# CLIMATE CHANGE MODELING FOR WATER RESOURCES MANAGEMENT: TANA SUB-BASIN, ETHIOPIA

Submitted in the fulfillment of the requirements for the degree of

**Doctor of Engineering**

in the Department of Civil Engineering (Midlands)

Faculty of Engineering and the Built Environment

**Durban University of Technology**

**Bewuketu Abebe Tesfaw**

**Supervisor:** _____ **Date:** 23 April 2025

Bloodless Dzwairo (DTech Eng: Civil)

**Co-Supervisor:** **Date:** 21 April 2025

Dejene Sahlu (PhD in Water Resources Engineering and Management)

## EXECUTIVE SUMMARY

This study, conducted in the Tana Sub-basin, Ethiopia, aimed to model the impact of climate change on water resources management. The Soil and Water Assessment Tool (SWAT), SPI generator, and RStudio were employed to conduct a comprehensive analysis of climate variability, hydro-climatic extremes, and the impact of land use land cover change on water resources within the region. The findings highlight the significant impacts of both climate variability and land use land cover change on water resources management in the Tana Sub-basin. Changing climate patterns and hydro-climatic extremes were identified as key factors posing increasing challenges to water availability and sustainable management within the region.

In analyzing the variability and trends of climate parameters in the Tana Sub-basin, various statistical methods and indices were employed to assess precipitation and temperature patterns. The findings indicated a statistically non-significant increasing trend in rainfall across the Sub-basin, with values ranging from 1.64 to 5.37 mm/year. With regard to temperature, an increase was observed, but it was also not statistically significant. The seasonality index ranged between 0.87 and 1.03. In 36.69% of the Sub-basin, rainfall occurs in marked seasonal patterns with a long dry season and the remaining 63.31% is concentrated in three or fewer months, indicating a different rainfall distribution pattern. The assessment of precipitation concentration found that 57.5% of the rainfall data exhibited strong irregular concentration; 41.5% showed irregular concentration, and 1% exhibited moderate concentration. This decreasing trend in projected mean annual precipitation and increasing trend in temperature under the RCP4.5 and RCP8.5 scenarios from 2020 to 2100 indicated significant changes in climate conditions in the Tana Sub-basin. In conclusion, the study underscores the presence of climate change, variability, and trends in the Tana Sub-basin, highlighting the need to align agricultural and water resource management practices with the observed climate variability.

Hydro-climatic extremes in the Tana Sub-basin, including drought events, were investigated using several statistical measures and tests including coefficient of variation, seasonality index,

precipitation concentration index, Mann-Kendall trend test, and Sen's slope estimator. Three categories of drought were identified: meteorological drought, agricultural drought, and hydrological drought. The frequency of meteorological drought ranged from 1.05% to 10.04%, agricultural drought from 1.26% to 12.21%, and hydrological drought from 0.21% to 14.5% in the study area. The variability in drought occurrence indicates that certain areas and seasons in the Tana Sub-basin are more susceptible to drought conditions than others. The observation of a potential trend in drought and wet extent occurrences in the study area until 2100 suggests that it may experience significant shifts in hydro-climatic patterns due to climate change. This highlights the importance of considering both spatial and seasonal patterns when assessing drought risks and implementing appropriate measures for water resource management and agricultural practices. In conclusion, the study emphasizes the significance of understanding spatial and seasonal variations in drought occurrence and aligning agricultural practices and water resource management accordingly.

This study also assessed the impacts of land use land cover change on water resources using the Soil and Water Assessment Tool. Three land use land cover maps (1986, 2000, and 2014) were analyzed to assess and quantify the changes and their impact on water resources. The findings indicated that changes in land use land cover have a significant impact on various components of the water balance in the study area. Compared to the baseline year of 1986, the average annual water yield increased by 14.88% and 12.6% in 2000 and 2014, respectively. Baseflow exhibited an increase of 18.4% in 2000 but decreased by 7.16% in 2014. Surface runoff increased by 12% and 16.16% in 2000 and 2014, respectively. Evapotranspiration decreased by 18.39% and 13.49% in 2000 and 2014, respectively. The expansion of cultivated land and the decline of forestland and grassland have implications for water resources and hydrological processes. The study thus demonstrates that land use land cover changes in the Tana Sub-basin have significant implications for surface runoff, water yield, evapotranspiration, and baseflow.

The analysis of water consumption by different sectors in the Sub-basin in 2020 indicated total annual water consumption for irrigation and horticulture of approximately 555.76 and 46.52 MCM, respectively. Livestock consumes about 31.78 MCM annually. Urban and rural domestic

water consumption is estimated to be around 22.03 and 33.43 MCM/year, respectively. The highest water-consuming sectors in the Sub-basin are rainfed agriculture and hydropower, accounting for more than 3,700 MCM annually. The projected increase in water demand, as indicated by the estimated water requirements of 6079.01 MCM in 2025, 6423.99 MCM in 2030, and 7519.93 MCM in 2035, emphasizes the urgency of sustainable water resource management. The study proposes adaptive strategy options for integrated water resource management as a crucial step in addressing the scarcity of water and ensuring sustainable use of water resources in the area. Assessing and updating water demand and available water resources are fundamental for informed decision-making and effective management of water resources in the Tana Sub-basin. Implementation of the adaptive strategy options outlined is essential to mitigate the challenges posed by increasing water demand and consumption, ultimately contributing to sustainable management of water resources in the region.

## DECLARATION BY STUDENT

I hereby declare that this thesis for the degree of Doctor of Engineering in the Department of Civil Engineering at Durban University of Technology is my original work, and it has not been submitted previously to any other institution of higher education. I further declare that all the sources cited and quoted are indicated and acknowledged in the references.

**Bewuketu Abebe Tesfaw:** **Date:** 14 April 2025

**Student Number (22063693)**

## DEDICATION

This thesis is dedicated to the people who are proactively working to save water resources management before the problem happens.

## ACKNOWLEDGEMENTS

ለመጀመር ያነሳሳኝ፣ በመካከል ያበረታኝ፣ ለመፈጸም ያበቃኝ፣ በቸርነቱ የጠበቀኝ፣ በመግቡ ያልተለየኝ አምላከ ቅዱሳን ልዑል እግዚአብሄር የተመሰገነ ይሁን።

This research would not have become a reality without the support of many individuals and institutions. I would like to express my gratitude to Professor Bloodless Dzwairo, my supervisor, not only for her valuable guidance, encouragement, patience, and support throughout this study but also for her interesting discussions, continuous follow-up, and dedication to this work despite her busy schedule. I also extend my deepest gratitude to Dr. Dejene Sahlu, my co-supervisor, for his kind and valuable support, follow-up, constructive comments, and suggestions for improvement.

Sincere thanks to Mr. Tilik Tena, for his continuous encouragement, follow-up, and support which were instrumental in completing the study. I am also grateful to Ms. Tinebeb Yohannes, Mr. Habitamu Tamir, Mr. Sileshie Mesfin and Mr. Ayenew Desalegn for their kind and valuable technical support and assistance and their provision of valuable data. I gratefully acknowledge Mr. Dereje Tewachew for his encouragement, motivation, and social support throughout this journey.

Thank you to the BRICS multilateral R&D Project team and Durban University of Technology for hosting the grant. The University of Limpopo and South Africa's Agricultural Research Council - Natural Resources & Engineering played an important role as co-investigators in this NRF-BRICS research project. Thanks also go to the Ministry of Water and Energy, National Meteorological Agency, Abbay Basin Administration Office, and Amhara Design and Supervision Work Enterprise in Ethiopia for providing valuable data and information.

እናት (መቅዲዬ) ውዷ ባለቤቴ ውድ ጊዜሽን ተሻምቸ፣ ምኞትሽን ነስቼ፣ በትዕግስትና በጥበብ ጸባዬን ተሸክመሽ፣ በፍቅር እያበረታሽኝ ለዚህ አድርሰሽኛልና በፍፁም ምስጋና እግዚአብሄር ይስጥልኝ።

# TABLE OF CONTENTS

## LIST OF FIGURES

## LIST OF TABLES

# LIST OF EQUATIONS

## LIST OF ANNEXURES

# CHAPTER ONE: BACKGROUND

## 1.1 Introduction

Climate change is a significant global challenge in the 21st century (Field 2014; Abidoye *et al.* 2015; Reidmiller *et al.* 2018; Mengistu *et al.* 2021). Developing countries, particularly those in sub-Saharan Africa, are particularly affected by the rise in global average temperatures, commonly referred to as global warming (IPCC (2012). For instance, climate variability has negatively impacted Ethiopia's economy (Birara *et al.* (2018). Numerous studies have been conducted to examine historical climate change and variability trends in Ethiopia (McSweeney *et al.* 2008; Keller 2009; Eshetu *et al.* 2014; Shawul *et al.* 2020; Tofu *et al.* 2023). Fluctuating rainfall patterns have had a significant influence on agricultural productivity, pastoralist communities, and animal populations in Ethiopia (Seleshi *et al.* 2004). Lake Tana, situated in the Tana Sub-basin and covering 20% of the Sub-basin area, is highly sensitive to climate change (Kebede *et al.* (2006); Setegn *et al.* (2011). Researchers have employed different approaches and methods to analyze and comprehend climate variability, changes, and associated risks (Fu *et al.* 2009; Makenzi *et al.* 2013; Aladaileh *et al.* 2019; Ademe *et al.* 2020; Getachew *et al.* 2021; Harka *et al.* 2021; Worku *et al.* 2022). It is crucial to adopt appropriate methods to analyze climate variability, trends, changes, and associated risks in a specific study area to ensure accurate and reliable results.

Ethiopia's natural resources are influenced by a combination of interconnected factors. As noted by Wassie (2020), these include agricultural expansion, population pressure, rapid urbanization, migration and resettlement, climate change, and environmental pollution. The study area holds significant potential for future socio-economic development, particularly through increased utilization of water resources (McCartney *et al.* 2010). The impact of urban expansion and industrial development along the shoreline of Lake Tana has been the subject of investigation (NBI (2009). McCartney *et al.* (2010); Abera *et al.* (2020) noted that, the majority of the population in this region resides in rural areas, and their livelihoods depend on agriculture. The status of land cover and ongoing land use changes have been issues of concern due to uncontrolled land fragmentation, intensive sub-division, and deforestation, resulting in significant soil erosion across the watershed. This issue is prevalent in various parts of the study area (Bogale (2020) Tewabe *et*

*al.* (2020). Stonestrom *et al.* (2009) and Getachew *et al.* (2022) emphasized that land use land cover (LULC) changes can have substantial impacts on water resources, while Woldesenbet *et al.* (2017, 2018) demonstrated that changes in land use and land cover have an impact on the hydrological components of the Tana Sub-basin. These changes can influence the quantity and quality of water resources in the area. Understanding these dynamics is thus crucial for sustainable resource management and planning in the region.

Such research will offer policymakers and stakeholders valuable insights into the current state of water resources and enable them to understand the potential impacts of climate change and land use changes, and to develop appropriate strategies to ensure sustainable water resource management in the Tana Sub-basin. This type of analysis and planning is essential to address future water challenges and promote the long-term socio-economic development and well-being of the region.

Water is a crucial and essential natural resource that plays a vital role in social and economic development and supports life on Earth (Halli *et al.* (2022). Ethiopia's Tana Sub-basin is a populous area that is a growth corridor due to its significant productive potential (NBI 2009; McCartney *et al.* 2010; Taye *et al.* 2021). It is also home to the largest freshwater source for the River Abbay (SMEC 2008). Given the importance of water resources in the Tana Sub-basin, it is crucial to assess and analyze current demand and supply of water in the area in order to propose optimal solutions for future efficient and effective utilization and management of water resources.

This study aimed to model the impact of climate change on water resource management in the Tana Sub-basin. It assessed and analyzed climate variability, trends, and associated risks in the study area, providing insights into changing climate conditions. More specifically, it examined hydro-climatic extremes in order to understand the occurrence and characteristics of extreme weather events such as droughts, floods, or intense rainfall. This assisted the identification of potential risks and vulnerabilities associated with such hydro-climatic extremes. Furthermore, the study evaluated the impact of LULC changes on water resources using the Soil and Water

Assessment Tool (SWAT). Lastly, it developed adaptive strategic options for sustainable water resource management in the Tana Sub-basin aimed at mitigating the potential risks and challenges. Overall, the study provides valuable insights into the complex interactions between climate change, LULC, and water resources in the Tana Sub-basin.

### 1.2 Problem statement

The Tana Sub-basin in Ethiopia confronts numerous challenges related to climate change and LULC changes, which are impacting its water resources (Setegn *et al.* 2011; Wubneh *et al.* 2022). The region is experiencing global warming, leading to variations in rainfall, river inflows, and evaporation, particularly affecting Lake Tana. Climate change has been shown to have a significant impact on the hydrology of the Sub-basin, including increased flooding and landslides (Tenagashaw *et al.* 2022). The Sub-basin is also undergoing land cover shifts due to rapid population growth and agricultural expansion (Bogale 2020). Agriculture is a major economic activity in the area, but its impact on water resources is not well understood. Industrialization, urbanization, and forestry are also contributing to land cover changes and affecting water resources. These have consequences for the hydrological component and overall water resources in the study area, with river flows diminishing periodically, lake levels falling, and aquifer flows, and quality being impacted.

In addition to these challenges, the Tana Sub-basin is facing increasing demand for water resources from various sectors such as hydropower, irrigation, water supply, industry, tourism, navigation, and fisheries. However, there are no agreed limits on water abstraction from the lake, aquifers, or rivers within the Sub-basin, leading to uncontrolled and unsustainable water abstraction practices. This lack of effective water resource management has resulted in unfair distribution and utilization of natural resources, water use conflicts, and spatial and temporal water scarcity. Erosion, sediment problems, and decreased river flow exacerbate the challenges in the Sub-basin (Bogale 2020; Lemma *et al.* 2020).

To address these issues, it is crucial to model the impact of climate change and LULC changes on water resources and develop adaptive strategies. Assessing existing water demand and supply and developing scenarios for sustainable water resource management practices are important steps in improving the environmental, economic, and social prosperity of the study area.

### 1.3 Justification for the study

The Tana Sub-basin in Ethiopia is facing significant challenges related to population growth, urbanization, industrialization, agriculture, and irrigation expansion (Abera *et al.* 2020; Taye *et al.* 2021). These economic activities are putting pressure on the limited natural resources in the area, and the impacts of climate change are exacerbating the situation (Wubneh *et al.* 2024). However, current management of water resources and land use practices in the Sub-basin are not coordinated, integrated, participatory, or sustainable (McCartney *et al.* 2010). The lack of a well-defined and scientific water resource management system is aggravating the situation, and the effects of water resource management in the study area are not well understood. Despite this, the government is investing heavily in water resource development projects and economic activities, which is paradoxical considering the limited availability of natural resources.

While research has been conducted on the impact of climate and LULC changes on water resources using different tools, there is a need to assess and update the information on the impact of these changes on water balance components and their availability in the study area (Setegn *et al.* 2011; Gebretsadik 2021; Chakilu *et al.* 2022). Previous studies in the study area have utilized hydrological tools, programs, or statistical parameters independently, without proposing an adaptive strategy for sustainable water resources management. Considering this, the present study employed a rigorous, multidisciplinary, and integrated approach combining statistical analysis, hydrological modeling, and scenario-based projections to simulate the effects of climate and LULC changes on water resources management. Additionally, it aimed to develop adaptive strategy options for sustainable water resource management in the Tana Sub-basin. The results offer valuable insights for decision-makers, planners, and researchers, and can inform policy options for water resource management in Ethiopia.

Overall, the development and implementation of adaptive strategies are essential to ensure effective, efficient, and sustainable utilization of water resources in the Tana Sub-basin. Hence, this study contributes to the formulation of water resource management policies and strategies in the area.

## 1.4 Objectives of the study

### 1.4.1 Aim of the study

The aim of this study was to model the impact of climate change for water resources management in the Tana Sub-basin, Ethiopia using the SWAT.

### 1.4.2 Objectives

The study's objectives were to:

1. Analyze climate variability, trends, and associated risks in the Tana Sub-basin;
2. Explore the impacts of hydro-climatic extremes on the Tana Sub-basin;
3. Assess the impact of land use land cover change on water resources; and
4. Develop sustainable and efficient adaptive options for integrated water resources management of the Tana Sub-basin.

## 1.5 Scope of the study

The study's main objective was to assess the impact of LULC change on water resources, climate variability, trends, and hydro-climatic extremes within the Tana Sub-basin. However, it is important to note that this assessment was limited to the time period from 1986 to 2014. This means that the analysis of the impact of LULC change on water resources is based on the available data within that specific time frame. The study did not cover the period from 2014 to 2023. Furthermore, it did not incorporate climate change projections for the future alongside LULC changes to assess their combined impact on water resources in the study area. The research focused on current LULC change and its effects on the hydrological system, rather than incorporating

projected future climate scenarios. However, it projected climate parameters until 2100 and analyzed them, indicating a forward-looking approach to understanding the possible long-term effects of climate change. This kind of analysis can offer insightful information on the study area's long-term climate change effects, including temperature and precipitation patterns.

Despite these limitations, the study provides valuable insights into the historical impact of LULC change on water resources and the influence of climate variability on hydro-climatic extremes within the Tana Sub-basin. These findings can be used to develop adaptive strategic options for sustainable water resource management. By informing decision-making processes, they can help to ensure the long-term sustainability and resilience of the Tana Sub-basin's water resources.

### 1.6 Thesis structure

The executive summary (abstract) presents an overall summary of this thesis, which is organized into six chapters as follows:

Chapter One: Provides a general description of LULC change and climate change, and their impact on water resources in the Tana Sub-basin. It outlines the objectives and scope of the research and presents the motivation and justification for the study.

Chapter Two consists of a comprehensive literature review for each of the study’s objectives. It covers climate variability, trends, hydro-climatic extremes, LULC change’s impact on water resources, and adaptive strategies for water resource management. The review also includes an examination of hydrology modeling tools and their dynamic features in assessing the impact of LULC change on water resources and climate change. The programs and statistical parameters used in the study are also reviewed.

Chapter Three: Presents a detailed description of the study area. It includes information on the geographical location, LULC, soil, slope distribution, and climate features of the Tana Sub-basin.

Chapter Four: Provides a detailed explanation of the methods and materials used in the study, including the research methods employed for each of its objectives.

Chapter Five: Presents and discusses the study's results, including the model evaluation, performance, and sensitivity analysis. The results and discussion are aligned with the research objectives and provide insights into climate variability, hydro-climatic extremes, the impact of LULC change on water resources, and adaptive strategies in the Tana Sub-basin.

Chapter Six: Summarizes the study's key findings, draws conclusions, and offers recommendations for future research and/or policy implications.

Overall, the thesis follows a logical structure, starting with an introduction and motivation, followed by a literature review, a detailed description of the study area, the methodology, results, and discussions, and wrapping up with the main conclusions and recommendations derived from the research.

# CHAPTER TWO: LITERATURE REVIEW

## 2.1 Introduction

This chapter reviews different studies related to climate variability, trends, hydro-climatic extremes, the impact of climate and LULC changes on water resources, and sustainable water resource management. It also focuses on the hydrological model, programs, and statistical parameters adopted in this research to achieve the objectives in the study area.

### 2.1.1 Climate variability and trends

A recent study analyzing TAMSAT rainfall data from 1983 to 2020 across Africa applied the Mann–Kendall test and Sen's slope estimator to assess rainfall variability and trends at monthly, seasonal, and annual scales (Alahacoon *et al.* 2022). Results revealed significant spatial differences, with increasing trends in Central and Northern Africa most notably in Rwanda (11.97 mm/year) and the Gulf of Guinea (8.71 mm/year) and declining trends in regions such as Mozambique (−0.437 mm/year). The findings highlight that rainfall increases in certain climate zones, such as tropical grasslands and northern deserts, may enhance food security through improved rain-fed agriculture, while declining trends pose risks to climate resilience. It offers key insights for drought and flood management but does not incorporate other common statistical methods addressed in this study.

Belay *et al.* (2021) assessed climate variability and trends in southern Ethiopia using the coefficient of variation, standard anomaly index, standard precipitation index, precipitation concentration index, Mann-Kendall trend test and Sen's slope estimator. The results indicated climate variability with significant decreasing and increasing trends observed in southern Ethiopia. The findings and methods used align with this study, except for the non-significant trend found in the current research.

Kassie *et al.* (2014) study titled 'Climate variability and change in the Central Rift Valley of Ethiopia: Challenges for rainfed crop production' analyzed agro-climatic variability and changes

and associated risks with respect to rainfed crop production in the Central Rift Valley. The study used Sen's slope estimator and Mann-Kendall trend test methods. The results showed that total rainfall decreased, but not significantly, and annual mean temperatures showed a significant warming trend. Past and future climate trends and variability pose major risks to rainfed agriculture. The study recommended the development of adaptation strategies to cope with the risks and sustain farming. Thus, the methods used, and the findings are aligned with this study.

Harka *et al.* (2021) investigated the spatial temporal patterns or trends and spatial distribution, and variability of rainfall in seasonal and annual time-series in Upper Wabe Shebelle river basin, Ethiopia. The study evaluated rainfall variability and trends using the coefficient of variation, precipitation concentration index, standardized anomaly index, Mann-Kendall test, Sen's slope estimators, and the latest technique of innovative trend analysis. The results showed that most stations recorded high annual rainfall in the wet season, while greater rainfall variability occurred in the dry season. Although trends showed slight increases in the wet season and decreases in the dry season, these changes were statistically non-significant. The results have implications for water resources planning and management in the study area.

Asfaw *et al.* (2018) employed trend analysis to analyze changes in rainfall and temperature in northcentral Ethiopia using gridded monthly precipitation and temperature data with 0.5° by 0.5° resolution from 1901 to 2014. The coefficient of variation, anomaly index, precipitation concentration index, Palmer drought severity index, and Mann-Kendall test were used to analyze the data. The results showed intra- and inter-annual variability of rainfall and an increasing number of drought years. Annual rainfall during *Kiremt* (the primary rain season from mid-June to mid-September) and *Belg* (the secondary wet season from February to May) decreased at a rate of 15.03, 1.93 and 13.12 mm per decade, respectively while the change in temperature was 0.067 and 0.026, and 0.046 °C per decade for the minimum, maximum, and mean, respectively. The study recommended the formulation of agricultural strategies that align with the declining and variable nature of rainfall and increasing temperature.

Roth *et al.* (2018) research on the effects of climate change on water resources in Ethiopia's upper Blue Nile Basin focused on seasonal and temporal changes in long term flow in the country at the border with Sudan. Both parametric and nonparametric methods were used to examine long-term patterns in hydrological time series. Using data from the Climate Forecast System Reanalysis (CFSR) of the National Centers for Environmental Prediction (NCEP) based on three distinct climate change scenarios from the Coupled Model Intercomparison Project (CMIP3), the SWAT model was calibrated, and future climate change impacts were projected. Precipitation could increase from 7% to 48% and streamflow would increase from 21% to 97%, according to climate change scenario modeling. In two subsequent time periods (2046–2064 and 2081–2099), three models (CCCMA, CNRM, and MRI) were applied. The study concluded that a significant seasonal shift from June to September (existing main rainfall season) to an earlier beginning (January to May) with less dramatic peaks, but longer period of the rainfall season is projected under current climate change scenarios.

Analyzing the spatial-temporal distribution of rainfall and temperature and detecting trends are key to healthy ecosystem functions and sustainable agricultural production. Therefore, this study also analyzed climate variability, trends, and associated risks of the climate parameters temperature and rainfall in the Tana Sub-basin, Ethiopia. The seasonal and annual variability of rainfall and temperature were assessed, and the concentration of precipitation was computed.

### 2.1.2 Hydro-climatic extremes

Gebrechorkos *et al.* (2023) study examines the projected impacts of climate change on hydrology and extremes in East Africa using downscaled outputs from seven CMIP6 models. Using a high-resolution hydrological model, it finds that precipitation and streamflow are expected to increase in Ethiopia, Kenya, and Uganda, while parts of Tanzania may experience declines. Temperature and evapotranspiration are also projected to rise, intensifying hydrological extremes. These findings highlight the need for localized adaptation strategies to manage future droughts and floods in the region. More comprehensive results can be achieved by incorporating additional parameters, such as vegetation indices, to better understand their impact on hydroclimatic extremes.

The impact of climate change on hydrological drought in the Tana Sub-basin using the HBV model was the focus of Enyew (2014) study. It considered two future periods: the intermediate period (2021-2050) and the far future (2071-2100). According to HBV using CNCM3 force, the number of droughts in the Tana Sub-basin is expected to increase by 100% and 68.8% in the intermediate and far future, respectively. The finding aligns with this study's results using different magnitudes of drought. However, this study used three parameters (precipitation, temperature and soil moisture) rather than one to compute the drought index using RStudio, which was one of its advantages.

Hydro-climatic extremes such as droughts and floods have likely increased due to climatic change, with potentially severe socio-economic, structural and environmental impacts (Tan *et al.* 2020). Tan *et al.* (2020) reviewed 111 studies conducted on hydro climate extremes starting from 1999. These articles can be divided into extreme flow assessments, drought studies, flood studies, and drought and flood studies, SWAT coupling with other models, and SWAT improvements. Most of the extreme performance assessment studies reported "satisfactory" performance, with particular emphasis on peak flow comparisons. The study suggested that future research on hydro-extremes should employ a SWAT model.

Using an observation-driven approach, Neri *et al.* (2019) developed a statistical framework to attribute changes in the occurrence of flood peak incidents to changes in the climate system and LULC. The analyses were performed at the seasonal level and considered five predictors: precipitation, temperature, antecedent wetness conditions, agriculture, and population density. The results indicate that precipitation and antecedent wetness conditions are the strongest predictors, with the role of the latter increasing as the threshold for event identification is reduced. The study concluded that population growth (urbanization) and agriculture are less important than climate predictors.

Information on drought severity and frequency is crucial for drought monitoring, water resource management, and decision-making in drought-prone regions. Therefore, this study analyzed and

examined the severity and frequency of droughts and wet seasons in the Tana Sub-basin. It adopted RStudio and the SPI tool to compute the drought index by considering three parameters (precipitation, temperature, and vegetation cover) rather than only precipitation values.

### 2.1.3 Impact of land use land cover change on water resources

The impact of LULC change on water resources in a tropical catchment in Tanzania under different climate change scenarios was studied by Näschen *et al.* (2019) using the SWAT. The results showed that high flows increased by up to 84% for the combined LULC and climate change scenarios whereas low flows decreased by 6-8% for the LULC scenario. The study concluded that the effect of LULC change is lower than that of climate change, but it also poses fewer uncertainties. The findings and the tools used align with this research.

Sead *et al.* (2010) assessed the impact of land use change and climate change on hydrologic regimes and the water resources of the Blue Nile River Basin that is mainly located in Ethiopia and Sudan. Using general circulation and SWAT models, the results suggest that land use cover change has had a significant impact on the Basin's flow regime. The author concludes that LULC and climate change will have a significant impact on the Blue Nile River, calling for action to be taken by stakeholders and decision-makers.

The impact of LULC change on water balance responses in the Pra River, Ghana was the focus of Awotwi *et al.* (2019) research. Seven land use/cover maps were used, and the SWAT model was deployed for hydrological simulation. The results revealed a continuous increase in cropland, settlement, and mining to the detriment of forest areas. Conversely, they pointed to reduced surface runoff and water yield during the dry season and increased baseflow and evapotranspiration during the wet season. The study concluded that settlement and mining are the major contributors to changes in the components of the water balance. These results highlight the importance of controlling LULC to maintain the water balance components and guarantee access to water for current and future generations.

Zhang *et al.* (2020) simulated hydrological responses to land use change using an improved SWAT model in a catchment in tropical Australia. This study considered vegetation growth calibrated from MODIS LAI data. The North Johnstone River catchment in wet tropical eastern Australia was selected as the case study. The results showed that land use change impacted all hydrological variables, with the impact on surface runoff being the most notable at annual scale. The authors noted that the results had important implications for the formulation of effective adaptation strategies and future policy plans for sustainable water management in tropical eastern Australia.

Bormann *et al.* (2009) analyzed the effects of spatial resolution and the distribution of model input data on the results of regional-scale land use scenarios using three different hydrological catchment models. Simulation results were used to identify the grid size, distribution, and model dependent scenario effects. In the case of data aggregation, all the models reacted sensitively to the grid size. The WASIM and TOPLATS simulate constant water balances for grid sizes, and the SWAT is more sensitive to input data aggregation. The aggregation effects were stronger than the redistribution effects. The study concluded that spatial discretization is more important than spatial distribution. Since the aggregation effect was mainly associated with a change in land use fraction, it concluded that the accuracy of datasets is more important than high spatial resolution.

Land use land cover changes continuously over time and influences water resources. Therefore, it is crucial to assess and update the impact such changes have on the water resources in the study area. This research assessed the impact of LULC change on water resources in the Tana Sub-basin using the SWAT and three LULC scenarios of the study area.

### 2.1.4 Sustainable water resource management

Mukheibir (2008) developed a framework for strategy considerations for water resources management in South Africa to meet the development goals in the municipal and agricultural sectors. The northwestern part of South Africa experiences severe periods of drought and, according to climate change projections, will be the most vulnerable to future climate induced water supply stress. A series of potential adaptation strategies suitable for long term adaptation are

discussed and presented in the study, including both supply and demand side strategies. The study found that human and financial resource deficiencies at local municipal and community levels were barriers to implementing these strategies.

Institutional obstacles to integrated water management at the river basin scale have been discussed in detail in the water governance literature, but less attention has been paid to developing an analytical framework to understand local government cooperation (Christophe *et al.* 2015). Christophe *et al.* (2015) formulated a median voter model to describe the political processes that support land use control in river basin management planning. The results confirm the existence of a very strong political component in the process whereby a municipality decides whether or not to support a river basin plan. This decision can be linked to the preservation of natural landscape amenities in peripheral areas, while elsewhere it is connected to the protection of farming.

Zhao *et al.* (2022) proposed adaptive water resources management as a strategy to better coordinate surface water and groundwater resources in response to droughts. The authors applied a water resource management tool that represents integrated agriculture, water, energy, and social systems in the Yakima River Basin in Washington State, USA. The study found that severe, consecutive droughts call for the application of additional financial and natural resources to achieve well-implemented adaptation strategies.

A highly negative water balance system that highlights the shortcomings of both water management and adaptation in the Mygdonia agricultural basin, Greece was the focus of Kolokytha (2022) research. The study, which analyzed the hydrology of the basin and climate projections until 2100, revealed the urgent need for concerted action. Different development adaptation strategies were applied and assessed for their effectiveness. The study found that integrated watershed management is a prerequisite for successful adaptation. Radical reform is also required in the agricultural sector to reduce the amount of land devoted to crops and to introduce different ones. Furthermore, demand management, rather than a focus on supply options, was found to be a solution.

## 2.2 SPI generator

The SPI was developed to compute the drought index in a given location (McKee *et al.* 1993). It is one of the most well-known and widely used meteorological and hydrological drought indices (Svoboda *et al.* 2012) that can be used to monitor hydrological and meteorological drought characteristics under multiple temporal and spatial scales and thus provide a reliable method to obtain the response patterns of hydrological drought to meteorological drought. Its computation for any location depends on the availability of long-term precipitation data for the given time period (Tenagashaw *et al.* 2022). It is used to estimate and monitor dry and wet conditions on a variety of time scales from sub-seasonal to inter-annual. The long-term precipitation data is matched to a probability distribution, which is then converted into a normal distribution so that the average and standard deviation of the SPI for the given location and the given time period are zero and one, respectively (Edwards *et al.* 1997).

SPI values are expressed as standard deviations that the observed precipitation would deviate from the long-term mean, for a normal distribution and fitted probability distribution for the actual precipitation record (Lloyd-Hughes *et al.* 2002). The SPI calculation comprises transformation of one frequency distribution to another. To calculate the SPI, the first step is to select a specific probability distribution (McKee *et al.* 1993; McKee 1995; Guttman 1998, 1999) that reliably matches the long-term precipitation record time series data and conduct fitting to that distribution. According to McKee *et al.* (1993) and Svoboda *et al.* (2012) drought categories, negative SPI values indicate the dry condition less than median precipitation, whereas positive values reflect the wet condition more than median precipitation. The SPI has different output values ranging from −2.0 to 2.0 (Table 1) as in the studies conducted by McKee *et al.* (1993) and Svoboda *et al.* (2012).

The SPI can be calculated from one to 72 months. Statistically, 1-24 months is the best practice range of application (Guttman 1999). The 24-month cutoff is based on Guttman's recommendation of 50-60 years of available data. The sample is too small if the time series data spans less than 80-100 years and the statistical confidence of the probability estimations on both dry and wet extremes becomes weak beyond 24 months.

Table 1: Standard Precipitation Indices (SPI) and their interpretation

Source: McKee (1995)

| SPI Value | Interpretation |
|---|---|
| ≥ 2.0 | Extremely wet |
| 1.5 to 1.99 | Severely wet |
| 1.0 to 1.49 | Moderately wet |
| 0.99 to -0.99 | Near normal |
| -1.0 to -1.49 | Moderately dry |
| -1.5 to -1.99 | Severely dry |
| ≤ -2.0 | Extremely dry |

### 2.3 RStudio

R is a free open-source tool that allows users to write and execute code to analyze data (Hair *et al.* 2021). RStudio is an integrated development environment (IDE) for R (Nwanganga *et al.* 2020; Hair *et al.* 2021) that offers a well-designed graphical interface to assist with the creation of R code (Nwanganga *et al.* 2020). An IDE is a programming environment that offers tools such as project management, tabs to easily manage multiple script files, and additional developer tools (Hair *et al.* 2021).

RStudio was used to compute the combined drought index (CDI) in this study. The CDI is a comprehensive index that combines various variables and provides an integrated measure of drought. It assesses the deviation of the current drought situation from a reference level, typically the long-term average over multiple years (Balint *et al.* 2013; Aladaileh *et al.* 2019; Bayissa *et al.* 2022). The CDI calculation involves processing and analyzing relevant data such as precipitation, temperature, soil moisture, or other variables that contribute to drought assessment. RStudio's data manipulation, statistical analysis, and visualization capabilities rendered it an ideal tool to conduct this analysis.

The precipitation drought index (PDI) considers rainfall deficits and the persistence of dryness; the temperature drought index (TDI) examines temperature excesses and the persistence of high temperatures, and the vegetation drought index (VDI) considers soil moisture deficits and the persistence of dry soil conditions. The resulting CDI provides a quantitative measure of drought severity and can be used to evaluate current drought conditions in relation to historical averages. This information is crucial for drought monitoring, water resource management, and decision-making in drought-prone regions.

### 2.4 Hydrological model

Hydrological models have become an essential tool in studying hydrological processes and anthropogenic factors' impact on the hydrologic system (Dwarakish *et al.* 2015). Sidle (2021) stated that watershed models are widely used in fields ranging from water resources assessment and management to watershed management and its engineering design. Hydrological modeling is used as a tool in a data-scarce basin for water resources management (Dutta *et al.* 2020). It also plays a crucial role in assessing seasonal water availability, which is necessary to make decisions in water resources management (Dwarakish *et al.* 2015). It is designed to gain a better understanding of the hydrologic processes in a watershed and improve hydrologic prediction at different levels. It also provides important information to evaluate the potential impacts of LULC or climate change (Tadele *et al.* 2007). Thakuri *et al.* (2021) stated that a review and criteria-based evaluation of the hydrological model is important to identify a suitable model for water resources management purposes in a watershed.

Different criteria can be considered to select the appropriate hydrological model for a specific problem. These are project-oriented since all projects have specific needs and requirements. Among different project-oriented selection criteria, four common, fundamental ones are the required model outputs vital to the project (Cunderlik *et al.* 2007). The level of accuracy and availability of data to deal with the complexity of the modeling process are the key factors for hydrological model selection. The model can be "lamped", "semi-distributed" or "distributed" and the complexity of the modeling process will increase in the order from lumped to distributed (Thakuri *et al.* 2021). However, a semi-distributed model can overcome the limitation of a fully

distributed model with a relatively larger amount of data and computation complexity than a lumped model (Jajarmizadeh *et al.* 2012). Therefore, semi-distributed models were selected for this study to model the impact of climate change on water resources management (Koua *et al.* 2021; Tenagashaw *et al.* 2022).

### 2.4.1 The Soil and Water Assessment Tool

The SWAT model was developed by the United States Department of Agriculture's Agricultural Research Service (USDA-ARS) to model the hydrology of a given watershed (Arnold 1998). It is a semi-distributed hydrological model (Arnold 1998) which operates on a daily time step. It is also a physically-based continuous-time and spatially distributed model designed to simulate water, sediment, nutrient, and pesticide transport in a watershed scale on a daily time step (Kasuni 2017). The SWAT is widely used to evaluate and assess the influence of environmental and ecological changes and hydrological responses at different watershed scales, even with limited data (Fu *et al.* 2009; Liu *et al.* 2018). The SWAT model has been applied to understand hydrological processes and responses in various river basins (Akoko *et al.* 2021). It has been used worldwide for water management (quality and quantity), agricultural practices management, large watersheds simulation, surface water and subsurface management, and to model sediment, nutrient, and pesticide processes (Koua *et al.* 2021). It is employed to predict land management practices' impact on water, sediment, and agricultural chemical yields in watersheds with varying soils, land use, and management practices over long periods (Arnold *et al.* 2005). The application of the SWAT model in the study area was tested and validated by Setegn *et al.* (2009).

There are two main sections in the hydrological simulation of a watershed using the SWAT. The first is the land phase of the hydrologic cycle which controls the water, sediments, nutrients, and pesticides loads to the main channel in each sub-basin and is based on the water balance equation. The second part of the hydrologic cycle is the water or routing phase, which deals with the movement of water, sediments, nutrients, pesticides, and other materials through the watershed's channel network to outlet (Neitsch *et al.* 2009; Koua *et al.* 2021). The SWAT tool requires a digital elevation model (DEM), and land use/land cover and soil data for the delineation of watersheds

and to generate hydrological response units (HRUs) (Abbaspour *et al.* 2015; Samal *et al.* 2021). Figure 1 below shows a schematic representation of the hydrologic cycle in the SWAT tool.

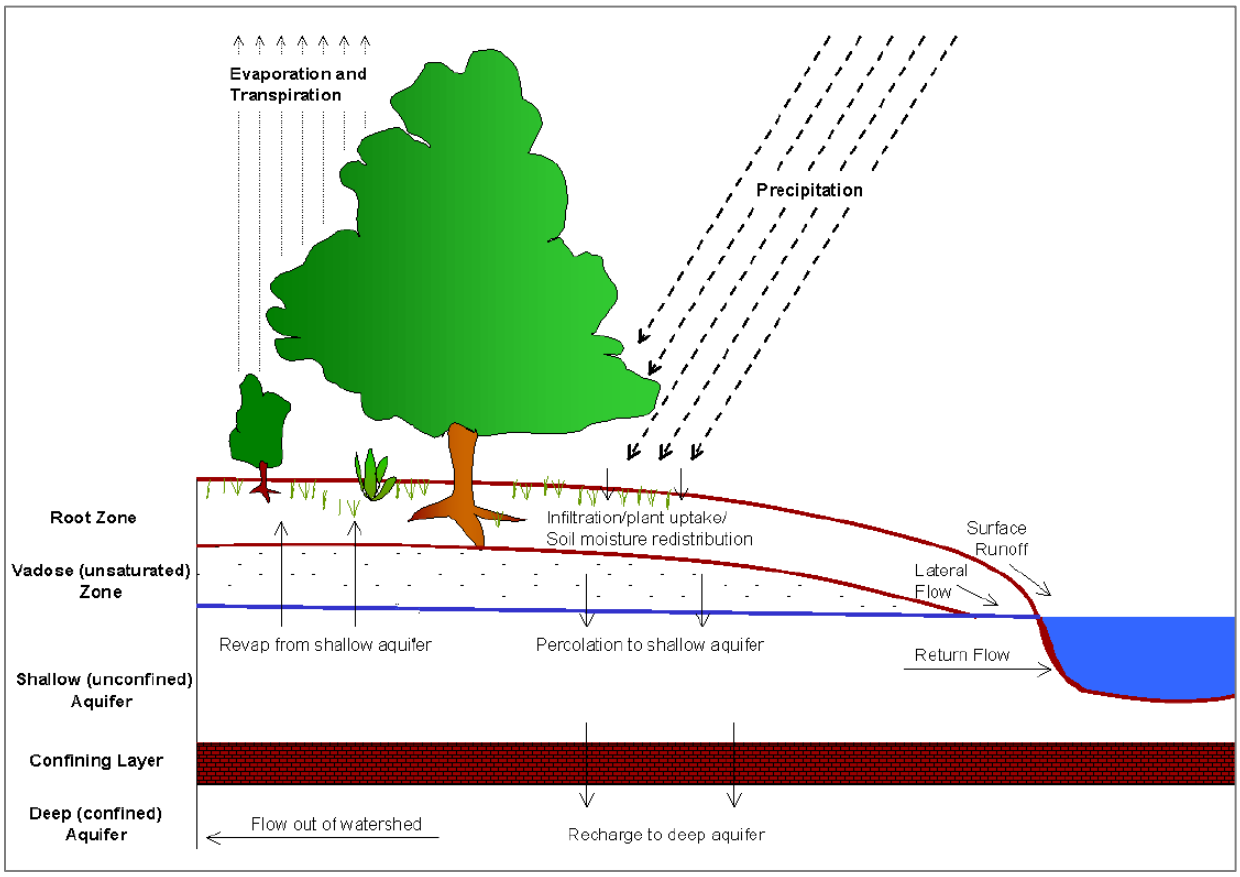


Figure 1: Schematic representation of Hydrologic cycle in SWAT

Source: Neitsch *et al.* (2009)

### 2.4.2 SWAT-CUP

Uncertainties in the hydrological model can be linked to either the input data (missing data or measurement error) or to the model itself (Refsgaard 1997; Schuol *et al.* 2008; Bastin *et al.* 2013). Considering these uncertainties, it is important to evaluate the differences and similarities between the observed data and the simulated data, either by objective parameters or graphically. SWAT Calibration and Uncertainty Programs (SWAT-CUP) was developed for calibration, validation, and uncertainty analysis of the SWAT model and is also used to optimize the SWAT model

parameters (Abbaspour 2013). Using this generic interface, any calibration, validation, and uncertainty or sensitivity analysis can easily be linked to the SWAT.

Five calibration, uncertainty, and sensitivity analysis algorithms are incorporated (Table 2). These are Sequential Uncertainty Fitting version 2 (SUFI-2) (Abbaspour *et al.* 2004; Abbaspour *et al.* 2007), the Generalized Likelihood Uncertainty Estimation (GLUE) (Beven *et al.* 1992), Particle Swarm Optimization (PSO) (Eberhart *et al.* 1995), Parameter Solution (PARASOL) (Van Griensven *et al.* 2006) and Markov Chain Monte Carlo (MCMC) (Kuczera *et al.* 1998). The SUFI2 algorithm considers all the sources of uncertainties (Yang *et al.* 2008); it was chosen to determine the global sensitivity of the parameters. This sensitivity analysis is governed by two criteria of uncertainty (Schuol *et al.* 2008; Koua *et al.* 2021).

The R-factor is calculated at 97.5% (Xu) which represents the average thickness of the “95PPU” band divided by the standard deviation of the measured data. The P-factor is calculated at 2.5% (Xl) which represents the percentage of measured data framed by the prediction uncertainty of 95% (95PPU). By computing the uncertainty derived from the percentage of measured data encircled by the maximum and minimum values of the "95PPU," the quality of the fit is evaluated (Abbaspour *et al.* 2015). The SUFI-2 is iterative; each iteration results in reduced parameter uncertainties causing a narrower “95PPU” band. For quantifying the inclusion of uncertainties and determining the optimal values to halt the simulations, it provides two indicators: the P-factor and R-factor (Abbaspour *et al.* 2015; Koua *et al.* 2021). Hence, a balance must be struck between the two indices (Abbaspour *et al.* 2015).

Table 2: Algorithms integrated in SWAT-CUP

Source: Koua *et al.* (2021)

| Algorithm | Description |
|---|---|
| SUFI-2 | Uncertainty in parameters is expressed as ranges (uniform distributions). The algorithm accounts for all sources of uncertainties. |
| GLUE | Many parameter sets are randomly selected from the previous distribution once the generalized likelihood measure has been defined. Each parameter set is then evaluated as behavioral or non-behavioral by comparing the likelihood measure with the specified threshold value. Next, a likelihood weight is assigned to each behavioral parameter. The uncertainty is finally forecast. |
| PSO | A population-based stochastic optimization method is represented by this algorithm. It starts with a collection of random particles, or solutions, and iteratively searches through generations in quest of optima. |
| PARASOL | Using the Shuffle Complex (SCE-UA) algorithm, the PARASOL approach minimizes objective functions (OF) in a global optimization criterion (GOC) and conducts uncertainty analysis. |
| MCMC | Samples from a random walk that adjusts to the posterior determination are produced by MCMC. |

#### 2.4.2.1 Model sensitivity analysis

The global sensitivity design method was utilized by SWAT-CUP's built-in tool to perform the sensitivity analysis (Yang *et al.* 2008; Abbaspour 2013; Abbaspour *et al.* 2015). Hydrological parameters are tested for sensitivity analysis for the simulation of the streamflow. The parameter with the high absolute value of “t-stat” and low “p-value” is the more sensitive parameter for streamflow sensitivity analysis in the model (Abbaspour 2013), and the list of the most sensitive parameters is used in order to perform further model calibration and validation analysis.

#### 2.4.2.2 Model performance

The model may or may not perform well. To evaluate the performance of models for water balance components, statistical parameters such as Nash Sutcliff efficiency (NSE) (Equation 1), coefficient of determination ($R^2$) (Equation 2), percent bias (PBIAS) (Equation 3), and the ratio of the root mean square error to the standard deviation of measured data (RSR) (Equation 4 and *Equation 5*) were used prior to further application and analysis as recommended by Krause *et al.* (2005) and Moriasi *et al.* (2007). These statistical parameters are widely used to evaluate the performance of hydrological models (Arnold *et al.* 1999; Gassman *et al.* 2007). The parameters are first computed by maximizing the NSE (Nash *et al.* 1970), then $R^2$ (Van Liew *et al.* 2003; Lemma *et al.* 2020), and, lastly, minimizing the magnitude of PBIAS (Gupta *et al.* 1999) and RSR (Moriasi *et al.* 2007).

The model performance is satisfactory and applied for further analysis if the NSE > 0.5 (Nash *et al.* 1970), PBIAS < 25% (Gupta *et al.* 1999) and RSR ≤ 0.7 (Moriasi *et al.* 2007) for monthly time step variable/flow. The values of $R^2$ greater than 0.5 are considered acceptable based on the previous criteria reported by Santhi *et al.* (2001) and Van Liew *et al.* (2003). Setegn *et al.* (2009) also stated that the model performance can be judged as satisfactory if $R^2$ is greater than 0.6 and NSE is greater than 0.5. The value NSE shows the level of reliability of the model in comparison to the mean, and the value of $R^2$ indicates how much the observed and simulated streamflow fit. The comparison between the observed and simulated streamflow indicated that there is a good agreement between the simulated and observed discharge which was verified by lower values of RSR and PBIAS and higher values of $R^2$ and NSE. RSR ranges from zero to a large positive value. The lower the RSR, the lower the RMSE and the better the model simulation performance.

Equation 1

$$\mathrm{NSE} = 1.0 - \frac{\sum_{i=1}^{n}(\mathrm{Qm,i} - \mathrm{Qs,i})^2}{\sum_{i=1}^{n}(\mathrm{Qm,i} - \overline{\mathrm{Q}}\mathrm{m})^2}$$

Equation 2

$$\mathrm{R2} = \left[\frac{\sum_{i=1}^{n}(\mathrm{Qm,i} - \overline{\mathrm{Q}}\mathrm{m})(\mathrm{Qs,i} - \overline{\mathrm{Q}}\mathrm{s})}{\sqrt{\sum_{i=1}^{n}(\mathrm{Qm,i} - \overline{\mathrm{Q}}\mathrm{m})^2}\sqrt{\sum_{i=1}^{n}(\mathrm{Qs,i} - \overline{\mathrm{Q}}\mathrm{s})^2}}\right]^2$$

Equation 3

$$\text{PBIAS} = 100 * \frac{\sum_{i=1}^{n}(\text{Qm,i} - \text{Qs,i})}{\sum_{i=1}^{n}\text{Qm,i}}$$

Equation 4

$$\text{RMSE} = \sqrt{\frac{1}{n}\sum_{i=1}^{n}(\text{Qs,i} - \text{Qm,i})^2}$$

Equation 5

$$\text{RSR} = \frac{\text{RMSE}}{\text{STDV}}$$

where Qm,i and Qs,i are observed and simulated variable/flow at time i respectively, $\overline{\text{Q}}m$ and $\overline{\text{Q}}s$ are average observed and simulated variables, respectively, and STDV is the standard deviation of the measured data.

### 2.5 Summary

The study area is somewhat complex and is home to ongoing anthropogenic activities. High population growth and urban expansion, the expansion of cultivated land accompanied by reduced forest and related plant cover and increased economic activities due to the Sub-basin being one of the growth corridors in Ethiopia, are the most common phenomena in the study area at different levels. Climate variability and climate and LULC change will affect the overall process.

Modeling the Sub-basin using hydrological modeling tools such as the SWAT can provide valuable insights into the study area's integrated and independent responses to climate variables and land use changes. The use of statistical analysis and programs such as RStudio can also enhance the quality of the outputs and provide a more comprehensive understanding of the hydrological processes in the area. However, it is critical to gather high-quality data and information to model the hydrological cycle and climate variability. The availability of multiple weather and hydrology variables, as well as remote sensing data, can aid in the development of more accurate models and predictions.

Overall, an integrated approach that considers climate variability and LULC changes is crucial for planners and decision-makers to develop appropriate adaptation and mitigation strategies in the study area. The use of hydrological modeling tools, statistical analysis, and programs can facilitate this process and provide valuable insights into the complex hydrological processes in the Tana Sub-basin.

# CHAPTER THREE: THE STUDY AREA

## 3.1 Location of the study area

The Tana Sub-basin is located in the headwaters of the Blue Nile Basin in northern Ethiopia. Its geographical coordinates extend from 36°04'5" E to 38°01'5" E longitude and from 10°05'7" N to 12°04'6" N latitude, as indicated in Figure 2. The Sub-basin is characterized by its elevated terrain, with a mean elevation of 2,026.54 meters above sea level (m.a.s.l.). The highest elevations are found in the eastern part around Mountain Guna, reaching up to 4,112 m.a.s.l. The lowest elevation is observed at the point where the outflow from Lake Tana enters the Blue Nile near the city of Bahir Dar (Abebe *et al.* 2017). This point has an elevation of approximately 1,786 m.a.s.l. The difference in elevation between the highest and lowest points highlights the topographic variation within the Sub-basin.

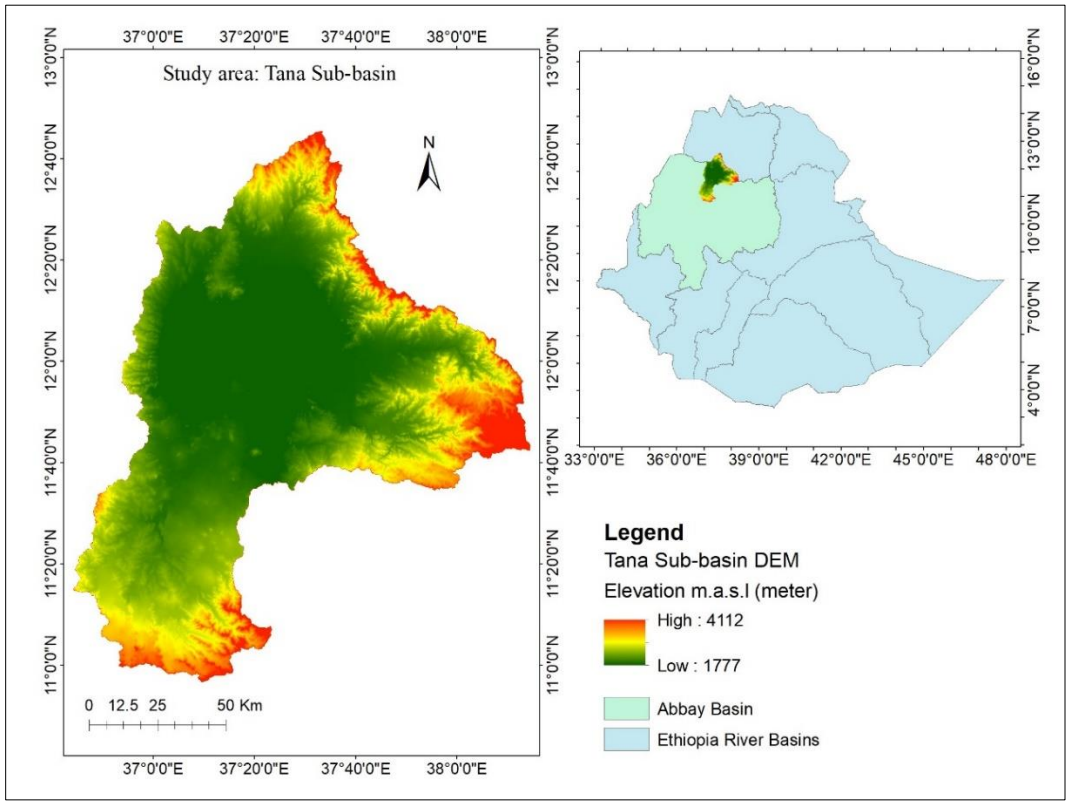


Figure 2: Location of the Tana Sub-basin in Ethiopia and Abbay Basin

Source: NASA's and ABAO

### 3.2 Climate of the study area

Ethiopia experiences three distinct rainy seasons (Gissila *et al.* 2004; Segele *et al.* 2005; Korecha *et al.* 2007; Haile *et al.* 2009). The main one occurs from June to September, followed by a dry season from October to January, and a smaller rainy season from February to May. A unimodal rainfall distribution is observed in the Tana Sub-basin (Getachew *et al.* 2021). The mean annual rainfall is estimated to be around 1,280 mm (Setegn 2008; Birara *et al.* 2018). The southern and southeastern parts of the region receive higher mean annual rainfall than the northern and northwestern parts (SMEC 2008). For example, at Bahir Dar in the southern part, mean annual rainfall is reported to be 1,433 mm. In Addis Zemen, located in the eastern part, it is 1,108 mm, and at Gondar airport in the northern part, it is 1,158 mm, indicating spatial variations in rainfall patterns (Dessie *et al.* 2015). The majority of the rainfall in the Tana Sub-basin occurs during the major rainy season from June to September (Alemu *et al.* 2020). This period is crucial for agriculture and water availability in the study area.

The mean annual temperature in the study area is documented at around 20°C (Weldegerima *et al.* 2018). Based on long-term climatic data in the Sub-basin, the temperature is comparatively uniform throughout the year with a mean annual temperature of 20.6°C and 20.2°C at Gonder and Bahir Dar, respectively (Wale *et al.* 2008; Dessie *et al.* 2015). Regarding evapotranspiration, Allam *et al.* (2016) reported annual actual evapotranspiration of 1,036 mm for the Sub-basin, while Setegn (2008) estimated it to be 733 mm. Understanding the rainfall patterns, temperature variations, and evapotranspiration rates in the Tana Sub-basin is crucial for water resource management, agricultural planning, and ecosystem conservation. It facilitates evaluation of the water balance, estimation of water availability, and implementation of appropriate measures for sustainable water use in the region.

### 3.3 Hydrology and water resources of the study area

The Tana Sub-basin covers an area of 15,070.14 $km^2$, and Lake Tana constitutes approximately 20%. Lake Tana is the largest freshwater lake in Ethiopia and the third-largest in the Nile Basin (Kebede *et al.* 2006; Woldesenbet *et al.* 2017; Lemma *et al.* 2020). It receives water inputs from

numerous smaller streams and a few larger rivers with catchments over 1,000 km$^2$. According to Kebede *et al.* (2006), the Gilgel Abbay, Ribb, Gumara, and Megech rivers are among the major contributors to the inflow of water into Lake Tana. These rivers have catchment areas of 1,656.35 km$^2$, 1,318.01 km$^2$, 1,354.35 km$^2$, and 515.06 km$^2$, respectively, as shown in Figure 3. Atanaw *et al.* (2018) emphasized their significant contribution to the inflow of water into Lake Tana. It is estimated that Gilgel Abbay River, which enters to the Lake Tana from the south, drains approximately 35% of the Tana Sub-basin and is the largest river in terms of the drainage area. The Gumara and Ribb rivers, entering the lake from the east, each drain approximately 27% of the Sub-basin. The Megech River, located in the northern part of the study area, covers 11% of the Sub-basin. Collectively, these four rivers (Megech, Ribb, Gumara, and Gilgel Abbay) contribute about three-quarters of the inflow of water into Lake Tana (Atanaw *et al.* 2018).

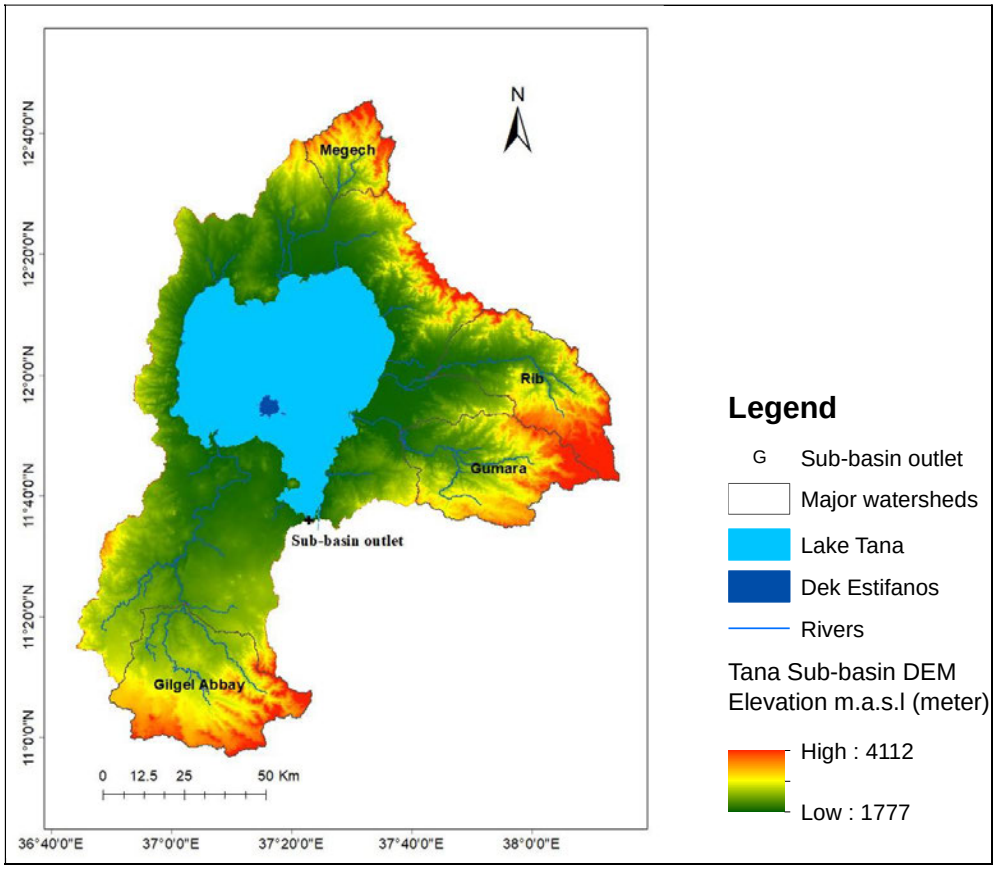


Figure 3: River network, Sub-basin outlet and major watersheds of the Tana Sub-basin

Source: NASA's and ABAO

Lake Tana receives water input from more than 40 rivers and streams. However, the majority of the water inflow, approximately 93%, is contributed by the four major rivers (Kebede *et al.* 2006). According to Dessie *et al.* (2015), between 1995 and 2008, the average annual outflow from Lake Tana through the Blue Nile River reached up to 133 m3/s. However, after 2011, it decreased to 75 $m^3$/s due to the diversion of lake water to the Tana-Beles hydropower plant. This likely resulted in a reduction in the water volume discharged from the lake to the downstream areas. In addition, the Tana Sub-basin experiences significant average annual discharge volumes at the four major hydrometric stations. These stations measure the flow of water in rivers and provide important data for water resource management. The average annual discharge volumes observed at the stations total approximately 3,490 $Mm^3$/year (SMEC 2008). These figures highlight the significant hydrological contributions of Lake Tana and the major rivers in the Tana Sub-basin. Understanding the inflow, outflow, and discharge volumes is crucial for assessing the water balance, evaluating water availability, and managing water resources effectively. It assists in making informed decisions regarding water allocation, hydropower generation, and conservation measures to ensure sustainable water management in the region.

### 3.4 Slope distribution of the study area

In the SWAT model, the HRUs represent spatially homogeneous land units within a watershed that have similar characteristics affecting water resources and runoff generation. One of the important factors considered in defining HRUs is the slope of the land. Major watershed of the Sub-basin MG representation Megech, RB Rib, GU Gumara, AB Abbay, and GA Gilgel Abbay watershed shown in Figure 4. According to the information provided, the study found that of the total drainage area, 63.18% has a slope ranging from 0-8%. This indicates that most of the watersheds consist of relatively gentle slopes. However, the remaining 36.82% of the drainage area has a slope above 8%. Within this portion, 15.65% has a slope between 8 and 15%, as shown in Figure 4. This suggests that a considerable portion of the watershed has moderate to steep slopes, which can have implications for water resources and runoff generation. Steeper slopes may contribute to higher amounts of surface runoff and erosion, potentially affecting water availability and quality within the watershed.

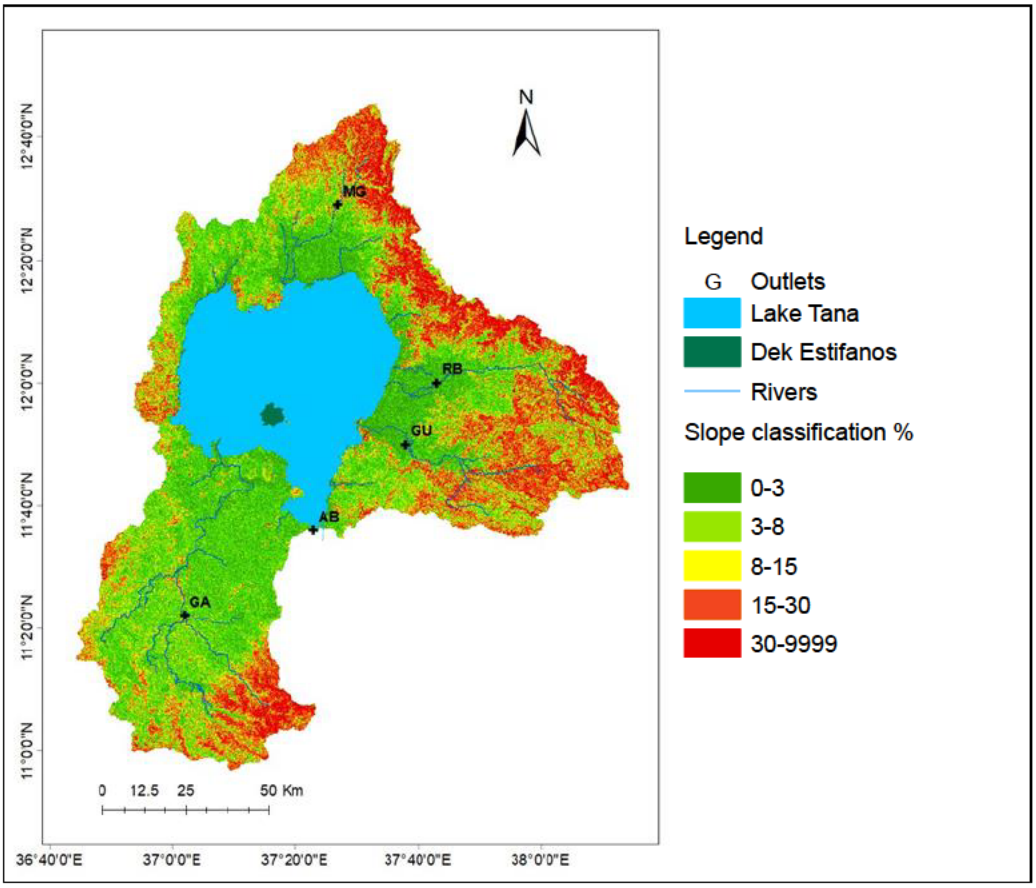


Figure 4: Drainage, major watersheds outlets, and slope distribution in the Tana Sub-basin

Source: NASA's

### 3.5 Land use land cover of the study area

The study area primarily consists of cropland, with limited areas of woodland and forest. Cropland refers to areas that are used for agricultural production, specifically for growing crops. This indicates that agriculture is a dominant land use in the study area. The woodland category refers to areas where trees are present, but they may be small or widely spaced. These areas may have some level of tree cover, but it is not as dense or continuous as in forests. The presence of woodland suggests that there are scattered trees or patches of vegetation in the study area, but they are not extensive. Water bodies, such as lakes and rivers, cover approximately 20% of the total study area. These contribute to the hydrological system and provide important resources for various purposes,

including irrigation, domestic water supply, and ecological habitats. Grassland is another land cover type found in the study area. Grasslands are biomes dominated by grass, with relatively few trees or shrubs. They are typically associated with areas where the climate and soil conditions are suitable for grass growth. Bare land refers to areas that are devoid of vegetation cover. These may be exposed to soil, rocks, or other surfaces without any significant vegetation.

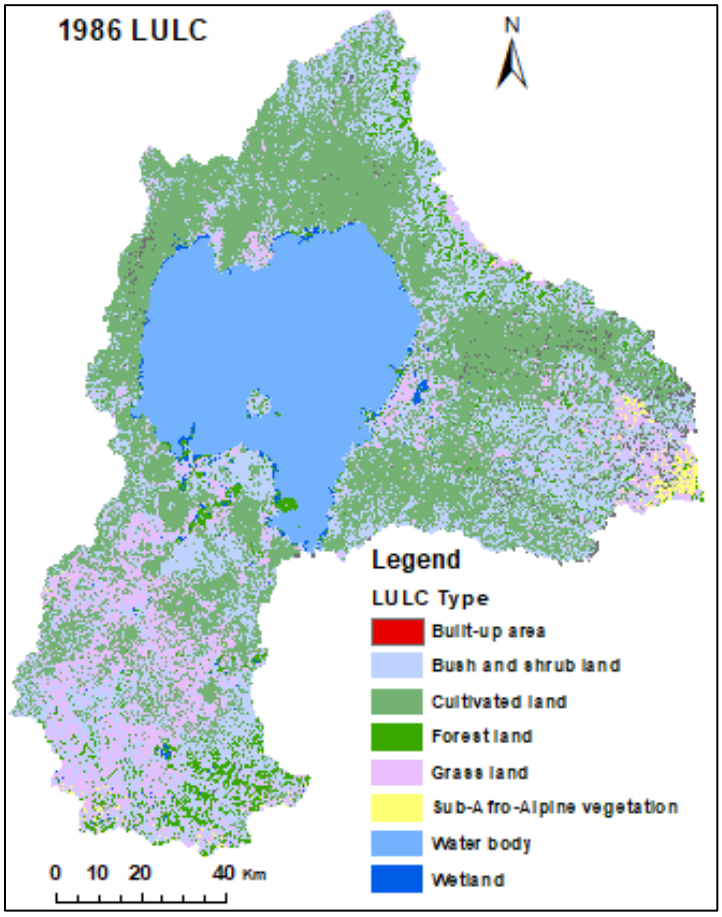


Figure 5: Land use land cover (LULC) at baseline year 1986

Source: ADSWE in Ethiopia

Forests are present in limited areas of the highlands within the study area. They are characterized by dense and continuous tree cover, supporting diverse ecosystems, and providing various ecological services. Lastly, urban and built-up areas are associated with cities or densely populated regions. These areas are characterized by infrastructure, buildings, and human settlements. By

identifying and characterizing these major land use and land cover types, the study provides insights into the spatial patterns of land use and the distribution of different land cover types within the study area. The study area LULC map at the baseline year of 1986 is shown in Figure 5.

### 3.6 Soil distribution of the study area

Soils in most of the study areas are derived from a weathered basalt profile, indicating the influence of volcanic activity in the region, and are highly variable in their properties and characteristics. There are five major soil groups: Eutric Luvisols, Eutric Leptosols, Fluvisols, Haplic Nitisols, and Eurtic Vertisols (refer to Figure 6). Haplic Nitisols is characterized by a moderate degree of weather and is a dominant soil type in the study area. In low-lying areas, particularly in the northern and eastern parts of Lake Tana and along parts of Gilgel Abbay, the soils have developed on alluvial sediments (SMEC 2008).

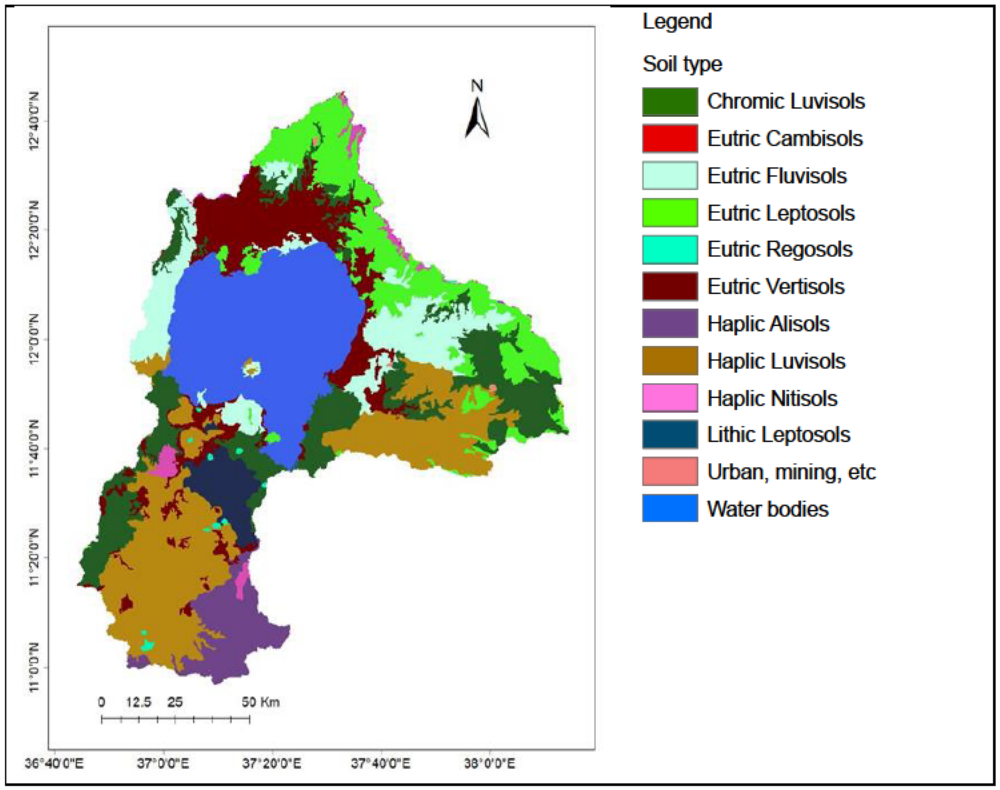


Figure 6: Soil distribution map in the Tana Sub-basin

Source: MoWIE in Ethiopia

Understanding the distribution and characteristics of these soil groups is important for agricultural planning, soil management, and land use decisions in the Sub-basin. It facilitates the identification of areas with high agricultural potential, areas prone to erosion, and those where soil conservation measures may be required.

# CHAPTER FOUR: METHODS AND MATERIALS

## 4.1 Introduction

This chapter provides a detailed explanation of the approaches used to collect information for the study, the data analysis methods, and how the Sub-basin was modeled. It discusses the research design, the tools utilized, the methodology employed to achieve the study's objectives, performance and validation of the model, validity, and reliability of the study and the ethical considerations taken into account.

## 4.2 Research design

The data collection and organization processes were prioritized. Various hydrological, meteorological, and spatial datasets were obtained from different institutions to support the research. Where data gaps were identified, remote sensing datasets were utilized to fill these gaps. Once the data was collected, a screening process was undertaken to ensure its quality and reliability. This involved checking for any errors, inconsistencies, or missing values in the datasets. Bias correction techniques were also applied to address any potential biases in the data. Statistical tools and MS Excel 365 were employed to analyze the data.

Secondly, a comprehensive literature review was conducted to gain a better understanding of the study area and identify suitable tools and approaches. It aimed to gather information on previous studies related to the study area, including those with similar research objectives or methodologies.

Thirdly, the input dataset was organized and imported into the model, specifically the SWAT model. The input dataset included various hydrological, meteorological, and spatial data relevant to the study area. Thereafter, simulation runs were performed. The model simulated hydrological processes and generated outputs such as streamflow, sediment yield, or nutrient loads based on the input data and the model's algorithms and equations. A performance, validation, and verification process were conducted to ensure the accuracy and reliability of the model. This involved

comparing the simulated results from the SWAT model with observed data collected from the study area.

Lastly, the simulation and interpretation and discussion of the results were conducted in line with the study's objectives. Based on the results, conclusions were drawn, and recommendations were formulated.

### 4.3 Research instrument

A variety of secondary data sources and tools were utilized to achieve the study objectives. The secondary data played a crucial role in providing the necessary information about the study area and its hydrological processes. The SWAT (ArcSWAT), SWAT-CUP2012, ArcGIS10.8.2, RStudio, SPI generator, WGNmaker, PCP stat, Dew02.exe, statistics tool software, and MS Excel 365 tools were used for data analysis, modeling, and statistical calculations. Sections 4.8 to 4.11 provide more detailed information on how these tools were applied and the specific analyses or calculations conducted to achieve each of the study's objectives.

### 4.4 Data collection

The data collection process involved a combination of primary and secondary sources. The researcher carefully observed and collected the key parameters required for the model. The primary data included field measurements or observations of climate, hydrology, water demand and supply, LULC, soil characteristics, and DEM data. The secondary data included existing datasets on climate parameters, remote sensing data (such as DEM, soil, and LULC maps), similar studies' results, and design documents. The secondary data were collected from various sources and reviewed to ensure their relevance to the study's objectives. They were analyzed and carefully reviewed to assess their quality and applicability to the study. Data screening and bias correction techniques were applied to identify and correct any errors, inconsistencies, or biases in the datasets.

The DEM used in this study was a 30 × 30-meter resolution Shuttle Radar Topographic Mission (SRTM) DEM, obtained from NASA's data portal (http://srtm.csi.cgiar.org/). This resolution is widely accepted for watershed-scale hydrological modeling, ensuring reliable simulation results. The soil data were sourced from Ethiopia's Ministry of Water, Irrigation and Energy (MoWIE), while the LULC map for the entire Tana Sub-basin and beyond was sourced from the Amhara Design and Supervision Work Enterprise (ADSWE) in Ethiopia. The study also utilized a full dataset of daily time series measurements including rainfall, maximum and minimum temperature, relative humidity, sunshine hours, and wind speed. These data were obtained from the National Meteorological Agency (NMA) in Ethiopia for six weather stations. The remaining stations were used to correct the bias of the CFSR rainfall data. Due to the limited spatial distribution of the meteorological stations and the fact that the records spanned a short period, the study incorporated additional meteorological data from the CFSR, including six climate variables. This data was sourced from the NCEP and accessed through the Global Weather Data site (https://globalweather.tamu.edu/). Rainfall data were sourced from CHIRPS (https://www.chc.ucsb.edu/data/chirps). Before using the CFSR and CHIRPS data, bias correction was performed using ground observations. In addition, CORDEX precipitation and temperature data (https://esgf-data.dkrz.de/search/cordex-dkrz/) were used to assess future climatic trends after correcting for bias.

The SWAT database files were adjusted and customized to suit the local conditions in the study area. The model was then simulated and calibrated at a monthly time scale using observed discharge data from four major river stations, namely Gilgel Abbay, Megech, Rib, and Gumara. To ensure model accuracy, the SWAT was used for simulating hydrological processes and assessing water balance components, while SWAT-CUP2012 was employed for model calibration, uncertainty analysis, and validation. The calibration process involves adjusting the model parameters to improve the agreement between the simulated and observed discharge data. The validation process uses statistical parameters to assess the model's performance to evaluate its accuracy and reliability in representing the hydrological processes in the context of the study area.

### 4.5 Data analysis

The missing data in the dataset were sourced and the quality of the data was checked to ensure its reliability. The analyses involved the interpretation of hydrological and meteorological data. Measured weather data from 1987 to 2013, including daily time series data on rainfall, maximum and minimum temperature, relative humidity, sunshine hours, and wind speed were available from the NMA for six weather stations.

To address the limited spatial distribution of the meteorological stations and the short period of time covered by the records, additional meteorological data from the CFSR sourced from the NCEP were used. This consisted of 42 rainfall grid points covering the extent of the Tana Sub-basin. Each grid provided information on six meteorological variables, including rainfall, minimum temperature, maximum temperature, relative humidity, wind speed, and solar radiation. Before using the CFSR data, bias correction was performed using ground observations. The rainfall dataset was sourced from CHIRPS available at https://www.chc.ucsb.edu/data/chirps. The CORDEX projected dataset was employed to assess future climate projections and trends. Like the CFSR data, bias correction was performed on the CHIRPS and CORDEX data using nearby observed data. Performance evaluation criteria such as Nash Sutcliffe efficiency (NSE), coefficient of determination ($R^2$), and Percent Bias (PBIAS) were used to evaluate the performance and accuracy of the corrected CFSR and CHIRPS datasets. Upper and lower outlier tests were also conducted to examine the data's distribution pattern. Statistical data analysis was carried out using MS Excel 365 to derive insights and draw conclusions from the analyzed datasets.

Three methods were used to estimate missing observation data at the stations: arithmetic mean, normal ratio, and linear regression. These were previously tested and applied in the same area by Mesfin *et al.* (2021). The arithmetic technique was employed to estimate missing observation data when the annual rainfall data at surrounding gauges fell within a range of 10% of the annual rainfall of the considered station. If this condition was met, the arithmetic mean of the available data from the surrounding gauges was used to estimate the missing data at the target station. However, the normal ratio method was applied when the annual rainfall data at surrounding gauges exceeded 10% of the annual rainfall of the considered station (Caldera *et al.* 2016). The linear regression

method was utilized when there was good correlation between the annual rainfall of the missing station and that of nearby stations for the same years (Caldera *et al.* 2016). By establishing a linear regression relationship between the available data from nearby stations and the missing station, the missing observation data could be estimated. Various tools and techniques were employed to facilitate the screening of precipitation data. Large time series files were carefully examined, and graphical tools and standard reports of precipitation data were utilized. These approaches assisted in the identification of missing data and the estimation process.

The DEM data was utilized to generate stream networks and classify slopes. The threshold value of 10% was used for LULC, soil, and slope layers. This means that land units below the threshold size were not considered in the analysis. The soil data obtained from the MoWIE in Ethiopia were reclassified to match the requirements of the SWAT database. The reclassification process ensured that the soil data were compatible with the SWAT database. Similarly, the slope data derived from the DEM were reclassified to correspond with the requirements of the SWAT database. The slope classification system used in this study was adopted from the Food and Agricultural Organization (FAO) system, as described in previous studies by Yimer *et al.* (2006) and Dagnachew *et al.* (2020). The study area's slope was calculated based on the DEM data. The calculated slope values were then classified into different categories. The slope classification used in this study was flat to very gently sloping (less than 3%), gently to sloppy sloping (ranging from 3% to 8%), strongly sloping (ranging from 8% to 15%), moderately steep (ranging from 15% to 30%), and steep to extremely steep (greater than 30%) slopes. By classifying the slope data into these categories, the study aimed to better understand the characteristics of the terrain and their potential impact on water resources within the study area.

The LULC map was obtained from ADSWE and was extracted using the study area boundary as defined by the shapefile, which encompassed the entire Tana Sub-basin. ArcGIS10.8.2 software was used to analyze the LULC data. The LULC maps were processed using ArcGIS, and various calculations were performed to derive important information about the land cover within the study area. The land cover was categorized into eight classes, namely, cultivated land (areas used for agricultural activities such as farming and cultivation of crops), forest land (areas covered by dense

vegetation and trees), shrub/bushland (areas dominated by shrubs and bushes), water bodies (including rivers, lakes, ponds, and other water features), Afroalpine (high-altitude areas characterized by alpine vegetation), grassland (areas covered by grass and herbaceous vegetation), and settlement/built-up areas (areas with human settlements, infrastructure, and built-up structures). Using ArcGIS, the areal estimates and the percentage of each LULC class within the study area were computed. These calculations provided valuable insights into the distribution and composition of different land cover types in the Tana Sub-basin.

### 4.6 Validity and reliability of data

In this study, the precision of the model performance was influenced by the availability of sufficient spatial and temporal data in the study area. Efforts were made to ensure the quantity and quality of the data used for analysis. Various methods of data collection, filling the data gaps, and analysis were employed to gather the necessary data. Data calibration and validation tests were conducted to assess the accuracy and reliability of the data. Statistical parameters and analysis were utilized to evaluate the performance of the calibrated and validated data. These tests and analyses ensured that the data reflected the situation in the study area. The credibility of the data was established, enabling reasonable and reliable conclusions to be drawn from the analysis.

### 4.7 Ethical considerations

The ethical codes of conduct and standards laid down by the Durban University of Technology were adhered to. Consent was obtained from the Abbay Basin Administration Office to conduct the study on the Tana Sub-basin. The results were shared with the Abbay Basin Administration Office and other stakeholders with a vested interest in the findings. This ensures that the relevant parties are informed about the outcomes of the research and can make informed decisions or take appropriate measures based on the results. All the information was kept confidential.

## 4.8 Method for objective 1

*To analyze climate variability, trends, and associated risks in the Tana Sub-basin*

Several statistical measures and tests were employed to assess the variability, trends, duration, and magnitude of annual, seasonal, and monthly precipitation and temperature in the study area, including the coefficient of variation (CV), seasonality index (SI), precipitation concentration index (PCI), Mann-Kendall trend test (MK), and Sen's slope estimator. The CMhyd tool sourced from https://swat.tamu.edu/ was used to correct bias and perform statistical analysis of the projected climate parameters. By utilizing these statistical measures and tests, the study aimed to gain insights into the variability, seasonality, concentration, and trends of precipitation and temperature in the study area across different time scales. These analyses can help to identify patterns, changes, and potential climate-related impacts in the region.

### 4.8.1 Coefficient of variation

The CV was computed to assess the variability of rainfall, minimum temperature, and maximum temperature in the study area. The CV values were calculated for annual, seasonal, and monthly time scales using Equation 6. The degree of variability was classified into three classes based on the CV values, namely, high (CV > 30), moderate (20 < CV < 30), and low (CV < 20). The classification of the variability classes was based on previous studies such as Hare (2003) and NMSA (1996). According to Belay *et al.* (2021), lower CV values indicate lower variability of rainfall and temperature in the study area, while higher CV values indicate higher variability.

Equation 6

$$CV = \frac{\sigma}{\bar{x}} * 100$$

where CV is the coefficient of variation, σ is the standard deviation and $\bar{x}$ is the mean precipitation and temperature of the recording period.

By computing and analyzing the CV values, the study aimed to assess the variability of rainfall and temperature in the study area, classify the degree of variability, and understand the patterns and characteristics of the recorded precipitation and temperature data.

### 4.8.2 Rainfall regime classification

The rainfall regime can be classified using the value of SI (Walsh *et al.* 1981). It was used to assess the standardized timing and duration of rainfall in the study area, without considering the influence of magnitude. The method adopted to compute the SI of the stations and define the rainfall regimes was proposed by Walsh *et al.* (1981) and is widely used in the literature. It allows the calculation of the SI and provides insights into the relative seasonality of rainfall, even in areas with two or three distinct rainfall peaks throughout the year. The SI is defined as the sum of the absolute deviation of the mean monthly rainfall from the overall monthly mean, divided by the mean annual rainfall. Equation 7 below was used to calculate the SI:

Equation 7

$$SI = \frac{1}{R}\sum_{n=1}^{n=12} abs\left(X_n - \frac{R}{12}\right)$$

By calculating SI values for various stations or time periods, the study sought to quantify and compare the relative seasonality of rainfall. This analysis facilitates understanding of the timing and duration of rainfall events throughout the year, providing insights into the patterns and characteristics of the rainfall regimes in the study area.

Table 3: Redefined classification of the seasonality index (SI) based on rainfall duration

| Class code | Rainfall regime | Seasonality index (SI) | Rainfall duration in day |
|---|---|---|---|
| 1 | Very equable | ≤0.19 | ≥270 |
| 2 | Equable with a definite wetter season | 0.20–0.39 | 180–269 |
| 3 | Rather seasonal with a short drier season | 0.40–0.59 | 150–179 |
| 4 | Seasonal | 0.60–0.79 | 120–149 |
| 5 | Markedly seasonal with a long drier season | 0.80–0.99 | 90–119 |
| 6 | Most rain in 3 or less months | 1.00–1.19 | 60–89 |
| 7 | Extreme, almost all rain in 1 to 2 months | ≥1.20 | <60 |

The value of the SI varies from 0 to 1.83. A value of 0 indicates that all months receive an equal amount of rainfall, while a value of 1.83 suggests that all the rainfall occurs in a single month. The classification of rainfall regimes based on SI values proposed by Walsh *et al.* (1981) was redefined based on the duration of annual rainfall (Table 3).

### 4.8.3 Precipitation concentration index

The PCI was employed to assess the distribution of rainfall in the Tana Sub-basin across various time scales, including annual, seasonal, and monthly. It provides insights into the concentration or dispersion of precipitation events over a specified period. The PCI is also used to indicate the hydrological risks associated with floods and drought occasions and was used by researchers such as De Luís *et al.* (2000) and Gocic *et al.* (2013). It can be calculated using Equation 8.

Equation 8

$$PCI = \frac{\sum_{i=1}^{12} Pi^2}{(\sum_{i=1}^{12} Pi)^2}$$

where Pi is the precipitation amount of $i^{th}$ month

In calculating the PCI values, the study aimed to evaluate the degree of precipitation concentration in the Tana Sub-basin. This analysis provides important information to understand the rainfall distribution patterns and their potential impact on the hydrological system in the study area. A value of PCI less than 10 indicates uniform distribution of precipitation; values between 11 and 15 represent moderate precipitation concentration; those between 16 and 20 point to irregular distribution of precipitation and a value above 20 units shows strong irregular precipitation distribution across the area (Oliver 1980; Belay *et al.* 2021; Harka *et al.* 2021).

### 4.8.4 Mann-Kendall test

The MK trend test is a widely used statistical method to detect monotonic trends (increasing or decreasing) in time series data, particularly in the field of climate research (Addisu *et al.* 2015; Asfaw *et al.* 2018). It examines the presence of trends in climate parameters on both seasonal and annual scales. The details of the MK test are provided in Mann (1945) and Kendall (1975). The

MK trend test and Sen's estimator were employed in this study to investigate long-term changes in rainfall and temperature indices. This analysis facilitates an assessment of whether there are significant trends over time in these climate variables. One advantage of using the MK test for trend detection is that it is less affected by climate outliers (Sen 1968; Birsan *et al.* 2005). This makes it a robust method for trend analysis, particularly in the presence of extreme values.

However, it is important to consider the potential impact of autocorrelation in the time series data as it may affect the accuracy of the MK test results. To address this issue, a pre-whitening procedure was performed to remove autocorrelation from the data. Based on the output, no significant serial autocorrelation was found, and the MK test was conducted without modification. The test can yield two types of statistics depending on the number of data values available. The S statistic is used when the number of data points is less than 10, while the Z statistic (normal approximation/distribution) is used for datasets with 10 or more values. S is calculated based on total signs (it is always between -1, 0, and 1). In cases where N > 10, the standard Z is calculated as follows using Equation 9.

Equation 9

$$S = \sum_{i=1}^{n-1} \sum_{j=i+1}^{n} sgn(Xj - Xi)$$

Where the Xi is the actual time data for the time series of i = 1, 2, 3, to n, and n is the sample size.

The value of sgn (Xj-Xi) is calculated as follows:

Equation 10

sgn (Xj-Xi) = 1, if Xj-Xi > 0

= *0, if Xj-Xi = 0*

= *-1, if Xj-Xi < 0*

The S-statistics approximately behave as normally distributed, and the test is performed with normal distribution with the mean and variation as shown in Equation 11.

Equation 11

$$E(s) = 0$$

$$Var\ (s) = \frac{n(n-1)(2n+5) - \sum_{i=1}^{m} t(t-1)(2t+5)}{18}$$

Standard Z for one limit test is computed using the equation shown in Equation 12. The positive value of Z shows an increasing trend, and the negative value shows a decreasing trend.

Equation 12

$$Z = \begin{cases} \frac{(S-1)}{\sqrt{\mathrm{Var}\ (S)}}, S > 0 \\ 0, \quad S = 0 \\ \frac{S+1}{\sqrt{\mathrm{Var}(S)}}, S < 0 \end{cases}$$

Following the serial autocorrelation test, the MK test from the Z value was computed based on monthly, seasonal, and annual rainfall time series data.

In applying the MK trend test and analyzing the results, this study aimed to identify and quantify long-term changes in rainfall and temperature indices in the study area. This helps to understand the trends and potential shifts in climate patterns, supports climate change assessments and informs adaptation and mitigation strategies.

### 4.8.5 Sen's slope estimator

Sen's slope method is a nonparametric approach used to estimate the magnitude of the drift or trend in time series data (Kassie *et al.* 2014; Belay *et al.* 2021). It offers a robust method to quantify the direction and magnitude of the trend, whether it is increasing or decreasing, without assuming a specific statistical distribution. Sen's slope method was employed to calculate the magnitude of the trend based on the monthly, seasonal, and annual rainfall and temperature time series data. This analysis facilitates understanding of the rate of change over time for these climate variables. A positive value of Sen's slope indicates an increasing trend in the time series, suggesting a systematic and consistent upward drift. In contrast, the negative value of Sen's slope indicates a decreasing trend, indicating a systematic and consistent downward drift over time.

### 4.8.6 Climate projection

The CORDEX data obtained from the website (https://esgf-data.dkrz.de/search/cordex-dkrz/) were processed using the CMhyd software to correct biases and obtain climatic data. Observed time series weather data from four stations, namely Bahir Dar, Dangila, Debre Tabor, and Gonder, were used for the bias correction, calibration, and validation processes (Table 4). There are various GCMs available, but a single GCM is recommended to be used in practice for more detailed impacts assessment studies (Gebrechorkos *et al.* 2019). Therefore, the study is used the CanRCM4 model. The CanESM2 model is mainly used because daily predictor variables are freely available to be directly fed into the SDSM. It also represents the latest plausible radiative forcing scenarios, used to produce high resolution future climate data, and outputs can be applied for further impacts analysis with high degree of certainty in the study area and beyond (Fenta Mekonnen *et al.* 2018; Gashaw *et al.* 2020; Getachew *et al.* 2021; Getachew Tikuye *et al.* 2021; Chakilu *et al.* 2022). The emission scenarios RCP4.5 and RCP8.5 were used to analyze the statistical parameters for future precipitation and minimum and maximum temperature. These scenarios cover the period from 1950 to 2100 and were projected using the CanRCM4 (Canadian Regional Climate Model 4) climate model.

Table 4: Location of weather stations in the Tana Sub-basin

| Station | Latitude | Longitude | Altitude (m.a.s.l) |
|---|---|---|---|
| Bahir Dar | 11.275 | 37.322 | 1827 |
| Dangila | 11.434 | 36.846 | 2116 |
| Debre Tabor | 11.867 | 37.995 | 2612 |
| Gonder | 12.521 | 37.432 | 1973 |

The CanRCM4 model, which is an extension of the CanESM2 large ensemble, simulates the local climate using output from a Global Climate Model (GCM) as input to a high-resolution climate model. The NMA provided the baseline temperature and precipitation data for 1986 to 2005, which were used to validate and calibrate the downscaling procedure. Future climate change was analyzed using the Climate Centre of Canada's CanESM2 RCM output. Historical reanalysis baseline climatic data covering 1986–2005 were utilized for calibration and validation.

## 4.9 Method for objective 2

*To explore the impact of hydro-climatic extremes in the Tana Sub-basin*

### 4.9.1 Standardized precipitation index

The Standardized Precipitation Index (SPI) is a widely used meteorological and hydrological drought index (Svoboda *et al.* 2012). It is a statistical transformation of a precipitation time series to standardized normal distribution. SPI provides a measure of precipitation's deviation from the long-term average at different timescales. In this study, it was computed using monthly time series data, considering different timescales such as 3, 6, 9, 12, and 24 months (McKee *et al.* 1993; Karabulut 2015). This allows for the assessment of drought conditions over different durations, ranging from short-term to long-term perspectives. As reported by McKee *et al.* (1993) and Svoboda *et al.* (2012), the SPI values can range from -2.0 to 2.0 (Table 1).

The SPI generator and RStudio program, which are commonly used tools for SPI analysis, were used to compute the SPI values. The input data, in this case, the precipitation time series, were organized and rearranged to meet the requirements of the software before conducting any analysis. The percentage of drought and wet condition occurrence was analyzed using Excel. By calculating the SPI at various timescales, the study assessed the severity and duration of drought in the Sub-basin. The SPI values provide standardized measures that allow for comparisons across different locations and time periods, aiding drought monitoring, early warning systems, and water resource management.

### 4.9.2 Combined drought index

The CDI is an integrated drought index that combines multiple variables in a single indicator (Balint *et al.* 2013; Aladaileh *et al.* 2019; Bayissa *et al.* 2022). It provides a comprehensive assessment of drought conditions by considering various factors simultaneously. Different variables such as temperature, precipitation, soil moisture, streamflow, or any other relevant parameters that influence drought conditions are considered. By integrating these variables, the

CDI aims to capture overall drought severity and its impact on the environment, agriculture, and water resources.

The study employed three individual drought indicators: The Temperature Drought Index (TDI), Precipitation Drought Index (PDI), and the Vegetation Drought Index (VDI). Each focus on specific aspects of drought conditions. The PDI considers rainfall deficits and the persistence of dryness. It quantifies precipitation's deviation from normal levels and considers the duration and severity of dry periods. The TDI considers excessive temperatures and the persistence of high temperatures. It captures the temperature's departure from normal conditions and evaluates the duration and intensity of hot periods. The VDI reflects the presence of soil moisture deficits and the persistence of dry soil conditions. It assesses the impact of moisture deficiency on vegetation health and growth, considering the duration and severity of dry soil conditions.

The PDI, TDI, and VDI were integrated to generate the CDI. The CDI assigns three warning levels: watch, warning, and alert. The watch level is triggered when there is a precipitation shortage. The warning level is reached when the precipitation shortage is accompanied by excessive temperatures. Finally, the alert level occurs when both the precipitation and soil moisture deficits result in an impact on vegetation. The specific equations used to calculate the PDI, TDI, and VDI values in the study area are provided in Equation 13, Equation 14, and Equation 15, respectively. After calculating the individual indices, the CDI value is derived using RStudio4.2.1 tools. The CDI is obtained by weighting the values of PDI, TDI, and VDI, as specified in Equation 20 and illustrated in Figure 7 hereunder.

Equation 13

$$\mathrm{PDIi,m} = \frac{\frac{1}{\mathrm{IP}}\sum_{\mathrm{j=1}}^{\mathrm{IP-1}} \mathrm{P^{*}i,(m-j)}}{\frac{1}{(\mathrm{n}*\mathrm{IP})}\sum_{\mathrm{k=1}}^{\mathrm{n}}\left[\sum_{\mathrm{j=0}}^{\mathrm{IP-1}} \mathrm{P^{*}(m-j),k}\right]} * \sqrt{\left(\frac{\mathrm{RL}_{\mathrm{m,i}}^{(\mathrm{P^{*}})}}{\frac{1}{\mathrm{n}}\sum_{\mathrm{k=1}}^{\mathrm{n}} \mathrm{RL}_{\mathrm{m,k}}^{(\mathrm{P^{*}})}}\right)}$$

Equation 14

$$VDI_{i,m} = \frac{\frac{1}{IP}\sum_{j=0}^{IP-1} NDVI_i^*,\ (m-j)}{\frac{1}{(n*IP)}\sum_{k=1}^{n}\left[\sum_{j=1}^{IP-1} NDVI_{(m-i),k}^*\right]} * \sqrt{\left(\frac{RL_{m,i}^{(NDVI^*)}}{\frac{1}{n}\sum_{k=1}^{n} RL_{m,k}^{(NDVI^*)}}\right)}$$

Equation 15

$$TDI_{i,m} = \frac{\frac{1}{IP}\sum_{j=0}^{IP-1}[T_i^*,\ (m-j)]}{\frac{1}{(n*IP)}\sum_{k=1}^{n}\left[\sum_{j=1}^{IP-1} T_{(m-i),k}^*\right]} * \sqrt{\left(\frac{RL_{m,i}^{(T^*)}}{\frac{1}{n}\sum_{k=1}^{n} RL_{m,k}^{(T^*)}}\right)}$$

where IP is the interest period, $RL^{(P)}$ is the maximum number of successive decades or months below long-term available rainfall in the IP, $RL^{(T)}$ is the maximum number of successive decades or months above long-term average temperatures, $RL^{(NDVI)}$ is the maximum number of successive decades or months below long-term average NDVI in the IP, n is the number of years where relevant data are available, j is the summation running parameter covering the IP and k is the summation parameter covering the years where relevant data are available.

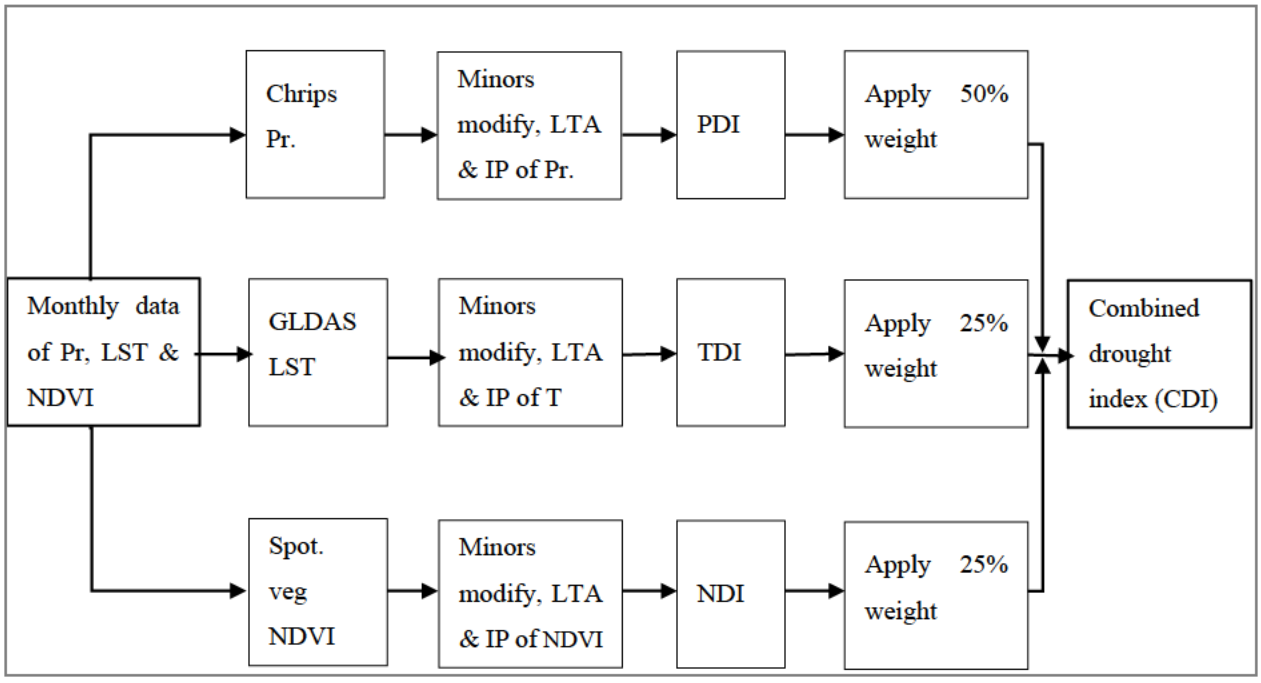


Figure 7: Schematic representation of CDI computation

Equation 16

$$T^* = (T_{max} + 1) - T$$

Equation 17

$$RL^* = (RL_{max} + 1) - RL$$

Equation 18

$$NDVI^* = NDVI - (NDVI_{max} - 0.01)$$

Equation 19

$$P^* = P + 1$$

The CDI is computed as the weighted average of the VDI, PDI, and TDI as indicated in Figure 7 above.

Equation 20

$$CDI_{i,m} = w_{PDI}*PDI_{i,m} + w_{TDI}*TDI_{i,m} + w_{VDI}*VDI_{i,m}$$

where w is the weights, 50% weight for PDI and 25-25% weight for TDI and VDI.

Table 5: Classification of drought categories based on CDI values

Source: Balint *et al.* (2013)

| CDI values | Drought severity | Description |
|---|---|---|
| >1.0 | Normal | No drought |
| 1.0 – 0.8 | Mild | Going into drought, short term dryness slowing planting, growth of crops. Also coming out of a drought – water deficits, partial loss of crops and pasture |
| 0.8 – 0.6 | Moderate | Damage to crops, pasture, drying of shallow reservoirs, voluntary water rationing |
| 0.6 – 0.4 | Severe | Wider scale of loss of crops and pasture, imposed water rationing and livestock migration |
| <0.4 | Extreme | Major loss of crops and pasture, extreme fire damage, total water shortage, drying of deep reservoirs and usage restrictions |

### 4.10 Method for objective 3

*To assess the impact of land use land cover on water resources in the Tana Sub-basin*

The DEM used in the study was generated from 30 × 30 m SRTM data obtained from NASA's website (http://srtm.csi.cgiar.org/). The DEM data were then utilized to generate stream networks and slope classification. The stream networks represent the flow paths of water in the area, while the slope classification categorizes the terrain based on its steepness. Based on the generated stream networks, the study delineated 69 sub-basins. Sub-basins are smaller drainage areas within the larger study area that contribute to the overall hydrological system.

Furthermore, the study created hydrologic response units (HRUs) based on dominant soil and LULC types for different years. A total of 942 HRUs were created for 1986, 886 for 2000, and 869 for 2014 (Annexure 42). It is worth noting that the HRUs varied due to changes in LULC over time, as depicted in Figure 29 and Annexure 42, as well as Table 16. These changes can impact the hydrological response of the sub-basins. To determine the HRUs, a 10% threshold value was considered for the LULC, soil, and slope layers. This means that land units below the threshold size were not included in the HRU delineation process. The soil data used in the study were sourced from the MoWIE in Ethiopia. These were reclassified to match the requirements of the SWAT database, a hydrological modeling tool used in the study. Overall, the elevation data, stream networks, LULC, soil information, and slope classification were integrated to create HRUs and analyze the hydrological processes within the sub-basins of the study area.

The slope data derived from the DEM were reclassified to match the requirements of the SWAT database. The reclassification was based on the FAO system, as referenced in the work of Yimer *et al.* (2006) and Dagnachew *et al.* (2020). Accordingly, the study area slope was calculated from the DEM and classified into flat to very gently sloping (<3%), gently to sloppy sloping (3-8%), strongly sloping (8-15%), moderately steep (15-30%), and steep to extremely steep (>30%). The reclassified slope data, along with other spatial data layers such as LULC and soil information, were integrated into the SWAT database for further analysis and modeling of the hydrological processes in the study area.

The study evaluated the impacts of LULC changes on water resources utilizing LULC maps obtained from ADSWE in Ethiopia. The LULC map covered the entire Tana Sub-basin and extended beyond its boundary. The study area boundary, obtained as a shapefile from ADSWE, was used to extract the LULC map specifically for the Tana Sub-basin area using ArcGIS 10.8.2 software. The LULC maps used in the study were for the years 1986, 2000, and 2014. They provide information on the spatial distribution and composition of different land cover types within the study area over time. The land cover classes were categorized into eight categories, namely, cultivated land, forest, shrub/bushland, water bodies, Afroalpine, grassland, and settlement/built-up area. These land cover classes were identified and delineated in the LULC maps, allowing for the assessment of their distribution and changes over time. The study computed areal estimates and percentages of each LULC class within the Tana Sub-basin area. These computations were used to quantify the extent and proportion of different land cover types within the study area for the years 1986, 2000, and 2014. The results of the LULC assessment, including the LULC maps, areal estimates, and percentage of each land cover class, are presented in Figure 30 and Table 16. These findings provide insights into the dynamics of LULC changes in the Tana Sub-basin and their potential impact on water resources.

Measured weather data for the period from 1987 to 2013 were used, with the full dataset including daily time series data for various weather variables, including rainfall, maximum and minimum temperature, relative humidity, sunshine hours, and wind speed. The measured weather data was obtained from NMA for six weather stations within the study area. In addition, data from the CFSR was utilized for 42 rainfall grid points. The CFSR data was bias corrected using ground observations to improve its accuracy and reliability. Several methods were used to estimate missing observations at the weather stations, namely, the arithmetic mean, normal ratio, and linear regression. These methods were previously tested and applied in the study area by Mesfin *et al.* (2021). The corrected CFSR data, along with nearby observed data, were evaluated using performance evaluation criteria. These criteria included the NSE, $R^2$, and PBIAS.

The NSE assesses how well the simulated data matches the observed data, with values ranging from negative infinity to 1. A higher NSE value indicates that the model provides a more reliable

simulation compared to the mean (Nash *et al.* 1970). The PBIAS value represents the average tendency of the simulated data to overestimate or underestimate the observed data. Positive values indicate overestimation, while negative values indicate underestimation. An optimal PBIAS value is 0.0, with low-magnitude values indicating accurate model simulations (Gupta *et al.* 1999). The $R^2$ value indicates the goodness of fit between the observed and corrected data, quantifying the proportion of the observed data that can be explained by the corrected data (Van Liew *et al.* 2003). These performance evaluation criteria were used to assess the accuracy and reliability of the corrected CFSR data in comparison to the observed data, ensuring the quality of the climate data used in the study.

Three weather stations were selected to represent the climate variability of the study area, namely, Bahir Dar, Dangila, and Gonder. Data for various meteorological variables, including daily maximum and minimum air temperature, solar radiation, wind speed, and one-hour rainfall were available for these representative stations. Statistical parameters were computed to analyze and simulate climatic patterns using the weather generator maker (WGNmaker) and precipitation (PCP stat) tools. These statistical parameters were then utilized by the weather generator component of the SWAT model. Daily dew point was calculated using Equation 23. For verification purposes, Dew02.exe was used to calculate the daily dew point. This software requires input of the minimum and maximum daily temperatures and the average daily humidity to compute the dew point temperature. WGEN users were developed based on the available data for the three selected weather stations. These incorporated daily rainfall, daily maximum and minimum temperatures, one-hour rainfall, daily solar radiation, daily wind speed, and daily dew point temperature. These inputs were used to generate synthetic weather data that mimic the statistical characteristics and variability of the observed meteorological variables.

The saturation vapor pressure (es) was computed using daily minimum and maximum air temperature values, and average actual saturation pressure (ea) was then computed using saturation vapor pressure (es) and average humidity data. The value of es and ea was computed according to Allen *et al.* (1998) studies as indicated in Equation 21 and Equation 22 below:

Equation 21

$$es = 0.6108 * \exp(\frac{17.27 * T}{T + 237.3})$$

Equation 22

$$ea = RF * \frac{es}{100}$$

The daily dew point temperature was calculated by the following equation:

Equation 23

$$dew = \frac{234.18 * log10(ea) - 184.2}{8.204 - log10(ea)}$$

where es is saturation vapor pressure (hPa), ea actual vapor pressure (hPa), RF relative humidity (%), T air temperature ($^{o}$C) and Dew is dew point temperature.

Flow data collected from the Abbay Basin Development Office was utilized for various purposes, including calibration, flow data generation for missing values, and estimations for ungauged stations. The available flow data from 1987 to 2013 were used for specific gauge stations, including Gilgel Abbay near Merawi, Megech near Azezo, Rib near Addis Zemen, and Gumara near Bahir Dar. The flow data played a crucial role in the modeling process. It was used for model simulation, sensitivity analysis, calibration, and validation.

Three different model setups were developed based on the LULC maps for the years 1986, 2000, and 2014 to evaluate the impact of LULC changes on the hydrological processes within the study area. The data sets used for the simulation were the same in all three, except for the LULC data, which varied with the respective years. The SWAT database files were adapted to represent conditions in the study area. The model was implemented in 69 watersheds or sub-basins within the study area, as depicted in Annexure 42. The simulation covered 27 years, from 1987 to 2013. The first three years (1987-1989) were considered as model warm-up periods, allowing the model to establish initial conditions and stabilize its performance. The subsequent 16 years (1990-2005) were used for calibration, where the model parameters were adjusted to minimize the differences between the simulated and observed discharge series. The last eight years (2006-2013) were allocated for model validation. During this period, the model's performance was evaluated by

comparing the simulated discharge with observed discharge data. The four major rivers in the Tana Sub-basin, namely, Gilgel Abbay, Megech, Rib, and Gumara, were selected to observe and validate the discharge. The model simulations and calibration/validation procedures were conducted at a monthly time scale, capturing the temporal dynamics of the hydrological processes, and ensuring consistency with the available observed discharge data.

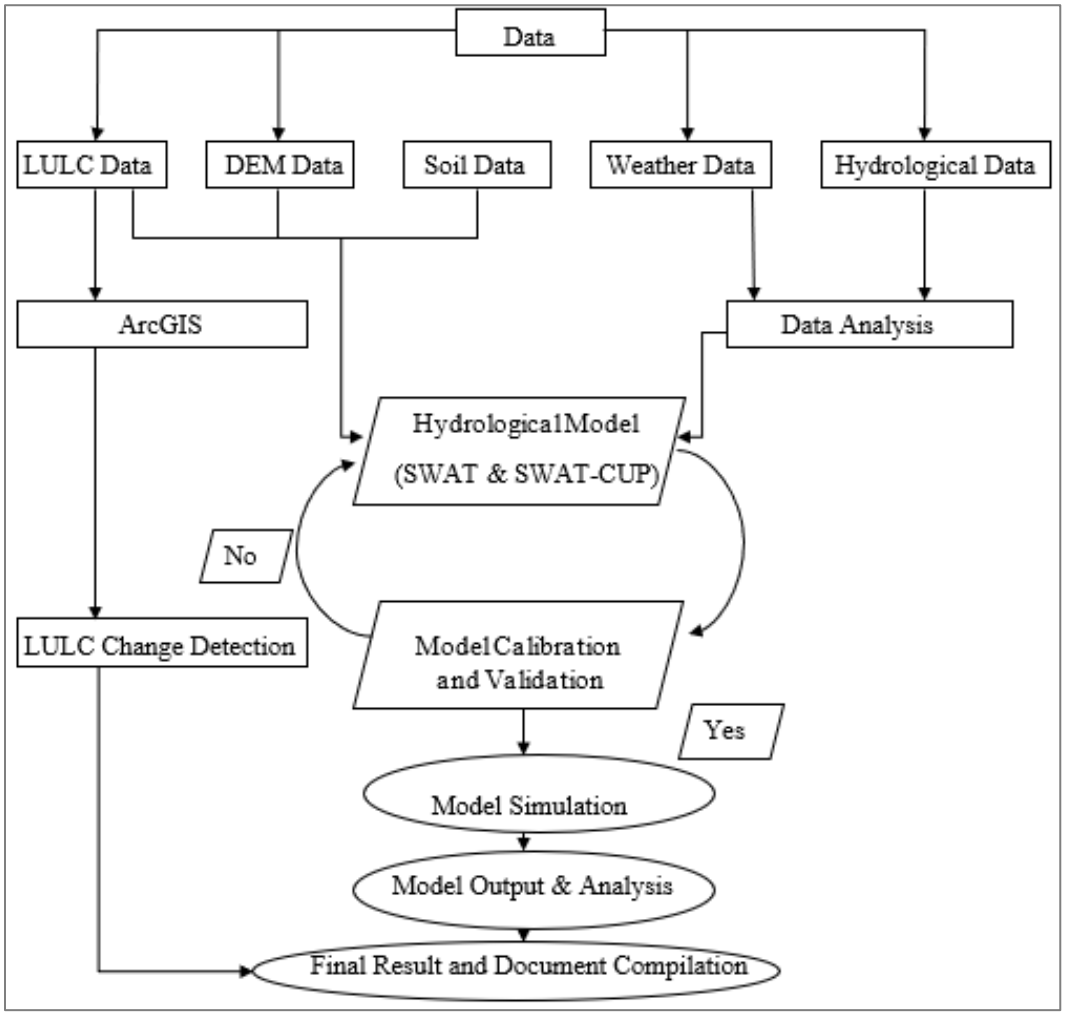


Figure 8: Schematic representation of SWAT modeling

The evaluation of the model's performance for water balance components in the study employed several statistical parameters, including NSE, $R^2$, PBIAS, and the ratio of the root mean square error to the standard deviation of measured data (RSR). The use of these statistical parameters is

recommended by Krause *et al.* (2005) and Moriasi *et al.* (2007) and they are widely utilized in hydrological model evaluation (Arnold *et al.* 1999; Gassman *et al.* 2007). Specific threshold values were considered to assess the model's performance. Satisfactory model performance was defined if the NSE exceeded 0.5 (Nash *et al.* 1970), PBIAS was less than 25% (Gupta *et al.* 1999), and RSR was equal to or less than 0.7 (Moriasi *et al.* 2007) for monthly time step variables or flow. In addition, $R^2$ values greater than 0.5 were deemed acceptable based on criteria reported by Santhi *et al.* (2001) and Van Liew *et al.* (2003). Setegn *et al.* (2009) suggested that a model's performance could be considered satisfactory if $R^2$ was greater than 0.6 and NSE was greater than 0.5. The evaluation of the goodness of fit between the simulated and measured data was conducted using five statistical parameters, and their calculations were performed based on the equations presented on page 22 and 23 of this thesis. The detailed schematic SWAT model is shown in Figure 8.

### 4.11 Method for objective 4

*To develop sustainable and efficient adaptive options for integrated water resources management of Tana Sub-basin*

Data collection formats were developed to facilitate the systematic collection of data and information. On-site data collection was carried out in each *woreda* (administrative divisions) within the Sub-basin, where different institutions were present. To enhance the knowledge base and understanding of the study area, various scientific research articles, findings, and reports were reviewed. The aim of the literature review was to gather valuable insights, build on previous knowledge, and identify gaps that the study could address. Discussions and interviews were also conducted as part of the data collection process and strategic development.

The data and information obtained were analyzed using Microsoft Excel 365, which facilitated data manipulation, calculations, and statistical analysis. The spatial distribution of water demand among various water users was mapped using ArcGIS 10.8.2. A water consumption rate of 0.9 liters per hectare per second adopted from the study by Taye *et al.* (2021) in the same area was assumed to calculate irrigation consumption. This assumption was made due to the absence of well-organized water consumption data and information in the study area. The data collected were

based on political administrative boundaries. The area ratio method was employed to incorporate these into the catchments or watersheds of the Sub-basin. This involved calculating the percentage area of a given *woreda* in relation to the overall watershed using GIS tools.

For domestic water demand (water consumption), the study adopted the second Growth and Transformation Plan (GTP-2) of Ethiopia's water supply service level standard. This standard specifies minimum daily water supply requirements for rural and urban areas. For rural areas, a minimum of 25 liters per capita per day was required, while for urban areas, the requirements varied based on population, ranging from 80 liters per capita per day to 40 liters per capita per day, as outlined in Adank *et al.* (2016). In urban areas, 80 lit/cap/day of water was required for a population within the range of 100,000 to 1 million, 60 lit/cap/day in the range of 50,000 and 100,000, 50 lit/cap/day for a population in the range of 20,000 and 50,000, and 40 lit/cap/day for population less than 20,000. Current livestock water demand was computed based on the water consumption rate per head for different types of animals. The rates used were 10 liters per head per day for cattle, 1.8 liters per head per day for sheep and goats, 5.8 liters per head per day for equines, and 0.1 liters per head per day for poultry (Taye *et al.* 2021).

Water demand computations were conducted at the watershed level within the study area and then aggregated to provide an overview of water demand at the Sub-basin level. Lastly, an annual comparison of water demand with available supply was made to assess the balance between demand and supply. In conducting these analyses and calculations, the study aimed to gain insights into the spatial distribution of water demand, assess current water demand in different sectors, and evaluate the balance between water demand and available supply in the Sub-basin.

Tana Sub-basin currently has few major dams to significantly modify its flow regime. Population growth, climate change and economic activities will create pressure on its natural resources. Scenario-based planning, development, and water resources management are thus critical in the study area. Projects are currently under investigation in the study area, with some in the process of being implemented. Three scenarios for the development of adaptive strategy options for

sustainable water resource management in the Tana Sub-basin were developed based on the study's results and the implementation level of individual projects as short, medium, and long-term development. The number of scenarios and development sequences could vary as determined by future planners and decision makers. It is important to note that these scenarios are among several possibilities and are based on information obtained from national and regional plans, assumptions, and projections. The scenarios considered are:

SC-0: Baseline scenario (2020): This represents the existing situation in the Sub-basin in 2020 taking into account current demand among various sectors, including irrigation, horticulture, Tana Beles hydropower, urban and rural domestic, and livestock demand. It also incorporates the minimum flow required for the environment to maintain a healthy ecosystem.

SC-1: Scenario one (2021-2025): This scenario includes several changes and developments in the Sub-basin. These include a 12% increase in domestic water demand, completion of the Megech Dam covering 7,311 hectares of irrigation, implementation of the Megech Serba pump irrigation project for 4,500 hectares, the commencement of irrigation for 18,700 hectares and water supply for Debre Tabor town from the Rib Dam, Gondar town water supply from the Megech reservoir, a 50% increase in irrigation efficiency, 50% increase in industrial water demand, and a population growth rate of 3.3% for urban areas and 3.8% for rural areas.

SC-2: Scenario two (2026-2030): This scenario also includes several changes and developments in the Sub-basin. These include construction of the Gilgel Abbay Dam and irrigation project for 14,552 hectares, utilization of Lake Tana pumping for a total of 44,650 hectares of irrigation, consideration of upcoming climate changes, an increase in irrigation water use efficiency to 55%, a 50% increase in industrial water demand, and population growth of 3.3% for urban areas and 3.8% for rural areas.

SC-3: Scenario three (2031-2035): This scenario considers several changes and developments in the Sub-basin. These include construction of the Jema dam for 7,786 hectares' irrigation,

construction of the Gumara dam for 14,000 hectares' irrigation, an increase in irrigation water use efficiency to 60%, a 50% increase in industrial water demand, a population growth rate of 3.3% for urban areas and 3.8% for rural areas, and implementation of micro-scale hydropower projects with a total capacity of 10.6 MW, including Jema (2 MW), Gilgel Abbay (5 MW), Megech (2.2 MW), and Gumara (1.4 MW).

An optimization model using Excel in the demand-supply analysis of the Sub-basin is a valuable approach. By maximizing the total benefit gained from each sector and efficiently allocating the available water resources, the model can inform decision-making and optimize water allocation. In this case, the model considers the satisfaction of domestic and environmental water demands as priorities. After meeting these demands, the remaining water is considered as allocable water, which can be allocated to different sectors based on their economic benefits. The objective function of the model, which includes the economic benefit generated by allocating each cubic meter of water to different sectors, helps to quantify the value and trade-offs associated with water allocation decisions.

Integrated approaches are crucial to address the challenges of limited water supply and ensure sustainable water resource management in the Sub-basin. The study followed a comprehensive process to formulate and develop adaptive strategic options for sustainable water resource management. Scientific research, resource documents, reports, group discussions, and the demand-supply analysis results were reviewed to achieve this objective.

# CHAPTER FIVE: RESULTS AND DISCUSSION

## 5.1 Results and discussion for objective 1

*To analyze climate variability, trends, and associated risks in the Tana Sub-basin*

### 5.1.1 Climatic variability

The study's findings indicated that the annual coefficient of variation (CV) for rainfall and temperature in the study area was less than 20% from 1981 to 2020 for rainfall and from 1981 to 2016 for temperature. This suggests that the study area experienced relatively low variability in both rainfall and temperature during these periods. However, when considering spatial variations within the study area, certain regions exhibited higher annual rainfall variability. The north, northeast, central, and eastern parts had high annual rainfall variability, indicating significant fluctuations in rainfall amounts in these regions. Similarly, the south and eastern parts of the Sub-basin showed relatively high annual minimum temperature variability, suggesting notable changes and fluctuations in the annual minimum temperature. Moreover, the north, northeast, east, and southern parts of the study area showed relatively high annual maximum temperature variability, indicating significant fluctuations in the annual maximum temperature.

The study area exhibited higher temporal variation in monthly rainfall than in monthly temperature. High rainfall variability (CV > 30) was observed from February to May and from October to December. This indicates significant fluctuations and variations in rainfall during these months. In addition, some parts of the area (30.99% of the Sub-basin) also experienced high rainfall variability in January. In January, moderate rainfall variability (20 < CV < 30) was observed in 61.36% of the Sub-basin. In June, 15.3% of the Sub-basin showed moderate rainfall variability, while in July, 20.23% of the Sub-basin experienced moderate rainfall variability. In September, 62.51% of the Sub-basin exhibited moderate rainfall variability. However, in August, the study area showed low rainfall variability for all regions (refer to Figure 9 and Figure 10). This result is more or less similar to that of Abera *et al.* (2020) study. This suggests that August had relatively stable and consistent rainfall patterns compared to other months.

The highest CV for rainfall was observed in March in the northeast part of the Sub-basin (Region 2). This indicates that, in March, this region experienced the most significant fluctuations and variations in rainfall compared to other months and regions within the study area (refer to Annexure *2*). The lowest CV for rainfall was recorded in August in the southeast region of the Sub-basin (Region 8). This suggests that, in August, this region had relatively stable and consistent rainfall patterns with less variability than in other months and regions. Overall, Figure 9 (a) illustrates the spatial distribution of annual rainfall, while Figure 9 (b) presents the degree of temporal variation of rainfall across each region for monthly rainfall.

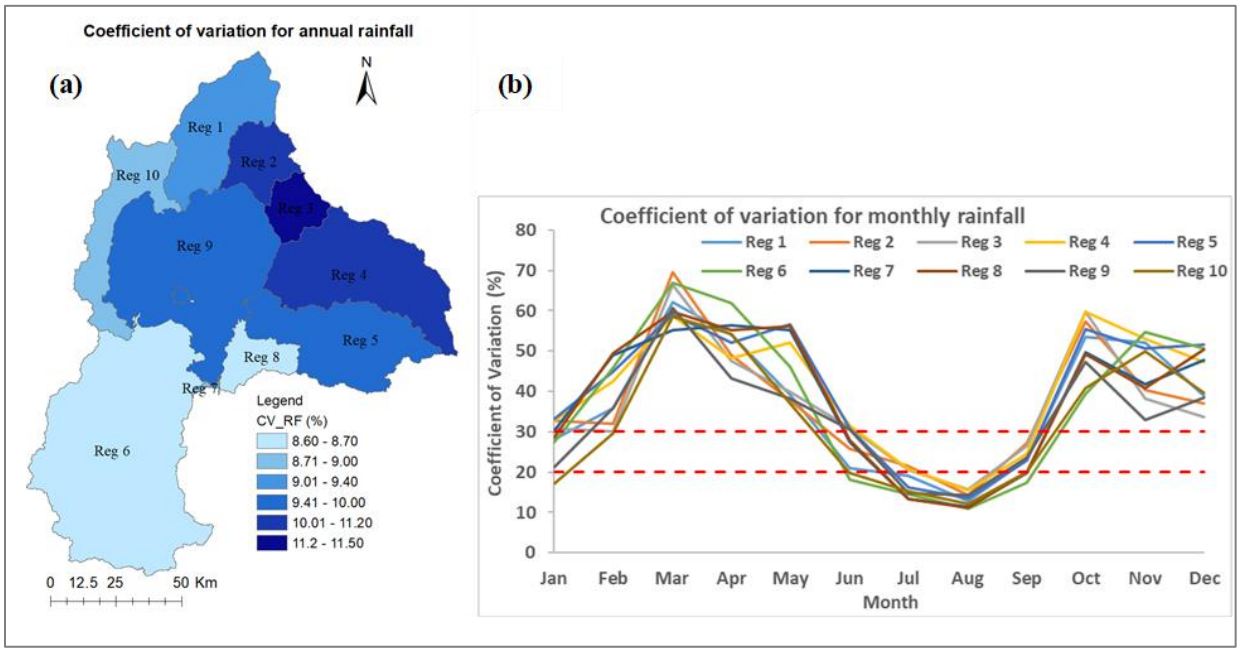


Figure 9: Coefficient of variation for (a) annual and (b) monthly rainfall across the regions

These findings highlight the spatial and temporal heterogeneity of rainfall variability within the study area. Variable rainfall patterns can have significant impacts on the rainfed dependent population, affecting crop production, livestock and overall livelihoods. Fluctuations in rainfall can disrupt agricultural activities, lead to water scarcity, and impact the availability of forage for livestock. It is thus important to implement mitigation measures and adaptation strategies to address the adverse impacts of climate change and rainfall variability. These may include the

development and promotion of nature-based solutions such as water harvesting techniques, conservation agricultural practices, crop diversification, and improved water management strategies. Furthermore, promoting climate-resilient livelihood options, providing access to climate information and early warning systems, and supporting sustainable agricultural practices can help to minimize the negative impacts of rainfall variability and enhance the rainfed-dependent population's resilience in the study area.

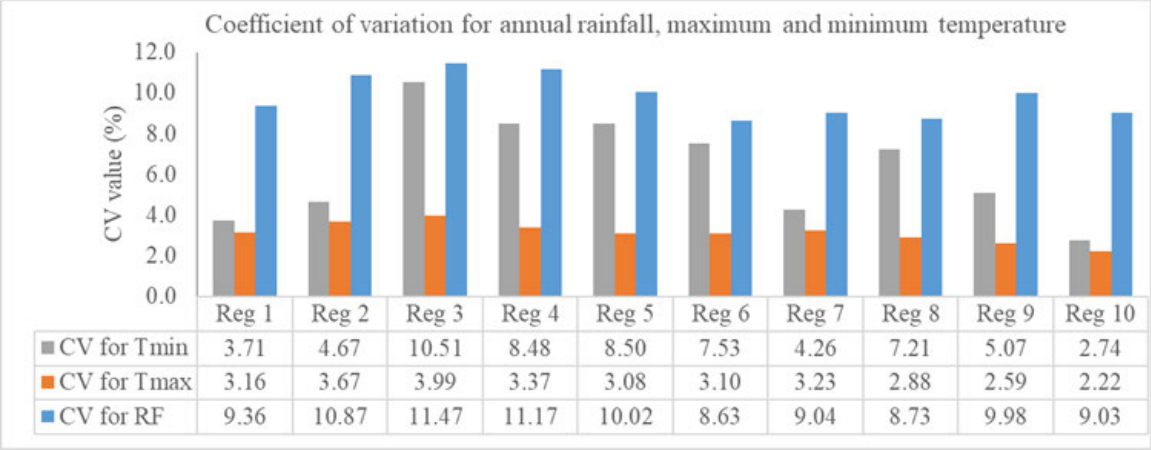


| | Reg 1 | Reg 2 | Reg 3 | Reg 4 | Reg 5 | Reg 6 | Reg 7 | Reg 8 | Reg 9 | Reg 10 |
|---|---|---|---|---|---|---|---|---|---|---|
| CV for Tmin | 3.71 | 4.67 | 10.51 | 8.48 | 8.50 | 7.53 | 4.26 | 7.21 | 5.07 | 2.74 |
| CV for Tmax | 3.16 | 3.67 | 3.99 | 3.37 | 3.08 | 3.10 | 3.23 | 2.88 | 2.59 | 2.22 |
| CV for RF | 9.36 | 10.87 | 11.47 | 11.17 | 10.02 | 8.63 | 9.04 | 8.73 | 9.98 | 9.03 |

Figure 10: Coefficient of variation across the regions in the study area

The maximum and minimum temperatures in the study area did not exhibit high variations in temporal trends compared to rainfall. Figure 10 illustrates this observation. However, variations in the minimum temperature were observed for January and December in some regions. These showed a certain degree of variability in the minimum temperature during these months, while the rest of the study area had lower variability (CV < 20) in minimum temperature. It is worth noting that areas with a CV greater than 30% are generally considered vulnerable to drought (Haile 1988; Hare 2003). In the study area, on average, approximately 58.04% of the year was classified as vulnerable to natural disasters. The highest CV for minimum temperature was found in January in the north of the study area, specifically in the Megech watershed (Region 1). The lowest CV for minimum temperature was recorded in December in the northeast region (Region 2). Figure 11 and Figure 12 present the value of the CV for annual and monthly minimum and maximum temperature across the regions of the Sub-basin, showing a CV of less than 20 in most.

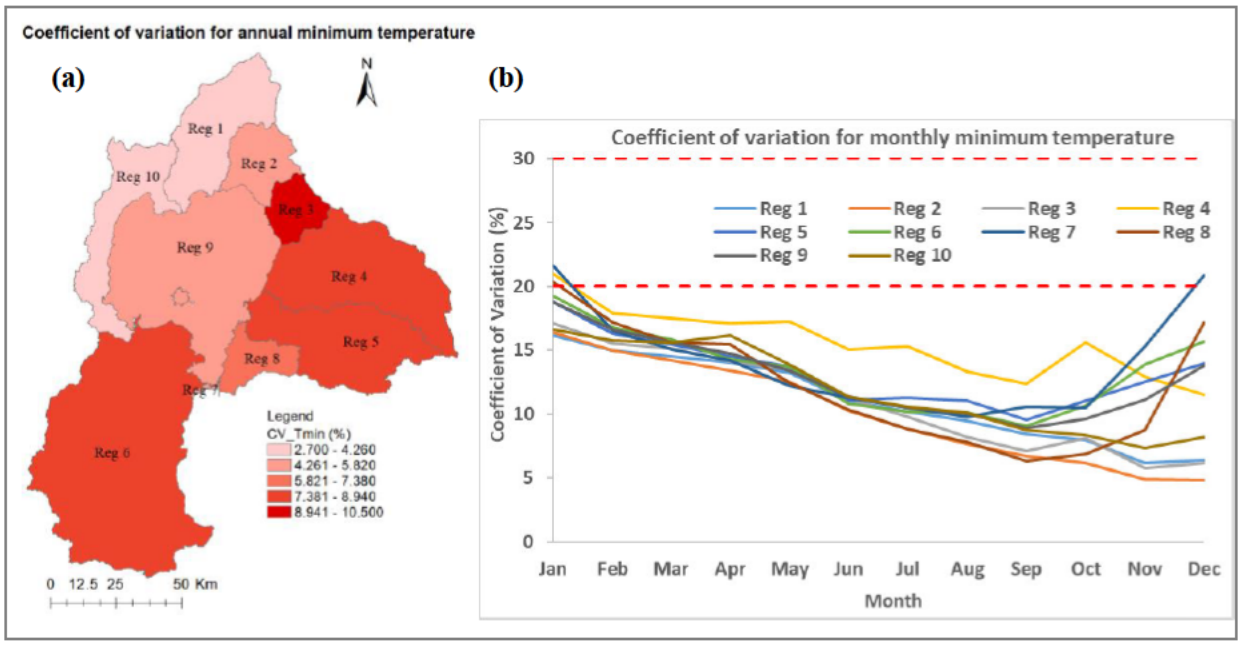


Figure 11: Coefficient of variation for (a) annual and (b) monthly minimum temperature

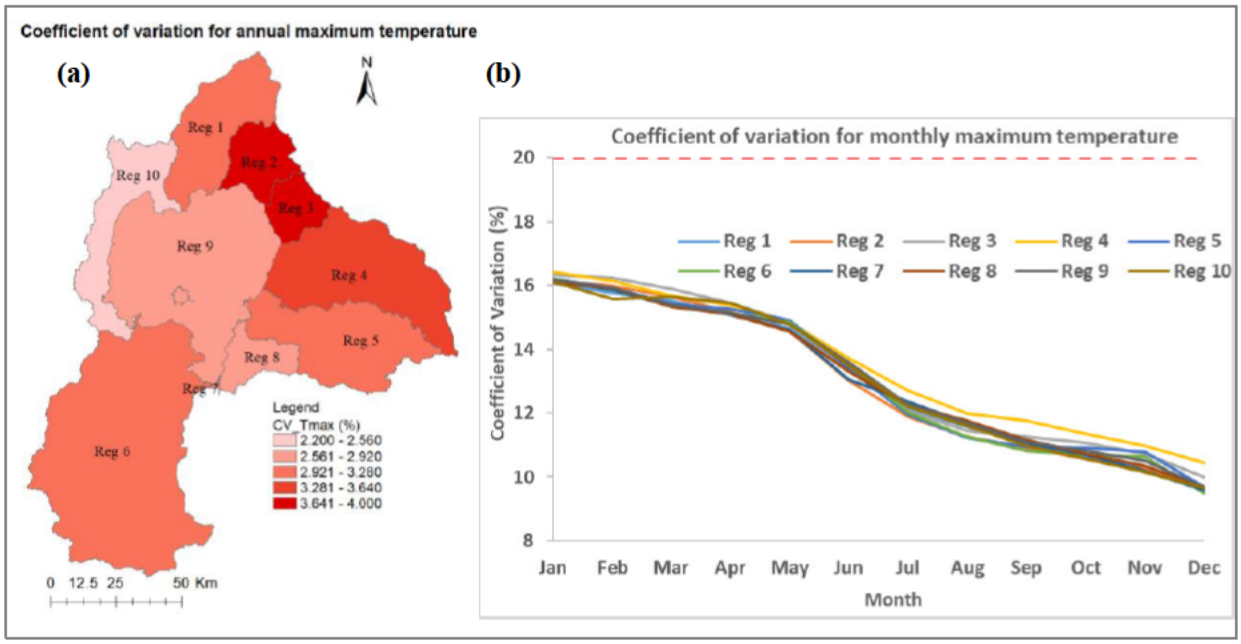


Figure 12: Coefficient of variation for (a) annual and (b) monthly maximum temperature

Regarding maximum temperature, the highest CV was found in January in the eastern part of the study area, specifically in the Rib watershed (Region 4). The lowest CV for maximum temperature was registered in December in the eastern part of the study area, particularly in the Gumara watershed (Region 5). These findings indicate that while temperature variability was generally lower than that of rainfall, there were still some variations in minimum and maximum temperatures within certain regions and months. Understanding these variations can assist in assessing the vulnerability of the study area to climate-related risks and in developing appropriate adaptation strategies to address the potential impacts of extreme temperatures and natural disasters like floods and droughts.

### 5.1.2 Trend analysis in climatic variables

The MK trend test and Sen's slope were applied at each month, annual mean, annual maximum, and annual minimum rainfall using significance level of 5% and confidence level of 95% across the regions. The results are presented in Table 6.

Table 6: Summary statistics for total annual rainfall

| Annual rainfall | | | | | | | |
|---|---|---|---|---|---|---|---|
| Regions | Obs. | Obs. with missing data | Obs. without missing data | Minimum | Maximum | Mean | Std. deviation |
| Reg 1 | 39 | 0 | 39 | 905.26 | 1243.09 | 1071.31 | 100.28 |
| Reg 2 | 39 | 0 | 39 | 797.71 | 1208.65 | 985.83 | 107.48 |
| Reg 3 | 39 | 0 | 39 | 858.25 | 1283.05 | 1060.50 | 121.75 |
| Reg 4 | 39 | 0 | 39 | 944.27 | 1434.87 | 1203.30 | 135.95 |
| Reg 5 | 39 | 0 | 39 | 1099.30 | 1701.18 | 1394.19 | 141.42 |
| Reg 6 | 39 | 0 | 39 | 1219.78 | 1770.20 | 1478.79 | 129.07 |
| Reg 7 | 39 | 0 | 39 | 1074.98 | 1588.37 | 1373.31 | 125.40 |
| Reg 8 | 39 | 0 | 39 | 1094.58 | 1596.65 | 1377.76 | 121.63 |
| Reg 9 | 39 | 0 | 39 | 949.04 | 1464.74 | 1183.08 | 118.28 |
| Reg 10 | 39 | 0 | 39 | 918.14 | 1341.79 | 1144.50 | 103.28 |

The annual rainfall in the study area was 797.71 mm to 1,770.2 mm. The results indicate significant variations in annual rainfall across the Sub-basin, with the highest annual rainfall observed in Region 6 with a value of 1,478.79 mm and the lowest in Region 2 with a value of 985.83 mm. This heterogeneous distribution of rainfall suggests that there are significant variations in rainfall patterns within the Sub-basin.

The MK trend test and Sen's slope were also applied each month, annual mean, annual maximum, and annual minimum for temperature with significance level of 5% and confidence level of 95% across the regions. The results are presented in Table 7. The annual minimum temperature in the study area ranged between 8.18 and 12.2 $^{o}$C while the maximum temperature ranged between 24.00 and 29.95 $^{o}$C. The results indicate significant variations in both annual minimum and maximum temperatures across the Sub-basin, with the highest annual maximum temperature observed in Region 4 with a value of 29.95 $^{o}$C and the lowest in Region 6 with a value of 8.17 $^{o}$C. This heterogeneous distribution of temperature further emphasizes the significant variations in temperature patterns within the Sub-basin.

Table 7: Summary statistics for minimum and maximum annual temperature

| Regions | | | | Annual minimum temperature | | | | Annual maximum temperature | | | |
|---|---|---|---|---|---|---|---|---|---|---|---|
| | Obs. | Obs. with missing data | Obs. without missing data | Minimum | Maximum | Mean | Std. deviation | Minimum | Maximum | Mean | Std. deviation |
| Reg 1 | 36 | 0 | 36 | 11.59 | 14.42 | 13.48 | 0.68 | 25.54 | 28.63 | 27.45 | 0.73 |
| Reg 2 | 36 | 0 | 36 | 11.66 | 13.44 | 12.75 | 0.47 | 24.08 | 27.12 | 25.93 | 0.82 |
| Reg 3 | 36 | 0 | 36 | 12.03 | 14.86 | 13.42 | 0.63 | 25.08 | 28.69 | 27.03 | 0.99 |
| Reg 4 | 36 | 0 | 36 | 9.65 | 15.34 | 12.79 | 1.34 | 25.75 | 29.95 | 27.94 | 1.12 |
| Reg 5 | 36 | 0 | 36 | 8.18 | 11.88 | 10.52 | 0.89 | 24.02 | 27.55 | 25.96 | 0.88 |
| Reg 6 | 36 | 0 | 36 | 8.17 | 12.04 | 10.55 | 0.90 | 24.00 | 27.20 | 25.93 | 0.80 |
| Reg 7 | 36 | 0 | 36 | 9.02 | 13.36 | 10.80 | 0.81 | 24.15 | 27.81 | 25.95 | 0.80 |
| Reg 8 | 36 | 0 | 36 | 11.11 | 13.15 | 12.08 | 0.52 | 25.24 | 28.69 | 27.41 | 0.89 |
| Reg 9 | 36 | 0 | 36 | 9.76 | 13.45 | 12.27 | 0.89 | 25.48 | 28.75 | 27.54 | 0.79 |
| Reg 10 | 36 | 0 | 36 | 12.20 | 15.62 | 14.54 | 0.80 | 25.15 | 28.22 | 27.02 | 0.70 |

Figure 13 and Figure 14 that represent the time series of annual rainfall and temperature in the Sub-basin provide valuable information about the temporal variations and spatial differences in these variables. The temporal variations observed in the time series indicate that there have been changes in the patterns of rainfall and temperature over time within the Sub-basin. These could include shifts in the timing, intensity, or duration of rainfall, as well as fluctuations in average temperatures. These temporal variations reflect the dynamic nature of the climate system and its response to various factors such as natural variability and human-induced climate change. In addition, the spatial increments depicted in the figures highlight the differences in rainfall and temperature across different regions within the Sub-basin. This suggests that certain regions may have experienced more significant changes or variations in these variables than others. These findings align with the results reported by Birara *et al.* (2020), suggesting temporal and spatial increments in rainfall and temperature within the Sub-basin.

The annual rainfall varied across different regions within the study area during the period 1981 to 2020 (refer to Annexure 1) with a significance level of 5% and confidence level of 95%. The maximum annual rainfall of 1,770.2 mm was recorded in 2017 in Region 6 while the minimum annual rainfall of 797.71 mm occurred in 1990 in Region 2. The annual rainfall exhibited variability with location. The results of the MK test for annual rainfall data revealed a statistically non-significant increasing trend at 5% level of significance. A statistically non-significant increasing trend was observed in summer, spring, autumn, and winter rainfall at 5% significance level across the regions while Regions 2 and 3 in winter and Region 6 in summer show a statistically non-significant decreasing trend.

In Region 1, the annual rainfall ranged from 905 mm in 1990 to 1,243 mm in 1998, but the trend was not statistically significant ($p > 0.05$), indicating no clear increasing or decreasing trend in annual rainfall for the region. Similarly, the areal annual rainfall for the entire study area did not show a significantly increasing trend ($p > 0.05$) across all regions (refer to Table 8 and Figure 13). In Region 2, the annual rainfall ranged from 797.71 mm to 1,209 mm, and a non-significant increasing trend with ($p > 0.05$) was observed. Other studies also did not find a statistically significant trend in the annual rainfall in other parts of Ethiopia (Viste *et al.* 2013; Mengistu *et al.*

2014). As depicted in the table below, annual rainfall in the Sub-basin showed an increasing trend in most parts of the study area. Only small sections in the southern and southeastern parts revealed no trend in annual rainfall.

Table 8: MK test results on annual time series rainfall with 5% significance

| Regions | Mann-Kendall test | | | | Sen's nonparametric estimator of slope | | |
|---|---|---|---|---|---|---|---|
| | Kendall's tau | S | P | Result | Sen's slope | Lower limit (95%) | Upper limit (95%) |
| Reg 1 | 0.247 | 183 | 0.028 | trend | 3.411 | 0.421 | 6.237 |
| Reg 2 | 0.271 | 201 | 0.016 | trend | 3.778 | 0.705 | 6.411 |
| Reg 3 | 0.260 | 193 | 0.020 | trend | 3.822 | 0.751 | 7.418 |
| Reg 4 | 0.271 | 201 | 0.016 | trend | 5.021 | 1.004 | 8.587 |
| Reg 5 | 0.301 | 223 | 0.007 | trend | 5.373 | 1.503 | 9.396 |
| Reg 6 | 0.104 | 77 | 0.358 | no trend | 1.639 | -1.868 | 5.935 |
| Reg 7 | 0.190 | 141 | 0.090 | no trend | 3.033 | -0.991 | 6.637 |
| Reg 8 | 0.220 | 163 | 0.050 | no trend | 3.468 | 0.077 | 6.943 |
| Reg 9 | 0.225 | 167 | 0.045 | trend | 3.614 | 0.049 | 6.773 |
| Reg 10 | 0.255 | 189 | 0.023 | trend | 3.534 | 0.527 | 6.563 |

The analysis of Sen's slope, which assesses the magnitude and direction of trends, indicated that rainfall in all regions of the study area showed an increasing trend, but it was not statistically significant. Non-significant increasing trends were observed for the months of May, September and December in all regions, while the remaining months showed non-significant increasing and decreasing trends in different regions. The magnitude of the rainfall increment, as indicated by Sen's slope, ranged from 1.64 to 5.37 mm/year. Most regions had an annual increment of rainfall of between 3 and 4 mm/year, except for Region 5, which had the highest annual increment of 5.37 mm/year, and Region 6, which had the lowest annual rainfall increment of 1.64 mm/year (refer to Table 8 and Figure 14). Overall, the study found a statistically non-significant increasing trend in rainfall across all regions of the Sub-basin. The increments were relatively small, with values ranging from 1.64 to 5.37 mm/year. These findings align with the results reported by Birara *et al.* (2020), suggesting a non-significant increment trend in annual rainfall across all regions of the Sub-basin.

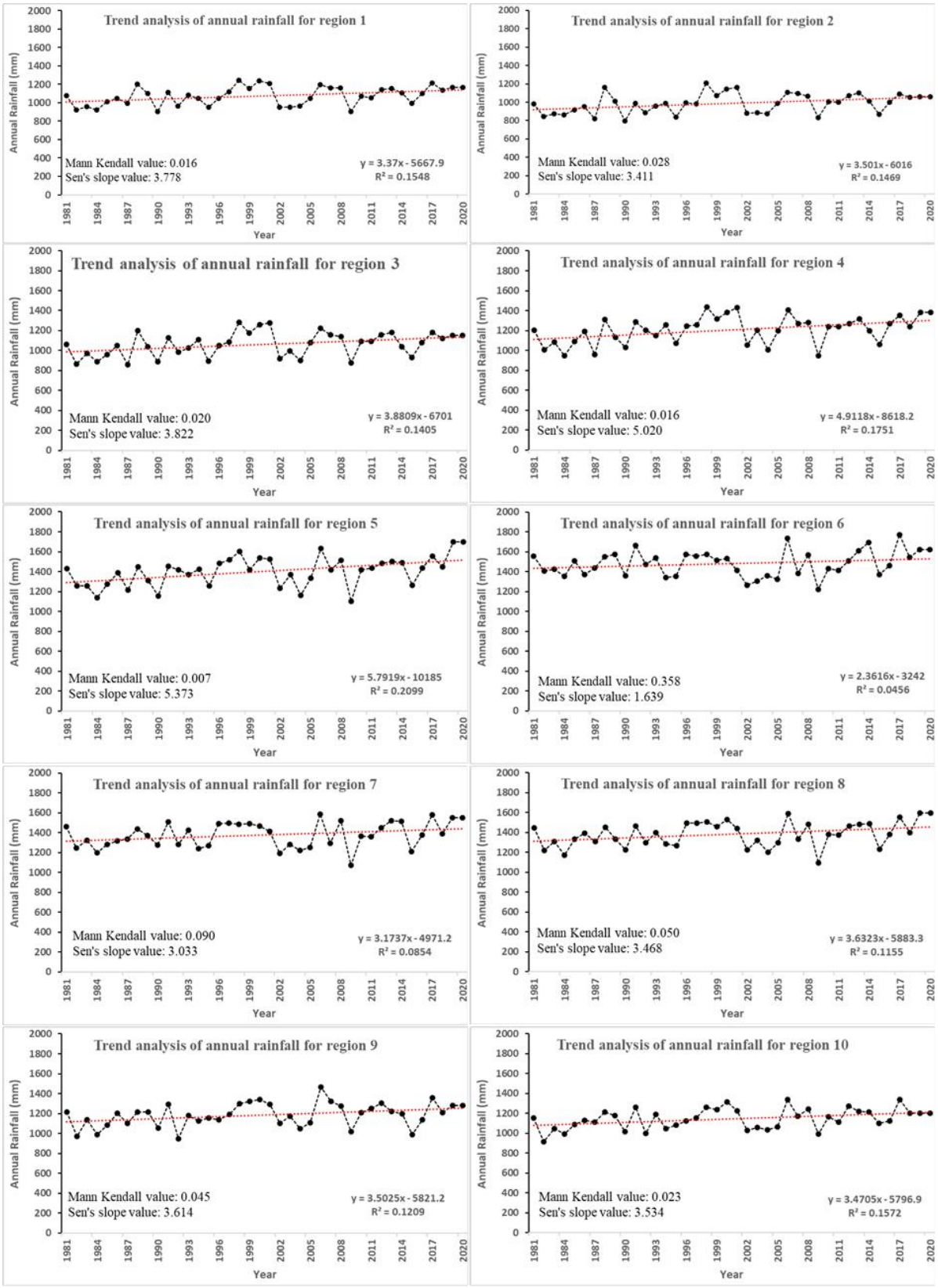


Figure 13: Annual total rainfall trend from 1981-2020

The results of the trend analysis, including the p-value from the MK test and the trend's slope (β) from Sen's estimator, are presented in Table 9 and

Table 10. Most regions showed a statistically non-significant increasing trend in annual minimum temperature except for Regions 7, 8 and 10, which showed no trend at 5% level of significance. Similarly, a statistically non-significant increasing trend was observed in summer, spring, autumn, and winter minimum temperatures at 5% significance level across the regions, with Regions 7 and 8 showing a statistically non-significant decreasing trend in winter. The magnitude of the increasing range, as indicated by Sen's slope method, ranged from 0.001 to 0.080 $^{o}$C/year. According to the Sen's slope annual minimum temperature increment, Region 4 had the highest annual increment of 0.080 $^{o}$C/year, and Region 8 had the lowest annual minimum temperature increment of 0.001 $^{o}$C/year. Overall, the study found a statistically non-significant increasing trend in annual minimum temperature in most regions of the Sub-basin.

Table 9: MK test results on annual time series minimum temperature with 5% significance

| Regions | Mann-Kendall test | | | | Sen's nonparametric estimator of slope | | |
|---|---|---|---|---|---|---|---|
| | Kendall's tau | S | P | Result | Sen's slope | Lower limit (95%) | Upper limit (95%) |
| Reg 1 | 0.371 | 234 | 0.0015 | trend | 0.034 | 0.015 | 0.050 |
| Reg 2 | 0.429 | 270 | 0.0002 | trend | 0.028 | 0.016 | 0.038 |
| Reg 3 | 0.667 | 420 | <0.0001 | trend | 0.049 | 0.039 | 0.059 |
| Reg 4 | 0.556 | 350 | <0.0001 | trend | 0.080 | 0.057 | 0.108 |
| Reg 5 | 0.486 | 306 | <0.0001 | trend | 0.051 | 0.035 | 0.070 |
| Reg 6 | 0.530 | 334 | <0.0001 | trend | 0.054 | 0.039 | 0.070 |
| Reg 7 | 0.219 | 138 | 0.0620 | no trend | 0.018 | -0.001 | 0.038 |
| Reg 8 | 0.019 | 12 | 0.8809 | no trend | 0.001 | -0.016 | 0.020 |
| Reg 9 | 0.530 | 334 | <0.0001 | trend | 0.055 | 0.037 | 0.073 |
| Reg 10 | 0.222 | 140 | 0.0583 | no trend | 0.027 | -0.002 | 0.051 |

The analysis presented in Table 10 indicates that the study area experienced a statistically non-significant increasing trend in annual maximum temperature across the regions at a 5% level of

significance. Similarly, a statistically non-significant increasing trend was observed in summer, spring, autumn, and winter maximum temperatures at 5% significance level in all regions. The magnitude of the increment in maximum temperatures, as indicated by Sen's slope, ranged from 0.043 to 0.096 $^{o}$C/year. According to Sen's slope value, Region 7 exhibited the highest increment and Region 4 (located in the eastern part of the study area) showed the lowest increment in annual maximum temperature. Overall, the study found an increasing trend in annual maximum temperature across the regions of the Sub-basin based on the MK test results and Sen's slope analysis with a 5% significance level.

Table 10: MK test results on annual time series maximum temperature with 5% significance

| Regions | Mann-Kendall test | | | | Sen's nonparametric estimator of slope | | |
|---|---|---|---|---|---|---|---|
| | Kendall's tau | S | P | Result | Sen's slope | Lower limit (95%) | Upper limit (95%) |
| Reg 1 | 0.625 | 394 | <0.0001 | trend | 0.055 | 0.041 | 0.071 |
| Reg 2 | 0.689 | 434 | <0.0001 | trend | 0.064 | 0.050 | 0.078 |
| Reg 3 | 0.635 | 400 | <0.0001 | trend | 0.078 | 0.054 | 0.100 |
| Reg 4 | 0.717 | 452 | <0.0001 | trend | 0.096 | 0.078 | 0.114 |
| Reg 5 | 0.584 | 368 | <0.0001 | trend | 0.067 | 0.047 | 0.087 |
| Reg 6 | 0.505 | 318 | <0.0001 | trend | 0.053 | 0.030 | 0.074 |
| Reg 7 | 0.378 | 238 | 0.0012 | trend | 0.043 | 0.020 | 0.064 |
| Reg 8 | 0.683 | 430 | <0.0001 | trend | 0.069 | 0.055 | 0.088 |
| Reg 9 | 0.562 | 354 | <0.0001 | trend | 0.054 | 0.034 | 0.071 |
| Reg 10 | 0.495 | 312 | <0.0001 | trend | 0.048 | 0.028 | 0.067 |

Figure 14 illustrates the long-term trend in the minimum and maximum monthly temperatures observed in the Sub-basin during the period 1981 to 2016. A monthly minimum temperature of 4.2 $^{o}$C was recorded in December with a monthly maximum temperature of 34.5 $^{o}$C observed in March. These values are similar to those reported by Abera *et al.* (2020) for maximum temperature, but the minimum temperature recorded in February differs. The monthly average minimum temperature (Tmin) ranged from 7.66 to 11.61 $^{o}$C, while the monthly average maximum temperature (Tmax) was in the range of 28.01 to 30.56 $^{o}$C. These values indicate the variability in temperature throughout the year within the Sub-basin.

According to the long-term average monthly temperature values, the Gumara watershed had lower values while the Rib watershed had higher values. An increasing trend was observed in both Tmin and Tmax across all regions during the period 1981 to 2016 (refer to Annexure *3* and Annexure 4). However, as indicated in these annexes, the trend was non-significant. This suggests that while there was an increase in temperature, it was not statistically significant.

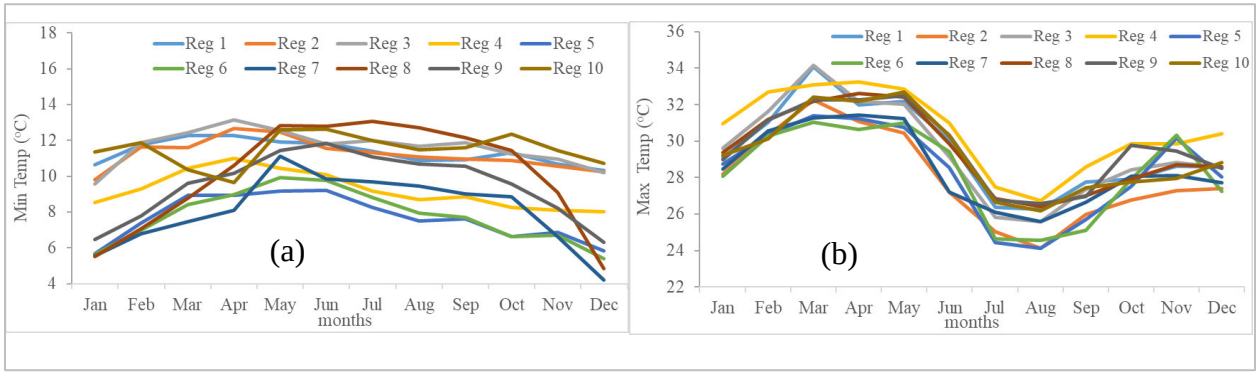


Figure 14: Mean monthly (a) minimum temperature and (b) maximum temperature

Birara *et al.* (2020) study supports the numerical increment in temperature, but with a significant trend. The rise in temperature can be attributed to factors for instance deforestation, over-cultivation, climate change, and excessive pressure on natural resources (Anteneh 2022). Increased temperatures can have several impacts on the study area. They can lead to increased evapotranspiration, and changes in precipitation patterns and amounts, and potentially impact water resources. In addition, they can influence the intensity of extreme weather events. This highlights the need to understand and manage the impacts of rising temperatures and climate change in the Sub-basin.

Temperature and rainfall variations in the Sub-basin could impact agricultural activities, cropping patterns, livelihoods, and natural resources. The high population pressure and dependence on agriculture in the study area renders rural livelihoods particularly vulnerable to these changes. The direct effects of temperature and rainfall variations can disrupt agricultural activities by affecting crop growth, water availability, and pest dynamics. Changes in cropping patterns may be required

to adapt to shifting climate conditions. This could challenge farmers who rely on specific crops or traditional farming practices.

The impact on livelihoods could be severe, particularly for rural households that depend heavily on agriculture for their income and sustenance. These households are more directly exposed to the risks associated with climate variability such as droughts, floods, and natural resource losses. The consequences could include reduced agricultural productivity, the loss of livestock, food insecurity, and increased vulnerability to poverty. It is crucial to develop and implement appropriate adaptation strategies to address these challenges. These should focus on building resilience in agriculture, promoting sustainable resource management, and diversifying livelihood options. By considering the potential impacts and implementing appropriate adaptation measures, it is possible to reduce the vulnerability of rural households and enhance their resilience to climate variability in the Sub-basin.

### 5.1.3 Rainfall seasonality

Figure 16 illustrates that the value of the seasonality index ranged between 0.87 and 1.03 for Region 6 and Region 3, respectively, in the Tana Sub-basin. The SI value increases from the southwest, southeast, south, and north to the east of the Sub-basin, indicating a gradient in the seasonality of rainfall.

The amount of rainfall received, and its seasonal distribution have significant implications for agricultural activities, natural vegetation, and regional moisture. As noted by Mesfin *et al.* (2021), the seasonal characteristics of rainfall play a crucial role in shaping these aspects. For the purposes of the study, the seasonality index was categorized into two groups. Region 1 represents areas with 80-99% of rainfall occurring in marked seasonal patterns with a long dry season. This category accounts for 36.69% of the total area. Region 2 includes areas with a seasonality index of 100-119%, indicating that most of the rain is concentrated in three or fewer months. This category covers 63.31% of the total area, as depicted in Figure 15.

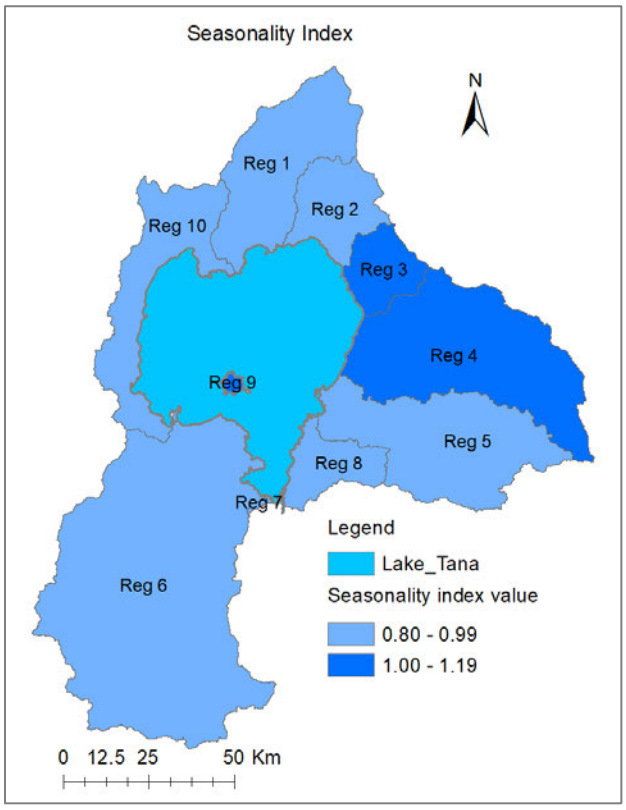


Figure 15: Seasonality index value across the regions

The findings reveal that while most regions in the Sub-basin receive ample amounts of rainfall, it is concentrated in three or fewer months each year, leading to significant variability and trends. This underscores the importance of adjusting agricultural practices in the area to account for the variability and trends in rainfall. This could include strategies such as adopting drought-tolerant crop varieties, implementing efficient irrigation techniques, and employing water harvesting and storage systems. These measures enable farmers to better manage water resources and optimize crop production in the face of variable and changing rainfall patterns. By considering the seasonality of rainfall and implementing appropriate agricultural adjustments, the Sub-basin can enhance its resilience to climate variability and optimize its agricultural productivity.

In terms of the rainfall variability and seasonality results in different regions, it is interesting to note that the highest CV in rainfall and the highest value of seasonality index are observed in

Regions 3 and 4 in the eastern part of the study area. In addition, the results show that the rainfall seasonality derived from the mean PCI and the seasonality index exhibit similar and direct graphical patterns in the study area. The regions with higher values of the seasonality index are likely to experience rain for many months. Region 3 has the highest rainfall variability and seasonality index, followed by Region 4, while Region 6 in the southern part of the study area has the lowest rainfall variability and seasonality index. The results of the correlation between CV and SI across the regions are presented in Figure 19.

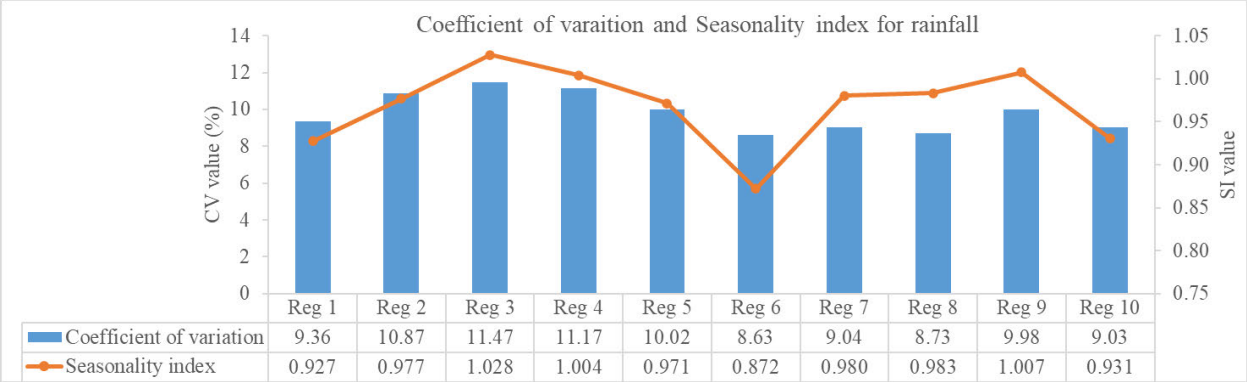


Figure 16: Correlation of seasonality index with coefficient of variation for rainfall

Figure 17 presents the distribution of the mean PCI of annual rainfall of the Tana Sub-basin across the regions from 1981 to 2020. As shown in the figure, there was no uniform distribution of rainfall (PCI<10) during this period. The value of the PCI varied from 13.67 to 27.58. The minimum values of PCI were observed in Region 9 at the center of the study area whereas the maximum values of PCI were observed in Region 3, predominantly in the northeastern part of the study area.

The analysis presented in Figure 17 indicates that the study area did not experience uniform distribution of precipitation (PCI<10) during the period from 1981 to 2020. Instead, about 57.5% of the rainfall data exhibited a strong irregular precipitation distribution (PCI>20), which is consistent with the findings reported by Dawit *et al.* (2019). In addition, approximately 41.5% of the PCI values represented irregular precipitation concentration, while only about 1% indicated

moderate precipitation concentration. The marked irregularity of annual, seasonal, and monthly precipitation distribution observed in the study area implies significant variability in rainfall patterns that could have implications for hydrological risks, including floods and droughts. For example, in certain years such as 1983, 1988, 1990, 2001, 2009, and 2010, flood occurrences were observed in the northeast parts of the Sub-basin. These may have been influenced by backflow from Lake Tana during the rainy season.

The irregularity in rainfall distribution, including the amount, intensity, and onset and offset days, directly impacts agricultural activities, crop patterns, and livelihoods. The spatial distribution of PCI values further demonstrates the irregularity in rainfall across the study area. It is worth noting that the year 1984 showed the lowest variation in PCI values, indicating marked irregular occurrence of rainfall. On the other hand, the years 1985-1986, 1996-1997, 2014-2015, and 2019 exhibited small variation/range differences in PCI values across all regions of the Sub-basin. This irregularity in rainfall distribution highlights the need for adaptive measures in agriculture and water resource management to cope with the associated risks.

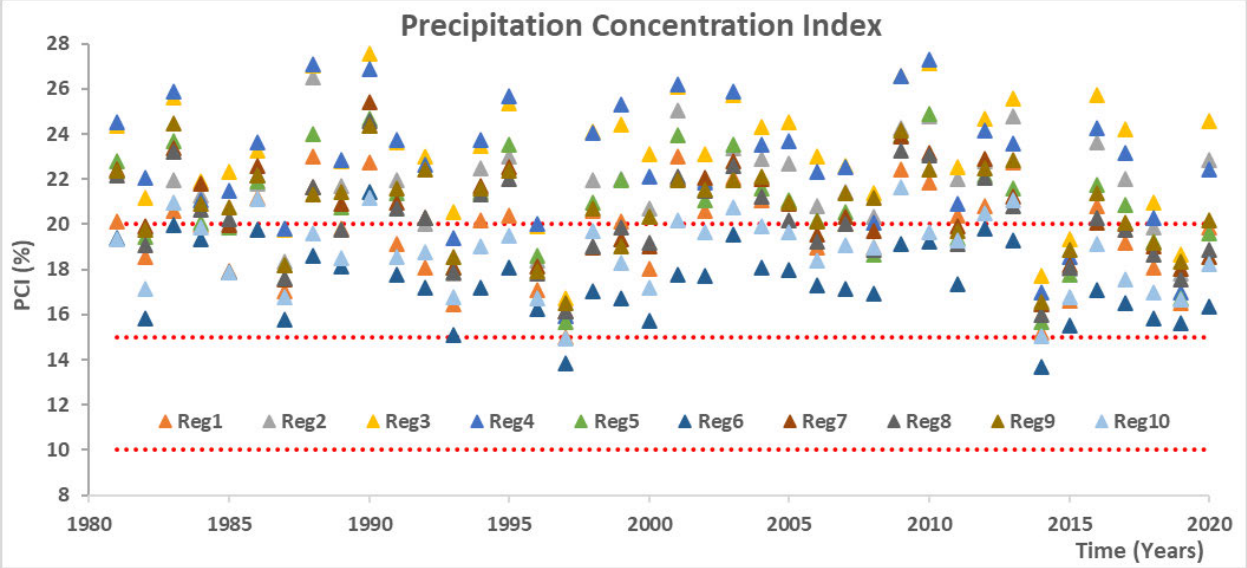


Figure 17: Precipitation concentration index (PCI) across the regions in the study area

### 5.1.4 Climate projection

#### 5.1.4.1 Precipitation projection

Using the CanRCM4 model and the RCP4.5 and RCP8.5 emission scenarios, the precipitation change forecasts at the Dangila, Bahir Dar, Gonder, and Debre Tabor stations were compared to the baseline period (1991-2020) (refer to Annexure 6, Annexure 10, Annexure 14 and Annexure 18). As shown in Figure 18 and Figure 19, and Table 11, these projections did not show a consistent decreasing or increasing trend in all future time periods and scenarios for all stations. However, on average, the model predicted the probability of a decreasing trend in mean annual precipitation between 2081 and 2100 and between 2021-2050 as compared to the baseline period in all scenarios.

For example, under the RCP4.5 scenario mean annual precipitation is projected to decrease by 30.88%, 29.96%, 33.06%, and 33.57% by the 2100s for Dangila, Bahir Dar, Gonder, and Debre Tabor, respectively. Similarly, under the RCP8.5 scenario it is predicted to decrease by 33.25%, 34.57%, 28.88%, and 32.3% by the 2100s for Dangila, Bahir Dar, Gonder, and Debre Tabor, respectively. Based on the analysis, the highest percentage change in mean annual precipitation projection was observed at Debre Tabor and Bahir Dar stations for the RCP4.5 and RCP8.5 scenarios, respectively, indicating a greater decrease in precipitation compared to the other stations. The lowest percentage change was recorded in Bahir Dar and Gonder, suggesting a relatively smaller decrease in precipitation.

Furthermore, when comparing the two emission scenarios, it was observed that the decrement in mean annual precipitation increased for stations Bahir Dar and Dangila when moving from RCP4.5 to RCP8.5 scenarios. This implies that under the RCP8.5 scenario there is a higher expected decrease in precipitation for these stations. For the stations Debre Tabor and Gonder, reverse trend was observed. The decrement in mean annual precipitation for these stations was lower under the RCP8.5 scenario than in the RCP4.5 scenario. This suggests that the projected decrease in precipitation is relatively smaller for these stations under the RCP8.5 scenario. These findings imply a high probability of decreased precipitation in the future for all stations which could have

significant impacts on the region's water resources and agricultural productivity. They also highlight the importance of considering different emission scenarios when assessing future precipitation changes and their potential impacts on different regions. It is crucial to account for these variations in order to develop appropriate adaptation and mitigation strategies to address the potential challenges posed by changing precipitation patterns.

According to the analysis, on a monthly scale, the mean monthly precipitation projection showed an increasing trend during most of the dry season (December to April) in all scenarios and at all stations (refer to Annexure 5, Annexure 9, Annexure 13 and Annexure 17). This suggests that there is a likelihood of higher precipitation during the dry season in the future. In contrast, a decreasing trend was observed for the wet season (July to September) in all scenarios and at all stations, indicating a potential reduction in precipitation during the wet season in the future. With regard to the percentage change, the month of February showed the highest percentage change compared to other months of the year in all scenarios and at all stations. This implies a greater projected increase in precipitation during February compared to other months. Conversely, the month of April consistently showed the lowest percentage change in mean monthly precipitation at all stations and in all scenarios. This suggests that there is a relatively smaller projected change in precipitation for April compared to other months.

During the wet season, the month of September showed the highest percentage decrement in mean monthly precipitation under the RCP4.5 scenario. This implies the presence of a significant projected decrease in precipitation during September. Likewise, under the RCP8.5 scenario the highest percentage change in mean monthly precipitation was observed in September for Bahir Dar and Debre Tabor stations, whereas the highest was noted in October for Dangila and Gonder stations. This suggests that there is a greater projected increase in precipitation during these months under the RCP8.5 scenario. These findings also provide insights into potential seasonal variations in precipitation changes that could be valuable for understanding the future hydrological patterns and planning for water resource management and agricultural activities in the region.

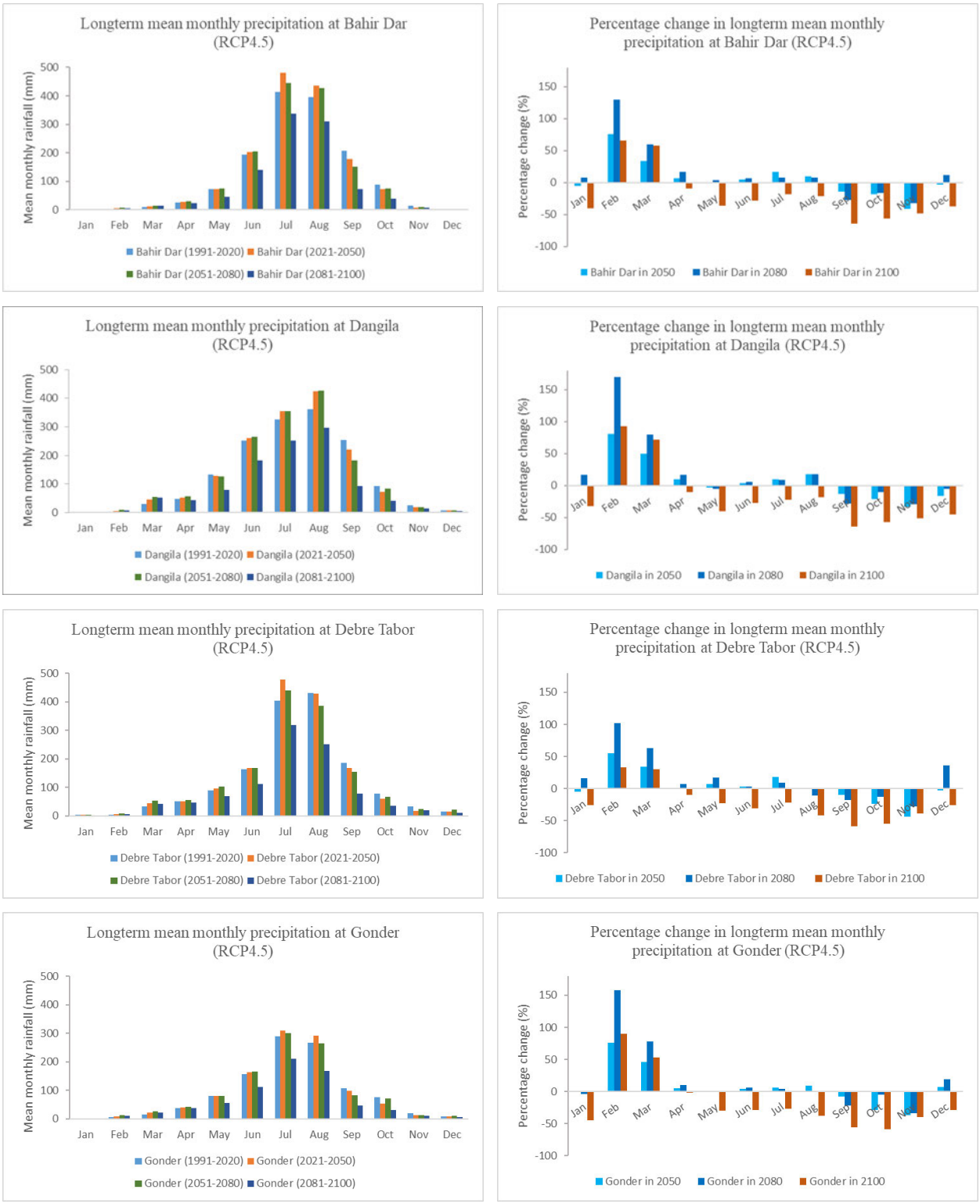


Figure 18: Long-term mean monthly precipitation and percentage changes using RCP4.5

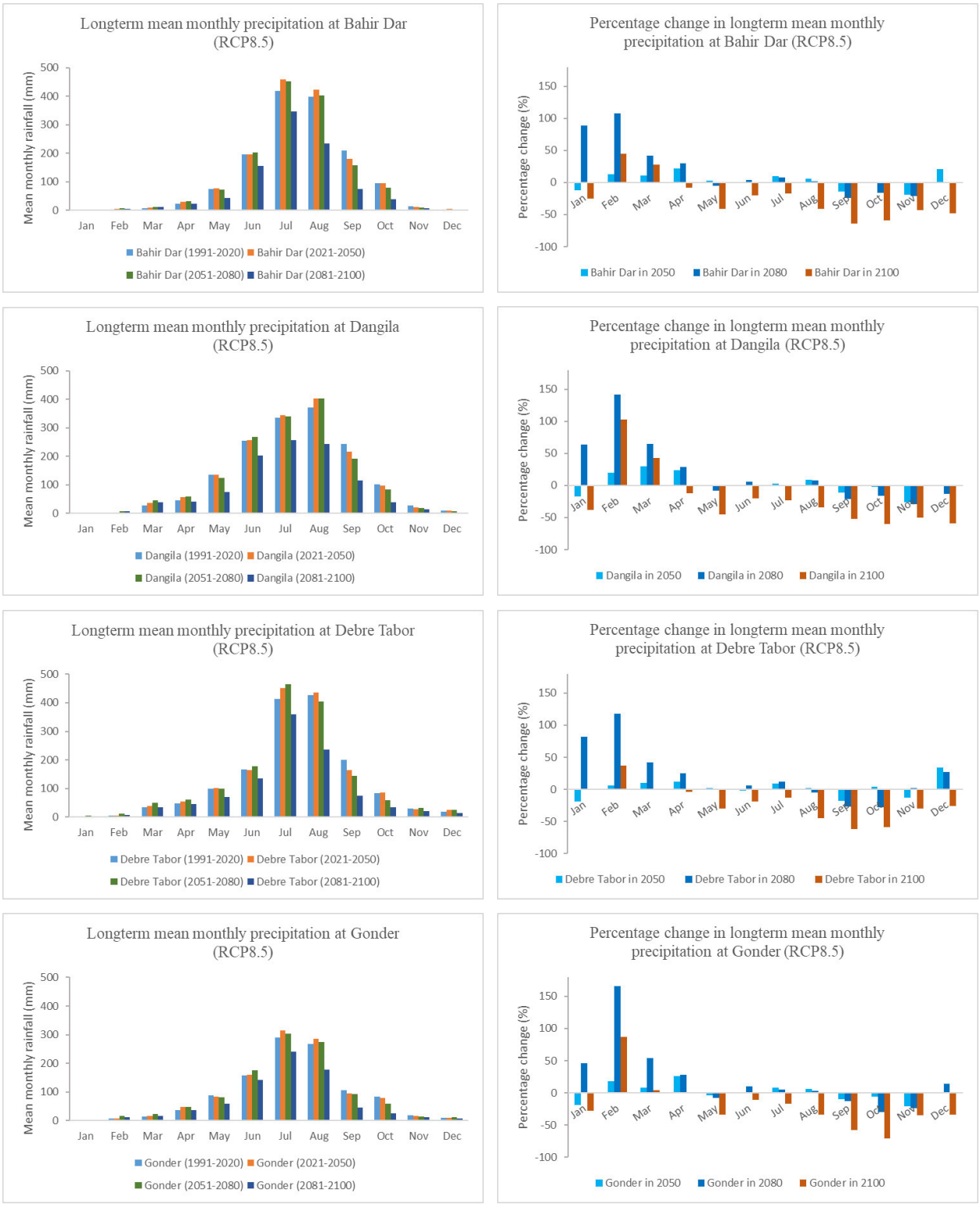


Figure 19: Long-term mean monthly precipitation and percentage changes using RCP8.5

Based on the precipitation projections, it is expected that the area near Dangila station will experience the highest mean annual precipitation in the future, followed by the area near Debre Tabor station. However, a decreasing trend in mean annual precipitation is observed in all scenarios and at all stations. By the 2100s, under the RCP4.5 scenario, Dangila station is projected to receive approximately 1,582.29 mm of mean annual precipitation. Under the RCP8.5 scenario, the projected mean annual precipitation for Dangila station is slightly lower at 1,582.11 mm. For Gonder station, the projected mean annual precipitation by the 2100s is 1,075.79 mm under the RCP4.5 scenario and 1,102.32 mm under the RCP8.5 scenario.

These findings indicate significant variations in precipitation patterns for the different stations in the future. Annexure 5, Annexure 9, Annexure 13 and Annexure 17 provide more detailed information and data in this regard. It is also important to consider these projected changes in precipitation when planning for water resource management, agriculture, and other sectors that depend on reliable and sustainable water availability. Adaptation strategies might also be necessary to mitigate the potential impacts of decreased precipitation on the region's ecosystems and socio-economic systems.

Table 11: Projected long-term mean annual precipitation and percentage changes

| | | Long-term mean annual precipitation (mm) | | | | Percentage change (%) | | |
|---|---|---|---|---|---|---|---|---|
| Model | Station | 1991-2020 | 2021-2050 | 2051-2080 | 2081-2100 | 2050 | 2080 | 2100 |
| RCP4.5 | Dangila | 1532.60 | 1590.35 | 1582.29 | 1059.28 | 3.77 | 3.24 | -30.88 |
| | Bahir Dar | 1424.77 | 1497.60 | 1440.09 | 997.94 | 5.11 | 1.08 | -29.96 |
| | Gonder | 1066.67 | 1090.55 | 1075.79 | 714.00 | 2.24 | 0.86 | -33.06 |
| | Debre Tabor | 1493.42 | 1536.94 | 1486.25 | 992.02 | 2.91 | -0.48 | -33.57 |
| RCP8.5 | Dangila | 1558.51 | 1582.11 | 1557.35 | 1040.33 | 1.51 | -0.07 | -33.25 |
| | Bahir Dar | 1448.90 | 1490.46 | 1439.33 | 948.02 | 2.87 | -0.66 | -34.57 |
| | Gonder | 1084.20 | 1115.88 | 1102.32 | 771.14 | 2.92 | 1.67 | -28.88 |
| | Debre Tabor | 1529.27 | 1554.62 | 1531.41 | 1035.35 | 1.66 | 0.14 | -32.30 |

#### 5.1.4.2 Temperature projection

Figure 20 and Figure 21 provide a detailed analysis of temperature projections from 2005 to 2100 using both the RCP4.5 and RCP8.5 scenarios. The analysis was conducted using the CMhyd tool,

which utilizes historical data and climate models to estimate future temperature patterns. An increasing trend in temperature was observed at all stations for both scenarios in all time periods. This suggests that temperatures are projected to rise in the future. Furthermore, the analysis revealed that the highest percentage increment was observed in minimum temperature compared with maximum temperature at all stations and in all time periods for both scenarios. This implies that minimum temperatures are increase at a higher rate than maximum temperatures in the study area projection.

The specific details and findings of this analysis are presented in Figure 20 and Figure 21 that provide graphical representations of the temperature projections, showcasing the trends and variations in temperature patterns over time. The characteristics of long-term mean monthly minimum and maximum temperature under RCP4.5 scenarios are shown in Annexure 7, Annexure 11, Annexure 15and Annexure 19 while those under RCP8.5 scenarios are in Annexure 8, Annexure 12, Annexure 16 and Annexure 20. Understanding temperature projections is crucial to assess climate change potential impacts on various sectors such as agriculture, water resources, and human health. It can also assist decision-making processes and the development of adaptation strategies.

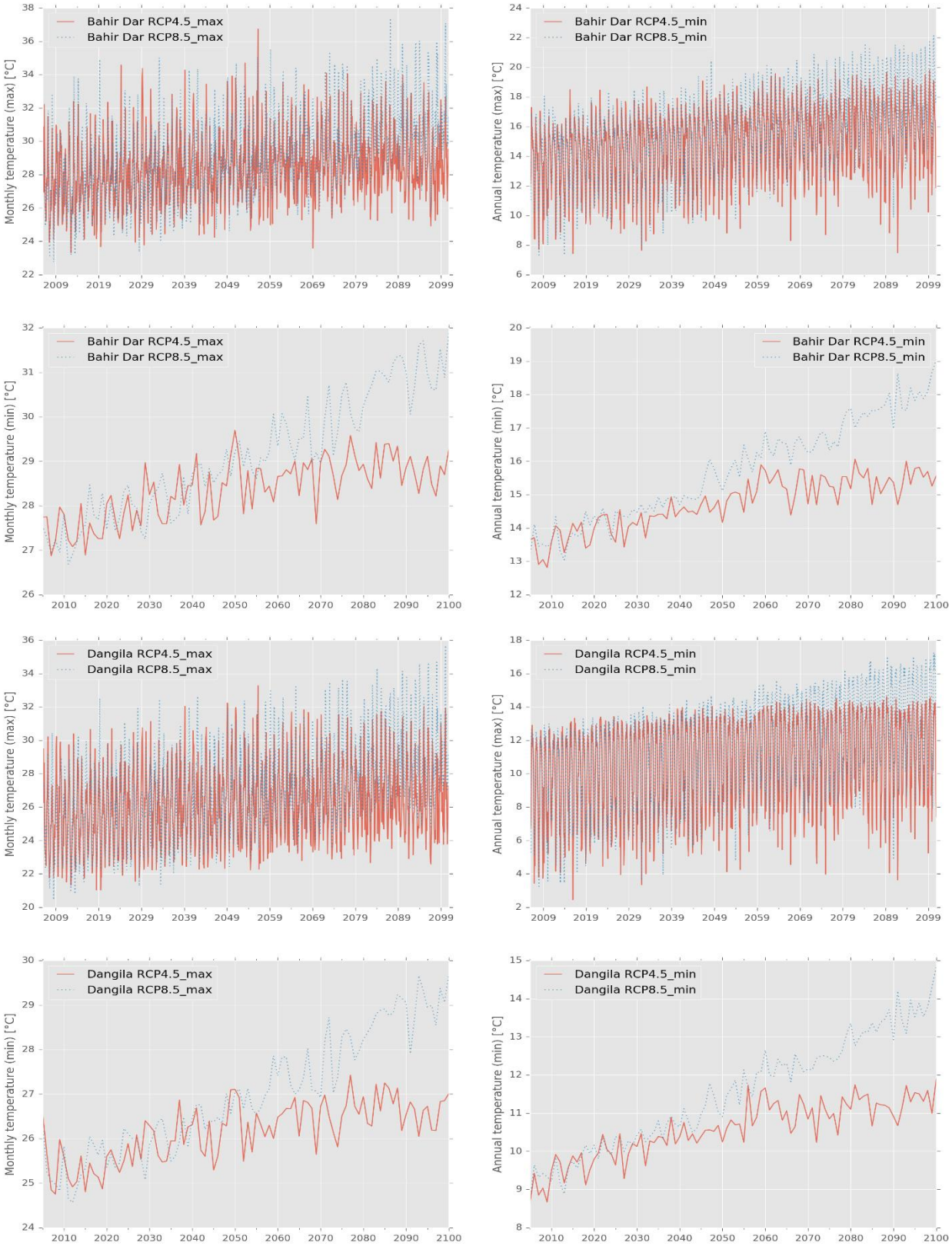


Figure 20: Projected maximum and minimum temperature for Bahir Dar & Dangila

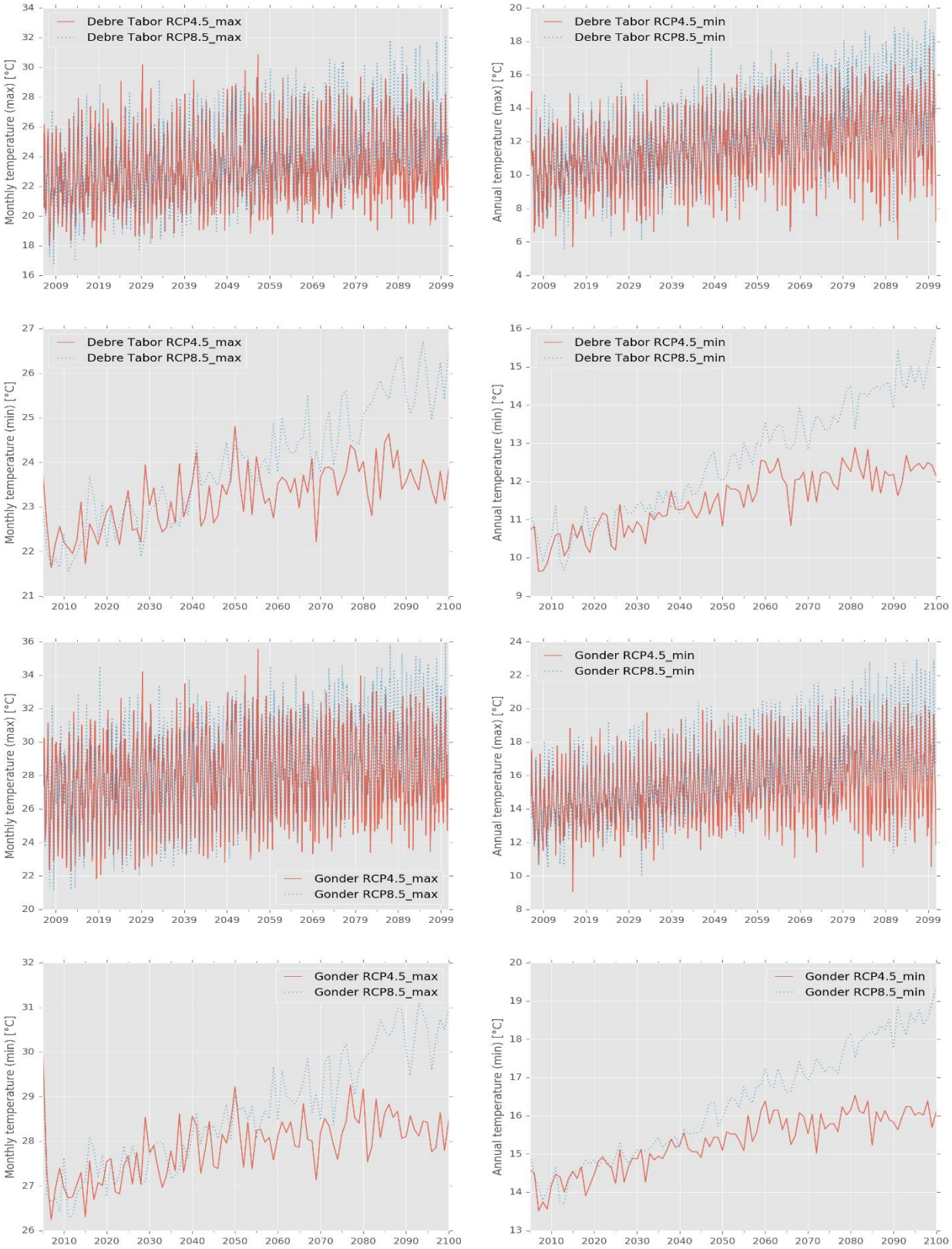


Figure 21: Projected maximum and minimum temperature for Debre Tabor & Gonder

- **Maximum temperature projection**

This section describes the projected changes in maximum temperature at the four stations (Dangila, Bahir Dar, Gonder, and Debre Tabor) under two emission scenarios (RCP4.5 and RCP8.5) compared to the baseline period (1991-2020). The projected changes are shown in Figure 22 and Figure 23 and the corresponding values are summarized in Table 12. The monthly percentage change in maximum temperature for both scenarios is presented in Figure 22 and Figure 23.

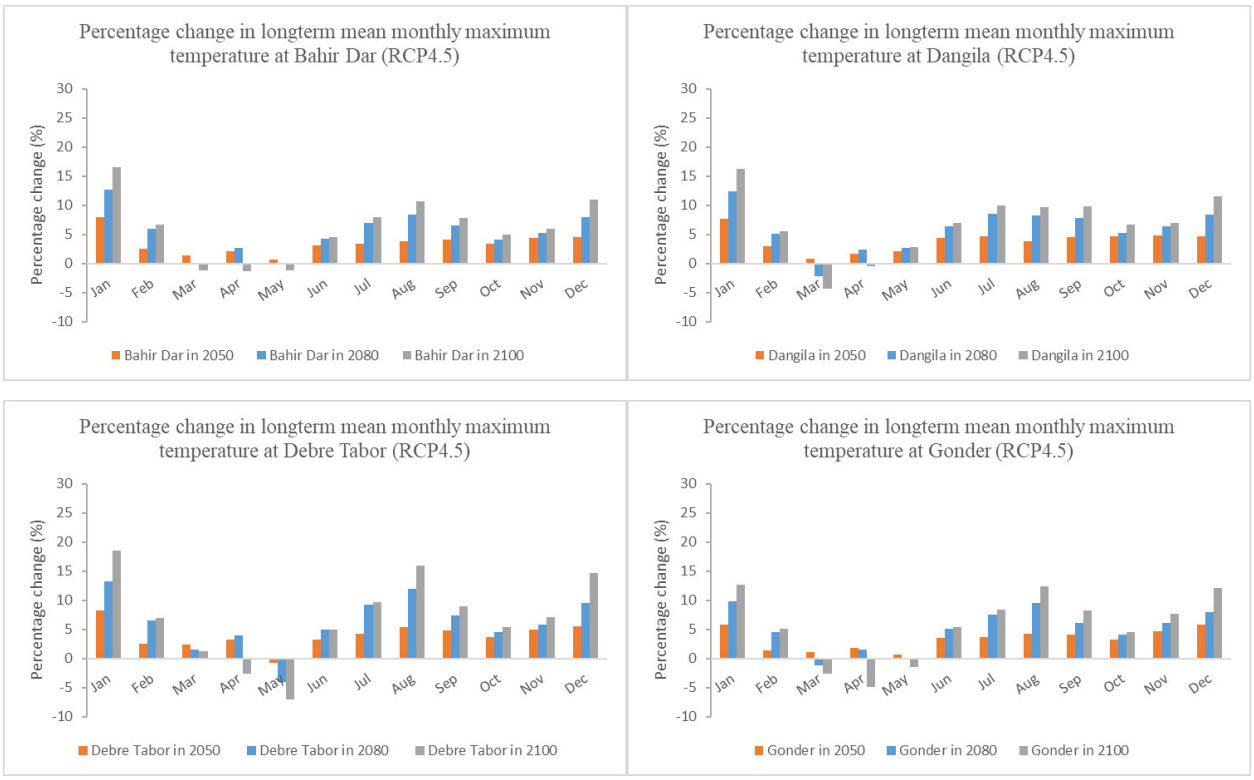


Figure 22: Change in mean monthly maximum temperature (1991-2100) using RCP4.5

The analysis shows that the increase in maximum temperature is most noticeable from November to January for all stations and in all time periods. From March to May under the RCP4.5 scenario, lowest increment in maximum temperature is observed and a decreasing trend is recorded in the same months under the RCP8.5 scenario. The projection shows the highest percentage changes in mean monthly maximum temperature for all scenarios during the summer, specifically from July to September. Lowest percentage change in temperature is observed in March, April, and May.

However, across all time periods, the maximum percentage increase in maximum temperature appears in January for all stations under both the RCP4.5 and RCP8.5 scenarios. Figure 22 and Figure 23 provide a visual representation of mean monthly maximum temperatures at each of four stations for the baseline, future, and all scenarios.

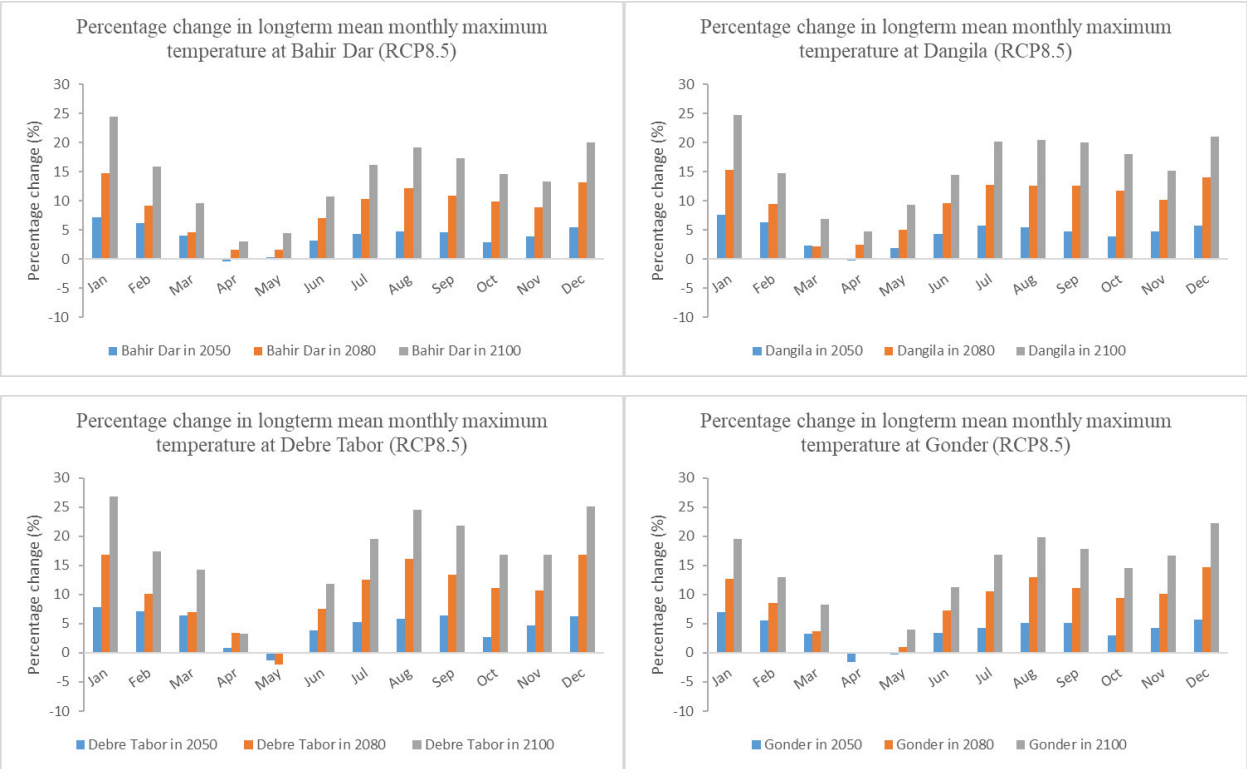


Figure 23: Change in mean monthly maximum temperature (1991-2100) using RCP8.5

For the future time periods and scenarios, the mean monthly and annual maximum temperature indicates an increasing tendency overall according to the anticipated maximum temperature. For example, under the RCP4.5 scenario at Bahir Dar station, the mean annual maximum temperature is projected to increase by 0.92 °C by the 2050s, 1.43 °C by the 2080s, and 1.58 °C by the 2100s compared to the baseline period. Under the RCP8.5, maximum temperature is projected to increase by 1.03 °C by the 2050s, 2.3 °C by the 2080s, and 3.75 °C by the 2100s (refer to Table 12). Similar patterns are observed for the station Dangila, Gonder, and Debre Tabor. The highest increases (3.91 °C, 3.59 °C, and 3.53 °C by the 2100s) are projected under the RCP8.5 scenario, while the

lowest (1.64 °C, 1.43 °C, and 1.48 °C by the 2100s) are projected under the RCP4.5 scenario for the stations Dangila, Gonder, and Debre Tabor, respectively.

Table 12: Projected long-term mean annual maximum temperature and percentage changes

| | | Long-term mean annual maximum temperature ($^{O}$C) | | | | Percentage change (%) | | |
|---|---|---|---|---|---|---|---|---|
| Model | Station | 1991-2020 | 2021-2050 | 2051-2080 | 2081-2100 | 2050 | 2080 | 2100 |
| RCP4.5 | Dangila | 25.03 | 25.99 | 26.47 | 26.67 | 3.85 | 5.77 | 6.57 |
| | Bahir Dar | 27.27 | 28.19 | 28.70 | 28.85 | 3.38 | 5.24 | 5.81 |
| | Gonder | 26.85 | 27.73 | 28.18 | 28.28 | 3.31 | 4.95 | 5.35 |
| | Debre Tabor | 22.21 | 23.07 | 23.55 | 23.69 | 3.89 | 6.04 | 6.66 |
| RCP8.5 | Dangila | 25.03 | 26.13 | 27.46 | 28.94 | 4.30 | 9.62 | 15.50 |
| | Bahir Dar | 27.27 | 28.30 | 29.57 | 31.02 | 3.77 | 8.45 | 13.77 |
| | Gonder | 26.85 | 27.85 | 29.09 | 30.44 | 3.65 | 8.30 | 13.30 |
| | Debre Tabor | 22.22 | 23.19 | 24.40 | 25.75 | 4.59 | 10.05 | 16.13 |

- **Minimum temperature projection**

Figure 24 displays the expected variations in the mean monthly minimum temperature over the upcoming time periods and scenarios for the stations (i.e., Bahir Dar, Dangila, Debre Tabor, and Gonder). The analysis indicates that an increase in minimum temperature is more prominent during the offset of dry seasons, particularly January to April under all emission scenarios and at all stations. This suggests that the warming trend is more pronounced during these months. The lowest increase in minimum temperature is projected to occur in the month of September across all time horizons and emission scenarios for all stations. This indicates that September is expected to experience the smallest change in minimum temperature compared to other months.

The highest percentage increase in mean monthly minimum temperature is observed from December to June for all stations in all scenarios over the entire time period. This indicates that these months are expected to experience the most significant increase in minimum temperature compared to other months. In Gonder, the least noticeable percentage change in monthly minimum temperature is observed under both the RCP4.5 and RCP8.5 scenarios. This signals that Gonder may experience relatively smaller changes in minimum temperature than the other stations. March

is the month that Bahir Dar experiences the highest increase in the monthly minimum temperature, followed by Debre Tabor.

Under the RCP4.5 scenario, the Bahir Dar station is projected to experience a minimum temperature increase of 4.05 °C by the 2100s in March. Similarly, under the RCP4.5 scenario, the Gonder station is projected to experience an increase of 3.84 °C in March by the 2100s. For Debre Tabor station, the highest increase in monthly minimum temperature is projected to be 6.15 °C by the 2100s in February, followed by Bahir Dar under the RCP8.5 scenario. Likewise, under the RCP8.5 scenario, the stiation Bahir Dar is projected to experience an increase of 6.03 °C in February by the 2100s. These values represent the highest projected changes in mean monthly minimum temperature for the respective stations and scenarios in February. Figure 24 presents a visual representation of the mean monthly minimum temperature projections for the baseline and future time periods, showcasing the percentage changes expected under different emission scenarios at the four stations.

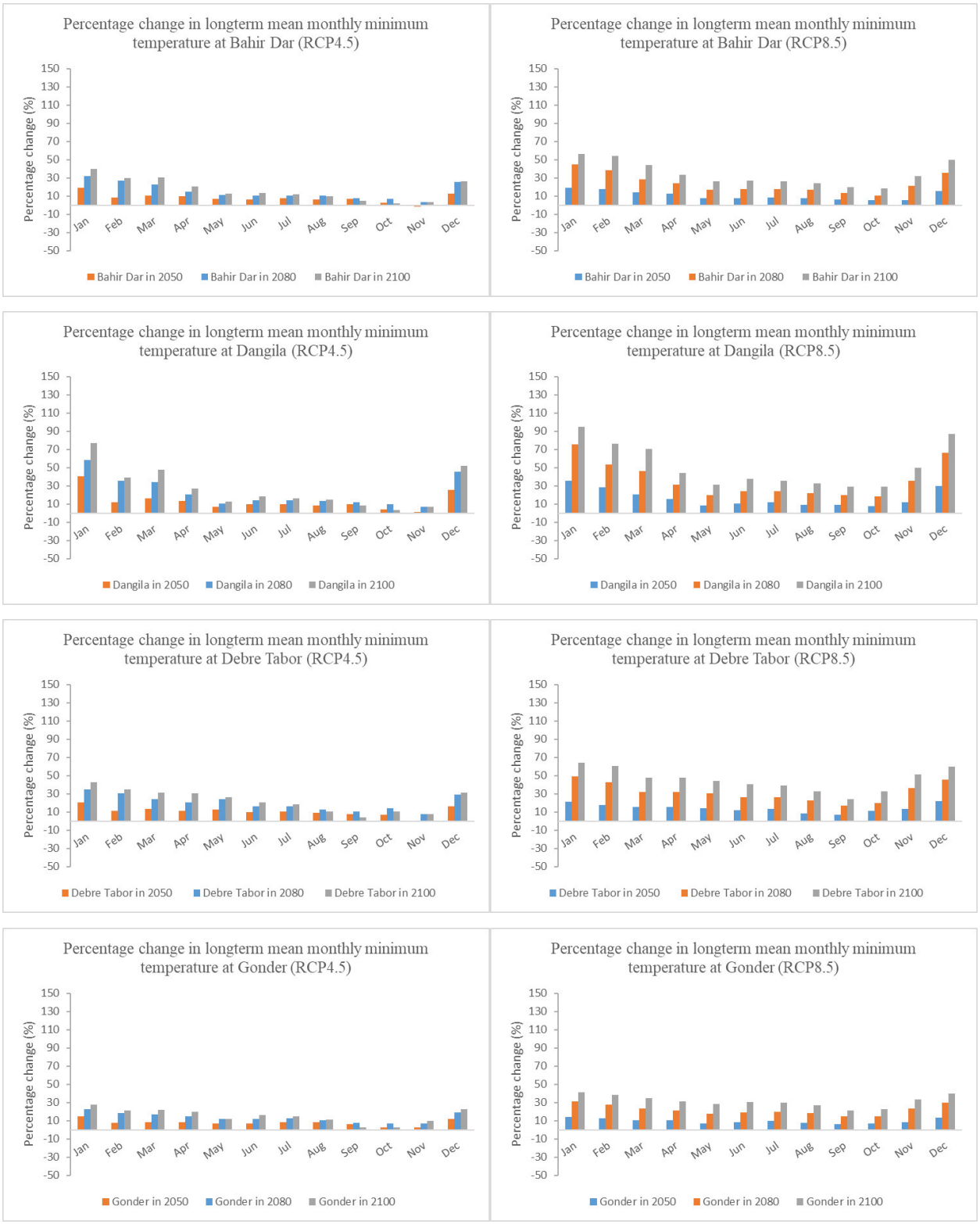


Figure 24: Change in mean monthly minimum temperature (1991-2100) using RCP4.5 & 8.5

According to the RCP4.5 scenario, the mean annual minimum temperature in Bahir Dar station is estimated to rise above the baseline by 1.01 °C by the 2050s, 1.9 °C by the 2080s, and 2.13 °C by the 2100s. Under the RCP8.5 scenario, the projected increases are 1.36 °C by the 2050s, 3.01 °C by the 2080s, and 4.38 °C by the 2100s. For Debre Tabor station, under both the RCP4.5 and RCP8.5 scenarios, the mean annual minimum temperature is projected to increase by 2.28 °C and 4.53 °C, respectively, by the end of the 21$^{st}$ century. At Dangila station, under the RCP4.5 scenario, the mean annual minimum temperature is projected to rise by 1.06 °C by the 2050s, 1.79 °C by the 2080s, and 2.10 °C by the 2100s compared to the baseline. Under the RCP4.5 scenario, the highest mean annual minimum temperature recorded is in Gonder, with projected values of 14.49 °C, 15.76 °C, and 16.03 °C by the 2050s, 2080s, and 2100s, respectively. These values represent the projected increases in mean annual minimum temperature for the respective stations and scenarios during the specified time periods. Table 13 provides a summary of the mean annual minimum temperature projections for the baseline and future time periods, showcasing the percentage changes expected under different emission scenarios at the four stations.

Table 13: Projected long-term mean annual minimum temperature and percentage changes

| | | Long-term mean annual minimum temperature | | | | Percentage change (%) | | |
|---|---|---|---|---|---|---|---|---|
| Model | Station | 1991-2020 | 2021-2050 | 2051-2080 | 2081-2100 | 2050 | 2080 | 2100 |
| RCP4.5 | Dangila | 9.20 | 10.26 | 10.99 | 11.30 | 11.46 | 19.49 | 22.85 |
| | Bahir Dar | 13.33 | 14.34 | 15.23 | 15.46 | 7.62 | 14.26 | 16.04 |
| | Gonder | 13.89 | 14.98 | 15.76 | 16.03 | 7.84 | 13.44 | 15.37 |
| | Debre Tabor | 9.99 | 11.08 | 12.00 | 12.27 | 10.85 | 20.05 | 22.79 |
| RCP8.5 | Dangila | 9.27 | 10.60 | 12.20 | 13.52 | 14.35 | 31.63 | 45.90 |
| | Bahir Dar | 13.41 | 14.77 | 16.42 | 17.79 | 10.07 | 22.42 | 32.66 |
| | Gonder | 13.97 | 15.32 | 16.99 | 18.36 | 9.67 | 21.58 | 31.45 |
| | Debre Tabor | 10.09 | 11.52 | 13.24 | 14.62 | 14.24 | 31.28 | 44.98 |

## 5.2 Results and discussion for objective 2

*To explore the impact of hydro-climatic extremes in the Tana Sub-basin*

### 5.2.1 Spatial pattern of historical drought frequency

Ethiopia is highly vulnerable to drought, and most areas of the country experience frequent and severe drought events (Degefu 1987; NMSA 1996). Indeed, it is the most significant climate-

related natural hazard that periodically affects the country. It is worth noting that drought is not confined to Ethiopia and occurs in various regions around the world. However, its impacts in Africa, including Ethiopia, can be particularly severe due to factors such as limited adaptive capacity and high dependence on rain-fed agriculture.

The analysis conducted on the Sub-basin using the Standardized Precipitation Index values on 3, 6, and 12-month time scales provides insights into the drought conditions experienced in the area over a period of 480 months from 1981 to 2020. The results are presented in Figure 25. The SPI values indicate deviation of precipitation from the long-term average, with positive values indicating wet conditions and negative values indicating drought conditions. Based on the SPI analysis, the study area has experienced a range of drought seasons, ranging from extremely wet to extremely dry.

The SPI values on the 3, 6, and 12-month time scales identify the months characterized by wet or drought conditions, showing the temporal variation in rainfall distribution across the Sub-basin. Since drought occurrences can vary both in time and space, the distribution of drought events was computed for all regions in the study area using the SPI values on the 3, 6, and 12-month time scales. This allowed for an assessment of the relative frequency of drought events across different regions within the Sub-basin. The spatial distribution of the relative frequency of drought events, expressed as a percentage, exhibits variation from Region 1 to Region 10, as depicted in Figure 25. This suggests that different parts of the Sub-basin have experienced varying levels of drought frequency over the analyzed period.

The analysis of drought frequency reveals that the occurrence of drought varies based on the spatial and seasonal variation of precipitation. However, an overall similar pattern of the relative frequency of drought is observed across all regions within the Sub-basin, as indicated in Annexure 21, Annexure 22 and Annexure 23. Using the drought categories defined by McKee *et al.* (1993) and Svoboda *et al.* (2012), it can be observed that spatially the highest mild, moderate, severe, and extreme drought was observed in the Tana Sub-basin. For the 3-month SPI, Region 10 experiences

the highest frequency of mild drought (39.12%), Regions 5 and 6 have the highest frequency of moderate drought (10.04%), Region 4 has the highest frequency of severe drought (5.44%), and Region 9 has the highest frequency of extreme drought (2.72%). For the 6-month SPI, Region 10 has the highest frequency of mild drought (34.53%), Regions 1 and 3 have the highest frequency of moderate drought (12.21%), Region 4 has the highest frequency of severe drought (6.32%), and Regions 7, 8, and 9 have the highest frequency of extreme drought (2.95%). For the 12-month SPI, Region 10 has the highest frequency of mild drought (33.9%), Region 2 has the highest frequency of moderate drought (14.5%), Region 4 has the highest frequency of severe drought (8.32%), and Region 10 has the highest frequency of extreme drought (2.56%). These findings highlight the variability in the spatial distribution of different drought intensities across the Sub-basin, with certain regions consistently experiencing higher frequencies of specific drought categories.

Of the 480 months analyzed, 245 months (approximately 51% of the time period) represented a negative precipitation anomaly, indicating drought conditions in the study area. The analysis further reveals that there is no significant difference in the total number of drought years among the different regions of the Sub-basin. Moreover, the frequencies of important drought categories do not differ significantly across regions. The occurrence of meteorological drought ranges from 1.05% to 10.04%, agricultural drought from 1.26% to 12.21%, and hydrological drought from 0.21% to 14.5%, considering the occurrence of moderate to extreme drought events. These findings are consistent with recent studies that highlighted the changing frequency of drought cycles over time in Ethiopia (see Amsalu *et al.* (2009) and Shawul *et al.* (2020).

Based on the analysis of the spatial precipitation index, several extremely wet and extremely dry years were identified in the watersheds of the Sub-basin. The years 1998, 2001, 2007, 2014, 2017, 2019, and 2020 were characterized as extremely wet (with SPI values of 2.0 or higher), while 1982, 1985, 1988, 1992, and 2010 were identified as extremely dry (with SPI values of -2.0 or lower). The remaining years exhibited a mix of extreme rainfall distributions, indicating variability in precipitation patterns over time in the watershed. These findings align with recent studies such as the work by Amsalu *et al.* (2009), which suggest that drought frequency in Ethiopia has been changing over time.

More specifically, the analysis reveals that extreme drought frequencies were observed in the western part of the Sub-basin for 3-month and 12-month SPI, while the southeast and central parts experienced extreme drought frequencies for the 6-month SPI. In considering the relative drought frequency across all regions of the Sub-basin, it is observed that less than approximately 50% of the relative drought frequency was for SPI3. However, for SPI6, more than 50% of extreme wet to normal range drought frequencies were observed in all regions except for Regions 1, 2, and 6. Similarly, for SPI12, Regions 6 and 10 were the exceptions, with the rest of the regions showing more than 50% of extreme wet to normal range drought frequencies.

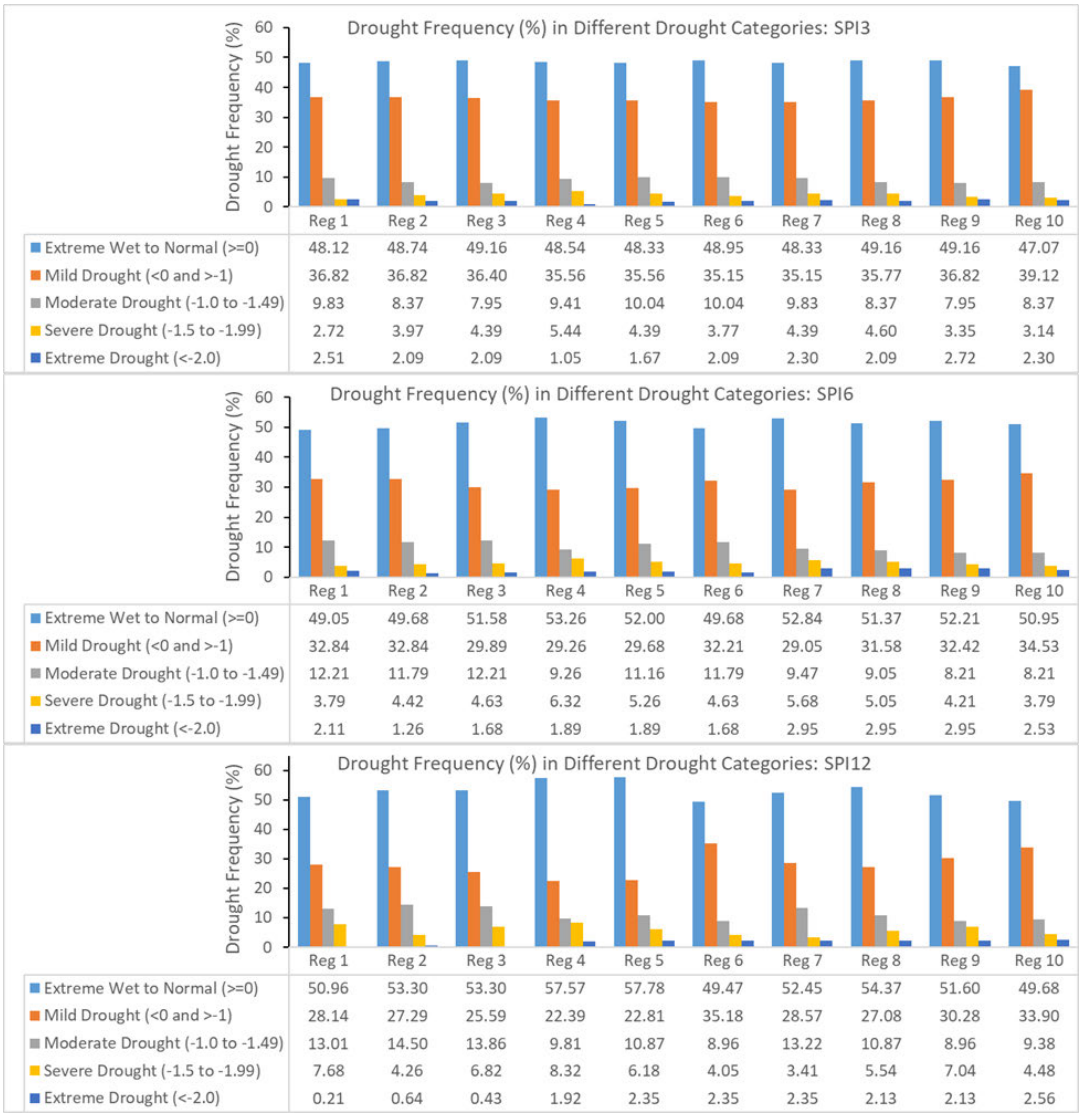


Figure 25: Spatial drought frequency in the Tana Sub-basin: SPI3, SPI6 and SPI12

Furthermore, the analysis indicates that the study area experienced a higher occurrence of agricultural drought compared to hydrological drought, with meteorological droughts being the most frequent overall. The eastern part of the Tana Sub-basin exhibited the highest drought frequencies throughout the year, while the south, north, and west of the Sub-basin were also identified as areas with expected frequent drought events. These findings provide insights into the spatial and temporal patterns of drought occurrences within the Sub-basin, highlighting areas that are more prone to drought and emphasizing the prevalence of agricultural drought. They could assist in developing targeted drought management and adaptation strategies in the affected regions.

### 5.2.2 Historical drought and flood severity

The analysis of different SPI time scales, including SPI1, SPI3, SPI6, SPI9, SPI12, and SPI24, revealed historical drought events within the study area. However, it was observed that SPI1 and SPI3 values (refer to Annexure 21) were highly sensitive to short-term precipitation deficits while SPI6 (refer to Annexure 22) and longer time scales (SPI9, SPI12, and SPI24) (refer to Annexure 23) were found to be more suitable to assess mid- to long-term droughts. Frequency, duration, and severity are important characteristics of drought events. The temporal pattern of SPI values in the study area shows the presence of drought severity indicators during certain periods, including 2003 to 2006, 2010, 2011, and 2016 (refer to Figure 26). In particular, the SPI value in 2010 was lower than -1.5, indicating the occurrence of severe drought in the study area. The temporal pattern illustrated in Figure 26 also reveals a wet season from 2017 to 2020, which may increase flooding events in the Sub-basin, especially when the SPI values exceed 1.5. Detailed information on spatial precipitation index values for 3-month, 6-month, 12-month, and 24-month time scales for all regions of the Sub-basin is presented in Annexure 24 and Annexure 25.

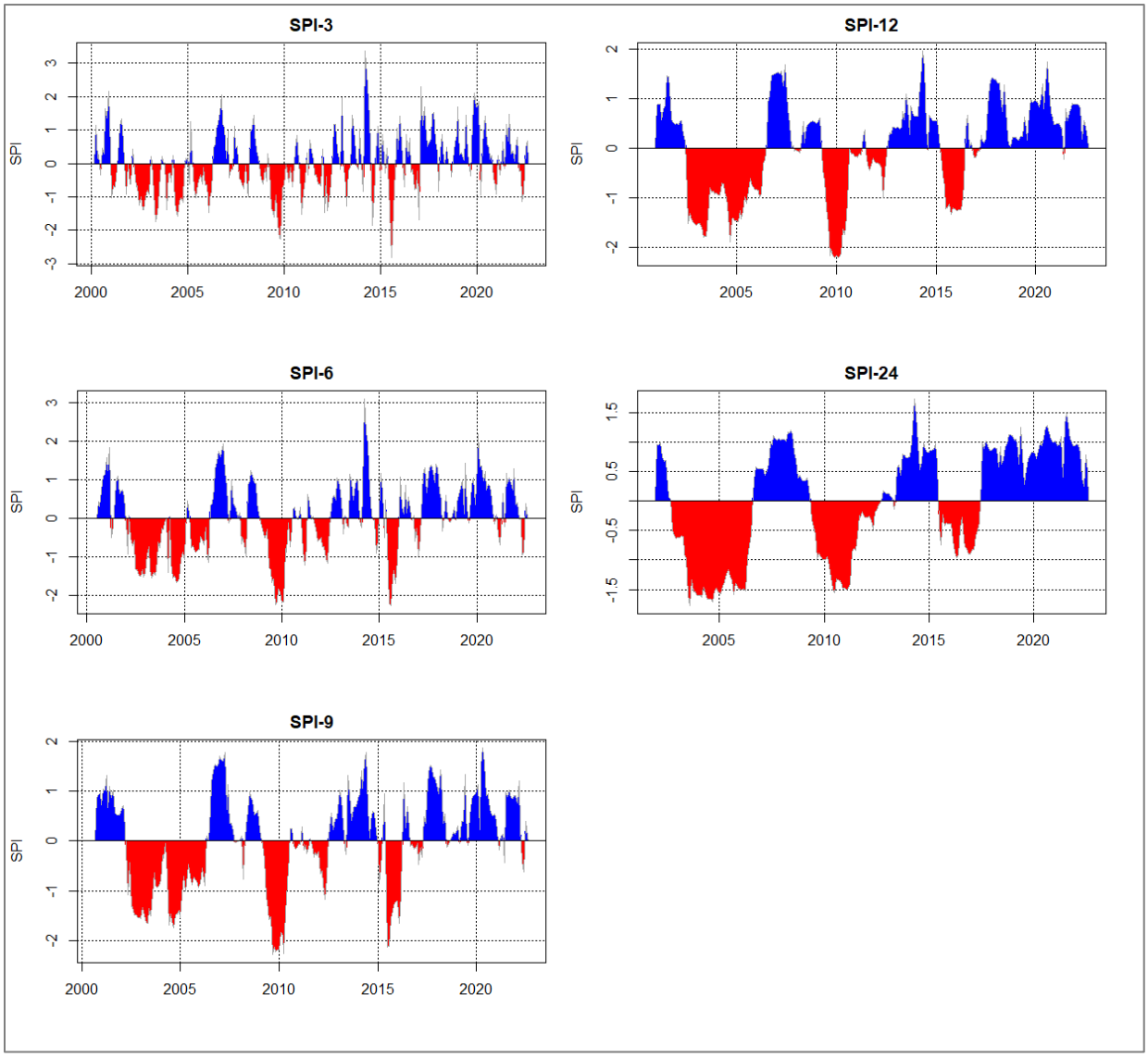


Figure 26: Spatial precipitation index for 3, 6, 9, 12, and 24 months in Tana Sub-basin

Ethiopia has experienced major floods, resulting in loss of life and property in various years. According to the NMA (2006), significant floods occurred in 1988, 1993, 1994, 1995, 1996, and 2006, affecting different parts of the country. The study area itself experienced serious flooding in 1964, 1988, 1993, 1994, and 1995, with the 1995 flood event resulting in the loss of 44 lives (GIRDC 2014).

The flood event in 1988 is particularly noteworthy as it caused massive evacuation of residents and damage to crops. Another significant flood event occurred in Libo Kemkem and Fogera Woredas (in the eastern part of Lake Tana) on 7 August 2006. This was caused by the overflow of the Gumera and Rib Rivers, resulting in the loss of one life and the displacement of 30,000 people. Furthermore, on 30 August 2006, rising lake levels in the same area led to the displacement of more than 10,000 people. In the Fogera plains, floods caused significant damage and losses. Three people lost their lives, 36,000 were left homeless, over 6,600 hectares of cropland were inundated, more than 320 beehives were destroyed, a school and several water points were damaged, stored seeds were spoiled, and large volumes of gravel and sand were deposited on farmlands.

The severity or scale of drought in the study area was assessed using CDI. It is calculated based on a weighted combination of three parameters: the precipitation drought index (refer to Annexure 26), temperature drought index (refer to Annexure 27), and vegetation drought index (refer to Annexure 28). According to the CDI values and the map presented in Figure 27, most regions in the study area were not severely affected by extreme or severe drought. Instead, mild to moderate drought conditions were observed in certain areas. This indicates that the study area experienced a moderate level of drought, which may have resulted in reduced soil moisture, slowed planting and crop growth, and caused water deficits, and partial loss of crops and pasture. In some cases, when drought severity is below 0.8, there may be damage to crops and pasture. Shallow reservoirs may also experience drying, and voluntary water rationing measures may be implemented.

The temporal pattern of CDI values shows that the month of January has the highest CDI value compared to other months, indicating a wider scale of crop and pasture loss, potential water rationing measures, and livestock migration. The month of September is identified as the wet season in the study area, suggesting a higher probability of flood occurrence. The lowland areas in the eastern part of Lake Tana are particularly susceptible to flood hazards, and this finding aligns with the NMA (2006) report. The study also highlights that the southern and eastern parts of the Sub-basin are sensitive to mild to moderate drought, while the area near the eastern part of the lake is prone to floods and may be impacted by the backflow from Lake Tana.

It is important to note that the researcher acknowledges potential uncertainties in the model used and data quality gaps, which could affect the accuracy of the results. There were discrepancies between the wetness shown in the model outputs for December and the actual conditions of the study area in the southeast parts. This highlights the need for on-going monitoring, improved modeling techniques, and data quality assurance to enhance the accuracy and reliability of flood and drought assessments in the Tana Sub-basin.

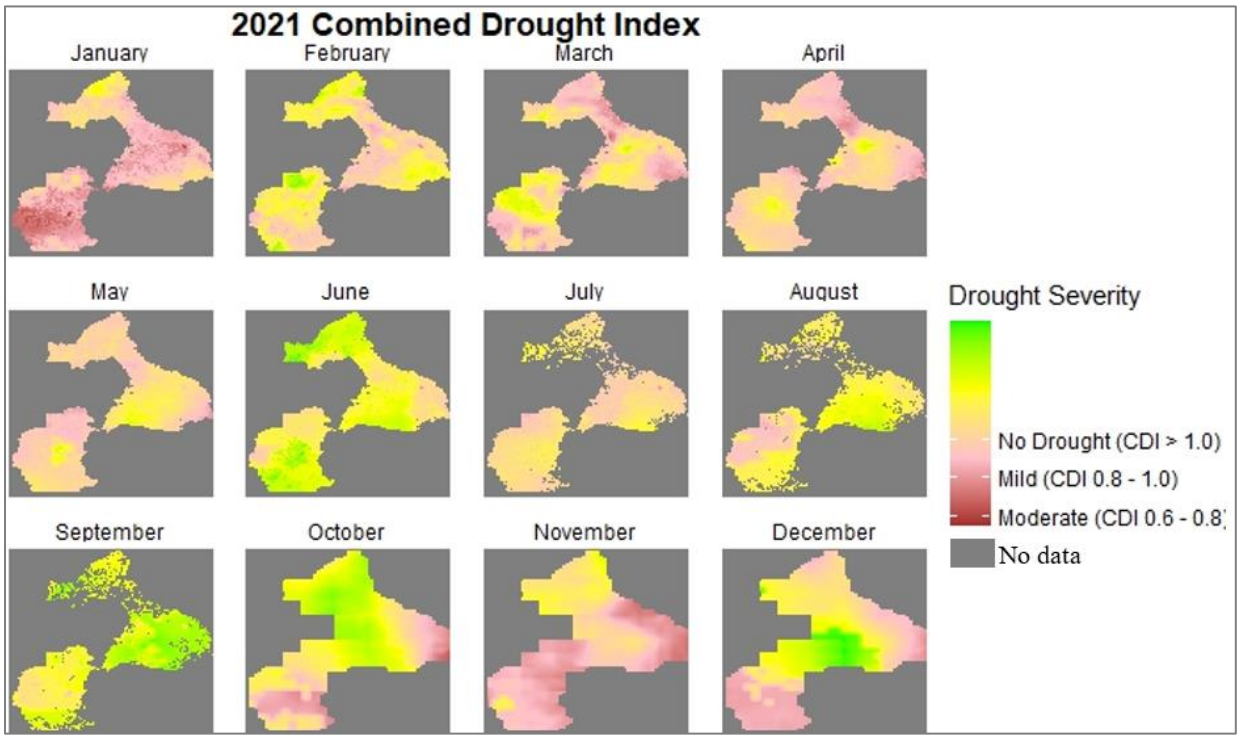


Figure 27: Spatial and temporal pattern of drought using CDI values

It is recognized that short-term dryness, which can have several impacts on agricultural activities and water resources, occurs in the study area. During such periods, the availability of moisture for planting and crop growth is reduced. This can delay planting and may hinder the growth and development of crops. Short-term dryness often results in a scarcity of water for agricultural needs and other purposes. Insufficient water supply can also affect irrigation practices, resulting in inadequate moisture for crops and potential water stress. Moreover, short-term dryness can cause partial loss of crops and pasture. Insufficient moisture and prolonged dry spells can negatively

impact crop yields and the condition of pastureland, thereby leading to reduced agricultural productivity and potential economic losses. During dry periods, shallow reservoirs and water bodies may experience reduced water levels or even complete drying. This affects water availability for irrigation, livestock watering, and other water-dependent activities.

The spatial distribution and percentage occurrence of drought severity for five drought categories are indicated in Table *5*. Based on the findings across all regions of the study area, it is observed that more than 50% of the time, the condition of drought is categorized as normal or above normal (indicating a wet situation). This suggests that the study area experiences relatively normal or wet conditions in terms of drought severity most of the time. Extreme drought, which is the most severe category, occurs for about 2% of the time in six regions (Regions 5 to 10) of the study area. Among these, Region 10 has the highest percentage of extreme drought occurrence (2.56%), while Region 1 has the lowest (0.21%).

The occurrence of severe drought varies across the regions. Region 7 has the lowest percentage of severe drought occurrences (3.41%), while Region 1 has the highest (7.68%). Severe drought conditions are experienced for a significant portion of the time in Region 1. Region 2 in the northeast part of the study area has the highest percentage of moderate drought occurrence (14.5%). In contrast, the central part of the Sub-basin has the lowest percentage of moderate drought occurrence (8.96%). The study thus highlights that the severity of drought varies spatially and temporally with different magnitudes observed across the study area. This indicates that different regions experience varying levels of drought severity at different times.

According to Table *5* n drought category classification, most of the study areas are categorized as having normal to wet conditions for drought severity with occurrence percentages above 50%. This suggests that it experiences drought conditions that are within normal or wet ranges most of the time. These findings emphasize the spatial and temporal variability of drought severity within the study area. It is important to consider these variations when assessing drought impacts,

formulating and implementing mitigation measures, and planning for water resource management in different regions.

Table 14: Spatial distribution of the severity of drought in Tana Sub-basin

| Catchment | Normal (>= 0) | Mild drought (<0 and >-1) | Moderate drought (-1.0 to -1.49) | Severe drought (-1.5 to -1.99) | Extreme drought (< -2.0) |
|---|---|---|---|---|---|
| Reg 1 | 50.96 | 28.14 | 13.01 | 7.68 | 0.21 |
| Reg 2 | 53.30 | 27.29 | 14.50 | 4.26 | 0.64 |
| Reg 3 | 53.30 | 25.59 | 13.86 | 6.82 | 0.43 |
| Reg 4 | 57.57 | 22.39 | 9.81 | 8.32 | 1.92 |
| Reg 5 | 57.78 | 22.81 | 10.87 | 6.18 | 2.35 |
| Reg 6 | 49.47 | 35.18 | 8.96 | 4.05 | 2.35 |
| Reg 7 | 52.45 | 28.57 | 13.22 | 3.41 | 2.35 |
| Reg 8 | 54.37 | 27.08 | 10.87 | 5.54 | 2.13 |
| Reg 9 | 51.60 | 30.28 | 8.96 | 7.04 | 2.13 |
| Reg 10 | 49.68 | 33.90 | 9.38 | 4.48 | 2.56 |

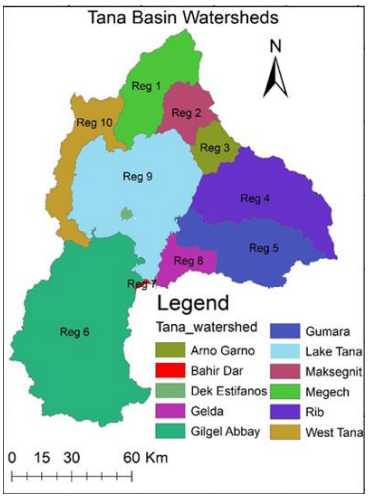


### 5.2.3 Projected drought and wet extent

Table 15 shows the projection of drought and wet extent occurrence for four different stations: Bahir Dar, Dangila, Debre Tabor, and Gonder. The projection does not show a consistent decreasing or increasing patterns for future time periods in all scenarios and at all stations. However, on average, there is a possibility of a trend in drought and wet extent occurrences in all scenarios at all stations from 2021 until 2100.

Under the RCP4.5 scenario, the highest probability of extremely wet occurrences is in Debre Tabor station for all SPIs (3-month, 6-month, and 12-month) with values of 4.64%, 4.70%, and 4.39%, respectively, between 2081 and 2100. The highest probability of extremely dry occurrences is in Bahir Dar station for both 3-month and 6-month SPIs with values of 2.53% and 2.14%, respectively, whereas for the 12-month SPI, the highest percentage of occurrences (3.95%) is in Debre Tabor. Under the RCP8.5 scenario, the highest probability of extreme drought occurrences

is in Dangila station for all SPIs (3-month, 6-month, and 12-month) with values of 1.69%, 0.85%, and 0.44%, respectively. The highest probability of extremely wet occurrences is in Gonder town for the 6-month and 12-month SPIs, whereas for the 3-month SPI, the highest probability of wet occurrences is in Debre Tabor station. In general, the projection suggests that there is a possibility of both drought and wet extent occurrences in all scenarios and at all stations from 2021 to 2100.

The comparison of the two emission scenarios revealed that RCP4.5 projected a higher percentage of extremely dry condition occurrence than RCP8.5, while RCP8.5 projected a higher percentage of extremely wet condition occurrence than RCP4.5. This indicates that the occurrence of drought is inversely related to the amount of precipitation but directly related to the probability of extremely wet occurrences in the station. Furthermore, the projection of precipitation is higher in RCP8.5 than RCP4.5. This implies that under the RCP8.5 scenario, there is a higher projected drought for all stations than RCP4.5 at all time periods. Under the RCP4.5 scenario, there is a higher projected wet condition for all stations than RCP8.5 at all time periods. Despite these differences, all stations behaved under normal conditions with a probability of more than 61% occurrence at all time periods in both scenarios.

Overall, the highest percentage of extremely wet occurrences was observed in Gonder station under the RCP8.5 scenario for the period 2021-2100 with a value of 10.09%. The highest percentage of extremely wet occurrence under the RCP4.5 scenario was observed in Debre Tabor station for the period 2021-2050 with a value of 5.44%. The highest percentage of extremely dry occurrence was observed in Debre Tabor station for the period 2021-2050 under the RCP4.5 scenario with a value of 3.15%. The highest extreme drought was observed in Dangila station for the period 2081-2100 under the RCP8.5 scenario with a value of 1.69%. It is worth noting that the existence of wet conditions may lead to flood problems in the study area. Therefore, appropriate measures should be taken to mitigate the impact of floods and droughts in the region.

Table 15: Percentage of future drought and wet occurrence in the Tana Sub-basin

| Model | SPI | Station | Drought and wet extent (%) | | | | | | | | | | | | | | | | | | | |
|---|---|---|---|---|---|---|---|---|---|---|---|---|---|---|---|---|---|---|---|---|---|---|
| | | | Extreme wet | | | Severe wet | | | Moderate wet | | | Normal | | | Moderate drought | | | Severe drought | | | Extreme drought | | |
| | | | 1 | 2 | 3 | 1 | 2 | 3 | 1 | 2 | 3 | 1 | 2 | 3 | 1 | 2 | 3 | 1 | 2 | 3 | 1 | 2 | 3 |
| RCP4.5 | SPI 3 | Bahir Dar | 3.63 | 2.51 | 2.53 | 4.47 | 5.59 | 6.75 | 6.98 | 10.61 | 8.44 | 69.55 | 63.97 | 68.78 | 10.34 | 12.29 | 7.17 | 3.35 | 3.63 | 3.80 | 1.68 | 1.40 | 2.53 |
| | | Dangila | 1.40 | 2.23 | 2.95 | 4.75 | 4.19 | 5.49 | 10.61 | 8.66 | 11.39 | 65.64 | 70.39 | 63.71 | 10.89 | 8.38 | 12.24 | 5.59 | 4.75 | 2.53 | 1.12 | 1.40 | 1.69 |
| | | Debre Tabor | 3.91 | 3.91 | 4.64 | 4.47 | 5.31 | 5.06 | 6.42 | 6.15 | 8.44 | 72.07 | 70.67 | 65.82 | 8.66 | 8.94 | 10.13 | 2.51 | 3.35 | 4.22 | 1.96 | 1.68 | 1.69 |
| | | Gonder | 4.19 | 2.79 | 2.95 | 2.79 | 6.15 | 6.33 | 8.66 | 8.10 | 7.59 | 67.32 | 68.99 | 66.24 | 11.45 | 9.22 | 11.39 | 4.19 | 2.79 | 3.80 | 1.40 | 1.96 | 1.69 |
| | SPI 6 | Bahir Dar | 3.66 | 1.41 | 2.14 | 5.63 | 5.07 | 5.56 | 5.63 | 12.11 | 12.82 | 70.14 | 64.51 | 65.81 | 11.27 | 9.01 | 6.84 | 3.10 | 7.04 | 4.70 | 0.56 | 0.85 | 2.14 |
| | | Dangila | 1.97 | 3.38 | 2.14 | 5.07 | 2.54 | 5.98 | 8.73 | 7.89 | 10.26 | 68.73 | 72.39 | 63.68 | 6.48 | 9.01 | 11.54 | 8.17 | 3.38 | 4.27 | 0.85 | 1.41 | 2.14 |
| | | Debre Tabor | 5.35 | 3.38 | 4.70 | 2.25 | 4.79 | 2.99 | 7.61 | 7.61 | 10.26 | 73.80 | 68.45 | 67.52 | 7.89 | 10.42 | 9.83 | 1.97 | 4.23 | 2.56 | 1.13 | 1.13 | 2.14 |
| | | Gonder | 4.23 | 3.10 | 3.42 | 3.10 | 3.38 | 5.13 | 10.99 | 12.11 | 8.12 | 67.04 | 66.48 | 68.80 | 10.70 | 10.42 | 9.40 | 2.54 | 2.25 | 4.70 | 1.41 | 2.25 | 0.43 |
| | SPI 12 | Bahir Dar | 3.72 | 0.00 | 0.00 | 7.16 | 4.30 | 3.95 | 2.87 | 12.03 | 20.18 | 73.35 | 63.90 | 61.40 | 11.46 | 8.60 | 4.39 | 1.43 | 8.60 | 9.21 | 0.00 | 2.58 | 0.88 |
| | | Dangila | 1.43 | 3.44 | 0.00 | 5.16 | 3.15 | 7.02 | 9.17 | 8.02 | 11.40 | 67.05 | 73.64 | 61.40 | 8.31 | 5.73 | 13.16 | 6.59 | 5.73 | 5.26 | 2.29 | 0.29 | 1.75 |
| | | Debre Tabor | 5.44 | 1.43 | 4.39 | 4.30 | 7.16 | 0.88 | 4.87 | 9.74 | 8.33 | 77.36 | 68.19 | 71.93 | 7.45 | 5.44 | 7.89 | 0.57 | 4.87 | 2.63 | 0.00 | 3.15 | 3.95 |
| | | Gonder | 4.58 | 0.86 | 4.39 | 4.87 | 6.59 | 2.19 | 6.02 | 11.46 | 6.14 | 70.77 | 64.76 | 73.25 | 9.17 | 7.16 | 6.14 | 4.58 | 7.16 | 7.02 | 0.00 | 2.01 | 0.88 |
| RCP8.5 | SPI 3 | Bahir Dar | 2.23 | 3.35 | 2.95 | 4.19 | 4.47 | 5.06 | 8.66 | 7.54 | 8.02 | 70.39 | 68.44 | 67.51 | 8.38 | 13.13 | 10.55 | 4.75 | 2.23 | 4.64 | 1.40 | 0.84 | 1.27 |
| | | Dangila | 3.35 | 4.19 | 3.38 | 4.75 | 4.19 | 4.64 | 7.54 | 7.26 | 7.59 | 69.55 | 70.67 | 68.35 | 9.22 | 9.22 | 10.55 | 4.75 | 3.07 | 3.80 | 0.84 | 1.40 | 1.69 |
| | | Debre Tabor | 3.35 | 3.63 | 5.06 | 2.79 | 4.75 | 3.38 | 10.89 | 8.10 | 6.33 | 68.44 | 70.39 | 73.00 | 8.66 | 9.22 | 8.86 | 4.19 | 3.07 | 2.95 | 1.68 | 0.84 | 0.42 |
| | | Gonder | 3.35 | 4.19 | 3.80 | 3.07 | 4.19 | 4.64 | 8.10 | 6.15 | 7.17 | 70.95 | 72.07 | 67.51 | 10.06 | 10.34 | 12.66 | 2.79 | 2.51 | 3.80 | 1.68 | 0.56 | 0.42 |
| | SPI 6 | Bahir Dar | 3.38 | 4.51 | 2.99 | 2.54 | 3.94 | 7.69 | 7.89 | 5.07 | 7.26 | 72.39 | 69.30 | 64.96 | 9.01 | 14.65 | 12.82 | 3.38 | 1.69 | 3.85 | 1.41 | 0.85 | 0.43 |
| | | Dangila | 3.66 | 4.79 | 3.42 | 5.07 | 3.94 | 4.70 | 7.89 | 6.48 | 6.84 | 66.76 | 69.58 | 68.80 | 12.96 | 12.68 | 12.82 | 2.82 | 1.69 | 2.56 | 0.85 | 0.85 | 0.85 |
| | | Debre Tabor | 3.10 | 3.10 | 5.56 | 4.79 | 4.51 | 3.42 | 10.14 | 5.63 | 4.70 | 66.20 | 73.24 | 77.35 | 10.14 | 9.30 | 4.70 | 4.51 | 3.10 | 4.27 | 1.13 | 1.13 | 0.00 |
| | | Gonder | 3.66 | 3.38 | 6.84 | 3.10 | 5.07 | 2.14 | 6.76 | 7.61 | 4.27 | 72.11 | 69.30 | 74.36 | 11.55 | 11.83 | 11.11 | 2.25 | 2.25 | 1.28 | 0.56 | 0.56 | 0.00 |
| | SPI 12 | Bahir Dar | 3.44 | 6.02 | 4.39 | 3.15 | 3.44 | 7.02 | 8.02 | 3.44 | 5.26 | 73.64 | 68.19 | 64.47 | 5.73 | 17.19 | 15.35 | 5.73 | 1.72 | 3.07 | 0.29 | 0.00 | 0.44 |
| | | Dangila | 2.87 | 3.72 | 5.26 | 5.73 | 7.45 | 2.19 | 9.46 | 5.16 | 7.46 | 62.18 | 66.76 | 67.11 | 15.19 | 14.90 | 14.47 | 4.58 | 2.01 | 3.51 | 0.00 | 0.00 | 0.00 |
| | | Debre Tabor | 3.72 | 4.30 | 8.77 | 3.72 | 2.87 | 1.32 | 12.32 | 6.02 | 1.32 | 62.75 | 71.92 | 78.51 | 11.46 | 12.89 | 6.58 | 5.16 | 1.72 | 3.51 | 0.86 | 0.29 | 0.00 |
| | | Gonder | 4.58 | 6.02 | 10.09 | 2.29 | 1.43 | 0.44 | 5.44 | 7.74 | 0.88 | 72.21 | 67.34 | 76.75 | 12.61 | 16.62 | 10.96 | 2.87 | 0.86 | 0.88 | 0.00 | 0.00 | 0.00 |

*1 represents 2021-2050, 2 represents 2050-2080, and 3 represents 2080-2100

## 5.3 Results and discussion for objective 3

*To assess the impact of land use land cover on water resources in the Tana Sub-basin*

### 5.3.1 Land use land cover changes: 1986, 2000 and 2014

Figure 30 and Table 16 provide information on the changes in LULC distribution and patterns over time in the study area for the years 1986, 2000, and 2014. In 1986, cultivated land accounted for approximately 36.64% of the study area. Water bodies, grassland, and bush/shrubland collectively represented about 56.48% of the land cover. The built-up area, forest land, Afroalpine, and wetland combined covered only 6.88% of the study area. In 2000, cultivated land covered approximately 40.71% of the study area, an increase compared to 1986. Water bodies, grassland, and bush/shrubland still dominated the land cover, collectively representing about 55.95% of the study area. The built-up area, forest land, Afroalpine, and wetland accounted for only 3.35% of the Tana Sub-basin. By 2014, cultivated land covered about 48.82% of the study area. Water bodies, grassland, and bush/shrubland collectively represented approximately 48.02% and the built-up area, forest land, Afroalpine, and wetland accounted for only 3.15% of the Tana Sub-basin.

### 5.3.2 Change detection

The changes in LULC in the study area over the past 28 years were assessed (refer to Table 16). The findings indicate that most of the vegetation cover in the study area has decreased. Forestland and grassland experienced continuous reduction throughout this period. This suggests deforestation and conversion of grassland areas to other land uses. Sub-Afroalpine vegetation, a specific type of vegetation, showed a dramatic decrease in the second period of assessment. This suggests a significant loss of this particular vegetation type. Bushes and shrubs recorded a 1% increase in the entire 28-year period. However, there was an unexpectedly fast decline in the second period, pointing to a complex pattern of change in this particular land cover type. Forest land showed continuous reduction over the years, indicating ongoing deforestation. Conversely, water bodies, including rivers, lakes, and other water features, and wetlands, showed relatively small variations compared to other land cover types in the study area. Water bodies occupied a fairly stable percentage of the total area throughout the assessed periods while wetlands

experienced a slight decrease in the first period and a subsequent increase in the second. Water bodies occupied approximately 20.29%, 20.37%, and 20.62% of the Tana Sub-basin in the years 1986, 2000, and 2014, respectively. Wetlands accounted for 0.72% in the first assessment period, decreased to 0.67% in the second, and then increased to 0.80%.

The study's findings indicate a significant change in LULC over the past 28 years in the Tana Sub-basin. A significant increase is observed in cultivated land, with a corresponding decrease in grassland and bush/shrubland. The expansion of cultivated land suggests potential changes in land use practices and agricultural activities in the study area. The decrease in forestland and grassland, as well as the loss of sub-Afroalpine vegetation, highlight potential environmental challenges such as deforestation and habitat degradation. The increase in bushes and shrubs suggests a complex dynamism in this land cover type. The relatively stable percentages of water bodies and wetlands indicate their persistence in the landscape although wetlands experienced some fluctuations. It is important to note that the built-up area, forest land, Afroalpine, and wetland cover relatively small percentages of the study area over the years, indicating their limited presence in comparison to other land cover types.

Table 16: Summary of LULC assessment for 1986, 2000, and 2014

| Land cover | Change assessment | | | | | |
|---|---|---|---|---|---|---|
| | 1986 | | 2000 | | 2014 | |
| | Area ($km^2$) | % | Area ($km^2$) | % | Area ($km^2$) | % |
| Afroalpine and sub-Afroalpine vegetation | 121.37 | 0.81 | 10.23 | 0.07 | 37.75 | 0.25 |
| Built-up area | 148.60 | 0.99 | 42.40 | 0.28 | 43.82 | 0.29 |
| Bush and shrubland | 3,619.32 | 24.06 | 3,773.61 | 25.09 | 2,688.23 | 17.87 |
| Cultivated land | 5,511.20 | 36.64 | 6,122.91 | 40.71 | 7,343.69 | 48.82 |
| Forest land | 656.51 | 4.36 | 351.09 | 2.33 | 272.75 | 1.81 |
| Grassland | 1,824.30 | 12.13 | 1,577.75 | 10.49 | 1,433.93 | 9.53 |
| Waterbody | 3,051.42 | 20.29 | 3,063.50 | 20.37 | 3,101.32 | 20.62 |
| Wetland | 108.80 | 0.72 | 100.03 | 0.67 | 120.03 | 0.80 |

Cultivated land expanded in the study area over the assessed periods. The significant increment from 36.64% in the first period to 40.71% in the second and 48.82% in the third period of assessment indicates substantial expansion of agricultural activities in the Sub-basin. Population pressure and the fact that the inhabitants are mainly engaged in agriculture explain this trend (Abera *et al.* 2020). The growing population and the need for agricultural production likely resulted in continuous pressure on the surrounding vegetation cover, leading to the expansion of cultivated land.

Understanding these changes in LULC is crucial to assessing their impact on water resources in the Tana Sub-basin. Expanding agricultural activities often require forests to be cleared, grasslands to be converted, or other land cover types to be modified to create arable land for crop cultivation. This can result in environmental changes, including deforestation, habitat loss, and alterations in ecosystem dynamics. Consequently, it is essential to strike a balance between meeting the needs of the growing population and protecting the environment and natural resources.

### 5.3.3 Transformed versus unchanged land use land cover

Due to the influx of people and agrarian activities in the Tana Sub-basin, the extent of LULC change was more than 25%. As indicated in Figure 28, the amount of land cover remains unchanged in the first period (1986-2000) at 73.47% and stood at 71.54% in the next period (2000-2014). However, the overall (1986-2014) changes recorded increased by slightly more than 30%, which pushed the unchanged down to 66.06%. In the first period (1986-2000), water bodies had by far the highest percentage of survival coverage, standing at 99.7% unchanged (refer to Table 17). There is also no significant cover transformation on cultivated land. More than half of the bush, shrub, and grasslands remain unchanged during this period. However, sub-Afroalpine vegetation (4.09%) followed by built-up areas (8.24%) had the lowest unchanged coverage. In other words, these land covers have been most transformed into other cover types in the past 28 years. The detailed transformed and unchanged LULC matrix analyses within the three scenarios (2000-1986, 2014-2000, and 2014-1986) in the study area are presented below in Table 17, Table 18 and Table 19.

Table 17: Transformed versus unchanged LULC matrix in Tana Sub-basin (2000-1986)

| 1986 | 2000 | | | | | | | |
|---|---|---|---|---|---|---|---|---|
| | Afroalpine and sub-afroalpine vegetation | Built-up area | Bush and shrub land | Cultivated land | Forest land | Grass land | Water body | Wetland |
| Afroalpine and sub-afroalpine vegetation | 4.97 | 0.19 | 69.08 | 5.60 | 5.44 | 35.99 | ..... | 0.10 |
| Built-up area | ..... | 12.25 | 50.50 | 81.60 | 0.35 | 3.01 | 0.05 | 0.84 |
| Bush and shrub land | 0.58 | 16.77 | 2,188.81 | 969.79 | 57.59 | 358.44 | 2.46 | 0.25 |
| Cultivated land | ..... | 11.20 | 721.33 | 4,573.38 | 6.90 | 186.26 | 0.12 | 12.01 |
| Forest land | 2.62 | 0.24 | 330.46 | 24.60 | 239.18 | 30.33 | 7.39 | 21.69 |
| Grass land | 2.05 | 1.51 | 377.81 | 465.28 | 13.57 | 957.73 | 0.14 | 6.20 |
| Water body | ..... | 0.08 | 4.22 | 0.08 | 2.45 | 0.05 | 3,042.28 | 2.26 |
| Wetland | 0.01 | 0.15 | 31.39 | 2.57 | 25.61 | 5.95 | 11.05 | 32.07 |

Table 18: Transformed versus unchanged LULC matrix in Tana Sub-basin (2014-2000)

| 2000 | 2014 | | | | | | | |
|---|---|---|---|---|---|---|---|---|
| | Afroalpine and sub-afroalpine vegetation | Built-up area | Bush and shrub land | Cultivated land | Forest land | Grass land | Water body | Wetland |
| Afroalpine and sub-afroalpine vegetation | 7.66 | ..... | 1.53 | 0.16 | 0.07 | 0.81 | ..... | ..... |
| Built-up area | ..... | 3.92 | 2.16 | 34.35 | 0.06 | 1.57 | 0.06 | 0.28 |
| Bush and shrub land | 21.39 | 27.28 | 1,728.83 | 1,626.45 | 72.58 | 230.91 | 21.22 | 44.93 |
| Cultivated land | 1.42 | 7.20 | 534.88 | 5,075.89 | 17.70 | 472.27 | 0.68 | 12.87 |
| Forest land | 1.24 | 2.11 | 113.39 | 36.28 | 153.54 | 7.23 | 15.86 | 21.45 |
| Grass land | 6.04 | 1.85 | 291.81 | 530.29 | 14.41 | 718.82 | 4.33 | 10.20 |
| Water body | ..... | 0.27 | 3.17 | 4.77 | 2.26 | 0.07 | 3,047.31 | 5.66 |
| Wetland | 0.00 | 1.19 | 12.45 | 35.50 | 12.14 | 2.24 | 11.87 | 24.65 |

Table 19: Transformed versus unchanged LULC in the Tana Sub-basin (2014-1986)

| 1986 | 2014 | | | | | | | |
|---|---|---|---|---|---|---|---|---|
| | Afroalpine and sub-afroalpine vegetation | Built-up area | Bush and shrub land | Cultivated land | Forest land | Grass land | Water body | Wetland |
| Afroalpine and sub-afroalpine vegetation | 22.23 | 0.19 | 31.18 | 12.28 | 4.93 | 50.53 | ..... | 0.03 |
| Built-up area | 0.06 | 4.32 | 14.49 | 105.23 | 0.35 | 23.34 | 0.19 | 0.61 |
| Bush and shrub land | 3.85 | 21.15 | 1,409.15 | 1,794.67 | 58.39 | 288.00 | 10.22 | 33.89 |
| Cultivated land | 0.04 | 8.35 | 478.95 | 4,619.37 | 19.53 | 363.53 | 0.81 | 20.62 |
| Forest land | 3.34 | 4.12 | 331.10 | 105.84 | 145.70 | 26.80 | 18.21 | 21.39 |
| Grass land | 8.20 | 4.53 | 402.45 | 674.10 | 31.69 | 678.34 | 9.18 | 15.82 |
| Water body | ..... | 0.19 | 3.55 | 4.08 | 2.15 | 0.15 | 3,035.31 | 6.00 |
| Wetland | 0.02 | 0.97 | 17.36 | 28.12 | 10.01 | 3.24 | 27.41 | 21.66 |

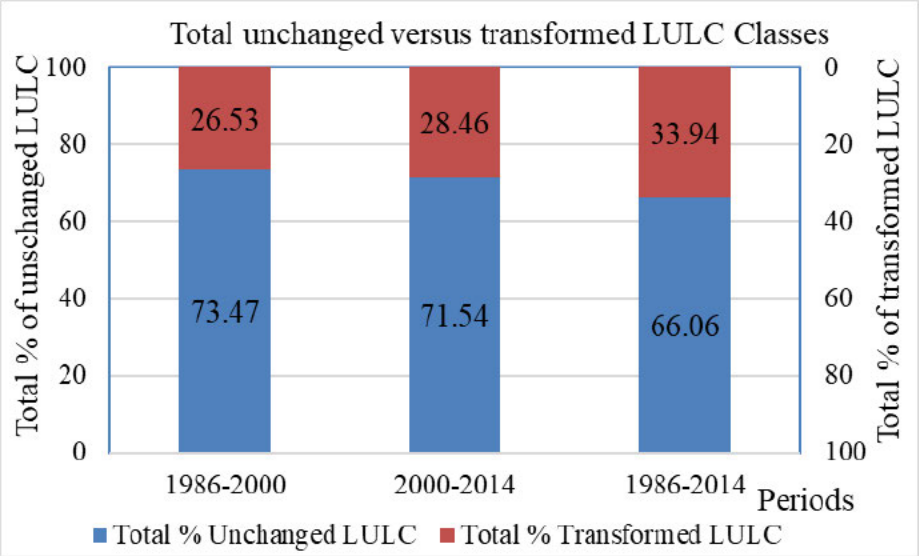


Figure 28: Summary of transformed versus unchanged land use land cover

Water bodies were well preserved over the assessment periods from 1986-2014, maintaining close to 99.87% coverage across the different timeframes. Built-up areas saw the most change/least preservation, maintaining only 9.24% of coverage over the whole assessment period. Wetlands also underwent significant changes, maintaining only 24.65% of their previous coverage areas.

This points to a loss of wetland habitats, likely due to development or conversion to other land uses. Comparing the first (1986-2000) and second (2000-2014) periods, water bodies preservation remained high but declined slightly from 99.7% to 99.47% (refer to Figure 29). This could be due to minor changes in water management or use overtime. Wetlands and built-up areas show the greatest changes/least preservation of all the land cover types assessed. Their protection and conservation seem to be lower than that of water bodies.

Despite increased expansion of cultivated land, the Tana Sub-basin still has a large area of grassland (grazing land) coverage. Grassland is the fourth largest in terms of coverage at 1,824.30 $km^2$ followed by cultivated land, water bodies, and bush, respectively. The government's recent conservation and rehabilitation program has resulted in significant coverage of bushes and shrubs inland, and current socio-economic pressures may influence it for the last year of assessment. The built-up areas are highly transformed and converted into other land cover types (refer to Figure 29). However, the transition statistics for these areas are not good indicators of the change actually expected on the ground. For instance, the Derg's villagization program, initiated in 1985, aimed to consolidate scattered farming communities into centralized villages. In subsequent years, some of these villages may have been transformed back into dispersed farming or cultivated land, further complicating the interpretation of land cover transitions.

Over the past 28 years, the waterbodies, including Lake Tana, have been the least disturbed in terms of coverage, while sub-Afroalpine vegetation is the most transformed. Cultivated land gained a large area from the other types.

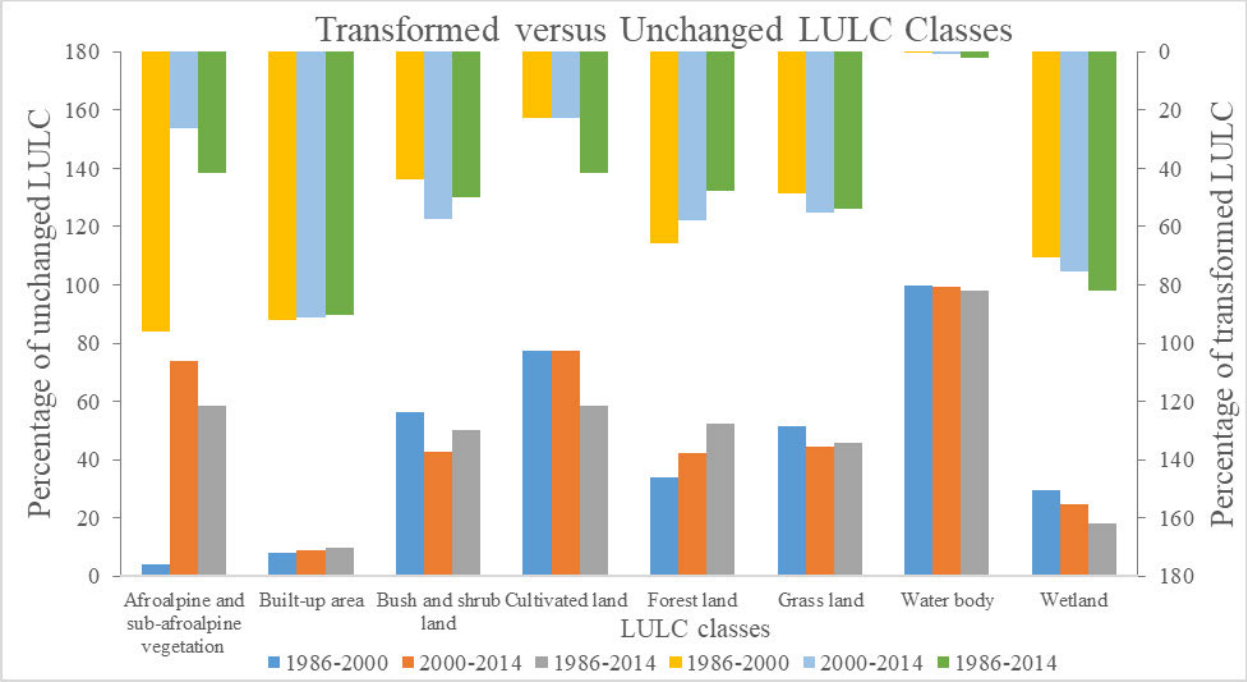


Figure 29: Transformed versus unchanged LULC: 1986-2000, 2000-2014, and 1986-2014

### 5.3.4 LULC change of four major watersheds

As indicated in Figure 30 and Table 20, the LULC of the major watersheds of the Tana Sub-basin changed in the past 28 years (1986-2014) (refer to Annexure 29). From 1986-2000 and 2000-2014, the highest LULC change was recorded in Rib (72.04%) (refer to Annexure 36 and Annexure 37) and Gumara watersheds (47.41%) (refer to Annexure 39, Annexure 40 and Annexure 41), respectively. Gilgel Abbay watershed showed highly transformed LULC (57.93%) for the past 28 years (Annexure 32, Annexure 31 and Annexure 30). The highest level of land cover remains unchanged in Megech (70.82%, 66.55%) from 1986-2000 (refer to Annexure 33) and 2000-2014 (Annexure 34), respectively. The overall LULC change in the whole study period for Megech is shown in Annexure 35. However, the overall (1986-2014) unchanged LULC recorded in the Rib watershed was 57.19% (refer to Annexure 38).

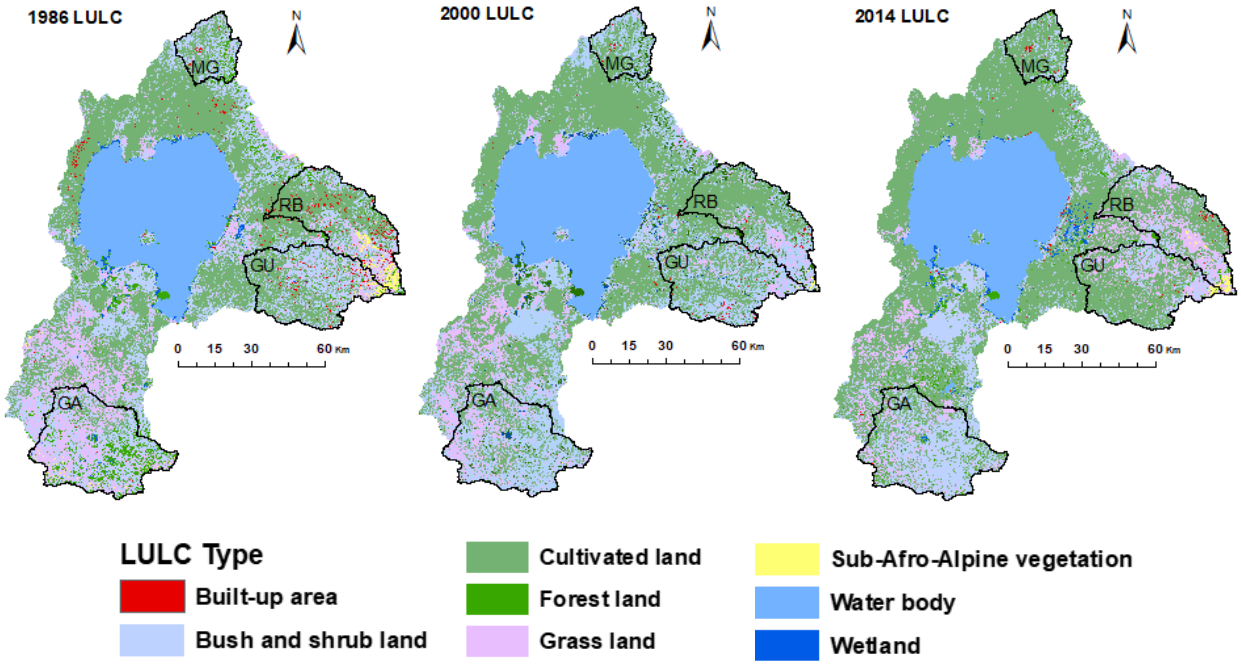


Figure 30: LULC change of four major watersheds in the Tana Sub-basin

Source: ADSWE Ethiopia

Afroalpine, wetland, and forest land were the most highly disturbed cover types in terms of transformation to other cover types in the past 28 years. In contrast, cultivated land increased over time in all the watersheds. Bush and shrubland coverage decreased in the past 28 years for the major watersheds, while it increased for Gilgel Abbay. Grassland increased for the Gumara and Rib watersheds and decreased for Gilgel Abbay and Megech (1986-2000). No significant cover conversion was observed on the water body in all eight major LULC types (refer to Figure 30). This transformed land use/land cover shows a significant impact on the water balance components (refer to Figure 33, Figure 34, Figure 35 and Figure 36).

Table 20: Percentage of unchanged and transformed LULC for major watersheds

| | Total unchanged LULC (%) | | | | Total transformed LULC (%) | | | |
|---|---|---|---|---|---|---|---|---|
| Year | Gumara | Rib | Megech | Gilgel Abbay | Gumara | Rib | Megech | Gilgel Abbay |
| 1986-2000 | 64.49 | 27.96 | 70.82 | 49.39 | 35.51 | 72.04 | 29.18 | 50.61 |
| 2000-2014 | 52.59 | 60.99 | 66.55 | 56.55 | 47.41 | 39.01 | 33.45 | 43.45 |
| 1986-2014 | 52.90 | 57.19 | 56.73 | 42.07 | 47.10 | 42.81 | 43.27 | 57.93 |

### 5.3.5 Sensitivity analysis, calibration, and validation

SWAT Calibration and Uncertainty Programs were developed for calibration, validation, and uncertainty analysis in the SWAT model. These programs were utilized to optimize the parameters of the SWAT model based on the study conducted by Abbaspour (2013). In the sensitivity analysis, streamflow data from four major rivers in the Tana Sub-basin were used for the period 1990-2013. The analysis employed a built-in tool in SWAT-CUP, which utilizes the global sensitivity design method. A total of 24 hydrological parameters were tested to assess their sensitivity for streamflow simulation in the study area (refer to Annexure 43). Table 21 presents the results of the sensitivity analysis, identifying the ten most sensitive parameters for streamflow simulation out of the 24 tested hydrological parameters. These parameters were selected based on their t-statistic and p-value, which are indicators of parameter sensitivity order for model calibration and validation.

The t-statistics measure the strength of the relationship between a parameter and the model output. A higher absolute value of the t-statistic indicates the parameter’s stronger influence on the streamflow simulation. However, the p-value represents the statistical significance of the parameter's sensitivity. A lower p-value suggests a higher level of confidence in the parameter's influence on the streamflow simulation. By considering both the t-statistic and p-value, the parameters with high absolute t-statistic values and low p-values are identified as the most sensitive for streamflow sensitivity analysis in the model. These parameters have a significant impact on the simulated streamflow and are crucial for accurate calibration and validation of the SWAT model in the study area.

The sensitivity analysis identified several key parameters for streamflow simulation in different rivers within the Tana Sub-basin. The curve number for moisture condition II (CN2) was found to be the most sensitive parameter for streamflow simulation in Gilgel Abbay and Megech rivers. The curve number represents the runoff potential of a watershed based on soil moisture conditions, land use, and hydrological characteristics. The groundwater "revap" coefficient (GW_REVAP) was identified as the most sensitive parameter for streamflow simulation in the Rib River. This represents the rate at which groundwater is returned to the atmosphere through evaporation. The groundwater delay (GW_DELAY) parameter was found to have the highest sensitivity for streamflow simulation in the Gumara River. This parameter reflects the time delay between groundwater recharge and its subsequent contribution to streamflow. In this study, the average curve number for the Tana Sub-basin ranges from 84 to 91, depending on the year and changes in LULC. The calibrated values of key SWAT model parameters: CH_K2, GW_REVAP, and RCHRG_DP are 19.89 mm/hr, 0.108, and 0.565, respectively.

Several parameters were identified as having high sensitivity order across multiple watersheds. These include the threshold depth of water in the shallow aquifer required for return flow to occur (GWQMN), baseflow alpha factor (ALPHA_BF), deep aquifer percolation fraction (RCHRG_DP), and depth from the soil surface to the bottom of the layer (Sol_Z). These parameters are crucial for accurately representing the hydrological processes and flow dynamics within the Tana Sub-basin. The results suggest that accurate estimation of these sensitive parameters is essential to improve streamflow simulations in the Sub-basin. They play key roles in the overall hydrological processes and should be carefully calibrated to ensure reliable model output. To visualize the findings, Annexure 44, Annexure 45, Annexure 46 and Annexure 47 provide graphical representations of the sensitivity analysis results, highlighting the relative importance of the identified parameters for each river.

Table 21: SWAT streamflow sensitive parameters and fitted values after calibration

| | Gumara River | | Rib River | | Megech River | | Gilgel Abbay River | |
|---|---|---|---|---|---|---|---|---|
| | Sensitive parameters | Fitted value | Sensitive parameters | Fitted value | Sensitive parameters | Fitted value | Sensitive parameters | Fitted value |
| 1 | A_GW_DELAY | -38.06 | V_GW_REVAP | 0.25 | R_CN2 | 1.68% | R__CN2 | 13.58% |
| 2 | R_CN2 | -3.05% | V_ALPHA_BF | 0.02 | A_GW_DELAY | -66.11 | R__SOL_Z | 15.81% |
| 3 | A_GWQMN | -257.03 | V_RCHRG_DP | 0.09 | A_GWQMN | 917.52 | A__GWQMN | -186.62 |
| 4 | V_GW_REVAP | 0.02 | A_GW_DELAY | -17.16 | V_GW_REVAP | 0.09 | R__SOL_ALB | 30.88% |
| 5 | V_RCHRG_DP | 0.21 | V_CH_EROD | 0.48 | V_RCHRG_DP | 0.52 | V__CH_EROD | 0.58 |
| 6 | R_SOL_AWC | -10.74% | R_CN2 | -3.33% | R_SLSUBBSN | -6.16% | R__SOL_AWC | -7.38% |
| 7 | V_CH_EROD | 0.40 | A_REVAPMN | -129.70 | A_EPCO | 0.51 | A__GW_DELAY | 2.19 |
| 8 | A_EPCO | 0.38 | R_SOL_ALB | 5.10% | V_SURLAG | 4.78 | V__SURLAG | 10.46 |
| 9 | V_BIOMIX | 1.00 | R_SOL_Z | 0.73% | V_CH_EROD | 0.53 | V__CH_COV | 0.85 |
| 10 | V_CH_N2 | 0.42 | R_OV_N | -5.89% | R_OV_N | 5.86% | V__ALPHA_BNK | 0.19 |

*R indicates multiple existing values, A adds on existing values, and V replaces the existing values

The results indicate that the SWAT model performed well in simulating streamflow in the Tana Sub-basin during the calibration and validation periods. The NSE values, which measure the agreement between observed and simulated streamflow, ranged from 0.72 to 0.88 during calibration and from 0.57 to 0.89 during validation. These indicate good performance of the model in the streamflow simulation. The performance of the best simulation, which utilizes the fitted parameter values obtained from calibration and validation, is presented in Figure 31. The figure shows that the model's streamflow simulation closely matches the observed streamflow data, indicating the applicability of the model in the Tana Sub-basin.

As stated by Santhi *et al.* (2001), NSE values that are greater than or equal to 0.50 are thought to be good enough for SWAT model application. Furthermore, Setegn *et al.* (2009) suggested that a model's performance can be considered satisfactory if $R^2$ is greater than 0.6 and NSE is greater than 0.5. The results in Table 22 demonstrate that most of the $R^2$ and NSE values in the Tana Sub-basin exceeded these threshold values, further indicating the SWAT model's strong performance in representing the hydrological conditions.

While the model generally performed well in simulating streamflow, there might be some discrepancies regarding peak flows and baseflows. It is important to note that these differences can occur due to various factors, such as uncertainties in input data, model limitations, or local hydrological processes that are not fully captured by the model. Overall, the findings indicate that the SWAT model provided a robust representation of the hydrological conditions in the Tana Sub-basin, with satisfactory to excellent performance in simulating streamflow.

Table 22: Model performance during calibration and validation periods

| Sub-basin | Major watersheds | Calibration | | | | Validation | | | |
|---|---|---|---|---|---|---|---|---|---|
| | | $R^2$ | NS | PBIAS | RSR | $R^2$ | NS | PBIAS | RSR |
| Tana | Gumara (GU) | 0.84 | 0.83 | 16.20 | 0.41 | 0.83 | 0.80 | 24.60 | 0.45 |
| | Megech | 0.72 | 0.72 | -9.4 | 0.53 | 0.74 | 0.57 | 44.1 | 0.65 |
| | Gilgel Abbay | 0.88 | 0.88 | 2.90 | 0.35 | 0.71 | 0.65 | -4.3 | 0.93 |
| | Rib | 0.83 | 0.82 | 4.10 | 0.42 | 0.90 | 0.89 | 11.60 | 0.33 |

In the calibration period, the monthly flow hydrograph of observed and simulated streamflow for the major watersheds in the Tana Sub-basin shows that the simulated streamflow generally replicates the observed streamflow (refer to Figure 31). However, some deviations are observed between simulated and observed flows. The model tends to overestimate the observed streamflow during the calibration period, except for the Megech watershed. This suggests that the model's simulated streamflow values are higher than the observed values in most of the watersheds. The model's performance in predicting peak flows and baseflow is not as accurate as its performance in capturing the rising and falling limbs of the hydrographs. This indicates that it may have difficulty in reproducing the extreme high and low flow of events, as well as the sustained baseflow contributions. These discrepancies could be due to limitations in the model's representation of flow routing processes, parameter calibration, or uncertainties in input data.

There are observed differences in the trend between the calibration and validation periods for the Megech watershed. This suggests that there are uncertainties in the simulated flow which potentially stem from errors in input data (e.g., temperature, rainfall), soil characteristics (e.g., infiltration capacity), or other unknown factors specific to the watershed. These observations align with similar findings in hydrological studies conducted by Setegn *et al.* (2009). This study likely encountered similar challenges and uncertainties in streamflow simulation, emphasizing the importance of recognizing and addressing these limitations in hydrological modeling.

The simulated streamflow did not accurately replicate the observed streamflow during the validation period. However, despite this discrepancy, the overall performance of the calibrated model was considered satisfactory for further analysis. The hydrographs of the Megech and Gilgel Abbay watersheds during the validation period indicate that the simulated streamflow poorly replicated the observed streamflow. This suggests that the model's ability to capture the dynamics and patterns of streamflow in these watersheds was limited. The discrepancies between observed and simulated streamflow could be attributed to various factors, including uncertainties in input data, errors in soil characteristics, or other unaccounted-for factors specific to these watersheds. The finding on poor replication of observed streamflow during the validation period in the Megech watershed align with previous studies conducted by Halefom *et al.* (2018a); (2018b). Similarly, the poor replication of observed streamflow in the Gilgel Abbay watershed is consistent with the findings of Worqlul *et al.* (2018). These previous studies likely encountered similar challenges and limitations in accurately simulating streamflow in these specific watersheds.

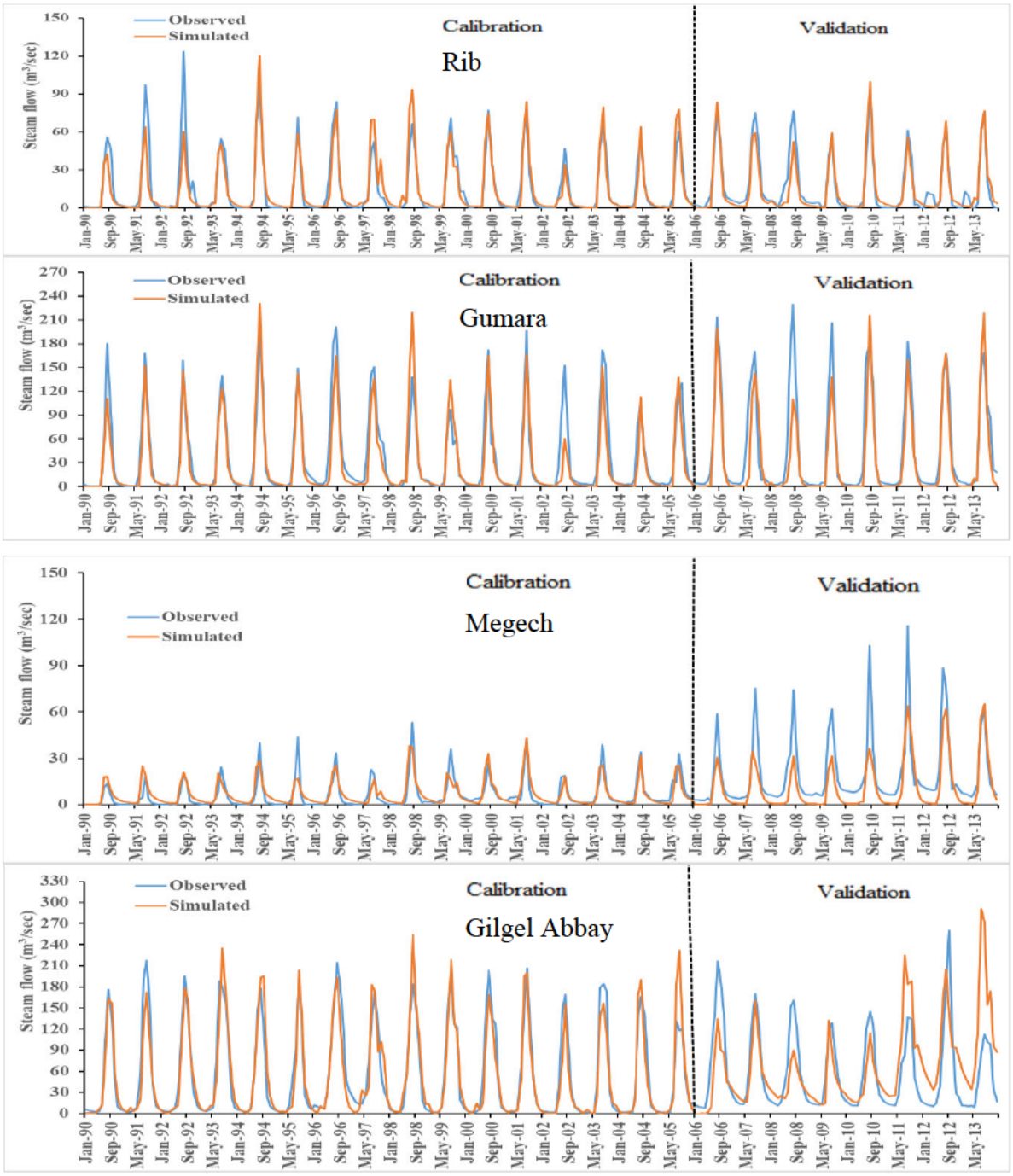


Figure 31: Streamflow hydrographs during calibration and validation

### 5.3.6 Impacts of LULC change on water resources

As indicated in Table 16, LULC changes occurred in the Tana Sub-basin over a period of 28 years, specifically in 1986, 2000, and 2014. The assessment of the LULC maps revealed notable changes

in various land cover classes within the study area. The results indicate that these LULC changes have an impact on water resources within the study area. Land use land cover change can affect hydrological processes such as infiltration, baseflow, runoff generation, and evapotranspiration, consequently influencing water availability and streamflow dynamics. The study considered baseflow (BF) as the combination of lateral flow and groundwater's contribution to streamflow for further analysis.

The changes in LULC classes and their corresponding average annual water balance components from 1986 to 2014 are shown in Figure 32, Annexure 48, Annexure 49, Annexure 50, Annexure 51, and Table 23. The average annual water yield in the Tana Sub-basin increased from 1986 to 2000 and 2014. Compared to the baseline year of 1986, the water yield was 93.57 mm and 79.26 mm higher in 2000 and 2014, respectively. This corresponds to an increase of 14.88% in 2000 and 12.6% in 2014 compared to 1986. The average annual baseflow also exhibited changes in response to LULC changes from 1986 to 2000 and 2014. It increased gradually from 291.5 mm in 1986 to 345.16 mm in 2000, representing an 18.4% increase. However, from 2000 to 2014, the baseflow decreased to 320.45 mm, a decrease of 7.16%. Overall, for the entire study period (1986 to 2014), the baseflow increased by 9.93%. The average annual surface runoff increased by 12% in 2000 and 16.16% in 2014 compared to 1986.

Table 23: LULC and annual average hydrological component changes in Tana Sub-basin

| Period | LULC (%) | | | | | | | | Water resources component (mm) | | | |
|---|---|---|---|---|---|---|---|---|---|---|---|---|
| | Afroalpine and sub-Afroalpine vegetation | Built-up area | Bush and shrubland | Cultivated land | Forest land | Grass land | Water body | Wetland | ET | SURQ | WYLD | BF |
| 1986 | 0.81 | 0.99 | 24.06 | 36.64 | 4.36 | 12.13 | 20.29 | 0.72 | 913.65 | 233.61 | 628.88 | 291.50 |
| 2000 | 0.07 | 0.28 | 25.09 | 40.71 | 2.33 | 10.49 | 20.37 | 0.67 | 745.62 | 261.65 | 722.45 | 345.16 |
| 2014 | 0.25 | 0.29 | 17.87 | 48.82 | 1.81 | 9.53 | 20.62 | 0.80 | 790.34 | 271.36 | 708.14 | 320.45 |
| 2000-1986 | -0.74 | -0.71 | 1.03 | 4.07 | -2.03 | -1.64 | 0.08 | -0.06 | -168.03 | 28.04 | 93.57 | 53.65 |
| 2014-2000 | 0.18 | 0.01 | -7.22 | 8.12 | -0.52 | -0.96 | 0.25 | 0.13 | 44.72 | 9.71 | -14.31 | -24.71 |
| 2014-1986 | -0.56 | -0.70 | -6.19 | 12.18 | -2.55 | -2.60 | 0.33 | 0.07 | -123.31 | 37.75 | 79.26 | 28.95 |

*ET - (Evapotranspiration); SURF - (Surface runoff); WYLD - (Water yield); and BF - (Baseflow)

In contrast to surface runoff and baseflow, average annual evapotranspiration (ET) decreased with LULC changes. In 2000, the ET was 168.03 mm lower than in 1986, representing an 18.39% decrease. Similarly, in 2014, the ET was 123.31 mm lower than in 1986, a 13.49% decrease. From 2000 to 2014, average annual surface runoff and evapotranspiration increased while the average annual water yield and baseflow decreased. The changes in the water balance components demonstrate the influence of LULC changes on the hydrological regime in the Tana Sub-basin. The increase in water yield and surface runoff suggests a greater contribution of runoff to the streamflow due to changes in LULC. However, the decrease in evapotranspiration and baseflow indicates potential impacts on water availability and groundwater recharge. Table 23 provides more details on these changes and the specific values for each LULC map and water balance components.

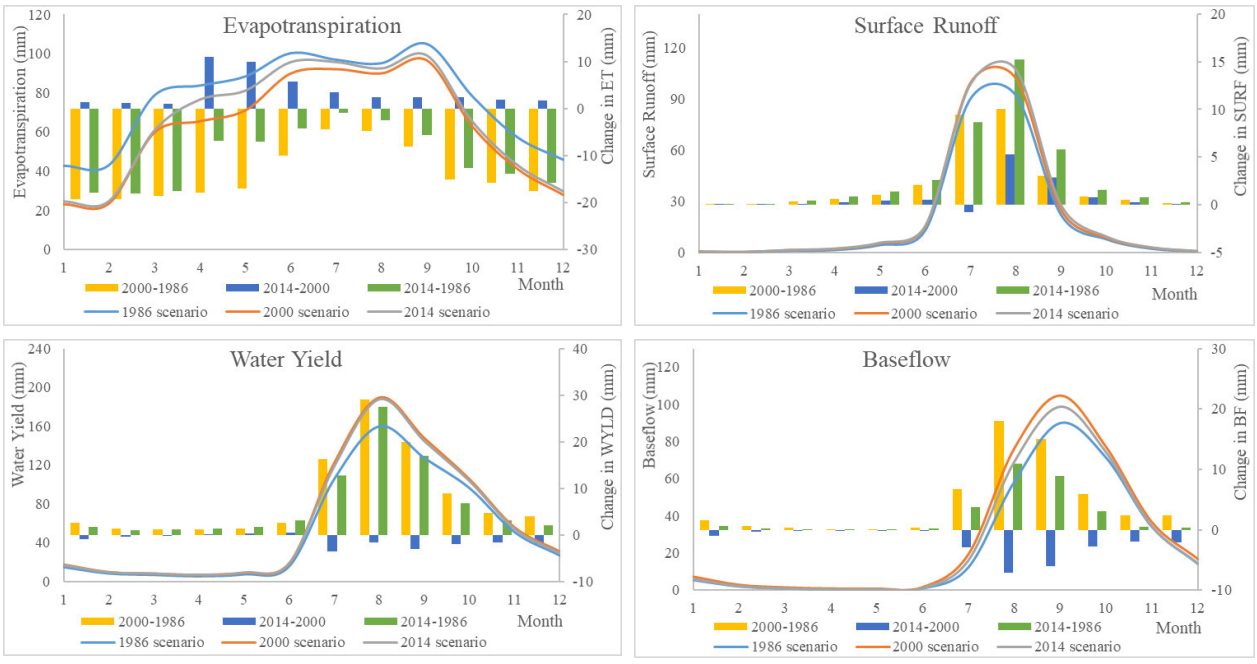


Figure 32: Monthly average response on water balance components for LULC change

The changes in average monthly evapotranspiration, surface runoff, water yield, and baseflow in the study area can be attributed to the LULC changes that occurred from 1986 to 2014 (refer to Table 16 and Figure 32). The expansion of cultivated land and the reduction of bush, shrubland,

grassland, and forest cover contribute to an increase in surface runoff and water yield, while evapotranspiration and baseflow are reduced. Woldesenbet *et al.* (2017) found a strong positive correlation between the extent of cultivated land and surface runoff components, indicating that expansion of the former contributes to an increase in the surface runoff. Conversely, there are strong negative correlations between shrubland and surface runoff components. This shows that areas with more shrubland tend to have lower surface runoff. In terms of baseflow, the expansion of cultivated land is negatively correlated, while the percentage of bush and shrubland shows a positive correlation. The expansion of cultivated areas has likely contributed to increased surface runoff by reducing the infiltration capacity of the soil (Franczyk *et al.* 2009).

The study reveals similar increases in average monthly and annual surface runoff due to the expansion of cultivated land and reduction of shrubland over the 28-year period. This implies that the changes in LULC have led to increased surface runoff and water yield. The reduction in forest cover also contributes to these changes, indicating the influence of forest cover on evapotranspiration. Forests with higher covers have higher rates of transpiration, resulting in increased evapotranspiration. This relationship is supported by the high negative correlation between open forests, surface runoff, and water yield (Awotwi *et al.* 2019). However, undisturbed water bodies in the Sub-basin show no significant changes in evaporation. On average, baseflow declined from 1986 to 2000 but increased from 2000 to 2014. The specific reasons for these changes and the values associated with them may require further investigation.

The study further emphasizes the influence of LULC changes on the water balance components in the Tana Sub-basin. The expansion of cultivated land in the study area has resulted in the replacement of grassland, bush, and shrubland. Compared to grassland and shrubland, cultivated land has a lower soil infiltration rate, percolation, and baseflow, while it increases surface runoff. This suggests that conversion of grassland and shrubland to cultivated land disrupts the natural water balance by reducing infiltration and increasing runoff. The comparison between changes in water yield and LULC changes in the Tana Sub-basin reveals that the increased water yield from 1986 to 2014 is primarily attributed to the gradual expansion of cultivated land and the

simultaneous decrease in bush and shrubland. This indicates that the changes in LULC, specifically conversion of natural vegetation to cultivated land, have a significant impact on water yield.

In summary, the study demonstrates that LULC changes have significant impacts on various components of the water balance, including infiltration rates, runoff production, total simulation flow, interflow, baseflow, water yield, evapotranspiration, and soil water retention capacity. These changes affect the overall water balance in the study area. This information adds to the understanding of the complex relationship between LULC dynamics and water resources in the Tana Sub-basin.

### 5.3.7 Impact of LULC change on evapotranspiration of major watersheds

The average monthly values of evapotranspiration simulated from each LULC map and its changes between each scenario for four major watersheds of the Tana Sub-basin are shown in Figure 33. The average monthly ET values increased over time in most of the major watersheds, except for Megech. The highest ET values were observed during the wet season (June to September). This indicates that evapotranspiration is influenced by both LULC changes and seasonal variations.

The average annual ET values in different watersheds exhibited varying trends. For example, in Megech, ET decreased by 5.42% in 2000 and 2.13% in 2014 compared to the baseline year of 1986, and in Rib, it decreased by 3.39% in 2000 but increased by 67.76% in 2014. In Gumara, ET increased by 16.71% in 2000 and 22.73% in 2014, and in Gilgel Abbay, it increased by 5.71% in 2000 and 6.79% in 2014. These variations indicate the influence of LULC changes on ET patterns in different watersheds. Expansion of cultivated land and reduction in forest and shrubland coverage, along with relatively unchanged water bodies, are observed in the watersheds. These changes can lead to a decrease in ET due to declining transpiration rates. The reduction in forest and shrubland cover affects the leaf area index (LAI), which in turn influences ET by controlling soil moisture content. In addition, vegetation growth, characterized by taller canopy height and abundant leaves, is possible when sufficient soil moisture is available (Wang *et al.* 2009).

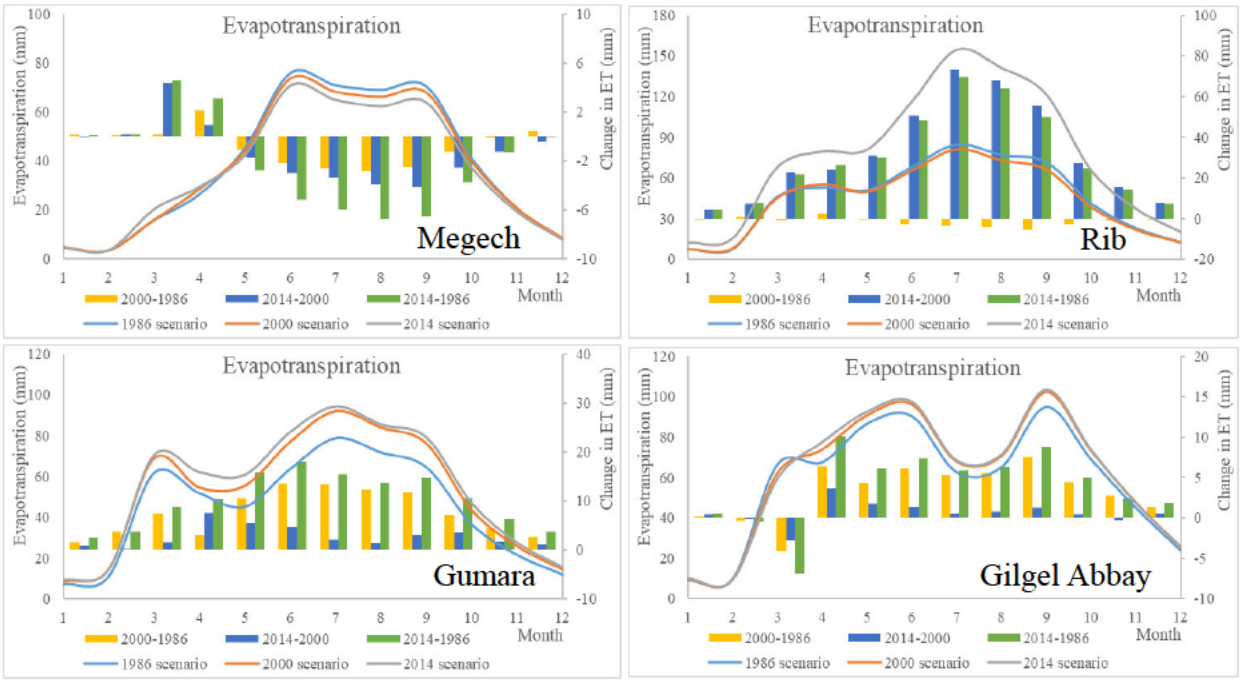


Figure 33: Monthly average response on watersheds' evapotranspiration for LULC changes

These findings highlight the significant impact of LULC changes on evapotranspiration in the Tana Sub-basin. Expansion of cultivated land, reduced forest and shrubland cover, and seasonal variations all contribute to the observed changes in evapotranspiration patterns.

### 5.3.8 Impact of LULC change on surface runoff of major watersheds

Figure 34 provides the average monthly values of surface runoff simulated from each LULC map and its changes within the three scenarios in the four major watersheds of the Tana Sub-basin. The average monthly surface runoff values increased over time for the four major watersheds. The response was particularly high during the wet season (June to September), while in the dry season, the increment in surface runoff was relatively smaller. This indicates that LULC changes, in conjunction with seasonal variations, play a significant role in surface runoff generation.

The average annual surface runoff values in different watersheds exhibited varying trends. In Megech, surface runoff decreased by 9.63% (17.13 mm) in 2000 but increased by 15.99% (31.76

mm) in 2014 compared to the baseline year of 1986. In Rib, it increased by 16.08% (41.22 mm) in 2000 and 93.54% (239.82 mm) in 2014. In Gumara, surface runoff increased by 8.74% (38.98 mm) in 2000 and 11.05% (49.32 mm) in 2014. Lastly, in Gilgel Abbay, it increased by 15.14% (132.42 mm) in 2000 and 20.69% (180.91 mm) in 2014. These variations indicate the impact of LULC changes on surface runoff in different watersheds.

The continuous increment in surface runoff observed in most scenarios suggests a general trend of increased runoff due to LULC changes. However, there may be uncertainties caused by errors in input data, such as temperature and rainfall, as well as errors in soil characteristics and infiltration capacity. Other unknown activities in the watersheds may also contribute to the observed variations in surface runoff. Overall, in the Tana Sub-basin, average annual surface runoff increased by 12% in 2000 and 16.16% in 2014 compared to the baseline year of 1986. This indicates a general increase in surface runoff for the entire Sub-basin, further emphasizing the impact of LULC changes on hydrological processes.

Figure 29 shows that cultivated land expanded over time, while shrub and forest land was reduced. This indicates a significant change in LULC patterns in the study area. The surface runoff response was positively correlated with the expansion of cultivated land and negatively correlated with reduced forest and shrubland coverage. Together, these factors led to increased surface runoff due to altered infiltration rates and decreased vegetation cover. The expansion of settlements/urbanization creates more impervious surfaces, such as roads and buildings, which inhibit the percolation of water into the soil and increase surface runoff. This further contributes to the positive correlation between LULC changes and surface runoff.

Changes in LULC within a watershed have a significant effect on water infiltration, accumulation, and flow over the land. These changes affect the runoff characteristics, which, in turn, influence the availability of surface and groundwater in the area. The observed surface runoff responses in the major watersheds of the study area (refer to Figure 29) can be attributed to these LULC changes. The study's outcomes align with previous research conducted in the Upper Blue Nile

Basin in Ethiopia by Woldesenbet *et al.* (2017, 2018). These studies also identified an increase in surface runoff as a result of expanding settlement/built-up areas and agriculture/cultivated land at the expense of closed and open forests.

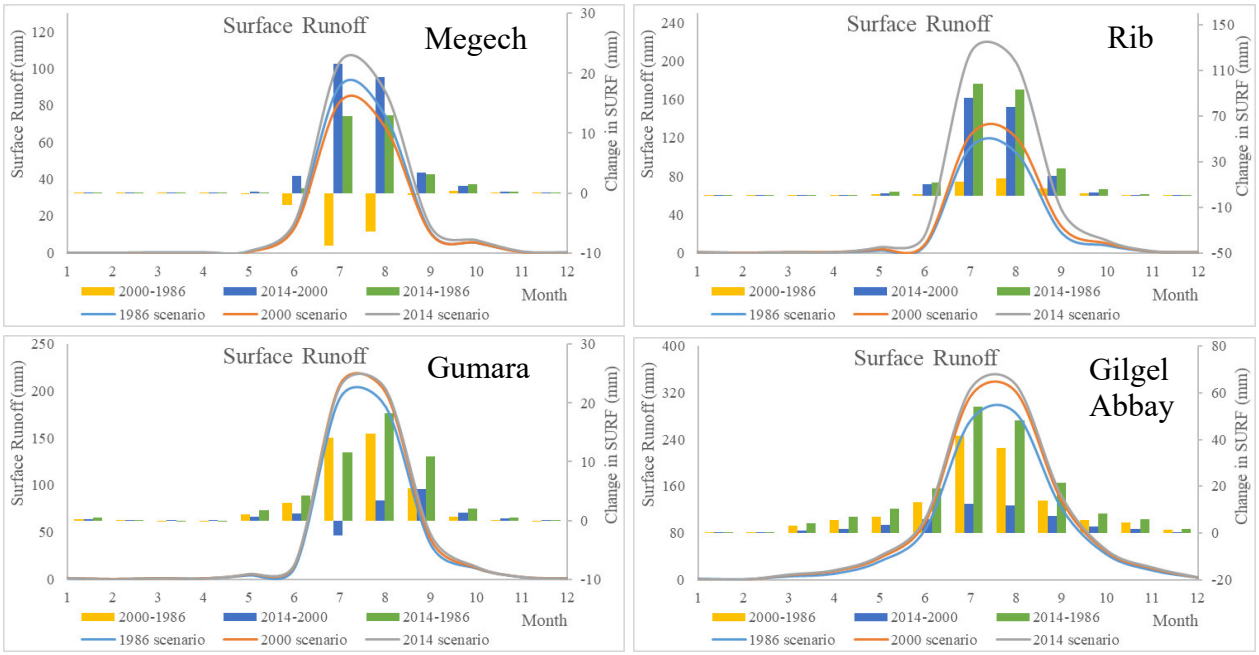


Figure 34: Monthly average response on watersheds' surface runoff for LULC changes

Overall, the study's findings highlight the significant impact of LULC changes, including the expansion of cultivated land and reduction of forest and shrubland, on surface runoff patterns in the Tana Sub-basin. The expansion of settlements/urbanization further exacerbates the increase in surface runoff. The increase in surface runoff, particularly during the wet season, suggests that LULC changes contribute to increased runoff generation. These findings are consistent with previous studies conducted in similar regions. However, it is important to consider uncertainties and potential error sources in the data analysis when interpreting the results.

### 5.3.9 Impact of LULC change on water yield of major watersheds

Figure 35 shows the average monthly water yield simulated from each LULC map and its changes within the three scenarios in the four major watersheds of the Tana Sub-basin. The average monthly water yield values increased over time for the four major watersheds. Similar to surface runoff, the response was particularly high during the wet season (June to September), while in the dry season, the increment in water yield was relatively smaller. This indicates that LULC changes, combined with seasonal variations in precipitation, play a significant role in water yield.

The average annual water yield values exhibited varying trends in different watersheds within the Tana Sub-basin. The changes in water yield were influenced by the specific characteristics and dynamics of each watershed, including the extent and nature of LULC changes. In the Megech watershed, there was a notable decrease in water yield, with values decreasing by 46.63% in 2000 and 11.42% in 2014 compared to the baseline year of 1986. This suggests that the LULC changes in this watershed, such as the expansion of cultivated land and reduced forest and shrubland, may have contributed to a decrease in water yield. In contrast, the Rib watershed experienced an increase in water yield, with values increasing by 4.2% in 2000 and 81.68% in 2014 compared to the baseline year. This indicates that the LULC changes in this watershed, such as the expansion of cultivated land and other factors, may have led to an increase in water yield.

Similarly, the Gumara and Gilgel Abbay watersheds showed an increase in water yield, with varying magnitudes. In Gumara, it increased by 27.09% in 2000 and 30.79% in 2014, while in Gilgel Abbay, water yield increased by 23.43% in 2000 and 14.19% in 2014. These variations indicate the influence of LULC changes on water yield patterns in different watersheds. A continuous increment in water yield was observed in all scenarios, except for the Megech watershed, where it declined. This suggests that LULC changes contribute to increased water yield, except in the specific case of the Megech watershed.

The average annual water yield in the Tana Sub-basin exhibited an overall increasing trend, with an increase of 14.88% in 2000 and 12.6% in 2014 compared to the baseline year of 1986. Figure

35 shows a monthly increasing trend in water yield for the Sub-basin. The expansion of cultivated land and reduction in shrub and forest land coverage over time are identified as factors contributing to the observed increase in water yield. These LULC changes can affect the hydrological processes within the study area, such as altering infiltration rates, vegetation cover, and surface runoff dynamics. The result is consistent with previous studies conducted in other regions, such as the Pra River Basin in Ghana (Awotwi *et al.* 2019) and the Upper Blue Nile River in Ethiopia (Sead *et al.* 2010), which reported similar effects of LULC changes on water yield.

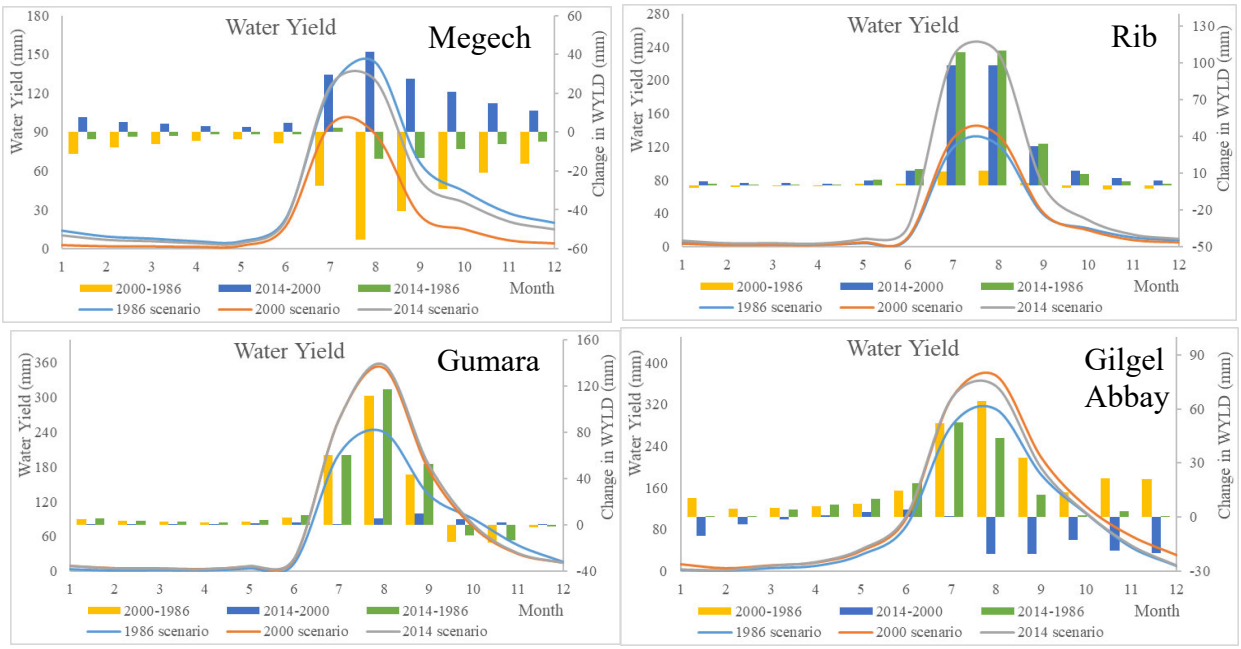


Figure 35: Monthly average response on watersheds' water yield for LULC changes

### 5.3.10 Impact of LULC change on baseflow of major watersheds

Average baseflow values simulated monthly from each LULC map and their changes within the three scenarios for the four major watersheds of the Tana Sub-basin are shown in Figure 36. The variation in baseflow was higher during the wet season than the dry season. This indicates that baseflow is influenced by seasonal variations in precipitation and hydrological processes. The average monthly baseflow values exhibited varying trends in the different watersheds. In the Rib and Gumara watersheds, there was an increasing trend in baseflow over time. This can be attributed

to the expansion of cultivated land and grassland, coupled with a reduction in shrubland. In contrast, the Megech and Gilgel Abbay watersheds experienced a decline in baseflow. Changes in LULC in these watersheds, such as the increase in cultivated land and reduction in grassland and shrubland, likely contributed to decreased baseflow. Such changes thus have significant implications for baseflow. As noted by Woldesenbet *et al.* (2017), expansion of cultivated land can decrease the soil infiltration rate and percolation, leading to a decrease in baseflow and an increase in surface runoff. The specific changes in each land cover category (cultivation, grassland, and shrubland) within the watersheds have varying impacts on hydrological components.

The average annual baseflow values exhibited different changes compared to the baseline year of 1986. For example, in the Megech watershed, baseflow decreased by 36.59% (24.55 mm) in 2000 and 41.06% (27.55 mm) in 2014. In Rib, it decreased by 1.27% (0.44 mm) in 2000 and increased by 116.97% (40.66 mm) in 2014. In Gumara, baseflow increased by 31.12% (90.72 mm) in 2000 and 36.15% (105.40 mm) in 2014. Lastly, in Gilgel Abbay, it increased by 63.15% (121.51 mm) in 2000 and then decreased by 13.74% (26.44 mm) in 2014. These findings highlight the influence of LULC changes on baseflow in the four major watersheds of the Tana Sub-basin. The expansion of cultivated land and changes in other land cover categories can thus have contrasting effects on baseflow, depending on the specific watershed dynamics.

In the Tana Sub-basin, the average annual baseflow exhibited an overall increasing trend, with the 18.4% increase in 2000 and 9.93% in 2014 compared to the baseline year of 1986. The graphical representation of the baseflow in Figure 36 demonstrates continuously increasing trends between 2000 and 1986 baseline years, as well as between 2014 and 1986. However, there is a declining trend between 2014 and 2000. These trends are likely influenced by variation in LULC changes and the proportional changes in LULC types within the Sub-basin. According to Woldesenbet *et al.* (2017), the expansion of cultivated land is strongly negatively correlated with the groundwater component of the water balance. In contrast, the percentage of bush and shrubland is strongly positively correlated with the groundwater component. This suggests that changes in LULC, particularly the expansion of cultivated land and reduced bush and shrubland, can have a

significant impact on baseflow characteristics and the availability of surface and groundwater resources.

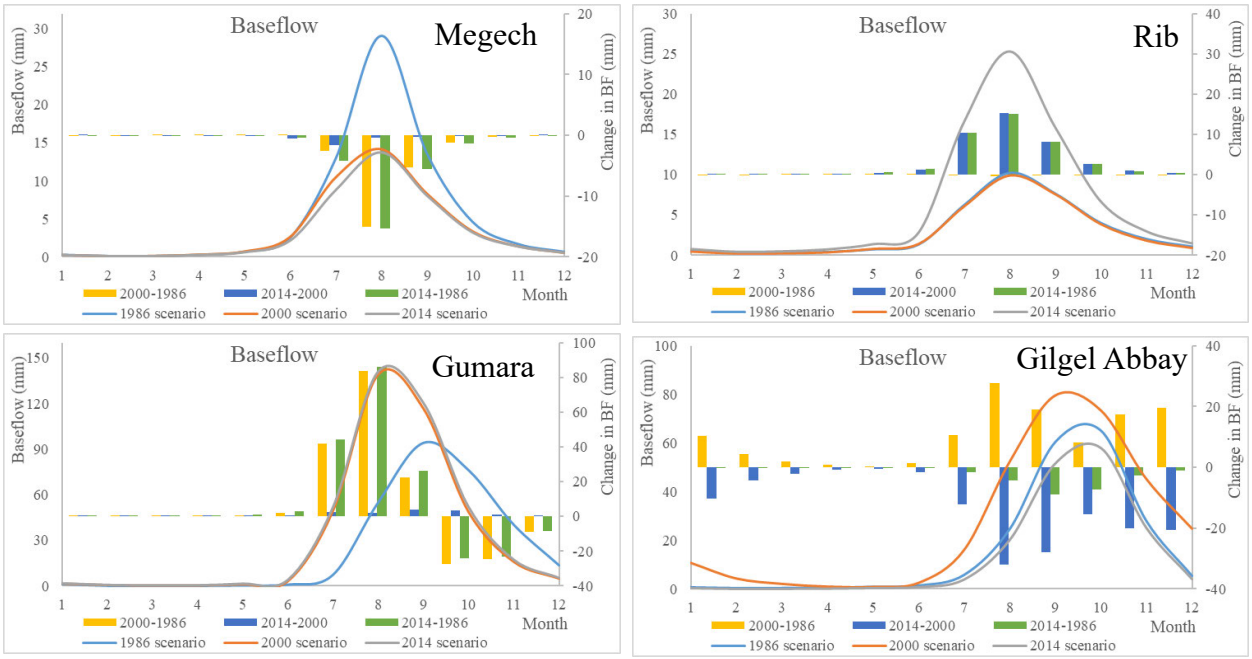


Figure 36: Monthly average response on watersheds' baseflow for LULC changes

The deviation of baseflow in each scenario, particularly from June to November, is high. This can be attributed to the combination of high rainfall intensity and variability during this period, as well as agricultural practices and the expansion of cultivated land. These factors contribute to changes in baseflow magnitude on an annual and monthly basis for the major watersheds within the study area. Therefore, it is essential to consider these changes in LULC when assessing water balance components and planning water management strategies in the Sub-basin.

## 5.4 Results and discussion for objective 4

*To develop sustainable and efficient adaptive options for integrated water resources management of Tana Sub-basin*

The study area is a populous area that has been identified as a growth corridor for Ethiopia because of its vast productive potential and economic development (Alemayhu 2006; NBI 2009; McCartney *et al.* 2010; Taye *et al.* 2021). Lake Tana at the center of the Sub-basin is also a valuable source of fresh water for the Sub-basin and the River Abbay (Blue Nile) (SMEC 2008); however, access to clean, reliable sources of water is a significant challenge for those living in the study area. Recent developments in the area include booming small, medium, and large-scale irrigation, horticulture, industries, hotels, and so on which depend on the Sub-basin's water resources (Taye *et al.* 2021). Given that such activities will continue to increase in the future, providing water for the Sub-basin will remain a challenge. It is, therefore, necessary to develop and manage water resources and water allocation plans.

### 5.4.1 Water demand assessment in the Tana Sub-basin

The area covered by rainfed agriculture, irrigation, and horticulture in the study area was assessed, alongside estimated water consumption. In the absence of well-organized recorded data on irrigation water consumption, a water abstraction rate of 0.9 liters per second per hectare recommended by Taye *et al.* (2021) was adopted to estimate total annual water consumption. Total annual water consumption for irrigation and horticulture was estimated at approximately 555.76 million cubic meters (MCM) and 46.52 MCM, respectively. The study found that approximately 38,694 hectares of land in the study area were covered by small-scale irrigation. In the 2020/21 dry season, an estimated volume of 430 MCM of water was extracted from the Sub-basin for irrigation purposes.

The regions in the eastern and southern parts of the Sub-basin such as Rib, Gumara, and the southern part of Gilgel Abbay, had the highest coverage of rainfed agriculture. In contrast, Rib, and the upper part of Gilgel Abbay had the highest coverage of irrigation areas. The study identified water shortages in the eastern parts of the Sub-basin during the dry season. This suggests

that water availability may be limited in these areas, potentially affecting agricultural practices and water abstraction for irrigation. The lowest water abstraction for rainfed agriculture was observed in Bahir Dar Zuria (138.47 MCM/year), while the lowest irrigation water abstraction was observed in West Tana (27.89 MCM/year) and Bahir Dar Zuria (8.17 MCM/year). High water abstraction by horticulture was observed in the lower (23.14 MCM/year) and upper (10.18 MCM/year) parts of Gilgel Abbay, Bahir Dar Zuria (3.9 MCM/year), and the Gumara watershed (3.78 MCM/year) (refer to Figure 37). The expansion of irrigation in the study area has implications for the sustainability of available water resources. This suggests that more precise irrigation technologies to minimize water losses, adaptive strategic options for sustainable water resource management, and alternative water sources may be necessary to sustain projected irrigation expansion (Abera *et al.* 2020; Tsakiris *et al.* 2023).

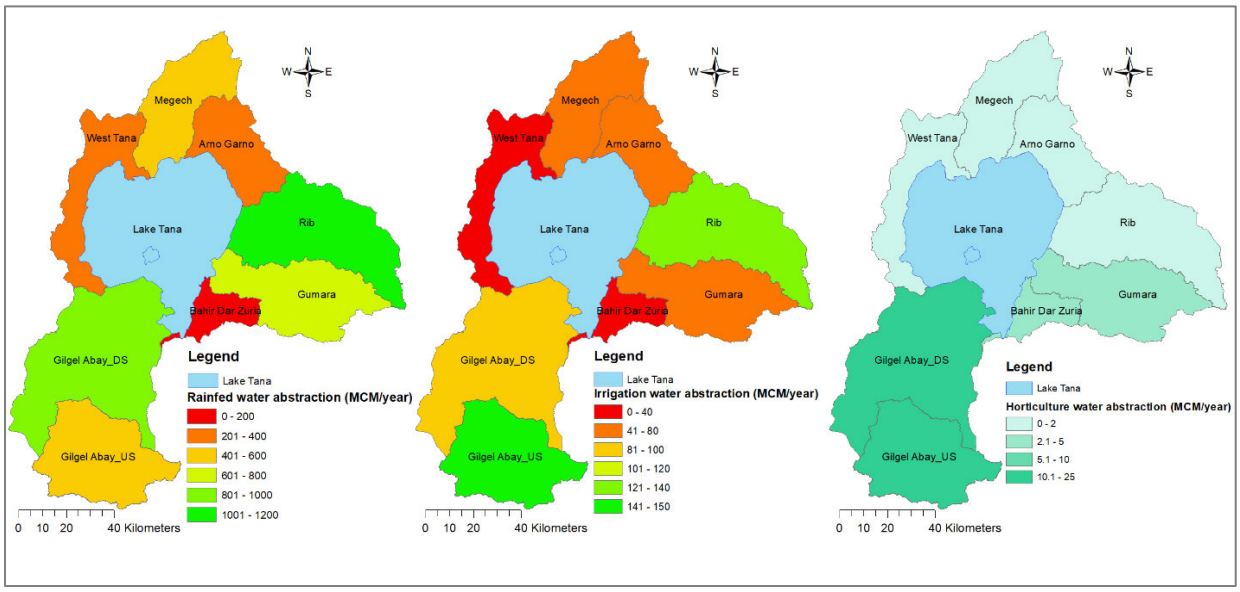


Figure 37: Rainfed, irrigation, and horticulture water abstraction (2020) in the Sub-basin

The livestock survey conducted in the study area considered cattle, sheep, goats, equines, and poultry. Livestock's annual water consumption in the Tana Sub-basin was estimated at approximately 31.78 million cubic meters (refer to Annexure 57). This estimation was based on the water consumption rate per head for each category of animal. Cattle accounted for the largest share of water consumption, at approximately 82% of the total, with the remaining 18% being

attributed to sheep, goats, equines, and poultry. Despite having the second highest population, poultry had the lowest water consumption rate per head.

Regions with the largest livestock populations experienced the highest water consumption. The lower part of Gilgel Abbay had the largest number of livestock, consuming approximately 8.35 MCM of water annually. Rib, Gumara, and the upper part of Gilgel Abbay watershed followed with annual water consumption of about 5.16, 4.22, and 4.22 MCM, respectively. In contrast, the areas of Bahir Dar Zuria and Arno Garno had the lowest livestock populations, consuming approximately 0.99 and 1.94 MCM of water annually, respectively (refer to Figure 38). These areas had lower water consumption than other parts of the study area. The findings highlight significant water consumption by livestock, particularly cattle, in the study area. The distribution of livestock populations across different regions correlates with variations in water consumption.

The study adopted a per capita water consumption rate of 25 liters per day, which was derived from Ethiopia's Growth and Transformation Plan 2 (GTP-2), to estimate rural water consumption (Adank *et al.* 2016). This was used as a basis to calculate the rural population's water consumption in the study area. The study estimated that approximately 33.43 MCM/year of water was abstracted for rural water consumption in the Sub-basin in 2020. This figure is nearly double the amount reported by Taye *et al.* (2021). Gilgel Abbay and Bahir Dar Zuria regions had the highest water consumption for rural domestic use. The Arno Garno area, with a scattered rural population, and Bahir Dar Zuria, with a relatively small rural population, consume lower amounts of water annually for rural domestic use. More specifically, 1.63 MCM and 1.37 MCM of water were abstracted annually in Arno Garno and Bahir Dar Zuria, respectively.

In 2020, an estimated 22.03 MCM of water was abstracted for urban water consumption in the study area. The regions of Gilgel Abbay and Bahir Dar Zuria had the highest water consumption for urban domestic use. The presence of major towns such as Bahir Dar in Bahir Dar Zuria and Gonder town in the Megech watershed contributed to high water abstraction for urban domestic demand in these areas (refer to Annexure 54 and Annexure 55). The volume of water abstracted

for urban domestic demand in the Sub-basin depended on the presence of towns and urban populations within the watersheds. Different watersheds exhibited varying levels of water demand. The areas of Arno Garno, West Tana, Gumara, and the upper part of the Gilgel Abbay watershed had the lowest water demand, with annual abstractions of 0.5, 0.33, 0.19, and 0.94 MCM of water, respectively (refer to Figure 38).

These findings highlight the varying water consumption patterns between urban and rural areas within the Tana Sub-basin. Urban centers with larger populations and major towns tend to experience higher demand for water, while rural areas with scattered populations generally have lower water consumption levels. Understanding these spatial variations is crucial for water resource management and planning in the Tana Sub-basin.

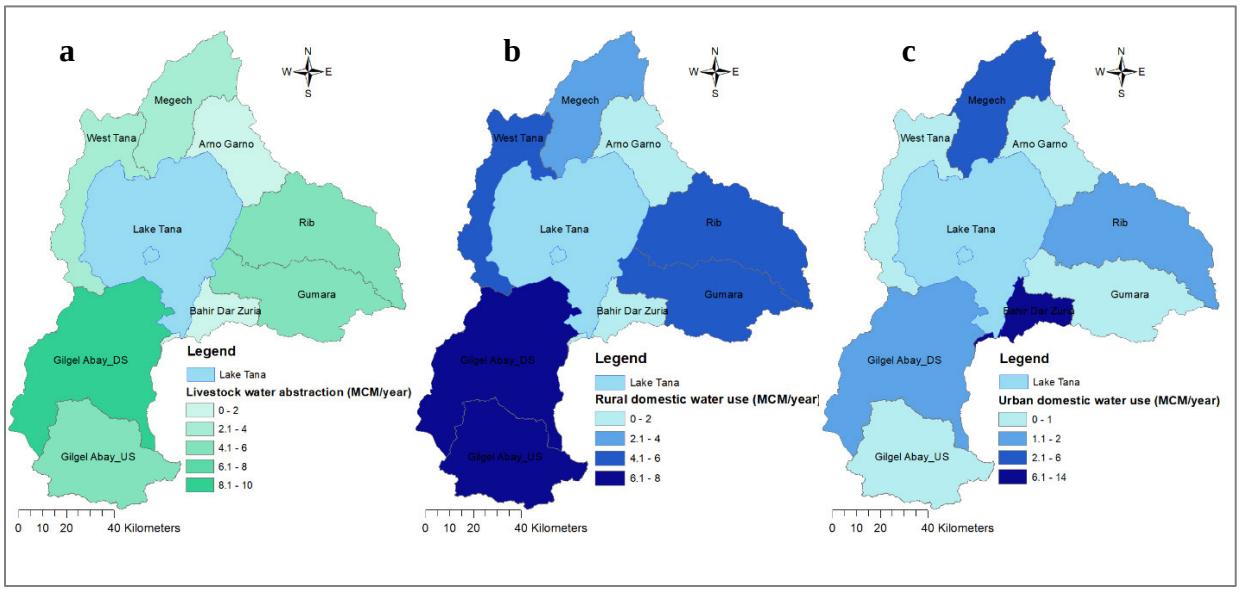


Figure 38. Water use in Tana Sub-basin for livestock, rural and urban population in 2020

The GTP-2 plan identifies five categories of water demand per capita for urban water supply that provide guidelines for the allocation of water based on population size in urban areas. The urban population's current water consumption in the study area was analyzed and compared with the per capita amounts of water allocated in the GTP-2 categories. For example, based on its population,

Bahir Dar town should have received an allocated amount of 80 liters per capita per day according to the GTP-2 plan. However, the study found that it distributed a slightly lower amount of water per head, approximately 78.44% (62.75 liters per capita per day). This indicates that Bahir Dar town was relatively close to meeting the recommended water allocation per capita, with a distribution rate of 78.44% of the standard in the GTP-2 plan (refer to Figure 39).

Based on its population, the GTP-2 plan allocated Chuahit town 50 liters per capita per day. However, the study found that Chuahit town distributed the least amount of water among the towns in the study area at approximately 7.48% (3.74 liters per capita per day) of the standard. This indicates that Chuahit town fell significantly short of meeting the recommended water allocation per capita, distributing only a fraction of the allocated amount. Figure 39 presents detailed data and an analysis of the towns in the study area.


Figure 39: Comparison of current water demand per head and GTP-2 standards

It was found that most of the domestic water supply in the study area came from groundwater sources. More than 80% of the water used in Gonder town, which is part of the study area, was sourced from surface water (refer to Annexure 55). Domestic urban water demand was fulfilled through a combination of groundwater, surface water, and spring sources. Based on the available data from 2020, the study revealed that groundwater accounted for the largest proportion of water supply for domestic purposes in the towns of the study area, amounting to approximately 76.24% of total supply. Spring water constituted the next significant source, providing approximately

12.19%, while surface water such as rivers or reservoirs accounted for a smaller share, approximately 11.27%, in meeting domestic water demand in the towns. These findings indicate that groundwater was the primary source of domestic water supply within the study area, followed by spring water and surface water.

The study found that in Bahir Dar town, approximately 2.07 MCM (16.59%) of water was lost annually. In Gonder town, the annual water loss was estimated at 1.27 MCM (27.2%). These figures represent the percentage of water lost compared to the total water supplied to these towns. The highest urban water loss was observed in Dangila town at approximately 38.63%. Shawura, Chuahit, and Delgie towns had relatively lower water losses, i.e., around 15% each (refer to Figure 40). The study also noted that the water yield from current source points or water points in Bahir Dar decreased by 43.37% compared to the design water yields (refer to Annexure 53). This suggests that the actual amount of water obtained from current sources was significantly lower than the expected or planned yields.

The study found that approximately 22.03 MCM of water was abstracted from both surface and groundwater sources for urban supply in the study area. Of this, 17.63 MCM of water was distributed to towns, while 4.40 MCM was lost annually. This represents a loss of 19.97% of the total water produced from the sources (refer to Annexure 56).

Several reasons were identified for water loss in urban water consumption, including illegal water abstraction from the system, the old pipe network and water meters, weak billing systems, and water leakages. These findings align with previous studies conducted by Ociepa *et al.* (2019) and Kitessa *et al.* (2022), which verified and highlighted similar reasons for water loss in water distribution systems.

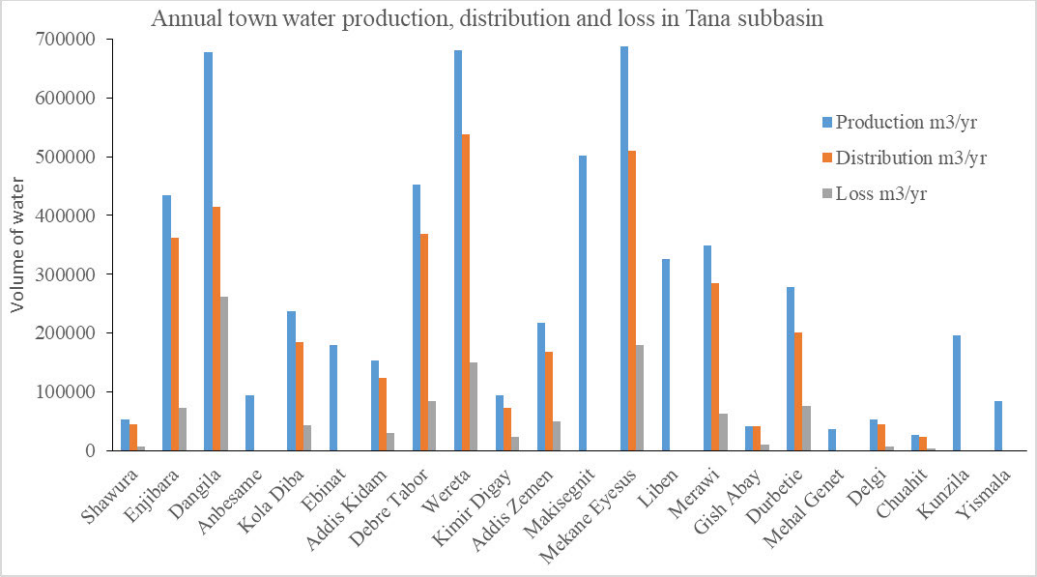


Figure 40: Current annual water production, distribution, and loss in the study area

In Gonder, the total number of customers increased steadily over the years. For instance, in 2005, the number of customers was below 8,856, but by 2020, it had reached 33,759. Thus, within a span of 16 years, Gonder experienced a significant increase of 24,903 new customers. Incremental trends in the number of customers, water production, and water consumption were observed in Gonder, similar to other towns in the Sub-basin. Over the 16-year period, water production increased from 2.1 million $m^3$/year to 4.7 million $m^3$/year. Similarly, water consumption rose from 1.4 million $m^3$/year to 3.3 million $m^3$/year (refer to Figure 41). The study also reported an improvement in efficiency from 67.76% in 2005 to 71.08% in 2020. This indicates that, compared to the total water produced, the percentage of water consumed increased over the 16-year timeframe, but the change is not significant.

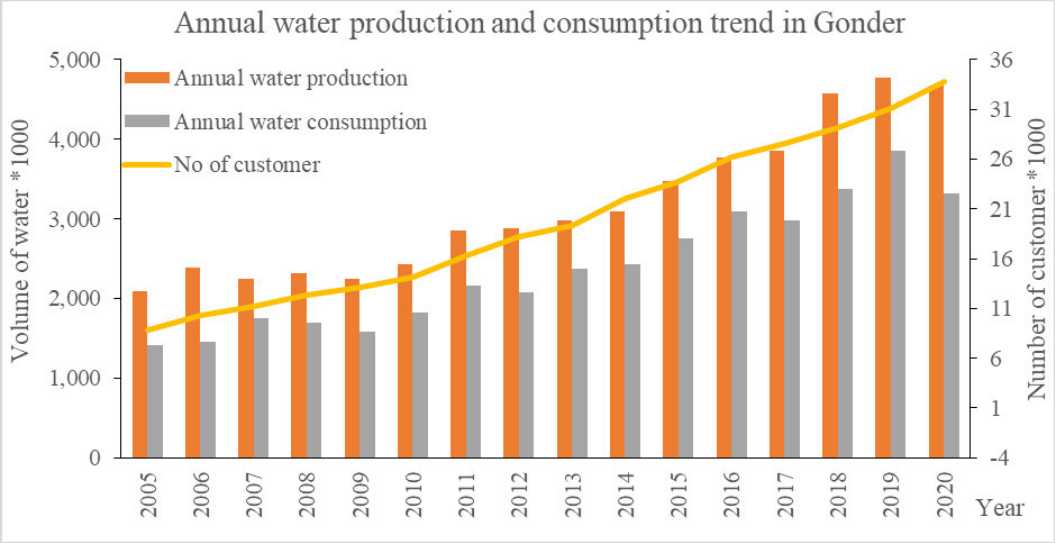


Figure 41: Trends in annual water production, distribution, and customers in Gonder

In Bahir Dar city, annual water production and consumption showed a consistent increase between 2009 and 2020. In 2009, total incoming water to the city was relatively lower compared to other years. However, over the years, there was a steady increase in the number of customers from approximately 15,197 in 2009 to 47,339 in 2020. Thus, within a 12-year period, Bahir Dar had 32,142 new customers. The amount of water produced increased from 5.11 million $m^3$/year to 12.95 million $m^3$/year over the 12-year period (refer to Figure 42). Correspondingly, water consumption rose from 4.35 million $m^3$/year to 10.39 million $m^3$/year. These findings highlight growing demand for water services in Bahir Dar, as evidenced by the increasing number of customers and the corresponding rise in water production and consumption.

The study found that in all towns and rural areas within the Sub-basin, the current yield of the water supply source or water point is lower than their initial design yield (see Annexure 52 and Annexure 53). However, it is worth noting that some towns and rural areas may lack organized initial water yield data; therefore, comparison is not possible. The decrease in the yield of water sources could be attributed to LULC changes in the water recharging areas surrounding each water point. These can affect the infiltration rate of water into the soil, subsequently impacting the recharge of groundwater and the overall yield of water sources.

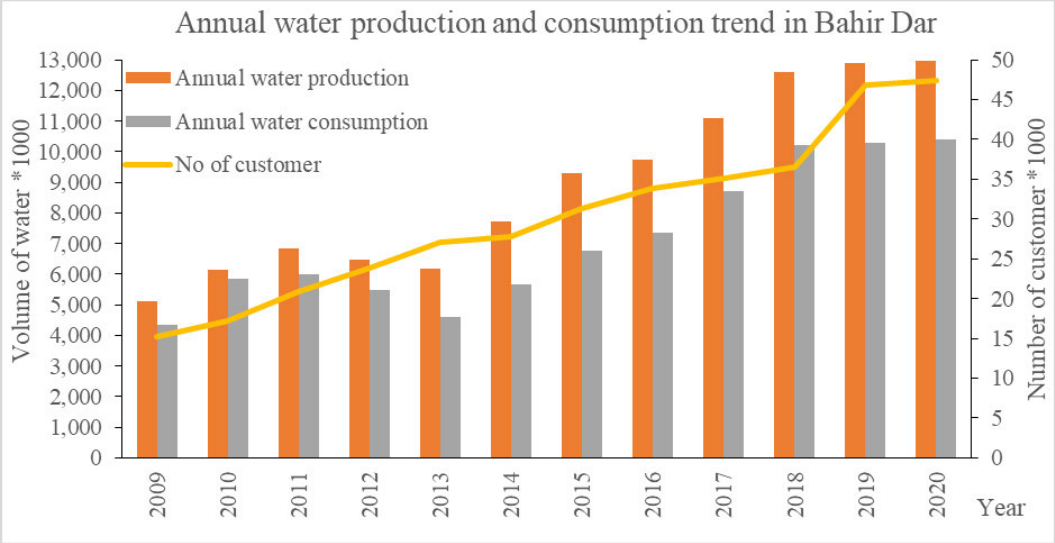


Figure 42: Trends in annual water production, distribution, and customers in Bahir Dar

The Tana Sub-basin has a major hydropower plant known as the Tana-Beles hydropower plant. Situated in the southern part of the West Tana watershed, it abstracts water from Lake Tana and diverts it to generate power. On an annual basis, approximately 3,790 million cubic meters of water are extracted from Lake Tana and utilized by the Tana-Beles hydropower plant to produce an energy output of 2,956.8 GWhr. The hydropower plant consists of four operational turbines, which collectively discharge an average of 38 $m^3/s$ of water. However, it is important to note that full-capacity hydropower production of the plant requires a higher discharge rate of 160 $m^3/s$ (Tesfaw 2016). The amount of water diverted from Lake Tana to the hydropower plant varies on a seasonal basis, depending on the power generation requirements and the operational rules of the reservoir.

### 5.4.2 Available water resources in the Tana Sub-basin

According to the SMEC (2008) study, the average annual runoff from the catchments upstream of the gauging stations in the study area is estimated at 3,490 million cubic meters. This includes the records observed at major tributaries such as Gilgel Abbay, Gumara, Rib, and Megech Rivers. In addition, ungauged areas are estimated to contribute around 1542 MCM/year of inflow, bringing the total river inflow into the lake to approximately 4986 MCM/year, including 46 MCM annual losses from flood plain inundation. However, other studies have suggested that the surface water

potential in the area could be as high as 12.1 BCM, which exceeds the estimates provided by the SMEC (2008) study (GIRDC 2014; Dessie *et al.* 2015). It is important to note that unreliable and limited data have posed challenges to development practitioners and researchers, leading to uncertainties in important studies and modeling practices. Regarding groundwater availability, the SMEC (2008) study estimates it to be approximately 1.8 BCM in the Sub-basin. In addition, it states that the available water resources range from 5553 to 8625 MCM per year, with surface water at the minimum Lake Tana operation level of 1784.0 m.a.sl estimated to be around 3753 MCM per year. These figures provide an overview of the estimated water resources and input for future scenarios in the study area. However, it is crucial to continue improving data collection and monitoring efforts to obtain more accurate and reliable information for future planning and management in the water sectors.

### 5.4.3 Projected water demand in the Tana Sub-basin

The optimization model used in the study aimed to maximize the total benefit gained from each sector by allocating available water resources. The amount of water remaining after satisfying domestic and environmental demand is considered as allocable water. The objective function of the model includes the economic benefit generated by allocating each cubic meter of water to different sectors, measured in Ethiopian birr per cubic meter. The results of the optimization model in Table 24 indicate increasing water demand in the coming years. In scenarios one and two, the highest percentage of water is required for hydropower. By the end of 2035, irrigation accounted for the highest percentage (54.34%) of water allocation in the study area, followed by hydropower. Furthermore, the amount of water required for industry is more than double in each scenario. This suggests a high level of industrial development in the study area, as it is identified as a growth corridor for Ethiopia.

The findings of the study highlight the need for special attention to be paid to increasing water demand with limited available resources in the study area. It is crucial to carefully manage and allocate water resources to ensure sustainable development and meet the growing demand of various sectors in the future.

Table 24: Projected water demand under future scenarios

| Demands in the Sub-basin | Total allocable water (MCM) | Base case 2020 | | Scenario one 2021-2025 | | Scenario two 2026-2030 | | Scenario three 2031-2035 | |
|---|---|---|---|---|---|---|---|---|---|
| | | Annual allocated (MCM) | Share (in %) | Annual allocated (MCM) | Share (in %) | Annual Allocated (MCM) | Share (in %) | Annual allocated (MCM) | Share (in %) |
| Hydro power | 5553/8625 | 3790 | 84.22 | 3322.3 | 54.65 | 3028.9 | 47.15 | 2902.8 | 38.60 |
| Irrigation | | 602.28 | 13.38 | 2561 | 42.13 | 3095 | 48.18 | 4086 | 54.34 |
| Domestic (urban & rural) | | 55.46 | 1.23 | 64.56 | 1.06 | 81.48 | 1.27 | 94.25 | 1.25 |
| Livestock | | 31.78 | 0.71 | 69.22 | 1.14 | 84.21 | 1.31 | 102.46 | 1.36 |
| Industry | | 20.54 | 0.46 | 61.93 | 1.02 | 134.4 | 2.09 | 334.42 | 4.45 |
| Total allocated water | | 4500.06 | 100 | 6079.01 | 100 | 6423.99 | 100 | 7519.93 | 100 |

### 5.4.4 Proposed adaptive strategic options

The availability of water in the Tana Sub-basin varies spatially and temporally. The area receives three months of rainfall, and the remaining months are relatively dry. This affects the balance between water supply and demand within the Sub-basin. It is important to note that the Sub-basin is experiencing significant growth and development, which is dependent on available water resources. Access to clean and reliable sources of water is crucial for the people living in the Sub-basin (Gebremichael *et al.* 2021). However, the limited availability of water resources poses a paradoxical challenge for the continued development of the area.

Beker *et al.* (2023) also recognized the growing scarcity of water in Ethiopia. In order to address this challenge and ensure sustainable water resource management, it is necessary to develop adaptive strategies (Tsakiris *et al.* 2023). These should focus on optimizing the use of the available water resources in the study area. This will involve implementing water-saving measures, prioritizing water allocation, and considering alternative water sources such as treated water reuse. By developing and implementing adaptive strategies for water resource management, the Sub-basin can better cope with the challenges posed by limited water availability and support its continued growth and development.

The study reviewed research and findings, reports, and documents and proposed adaptive strategic options for sustainable and integrated water resources management in the Tana Sub-basin. The detailed strategies based on this study are shown in Table 25. The proposed strategy is to develop and implement a water allocation plan that takes into account the efficient use of water resources. This plan is based on an adaptive framework that considers climate change, population growth, and economic activities as driving factors that put pressure on the water resources in the study area. The model for water allocation is presented in Figure 43. The framework includes consideration of different supply sources such as surface water and groundwater. In addition, the study recommends using treated water as an alternative resource to meet different demands, particularly for irrigation purposes (Abera *et al.* 2020). This approach aims to fill the gaps in water supply and ensure efficient use of available resources. The water allocation plan will involve accounting for the available water resources, analyzing demand, and considering the driving factors. Based on this analysis, an optimized water allocation plan will be developed, prioritizing water users and identifying areas where water resources are scarce.

Overall, the proposed strategy aims to ensure sustainable and efficient use of water resources in the study area by considering population growth, economic activities, and climate change. It emphasizes the need for continuous monitoring, evaluation, and improvement of the water allocation plan to adapt to changing conditions and incorporate new knowledge and technologies.

Table 25: Proposed adaptive strategies for sustainable water resources management

| Strategies | Strategic measures |
|---|---|
| Develop and implement water allocation plan based on efficient use of water resources in the Sub-basin | a) Develop and implement criteria to allocate Sub-basin water resources among different users. Prepare water allocation procedures and guidelines, and select appropriate tools,<br>b) Give special consideration and priority to drought-prone and water-scarce areas,<br>c) Adopt water transfer between different areas in the Sub-basin,<br>d) Implement supply and demand management measures in all water use and user sectors to improve water use efficiency, and<br>e) Improve water use efficiency by adopting, introducing and implementing technological alternatives. |
| Promote appropriate and integrated watershed management practices within the Sub-basin | a) Select and implement appropriate soil and water conservation measures to reduce soil erosion and reservoir siltation,<br>b) Develop and implement afforestation and terracing programs to improve infiltration of water into the soil and groundwater resources,<br>c) Rehabilitate deteriorated watersheds and regenerate natural vegetation and forest,<br>d) Establish soil and water conservation rules, regulations, and guidelines in relation to water resources and ecosystem management, and<br>e) Encourage and promote all stakeholders' participation and engagement in watershed management and water conservation practices. |
| Develop efficient and integrated data and information exchange and management in the water sector | a) Establish databases on all aspects of water resources,<br>b) Review and assess available water resources data and information and identify information gaps,<br>c) Design data and information collection, entry, storage, retrieval, review, analysis, and dissemination approaches,<br>d) Identify and define users' information requirements,<br>e) Improve cross-sectoral coordination, planning, and decision-making processes related to water, and<br>f) Develop guidelines on the dissemination of water resources information to enhance information exchange and networking. |

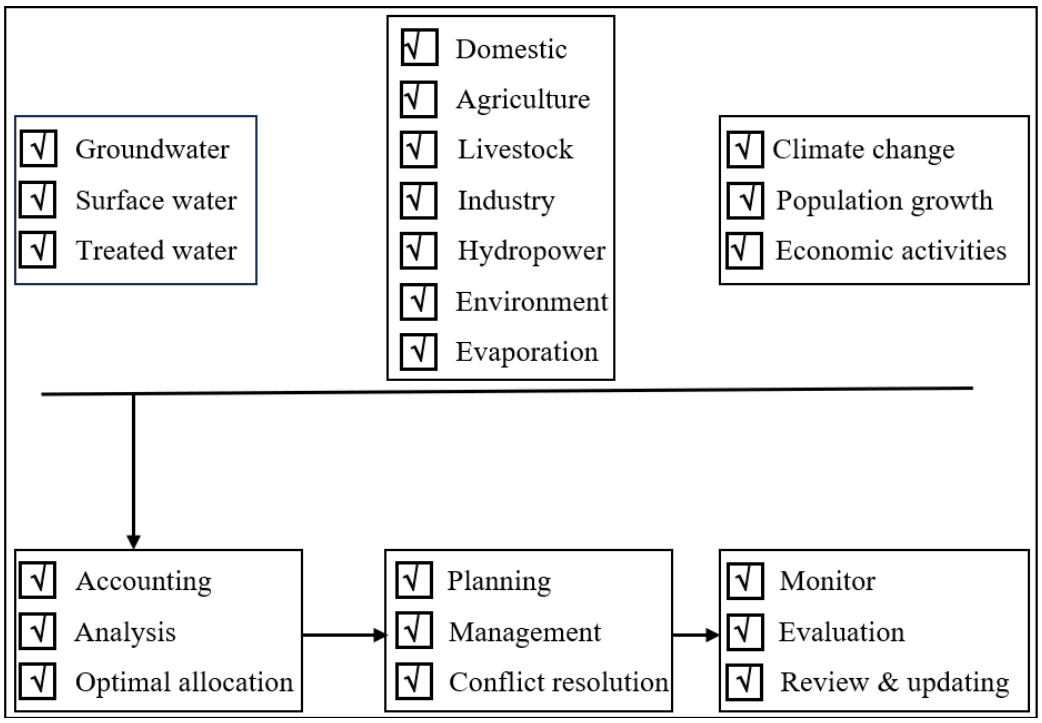


Figure 43: Proposed adaptive water allocation framework

# CHAPTER SIX: CONCLUSIONS AND RECOMMENDATIONS

## 6.1 Conclusions

### 6.1.1 Conclusion for objective 1

*To analyze climate variability, trends, and associated risks in the Tana Sub-basin*

Various statistical techniques such as the standardized precipitation index, CV, SI, PCI, nonparametric Sen's slope estimator, and MK trend test were applied in the study area. The study utilized monthly rainfall and temperature data from 1981 to 2020 and 1981 to 2016, respectively. These methods and data were used to analyze the variability and trend of climatic variables within the available data.

The study's results indicate a statistically non-significant increasing trend in climatic variables across the study area. The long-term minimum and maximum monthly temperatures were identified as 4.2 $^{o}$C in December and 34.5 $^{o}$C in March, respectively. Precipitation distribution in the Sub-basin was found to be non-uniform, with 57.5% of rainfall exhibiting strong irregular distribution spatially and temporally, and 41.5% showing irregular precipitation concentration, indicating significant variability in precipitation patterns. The study's precipitation projections revealed a decreasing trend in mean annual precipitation at all stations and scenarios. By the 2100s, the projected mean annual precipitation for Dangila station was approximately 1,582.29 mm under the RCP4.5 scenario and slightly lower at 1,582.11 mm under the RCP8.5 scenario. For Gonder station, the projected mean annual precipitation by the 2100s was 1,075.79 mm under the RCP4.5 scenario and 1,102.32 mm under the RCP8.5 scenario. Furthermore, the analysis showed an increasing trend in temperature at all stations for both scenarios and all time periods, indicating projected temperature rise in the future. Furthermore, the study revealed that the highest percentage increment was observed in minimum temperature compared with maximum temperature in both scenarios across all stations and time periods.

These findings highlight the significant climate variability and potential impacts of climate change on the study area. The projected decrease in mean annual precipitation and the increasing trend in temperature underscore the need for proactive measures to address climate change and its potential implications for water resources management and agriculture in the Tana Sub-basin. The study concludes that the temporal variation of monthly rainfall is higher than the temporal variation of monthly temperature in the Tana Sub-basin. This implies that rainfall patterns are more variable and subject to change over time than temperature patterns. The statistical parameters utilized in the study thus successfully examined climate variability and trends in the Tana Sub-basin. The findings are expected to contribute valuable information for future similar studies.

### 6.1.2 Conclusion for objective 2

*To explore the impact of hydro-climatic extremes in the Tana Sub-basin*

The study employed the standardized precipitation index and CDI as measures of dryness and wetness in the study area, providing a comprehensive assessment of the severity and frequency of drought events over different time intervals. The findings revealed spatial and seasonal variations in the frequency of drought, with similar patterns observed across all regions. The analysis considered meteorological, agricultural, and hydrological droughts, categorizing them from moderate to extreme levels. The study found that the percentage of areas affected by drought ranged from 1.05% to 10.04% for meteorological drought, 1.26% to 12.21% for agricultural drought, and 0.21% to 14.5% for hydrological drought; this indicates the diverse impacts of drought across different categories.

The study projected that in the future, the highest percentage of extremely wet occurrences would be observed in Gonder station under the RCP8.5 scenario for the 2021-2100 period, with a value of 10.09%. The highest percentage of extremely wet occurrences under the RCP4.5 scenario was projected to be observed in Debre Tabor station for the 2021-2050 period, with a value of 5.44%. The study also concluded that the highest percentage of extremely dry occurrence was projected to be observed in Debre Tabor station for the 2021-2050 period under the RCP4.5 scenario, with a value of 3.15%. Furthermore, the highest extreme drought occurrence was projected to be

observed in Dangila station for the 2081-2100 period under the RCP8.5 scenario, with a value of 1.69%.

The study concluded that extremely wet and drought situations will occur in the study area in the future. It is worth noting that the existence of wet conditions may lead to flood problems. Therefore, appropriate measures should be taken to mitigate the impact of floods and droughts in the region. Overall, the study stresses the use of SPI and CDI as measures of wet and drought situations in the study area.

### 6.1.3 Conclusion for objective 3

*To assess the impact of land use land cover change on water resources in the Tana Sub-basin*

The study used the SWAT to assess the impact of LULC on water resources in the Tana Sub-basin. This involved several steps, including the evaluation of the SWAT model, detection of LULC changes, and assessment of their impact on water resources. The SWAT model was successfully evaluated and used to analyze the impact of LULC changes on water resources employing the available data. The overall LULC changes recorded for the period from 1986 to 2014 amounted to 33.94%, indicating significant transformation of the land cover in the study area. The remaining unchanged land cover accounted for 66.06% of the total. The analysis revealed that the changes in LULC had a significant impact on the study area's water resources. The water balance components showed positive and negative responses to LULC changes in the Tana Sub-basin.

The study also highlighted the increment in the average annual water yield in the Tana Sub-basin over time. In 2014, compared to the baseline year of 1986, the water yield and average annual baseflow increased by 12.6% and 9.93%, respectively. In addition, the average annual surface runoff showed a significant increase of 16.16% in 2014 compared to 1986. However, in contrast to surface runoff and baseflow, the average annual evapotranspiration decreased with LULC changes. This indicates that changes in LULC have influenced the water balance components in the study area. The study concluded that the expansion of cultivation and the decrement in forest land are the main contributors to the changes in water balance components. These changes have

implications for natural resource management and development in the Tana Sub-basin. The results underscore the significance of controlling the change in LULC to maintain water balance components for optimum utilization of water resources in the future.

### 6.1.4 Conclusion for objective 4

*To develop sustainable and efficient adaptive options for integrated water resources management of Tana Sub-basin*

The study provided information on water consumption in the study area, highlighting growing demand for water resources across different sectors. It identified the Tana Sub-basin as a significant growth corridor for Ethiopia and emphasized increasing consumption of water despite the limited availability of water resources. The study computed water consumption across various categories, shedding light on the magnitude of water demand in different sectors. The findings revealed that total annual water consumption for irrigation and horticulture is approximately 555.76 and 46.52 MCM, respectively. Livestock consumption accounts for about 31.78 MCM annually. In addition, it noted that urban and rural domestic water consumption in the sub-basin amounts to approximately 22.03 and 33.43 MCM per year, respectively. The study projected future water demand in the study area, revealing a significant increase in water requirements over time. Water requirements are projected to increase from 555.76 MCM in 2017 to 6079.01 MCM in 2025, 6423.99 MCM in 2030, and 7519.93 MCM in 2035. These projections highlight the urgent need for sustainable and integrated water resource management in the Tana Sub-basin to address increasing water demand.

The study underscored the growing scarcity of water in the Tana Sub-basin, attributing it to factors such as population growth, urbanization, irrigation, and industrial development. It emphasized the need for comprehensive water resource planning and management that caters for increasing water demand from various sectors. To address this, the study developed three adaptive strategy options for sustainable integrated water resource management in the study area, aiming to balance social and natural water demands with the limited availability of water resources. The findings highlighted that irrigation/agriculture and hydropower are the highest water-consuming sectors,

emphasizing the need to prioritize water allocation and management in these sectors to ensure sustainable water use. Furthermore, the study emphasized the critical importance of assessing and updating water demand and available water resources as a fundamental step for water resource management in the Tana Sub-basin. By recognizing the challenges and developing adaptive strategies, it lays the foundation for sustainable and integrated water resource management in the region.

## 6.2 Recommendations

- The study highlights the significance of accurate datasets for hydrological model development. It emphasizes the need to analyze the model using the latest flow dataset and LULC information to understand the impact of land use changes on water resources in the study area. Furthermore, it suggests that more data is required for further studies to improve the calibration and validation process of the hydrological model. Future studies should explore and incorporate additional climate change scenarios to enhance the understanding of potential future impacts on the water resources of the study area.

- The study developed adaptive strategy options for sustainable water resource management in the Tana Sub-basin and highlighted the need to share data on current water demand with different sectors to develop these strategies effectively. However, it did not incorporate previous long-term time series water demand data and information to understand the trends and patterns of water demand in the study area over time due to lack of well-organized data. Such data could be crucial in identifying existing water demand patterns and assessing the effectiveness of current planned projects in meeting demand. Consideration of the previous long-term time series water demand data and information for current planned projects is critical for the development of strategic options. By incorporating this information, trends and patterns of water demand over time could be identified, the effectiveness of current planned projects could be assessed, and more robust and adaptive strategies for sustainable water resource management could be developed. It is also recommended that trends in long-term water demand data be incorporated to develop future scenarios in further studies. By developing

future scenarios, researchers can anticipate future water demand and plan sustainable water resource management.

In summary, the recommendations stress the need to continue this research utilizing the latest, real-time dataset to refine the models, and conduct validation processes. This will contribute to the development of more reliable and accurate adaptive strategy options for sustainable and integrated water resource management in the Tana Sub-basin.

## REFERENCES


Abbaspour, K. C. 2013. SWAT-CUP 2012: SWAT calibration and uncertainty programs–a user manual. Dübendorf, Switzerland, Eawag, pp. 103. Article ID: https://swat.tamu.edu/media/114860/usermanual_swatcup.pdf.

Abbaspour, K. C., Johnson, C. A. and van Genuchten, M. T. 2004. Estimating Uncertain Flow and Transport Parameters Using a Sequential Uncertainty Fitting Procedure. *Vadose Zone Journal*, 3 (4): 1340-1352.

Abbaspour, K. C., Rouholahnejad, E., Vaghefi, S., Srinivasan, R., Yang, H. and Kløve, B. 2015. A continental-scale hydrology and water quality model for Europe: Calibration and uncertainty of a high-resolution large-scale SWAT model. *Journal of Hydrology*, 524: 733-752.

Abbaspour, K. C., Yang, J., Maximov, I., Siber, R., Bogner, K., Mieleitner, J., Zobrist, J. and Srinivasan, R. 2007. Modelling hydrology and water quality in the pre-alpine/alpine Thur watershed using SWAT. *Journal of Hydrology*, 333 (2): 413-430.

Abebe, W. B., G/Michael, T., Leggesse, E. S., Beyene, B. S. and Nigate, F. 2017. Climate of Lake Tana Basin. *Social and Ecological System Dynamics: Characteristics, Trends, and Integration in the Lake Tana Basin, Ethiopia*, Article ID: 51-58.

Abera, A., Verhoest, N. E. C., Tilahun, S., Inyang, H. and Nyssen, J. 2020. Assessment of irrigation expansion and implications for water resources by using RS and GIS techniques in the Lake Tana Basin of Ethiopia. *Environ Monit Assess*, 193 (1): 13.

Abidoye, B. and Odusola, A. 2015. Climate Change and Economic Growth in Africa: An Econometric Analysis. *Journal of African Economies*, 24: 1-25.

Adank, M., Butterworth, J., Godfrey, S. and Abera, M. 2016. Looking beyond headline indicators: water and sanitation services in small towns in Ethiopia. *Journal of Water, Sanitation and Hygiene for Development*, 6 (3): 435-446.

Addisu, S., Selassie, Y. G., Fissha, G. and Gedif, B. 2015. Time series trend analysis of temperature and rainfall in lake Tana Sub-basin, Ethiopia. *Environmental Systems Research*, 4 (1): 25.

Ademe, D., Ziatchik, B. F., Tesfaye, K., Simane, B., Alemayehu, G. and Adgo, E. 2020. Climate trends and variability at adaptation scale: Patterns and perceptions in an agricultural region of the Ethiopian Highlands. *Weather and Climate Extremes*, 29: 100263.

Akoko, G., Le, T. H., Gomi, T. and Kato, T. 2021. A Review of SWAT Model Application in Africa. *Water*, 13 (9): 1313.

Aladaileh, H., Qinna, M. A., Barta, K., Al-Karablieh, E., Bakri, J. A. and Rakonczai, J. 2019. Applicability of a combined drought index to monitoring drought in Jordan. *International Journal of Engineering Research and Applications*, 9 (7): 20-39.

Alahacoon, N., Edirisinghe, M., Simwanda, M., Perera, E., Nyirenda, V. R. and Ranagalage, M. 2022. Rainfall Variability and Trends over the African Continent Using TAMSAT Data (1983–2020): Towards Climate Change Resilience and Adaptation. *Remote Sensing*, 14 (1): 96.

Alemayhu. 2006. GIS Applications in suitability modelling for livestock production in Tana Subbasin-Blue Nile River basin, Ethiopia. Master's Thesis. Addis Ababa, Ethiopia. Article ID: https://www.scribd.com/document/703944110/.

Alemu, M. L., Worqlul, A. W., Zimale, F. A., Tilahun, S. A. and Steenhuis, T. S. 2020. Water Balance for a Tropical Lake in the Volcanic Highlands: Lake Tana, Ethiopia. *Water*, 12 (10): 2737.

Allam, M. M., Jain Figueroa, A., McLaughlin, D. B. and Eltahir, E. A. 2016. Estimation of evaporation over the upper Blue Nile basin by combining observations from satellites and river flow gauges. *Water Resources Research*, 52 (2): 644-659.

Allen, R. G., Pereira, L. S., Raes, D. and Smith, M. 1998. Crop evapotranspiration-Guidelines for computing crop water requirements-FAO Irrigation and Drainage paper 56. *Fao, Rome*, 300 (9): D05109.

Amsalu, A. and Adem, A. 2009. Assessment of climate change-induced hazards, impacts and responses in the southern lowlands of Ethiopia. Forum for Social Studies and Cordaid. *Addis Ababa, Ethiopia Retrieved from http://publication. eiar. gov. et*, 8080.

Anteneh, M. 2022. Climate Variability Patterns and Farmers' Perceptions of Its Impact on Food Production: A Case Study of the Gelda Watershed in the Lake Tana Basin in Northwest Ethiopia. *Air, Soil and Water Research*, 15: 11786221221135093.

Arnold, J. G. and Fohrer, N. 2005. SWAT2000: current capabilities and research opportunities in applied watershed modelling. *Hydrological Processes*, 19 (3): 563-572.

Arnold, J. G., Srinivasan, R., Muttiah, R. S. and Allen, P. M. 1999. Continental Scale Simulation of the Hydrologic Balance. *JAWRA Journal of the American Water Resources Association*, 35 (5): 1037-1051.

Arnold, J. G. S., R. Muttiah, R.S. and Williams, J.R. 1998. Large area hydrologic modeling and assesment Part I: Model development. JAWRA J. Am. Water Resour. Assoc. 34, 73–89. Article ID: https://doi.org/10.1111/j.1752-1688.1998.tb05961.x.

Asfaw, A., Simane, B., Hassen, A. and Bantider, A. 2018. Variability and time series trend analysis of rainfall and temperature in northcentral Ethiopia: A case study in Woleka sub-basin. *Weather and Climate Extremes*, 19: 29-41.

Atanaw, F., Moges, M., Alemu, M., Ayana, E., Demissie, S., Tilahun, S. and Steenhuis, T. 2018. Budgeting suspended sediment fluxes in tropical monsoonal watersheds with limited data: The Lake Tana basin. *Journal of Hydrology and Hydromechanics*, 66: 65-78.

Awotwi, A., Anornu, G. K., Quaye-Ballard, J. A., Annor, T., Forkuo, E. K., Harris, E., Agyekum, J. and Terlabie, J. L. 2019. Water balance responses to land-use/land-cover changes in the Pra River Basin of Ghana, 1986-2025. *CATENA*, 182: 104129.

Balint, Z., Mutua, F., Muchiri, P. and Omuto, C. T. 2013. Chapter 23 - Monitoring Drought with the Combined Drought Index in Kenya. In: Paron, P., Olago, D. O. and Omuto, C. T. (Eds), *Developments in Earth Surface Processes*. Elsevier, 341-356. Available: https://www.sciencedirect.com/science/article/pii/B9780444595591000232 (Accessed 7/26/2022).

Bastin, L., Cornford, D., Jones, R., Heuvelink, G. B. M., Pebesma, E., Stasch, C., Nativi, S., Mazzetti, P. and Williams, M. 2013. Managing uncertainty in integrated environmental modelling: The UncertWeb framework. *Environmental Modelling & Software*, 39: 116-134.

Bayissa, Y., Srinivasan, R., Joseph, G., Bahuguna, A., Shrestha, A., Ayling, S., Punyawardena, R. and Nandalal, K. D. W. 2022. Developing a Combined Drought Index to Monitor Agricultural Drought in Sri Lanka. *Water*, 14 (20): 3317.

Beker, B. A. and Kansal, M. L. 2023. Complexities of the urban drinking water systems in Ethiopia and possible interventions for sustainability. *Environ Dev Sustain*, Article ID: 1-31.

Belay, A., Demissie, T., Recha, J. W., Oludhe, C., Osano, P. M., Olaka, L. A., Solomon, D. and Berhane, Z. 2021. Analysis of Climate Variability and Trends in Southern Ethiopia. *Climate*, 9 (6).

Beven, K. and Binley, A. 1992. The future of distributed models: Model calibration and uncertainty prediction. *Hydrological Processes*, 6 (3): 279-298.

Birara, H., Pandey, R. P. and Mishra, S. K. 2018. Trend and variability analysis of rainfall and temperature in the Tana basin region, Ethiopia. *Journal of Water and Climate Change*, 9 (3): 555-569.

Birara, H., Pandey, R. P. and Mishra, S. K. 2020. Projections of future rainfall and temperature using statistical downscaling techniques in Tana Basin, Ethiopia. *Sustainable Water Resources Management*, 6 (5): 77.

Birsan, M. V., Molnar, P., Burlando, P. and Pfaundler, M. 2005. Streamflow trends in Switzerland. *Journal of Hydrology*, 314: 312-329.

Bogale, A. 2020. Review, impact of land use/cover change on soil erosion in the Lake Tana Basin, Upper Blue Nile, Ethiopia. *Applied Water Science*, 10 (12): 235.

Bormann, H., Breuer, L., Gräff, T., Huisman, J. A. and Croke, B. 2009. Assessing the impact of land use change on hydrology by ensemble modelling (LUCHEM) IV: Model sensitivity to data aggregation and spatial (re-)distribution. *Advances in Water Resources*, 32 (2): 171-192.

Caldera, H. P. G. M., Piyathisse, V. and Nandalal, K. D. W. 2016. A Comparison of Methods of Estimating Missing Daily Rainfall Data. *Engineer: Journal of the Institution of Engineers, Sri Lanka*, 49: 1.

Chakilu, G. G., Sándor, S., Zoltán, T. and Phinzi, K. 2022. Climate change and the response of streamflow of watersheds under the high emission scenario in Lake Tana sub-basin, upper Blue Nile basin, Ethiopia. *Journal of Hydrology: Regional Studies*, 42: 101175.

Christophe, B. and Tina, R. 2015. Integrating water resource management and land-use planning at the rural-urban interface: Insights from a political economy approach. *Water Resources and Economics*, 9: 45-59.

Cunderlik, J. M. and Simonovic, S. P. 2007. Hydrologic models for inverse climate change impact modeling. In: Proceedings of *the 18th Canadian Hydrotechnical Conference, Challenges for Water Resources Engineering in a Changing World Winnipeg*. Citeseer, 1-9.

Dagnachew, M., Moges, A., Kebede, A. and Abebe, A. 2020. Effects of Soil and Water Conservation Measures on Soil Quality Indicators: The Case of Geshy Subcatchment, Gojeb River Catchment, Ethiopia. *Applied and Environmental Soil Science*, 2020: 1868792.

Dawit, M., Halefom, A., Teshome, A., Sisay, E., Shewayirga, B. and Dananto, M. 2019. Changes and variability of precipitation and temperature in the Guna Tana watershed, Upper Blue Nile Basin, Ethiopia. *Modeling Earth Systems and Environment*, 5 (4): 1395-1404.

De Luís, M., Raventós, J., González-Hidalgo, J. C., Sánchez, J. R. and Cortina, J. 2000. Spatial analysis of rainfall trends in the region of Valencia (east Spain). *International Journal of Climatology*, 20 (12): 1451-1469.

Degefu, W. 1987. Some aspects of meteorological drought in Ethiopia. In M. H. Glantz (Ed.), Drought and Hunger in Africa. Cambridge: Cambridge University Press. Article ID.

Dessie, M., Verhoest, N. E. C., Pauwels, V. R. N., Adgo, E., Deckers, J., Poesen, J. and Nyssen, J. 2015. Water balance of a lake with floodplain buffering: Lake Tana, Blue Nile Basin, Ethiopia. *Journal of Hydrology*, 522: 174-186.

Dutta, P. and Sarma, A. K. 2020. Hydrological modeling as a tool for water resources management of the data-scarce Brahmaputra basin. *Journal of Water and Climate Change*, 12 (1): 152-165.

Dwarakish, G. S. and Ganasri, B. P. 2015. Impact of land use change on hydrological systems: A review of current modeling approaches. *Cogent Geoscience*, 1 (1): 1115691.

Eberhart, R. and Kennedy, J. 1995. A new optimizer using particle swarm theory. In: Proceedings of *MHS'95. Proceedings of the Sixth International Symposium on Micro Machine and Human Science*. 4-6 Oct. 1995. 39-43.

Edwards, D. C. and McKee, T. B. 1997. *Characteristics of 20 th century drought in the United States at multiple time scales*. Colorado State University Fort Collins.

Enyew, B. 2014. Assessment of the Impact of Climate Change on Hydrological Drought in Lake Tana Catchment, Blue Nile Basin, Ethiopia. *Journal of Geology & Geosciences*, 03.

Eshetu, Z., Simane, B., Tebeje, G., Negatu, W., Amsalu, A., Berhanu, A., Bird, N., Welham, B. and Trujillo, N. C. 2014. Climate finance in Ethiopia. *Overseas Development Institute, London and Climate Science Centre, Addis Ababa*, Article ID: https://www.preventionweb.net/quick/43504.

Fenta Mekonnen, D. and Disse, M. 2018. Analyzing the future climate change of Upper Blue Nile River basin using statistical downscaling techniques. *Hydrol. Earth Syst. Sci.*, 22 (4): 2391-2408.

Field, C. B. 2014. *Climate Change 2014–Impacts, Adaptation and Vulnerability: Regional Aspects. Cambridge University Press: Cambridge, UK, 2014*.

Franczyk, J. and Chang, H. 2009. The effects of climate change and urbanization on the run-off of the Rock Creek basin in the Portland metropolitan area, Oregon, USA. Hydrol. Process, 23 (6), 805-815. Article ID: https://doi.org/10.1002/hyp.7176.

Fu, G., Charles, S. P., Yu, J. and Liu, C. 2009. Decadal Climatic Variability, Trends, and Future Scenarios for the North China Plain. *Journal of Climate*, 22 (8): 2111-2123.

Gashaw, T., Worqlul, A. W., Dile, Y. T., Addisu, S., Bantider, A. and Zeleke, G. 2020. Evaluating potential impacts of land management practices on soil erosion in the Gilgel Abay watershed, upper Blue Nile basin. *Heliyon*, 6 (8): e04777.

Gassman, P. W., Reyes, M. R., Green, C. H. and Arnold, J. G. 2007. The soil and water assessment tool: historical development, applications, and future research directions. *Transactions of the ASABE*, 50 (4): 1211-1250.

Gebrechorkos, S., Taye, M. T., Birhanu, B., Solomon, D. and Demissie, T. 2023. Future Changes in Climate and Hydroclimate Extremes in East Africa. *Earth's Future*, 11.

Gebrechorkos, S. H., Bernhofer, C. and Hülsmann, S. 2019. Impacts of projected change in climate on water balance in basins of East Africa. *Science of The Total Environment*, 682: 160-170.

Gebremichael, S. G., Yismaw, E., Tsegaw, B. D. and Shibeshi, A. D. 2021. Determinants of water source use, quality of water, sanitation and hygiene perceptions among urban households in North-West Ethiopia: A cross-sectional study. *PLOS ONE*, 16 (4): e0239502.

Gebretsadik, B. W. 2021. Lake Tana water balance assessment by the effect of climate change and land use interventions. Article IDUniversity of Twente.

Getachew, B. and Manjunatha, B. R. 2021. Climate change projections and trends simulated from the CMIP5 models for the Lake Tana sub-basin, the Upper Blue Nile (Abay) River Basin, Ethiopia. *Environmental Challenges*, 5: 100385.

Getachew, B. and Manjunatha, B. R. 2022. Impacts of Land-Use Change on the Hydrology of Lake Tana Basin, Upper Blue Nile River Basin, Ethiopia. *Global Challenges*, 6 (8): 2200041.

Getachew Tikuye, B., Manjunatha, B. R. and Gangadhara Bhat, H. 2021. Modeling impacts of projected climate and land use/land cover change on hydrological responses in the Lake Tana Basin, Upper Blue Nile River Basin, Ethiopia. *Journal of Hydrology*, Article ID: 125974.

GIRDC. 2014. *Topographic Survey in Lake Tana Sub basin Flood Plain Areas: Final Report*.

Gissila, T., Black, E., Grimes, D. I. F. and Slingo, J. M. 2004. Seasonal forecasting of the Ethiopian summer rains. *International Journal of Climatology*, 24: 1345-1358.

Gocic, M. and Trajkovic, S. 2013. Analysis of changes in meteorological variables using Mann-Kendall and Sen's slope estimator statistical tests in Serbia. *Global and Planetary Change*, 100: 172-182.

Gupta, H. V., Sorooshian, S. and Yapo, P. O. 1999. Status of Automatic Calibration for Hydrologic Models: Comparison with Multilevel Expert Calibration. *Journal of Hydrologic Engineering*, 4 (2): 135-143.

Guttman, N. B. 1998. Comparing the Palmer drought index and the standardized precipitation index. *JAWRA Journal of the American Water Resources Association*, 34 (1): 113-121.

Guttman, N. B. 1999. Accepting the standardized precipitation index: a calculation algorithm. *JAWRA Journal of the American Water Resources Association*, 35 (2): 311-322.

Haile, A. T., Rientjes, T., Gieske, A. and Gebremichael, M. 2009. Rainfall Variability over Mountainous and Adjacent Lake Areas: The Case of Lake Tana Basin at the Source of the Blue Nile River. *Journal of Applied Meteorology and Climatology*, 48 (8): 1696-1717.

Haile, T. 1988. Causes and Characteristics of Drought in Ethiopia. *Ethiopian Journal of Agricultural Sciences*, 10: 85-97.

Hair, J. F., Hult, G. T. M., Ringle, C. M., Sarstedt, M., Danks, N. P. and Ray, S. 2021. Overview of R and RStudio. In: Hair Jr, J. F., Hult, G. T. M., Ringle, C. M., Sarstedt, M., Danks, N. P. and Ray, S. (Eds), *Partial Least Squares Structural Equation Modeling (PLS-SEM) Using R: A Workbook*. Cham: Springer International Publishing, 31-47. Available: https://doi.org/10.1007/978-3-030-80519-7_2 (Accessed 7/26/2022).

Halefom, A., Teshome, A., Sisay, E. and Ahmad, I. 2018a. Dynamics of Land Use and Land Cover Change Using Remote Sensing and GIS: A Case Study of Debre Tabor Town, South Gondar, Ethiopia. *Journal of Geographic Information System*, 10: 165-174.

Halefom, A., Teshome, A., Sisay, E., Khare, D., Ulsido, M., Singh, L. and Tadesse, D. 2018b. Applications of Remote Sensing and GIS in Land Use/Land Cover Change Detection: A Case Study of Woreta Zuria Watershed, Ethiopia. Article ID: 1-9.

Halli, H. M., Hatti, V., Gupta, G., Raghavendra, M., Meena, M. P. and Gouda, R. 2022. Chapter 7 - Scientific approaches for water resources management in developing countries. In: Srivastav, A. L., Madhav, S., Bhardwaj, A. K. and Valsami-Jones, E. (Eds), *Current Directions in Water Scarcity Research*. Elsevier, 129-147. Available: https://www.sciencedirect.com/science/article/pii/B9780323918381000178 (Accessed 7/31/2023).

Hare, B. 2003. Assessment of Knowledge on Impacts of Climate Change - Contribution to the Specification of Art. 2 of the UNFCCC: Impacts on Ecosystems, Food Production, Water and Socio-economic Systems. Article ID: https://www.researchgate.net/publication/242460387.

Harka, A. E., Jilo, N. B. and Behulu, F. 2021. Spatial-temporal rainfall trend and variability assessment in the Upper Wabe Shebelle River Basin, Ethiopia: Application of innovative trend analysis method. *Journal of Hydrology: Regional Studies*, 37: 100915.

IPCC. 2012. *Managing the Risks of Extreme Events and Disasters to Advance Climate Change Adaptation. In: A Special Report of Working Groups I and II of the Intergovernmental Panel on*

*Climate Change (C. B. Field, V. Barros, T. F. Stocker, D. Qin, D. J. Dokken, K. L. Ebi, M. D. Mastrandrea, K. J. Mach, G.-K. Plattner, S. K. Allen, M. Tignor & P. M. Midgley (Eds). Cambridge University Press, Cambridge, UK and New York, USA, 582.*

Jajarmizadeh, M., Harun, S. B. and Salarpour, M. 2012. A review on theoretical consideration and types of models in hydrology. *Journal of Environmental Science and Technology*, 5: 249-261.

Karabulut, M. 2015. Drought Analysis in Antakya-Kahramanmaras Graben, Turkey. Journal of Arid Land, 7, 741-754. Article ID: https://doi.org/10.1007/s40333-40015-40011-40336.

Kassie, B. T., RÖTter, R. P., Hengsdijk, H., Asseng, S., Van Ittersum, M. K., Kahiluoto, H. and Van Keulen, H. 2014. Climate variability and change in the Central Rift Valley of Ethiopia: challenges for rainfed crop production. *The Journal of Agricultural Science*, 152 (1): 58-74.

Kasuni, S. 2017. Modeling the Impacts of Land Cover Changes on Stream Flow Response in Thiba River Basin in Kenya. *Journal of Water Resources and Ocean Science*, 6: 1.

Kebede, S., Travi, Y., Alemayehu, T. and Marc, V. 2006. Water balance of Lake Tana and its sensitivity to fluctuations in rainfall, Blue Nile basin, Ethiopia. *Journal of Hydrology*, 316 (1): 233-247.

Keller, M. 2009. Climate risks and development projects. *Assessment Report for a Community-level Project in Gudru, Oromyia, Ethiopia. Bread for All, Switzerland*, Article ID: https://www.iisd.org/cristaltool/documents/BFA-Ethiopia-Assessment-Report-Eng.pdf.

Kendall, M. G. 1975. *Rank correlation methods*. London: Griffin.

Kitessa, B. D., Ayalew, S. M., Gebrie, G. S. and Teferi, S. T. M. 2022. Optimization of urban resources efficiency in the domain of water-energy-food nexus through integrated modeling: a case study of Addis Ababa city. *Water Policy*, 24 (2): 397-431.

Kolokytha, E. 2022. Adaptation: A Vital Priority for Sustainable Water Resources Management. *Water*, 14 (4): 531.

Korecha, D. and Barnston, A. G. 2007. Predictability of June September Rainfall in Ethiopia. *Monthly Weather Review*, 135: 628.

Koua, T., Dhanesh, Y., Jeong, J., Srinivasan, R. and Anoh, K. 2021. Implementation of the Semi-Distributed SWAT (Soil and Water Assessment Tool) Model Capacity in the Lobo Watershed at Nibéhibé (Center-West of Côte D'Ivoire). *Journal of Geoscience and Environment Protection*, 09: 21-38.

Krause, P., Boyle, D. P. and Bäse, F. 2005. Comparison of different efficiency criteria for hydrological model assessment. *Adv. Geosci.*, 5: 89-97.

Kuczera, G. and Parent, E. 1998. Monte Carlo assessment of parameter uncertainty in conceptual catchment models: the Metropolis algorithm. *Journal of Hydrology*, 211 (1): 69-85.

Lemma, H., Frankl, A., Dessie, M., Poesen, J., Adgo, E. and Nyssen, J. 2020. Consolidated sediment budget of Lake Tana, Ethiopia (2012–2016). *Geomorphology*, 371: 107434.

Liu, G., He, Z., Luan, Z. and Qi, S. 2018. Intercomparison of a Lumped Model and a Distributed Model for Streamflow Simulation in the Naoli River Watershed, Northeast China. *Water*, 10 (8).

Lloyd-Hughes, B. and Saunders, M. A. 2002. A drought climatology for Europe. *International Journal of Climatology*, 22 (13): 1571-1592.

Makenzi, P., Ketiem, P., Omondi, P., Maranga, E. and Wekesa, C. 2013. Trend analysis of climate change and its impacts on crop productivity in the lower Tana River basin, Kenya. *Octa Journal of Environmental Research*, 1 (4).

Mann, H. B. 1945. Nonparametric Tests Against Trend. *Econometrica*, 13 (3): 245-259.

McCartney, M., Alemayehu, T., Shiferaw, A. and Awlachew, S. 2010. Evaluation of current and future water resources development in the Lake Tana Basin, Ethiopia. *IWMI Research Report*, 2010.

McKee, T. B. 1995. Drought monitoring with multiple time scales. In: Proceedings of *9th Conference on Applied Climatology. Boston, 1995*.

McKee, T. B., Doesken, N. J. and Kleist, J. 1993. The relationship of drought frequency and duration to time scales. In Proceeding of the 8th Conference on Applied Climatology, Anaheim, CA, USA. 17-22 January. 1993. Article ID: 179-183.

McSweeney, C., New, M. and Lizcano, G. 2008. "UNDP climate change Country profiles Ethiopia," 2008. Article ID: http://country-profiles.geog.ox.ac.uk.

Mengistu, D., Bewket, W., Dosio, A. and Panitz, H.-J. 2021. Climate change impacts on water resources in the Upper Blue Nile (Abay) River Basin, Ethiopia. *Journal of Hydrology*, 592: 125614.

Mengistu, D., Bewket, W. and Lal, R. 2014. Recent spatiotemporal temperature and rainfall variability and trends over the Upper Blue Nile River Basin, Ethiopia. *International Journal of Climatology*, 34 (7): 2278-2292.

Mesfin, S., Adem, A. A., Mullu, A. and Melesse, A. M. 2021. Historical Trend Analysis of Rainfall in Amhara National Regional State. In: Melesse, A. M., Abtew, W. and Moges, S. A. (Eds), *Nile and Grand Ethiopian Renaissance Dam: Past, Present and Future*. Cham: Springer International Publishing, 475-491. Available: https://doi.org/10.1007/978-3-030-76437-1_25 (Accessed 7/26/23).

Moriasi, D. N., Arnold, J. G., Van Liew, M. W., Bingner, R. L., Harmel, R. D. and Veith, T. L. 2007. Model evaluation guidelines for systematic quantification of accuracy in watershed simulations. *Transactions of the ASABE*, 50 (3): 885-900.

Mukheibir, P. 2008. Water Resources Management Strategies for Adaptation to Climate-Induced Impacts in South Africa. *Water Resources Management*, 22 (9): 1259-1276.

Näschen, K., Diekkrüger, B., Evers, M., Höllermann, B., Steinbach, S. and Thonfeld, F. 2019. The Impact of Land Use/Land Cover Change (LULCC) on Water Resources in a Tropical Catchment in Tanzania under Different Climate Change Scenarios. *Sustainability*, 11 (24): 7083.

Nash, J. E. and Sutcliffe, J. V. 1970. River flow forecasting through conceptual models part I - A discussion of principles. *Journal of Hydrology*, 10 (3): 282-290.

NBI. 2009. *The biodiversity, wetlands and water quality of the Lake Tana Sub Basin. Nile Basin Initiative (NBI), Bahir Dar*. https://nilebasin.org/node/12322:

Neitsch, S., Arnold, J., Kiniry, J. and Williams, J. 2009. Soil and water assessment tool theoretical documentation version 2009. 2011. *Texas Water Resources Institute*, Article ID: https://swat.tamu.edu/media/99192/swat92009-theory.pdf.

Neri, A., Villarini, G., Slater, L. J. and Napolitano, F. 2019. On the statistical attribution of the frequency of flood events across the U.S. Midwest. *Advances in Water Resources*, 127: 225-236.

NMA. 2006. *Agro-meteorology bulletin. Addis Ababa, Ethiopia*. http://wamis.gmu.edu/countries/ethiopia/Eth20061630.pdf:

NMSA. 1996. *Climatic and agro-climatic resources of Ethiopia. NMSA Meteorological Research Report Series. Vol. 1. Addis Ababa No. 1, 137.*

Nwanganga, F. and Chapple, M. 2020. *Practical machine learning in R*. John Wiley & Sons.

Ociepa, E., Mrowiec, M. and Deska, I. 2019. Analysis of Water Losses and Assessment of Initiatives Aimed at Their Reduction in Selected Water Supply Systems. *Water*, 11 (5): 1037.

Oliver, J. E. 1980. Monthly Precipitation Distribution: A Comparative Index. *The Professional Geographer*, 32 (3): 300-309.

Refsgaard, J. C. 1997. Parameterisation, calibration and validation of distributed hydrological models. *Journal of Hydrology*, 198 (1): 69-97.

Reidmiller, D., Avery, C., Easterling, D., Kunkel, K., Lewis, K., Maycock, T. and Stewart, B. 2018. *Fourth national climate assessment, Impacts, risks, and adaptation in the United States. US Global Change Research Program: Washington, D.C., USA, 2018; Volume 2*.

Roth, V., Lemann, T., Zeleke, G., Subhatu, A. T., Nigussie, T. K. and Hurni, H. 2018. Effects of climate change on water resources in the upper Blue Nile Basin of Ethiopia. *Heliyon*, 4 (9): e00771.

Samal, D. R. and Gedam, S. 2021. Assessing the impacts of land use and land cover change on water resources in the Upper Bhima river basin, India. *Environmental Challenges*, 5: 100251.

Santhi, C., Arnold, J., Williams, J. R., Dugas, W. A., Srinivasan, R. and Hauck, L. M. 2001. Validation of the SWAT Model on a Large River Basin with Point and Nonpoint Sources. *JAWRA Journal of the American Water Resources Association*, 37: 1169-1188.

Schuol, J., Abbaspour, K. C., Srinivasan, R. and Yang, H. 2008. Estimation of freshwater availability in the West African sub-continent using the SWAT hydrologic model. *Journal of Hydrology*, 352 (1): 30-49.

Sead, A., Bauwens, W. and Marwa, A. 2010. Analysis of the Impact of Land Use Change and Climate Change on the Flows in the Blue Nile River Using SWAT. *Unpublished Master's Thesis, KU Leuven, Belgium*, Article ID: https://www.academia.edu/6358202/.

Segele, Z. T. and Lamb, P. J. 2005. Characterization and variability of Kiremt rainy season over Ethiopia. *Meteorology and Atmospheric Physics*, 89: 153-180.

Seleshi, Y. and Zanke, U. 2004. Recent Changes in Rainfall and Rainy Days in Ethiopia. *International Journal of Climatology*, 24: 973-983.

Sen, P. K. 1968. Estimates of the Regression Coefficient Based on Kendall's Tau. *Journal of the American Statistical Association*, 63 (324): 1379-1389.

Setegn, S., Srinivasan, R., Melesse, A. and Dargahi, B. 2009. SWAT Model Application and Prediction Uncertainty Analysis in the Lake Tana Basin, Ethiopia. *Hydrological Processes*, 24: 357-367.

Setegn, S. G., Rayner, D., Melesse, A. M., Dargahi, B. and Srinivasan, R. 2011. Impact of climate change on the hydroclimatology of Lake Tana Basin, Ethiopia. *Water Resources Research*, 47 (4).

Setegn, S. G., Srinivasan, R. and Dargahi, B. 2008. Hydrological Modeling in the Lake Tana Basin, Ethiopia Using SWAT Model. The Open Hydrology Journal, 2, 49-62. Article ID: http://dx.doi.org/10.2174/1874378100802010049.

Shawul, A. A. and Chakma, S. 2020. Trend of extreme precipitation indices and analysis of long-term climate variability in the Upper Awash basin, Ethiopia. *Theoretical and Applied Climatology*, 140 (1): 635-652.

Sidle, R. C. 2021. Strategies for smarter catchment hydrology models: incorporating scaling and better process representation. *Geoscience Letters*, 8 (1): 24.

SMEC. 2008. *Hydrological Study of the Tana-Beles Sub-Basins: Main Report. Ethiopian Ministry of Water Resources, Addis Ababa.*

Stonestrom, D. A., Scanlon, B. R. and Zhang, L. 2009. Introduction to special section on impacts of land use change on water resources. *Water Resources Research*, 45 (7).

Svoboda, M., Hayes, M. and Wood, D. 2012. Standardized Precipitation Index User Guide; World Meteorological Organization: Geneva, Switzerland. Article ID: https://www.researchgate.net/publication/360653192.

Tadele, K. and Förch, G. 2007. Impact of land use/cover change on streamflow: the case of Hare River Watershed, Ethiopia. In: Proceedings of *Catchment and lake research, Lake Abaya Research Symposium (LARS), Arba Minch, Ethiopia*.

Tan, M. L., Gassman, P. W., Yang, X. and Haywood, J. 2020. A review of SWAT applications, performance and future needs for simulation of hydro-climatic extremes. *Advances in Water Resources*, 143: 103662.

Taye, M. T., Haile, A. T., Fekadu, A. G. and Nakawuka, P. 2021. Effect of irrigation water withdrawal on the hydrology of the Lake Tana sub-basin. *Journal of Hydrology: Regional Studies*, 38: 100961.

Tenagashaw, D. Y. and Andualem, T. G. 2022. Analysis and Characterization of Hydrological Drought Under Future Climate Change Using the SWAT Model in Tana Sub-basin, Ethiopia. *Water Conservation Science and Engineering*, 7 (2): 131-142.

Tesfaw, B. A. 2016. Optimize operations and future development on multi-purpose Tana Beles hydropower project. *Master's Thesis, Norwegian University of Science and Technology, Norway*, Article ID: http://hdl.handle.net/11250/2433628.

Tewabe, D. and Fentahun, T. 2020. Assessing land use and land cover change detection using remote sensing in the Lake Tana Basin, Northwest Ethiopia. *Cogent Environmental Science*, 6 (1): 1778998.

Thakuri, P. and Wijesekera, S. 2021. Selection of a Hydrological Model and Objective Function for Water Resources Management in Predominantly Rural Watershed using Criteria-Based Evaluation. *Journal of Water Engineering and Management*, 2.

Tofu, D. A. and Mengistu, M. 2023. Observed time series trend analysis of climate variability and smallholder adoption of new agricultural technologies in west Shewa, Ethiopia. *Scientific African*, 19: e01448.

Tsakiris, G. P. and Loucks, D. P. 2023. Adaptive Water Resources Management Under Climate Change: An Introduction. *Water Resources Management*, 37 (6): 2221-2233.

Van Griensven, A. and Meixner, T. 2006. Methods to quantify and identify the sources of uncertainty for river basin water quality models. *Water Science and Technology*, 53 (1): 51-59.

Van Liew, M., Arnold, J. and Garbrecht, J. 2003. Hydrologic simulation on agricultural watersheds: Choosing between two models. *Transactions of the ASAE*, 46 (6): 1539-1551.

Viste, E., Korecha, D. and Sorteberg, A. 2013. Recent drought and precipitation tendencies in Ethiopia. *Theoretical and Applied Climatology*, 112 (3): 535-551.

Wale, A., Rientjes, T., Dost, R. and Gieske, A. 2008. Hydrological Balance of Lake Tana Upper Blue Nile Basin, Ethiopia. In: Proceedings of. ITC The Netherlands,

Walsh, R. and Lawler, D. 1981. Rainfall seasonality: description, spatial patterns and change through time. *Weather*, 36 (7): 201-208.

Wang, L. and Qu, J. J. 2009. Satellite remote sensing applications for surface soil moisture monitoring: A review. *Frontiers of Earth Science in China*, 3 (2): 237-247.

Wassie, S. B. 2020. Natural resource degradation tendencies in Ethiopia: a review. *Environmental Systems Research*, 9 (1): 33.

Weldegerima, T. M., Zeleke, T. T., Birhanu, B. S., Zaitchik, B. F. and Fetene, Z. A. 2018. Analysis of Rainfall Trends and Its Relationship with SST Signals in the Lake Tana Basin, Ethiopia. *Advances in Meteorology*, 2018: 5869010.

Woldesenbet, T. A., Elagib, N. A., Ribbe, L. and Heinrich, J. 2017. Hydrological responses to land use/cover changes in the source region of the Upper Blue Nile Basin, Ethiopia. *Science of The Total Environment*, 575: 724-741.

Woldesenbet, T. A., Elagib, N. A., Ribbe, L. and Heinrich, J. 2018. Catchment response to climate and land use changes in the Upper Blue Nile sub-basins, Ethiopia. *Science of The Total Environment*, 644: 193-206.

Worku, M. A., Feyisa, G. L. and Beketie, K. T. 2022. Climate trend analysis for a semi-arid Borana zone in southern Ethiopia during 1981-2018. *Environmental Systems Research*, 11 (1): 2.

Worqlul, A. W., Ayana, E. K., Maathuis, B. H. P., MacAlister, C., Philpot, W. D., Osorio Leyton, J. M. and Steenhuis, T. S. 2018. Performance of bias corrected MPEG rainfall estimate for rainfall-runoff simulation in the upper Blue Nile Basin, Ethiopia. *Journal of Hydrology*, 556: 1182-1191.

Wubneh, M. A., Fikadie, F. T., Worku, T. A., Aman, T. F. and Kifelew, M. S. 2022. Hydrological impacts of climate change in gauged sub-watersheds of Lake Tana sub-basin (Gilgel Abay, Gumara, Megech, and Ribb) watersheds, Upper Blue Nile Basin, Ethiopia. *Sustainable Water Resources Management*, 8 (3): 81.

Wubneh, M. A., Worku, T. A., Fikadie, F. T., Aman, T. F. and Alemu, M. G. 2024. Operational analysis of lake Tana under climate change, Upper Blue Nile Basin, Ethiopia. *Scientific African*, 24: e02217.

Yang, J., Reichert, P., Abbaspour, K. C., Xia, J. and Yang, H. 2008. Comparing uncertainty analysis techniques for a SWAT application to the Chaohe Basin in China. *Journal of Hydrology*, 358 (1): 1-23.

Yimer, F., Ledin, S. and Abdelkadir, A. 2006. Soil property variations in relation to topographic aspect and vegetation community in the south-eastern highlands of Ethiopia. *Forest Ecology and Management*, 232 (1-3): 90-99.

Zhang, H., Wang, B., Liu, D. L., Zhang, M., Leslie, L. M. and Yu, Q. 2020. Using an improved SWAT model to simulate hydrological responses to land use change: A case study of a catchment in tropical Australia. *Journal of Hydrology*, 585: 124822.

Zhao, M. and Boll, J. 2022. Adaptation of water resources management under climate change. *Frontiers in Water*, 4: https://doi.org/10.3389/frwa.2022.983228.

# ANNEXURES

Annexure 1: Long term monthly average minimum and maximum rainfall (1981-2020)

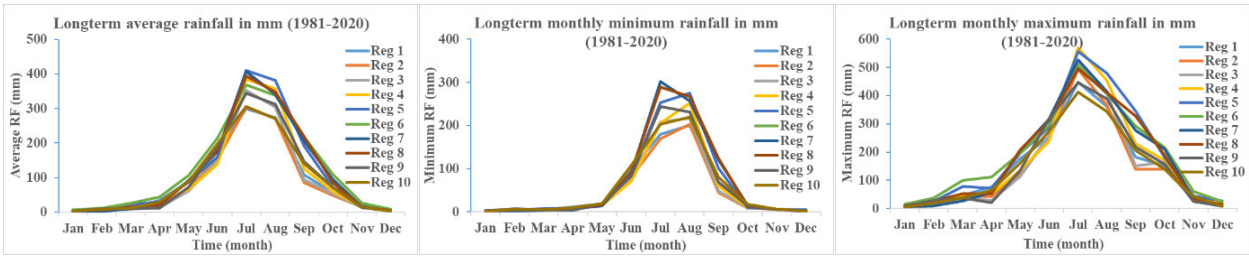


Annexure 2: Coefficient of variation for long-term monthly average rainfall (1981-2020)

| | Jan | Feb | Mar | Apr | May | Jun | Jul | Aug | Sep | Oct | Nov | Dec |
|---|---|---|---|---|---|---|---|---|---|---|---|---|
| Reg 1 | 28.10 | 35.87 | 62.25 | 54.12 | 39.26 | 20.92 | 19.13 | 12.77 | 23.07 | 53.59 | 52.16 | 39.02 |
| Reg 2 | 32.67 | 31.91 | 69.67 | 49.05 | 37.62 | 25.77 | 21.39 | 14.40 | 27.24 | 57.31 | 40.32 | 37.10 |
| Reg 3 | 30.87 | 30.08 | 66.48 | 47.51 | 39.96 | 31.06 | 20.48 | 15.81 | 26.37 | 59.77 | 38.30 | 33.61 |
| Reg 4 | 32.82 | 42.63 | 58.89 | 48.16 | 52.21 | 31.43 | 20.82 | 15.52 | 24.59 | 59.71 | 52.98 | 47.28 |
| Reg 5 | 33.15 | 44.85 | 58.95 | 52.10 | 56.59 | 30.71 | 16.15 | 13.56 | 22.87 | 55.36 | 50.57 | 51.70 |
| Reg 6 | 27.42 | 45.84 | 67.02 | 61.91 | 46.11 | 18.17 | 14.43 | 10.87 | 17.44 | 39.42 | 54.64 | 50.66 |
| Reg 7 | 30.21 | 49.03 | 55.15 | 56.29 | 55.14 | 27.36 | 13.30 | 11.40 | 19.85 | 49.68 | 41.86 | 47.69 |
| Reg 8 | 28.72 | 49.49 | 59.83 | 55.27 | 56.15 | 27.94 | 13.22 | 11.11 | 20.12 | 49.25 | 40.87 | 50.53 |
| Reg 9 | 21.33 | 35.87 | 60.76 | 43.23 | 38.27 | 30.61 | 14.72 | 14.28 | 23.54 | 47.22 | 32.83 | 38.54 |
| Reg 10 | 17.08 | 29.58 | 58.63 | 54.21 | 37.11 | 19.70 | 15.21 | 12.17 | 19.97 | 40.93 | 49.97 | 39.57 |

Annexure 3: Minimum temperature trend (Sen's slope and Mann-Kendall)

| MK | Jan | Feb | Mar | Apr | May | Jun | Jul | Aug | Sep | Oct | Nov | Dec | Spring | Summer | Autumn | Winter | Annual |
|---|---|---|---|---|---|---|---|---|---|---|---|---|---|---|---|---|---|
| Reg 1 | 0.00 | 0.00 | 0.00 | 0.04 | 0.01 | 0.01 | 0.04 | 0.01 | 0.00 | 0.00 | 0.05 | 0.02 | 0.00 | 0.03 | 0.00 | 0.00 | 0.00 |
| Reg 2 | 0.01 | 0.00 | 0.01 | 0.03 | 0.00 | 0.02 | 0.17 | 0.08 | 0.03 | 0.00 | 0.04 | 0.02 | 0.01 | 0.03 | 0.00 | 0.00 | 0.00 |
| Reg 3 | 0.24 | 0.00 | 0.00 | 0.00 | 0.00 | 0.00 | 0.00 | 0.00 | 0.00 | 0.00 | 0.00 | 0.02 | 0.00 | 0.00 | 0.00 | 0.00 | 0.00 |
| Reg 4 | 0.00 | 0.00 | 0.00 | 0.00 | 0.00 | 0.00 | 0.00 | 0.00 | 0.00 | 0.00 | 0.00 | 0.01 | 0.00 | 0.00 | 0.00 | 0.00 | 0.00 |
| Reg 5 | 0.12 | 0.00 | 0.00 | 0.00 | 0.00 | 0.00 | 0.00 | 0.00 | 0.00 | 0.00 | 0.00 | 0.03 | 0.00 | 0.00 | 0.00 | 0.00 | 0.00 |
| Reg 6 | 0.02 | 0.00 | 0.00 | 0.00 | 0.00 | 0.00 | 0.00 | 0.00 | 0.00 | 0.00 | 0.00 | 0.01 | 0.00 | 0.00 | 0.00 | 0.00 | 0.00 |
| Reg 7 | 0.23 | 0.75 | 0.32 | 0.27 | 0.06 | 0.04 | 0.04 | 0.01 | 0.00 | 0.02 | 0.45 | 0.73 | 0.07 | 0.02 | 0.02 | 0.88 | 0.06 |
| Reg 8 | 0.01 | 0.61 | 0.33 | 0.58 | 0.15 | 0.28 | 0.26 | 0.10 | 0.00 | 0.04 | 0.80 | 0.14 | 0.73 | 0.12 | 0.18 | 0.05 | 0.88 |
| Reg 9 | 0.02 | 0.00 | 0.00 | 0.00 | 0.00 | 0.00 | 0.00 | 0.00 | 0.00 | 0.00 | 0.00 | 0.01 | 0.00 | 0.00 | 0.00 | 0.00 | 0.00 |
| Reg 10 | 0.00 | 0.00 | 0.00 | 0.17 | 0.03 | 0.09 | 0.82 | 0.36 | 0.09 | 0.12 | 0.35 | 0.20 | 0.05 | 0.38 | 0.26 | 0.00 | 0.06 |

| Sen's Slope | Jan | Feb | Mar | Apr | May | Jun | Jul | Aug | Sep | Oct | Nov | Dec | Spring | Summer | Autumn | Winter | Annual |
|---|---|---|---|---|---|---|---|---|---|---|---|---|---|---|---|---|---|
| Reg 1 | 0.04 | 0.06 | 0.05 | 0.04 | 0.05 | 0.03 | 0.02 | 0.03 | 0.04 | 0.05 | 0.03 | 0.03 | 0.04 | 0.03 | 0.04 | 0.04 | 0.03 |
| Reg 2 | 0.03 | 0.04 | 0.03 | 0.03 | 0.04 | 0.03 | 0.02 | 0.02 | 0.03 | 0.04 | 0.02 | 0.02 | 0.03 | 0.02 | 0.03 | 0.03 | 0.03 |
| Reg 3 | 0.02 | 0.05 | 0.06 | 0.07 | 0.07 | 0.05 | 0.04 | 0.03 | 0.04 | 0.06 | 0.04 | 0.03 | 0.07 | 0.04 | 0.05 | 0.03 | 0.05 |
| Reg 4 | 0.07 | 0.09 | 0.09 | 0.10 | 0.11 | 0.09 | 0.07 | 0.06 | 0.07 | 0.09 | 0.07 | 0.05 | 0.10 | 0.07 | 0.08 | 0.07 | 0.08 |
| Reg 5 | 0.03 | 0.05 | 0.05 | 0.06 | 0.07 | 0.05 | 0.05 | 0.06 | 0.05 | 0.06 | 0.05 | 0.04 | 0.06 | 0.05 | 0.05 | 0.04 | 0.05 |
| Reg 6 | 0.04 | 0.06 | 0.06 | 0.06 | 0.07 | 0.05 | 0.05 | 0.05 | 0.05 | 0.06 | 0.06 | 0.05 | 0.07 | 0.05 | 0.06 | 0.04 | 0.05 |
| Reg 7 | -0.02 | 0.00 | 0.01 | 0.01 | 0.03 | 0.03 | 0.02 | 0.02 | 0.04 | 0.02 | 0.01 | -0.01 | 0.02 | 0.02 | 0.02 | 0.00 | 0.02 |
| Reg 8 | -0.04 | -0.01 | 0.02 | 0.02 | 0.03 | 0.01 | 0.01 | 0.01 | 0.02 | 0.03 | 0.00 | -0.04 | 0.01 | 0.01 | 0.01 | -0.02 | 0.00 |
| Reg 9 | 0.04 | 0.06 | 0.07 | 0.06 | 0.07 | 0.05 | 0.05 | 0.05 | 0.06 | 0.07 | 0.05 | 0.05 | 0.07 | 0.05 | 0.06 | 0.04 | 0.06 |
| Reg 10 | 0.05 | 0.08 | 0.06 | 0.04 | 0.05 | 0.02 | 0.00 | 0.02 | 0.02 | 0.02 | 0.02 | 0.02 | 0.05 | 0.01 | 0.02 | 0.05 | 0.03 |

Annexure 4: Maximum temperature trend (Sen's slope and Mann-Kendall)

| MK | Jan | Feb | Mar | Apr | May | Jun | Jul | Aug | Sep | Oct | Nov | Dec | Spring | Summer | Autumn | Winter | Annual |
|---|---|---|---|---|---|---|---|---|---|---|---|---|---|---|---|---|---|
| Reg 1 | 0.05 | 0.00 | 0.00 | 0.00 | 0.00 | 0.00 | 0.20 | 0.00 | 0.00 | 0.00 | 0.00 | 0.00 | 0.00 | 0.00 | 0.00 | 0.00 | 0.00 |
| Reg 2 | 0.00 | 0.00 | 0.00 | 0.00 | 0.00 | 0.00 | 0.01 | 0.00 | 0.00 | 0.00 | 0.00 | 0.00 | 0.00 | 0.00 | 0.00 | 0.00 | 0.00 |
| Reg 3 | 0.00 | 0.00 | 0.00 | 0.00 | 0.00 | 0.00 | 0.03 | 0.00 | 0.00 | 0.00 | 0.00 | 0.00 | 0.00 | 0.00 | 0.00 | 0.00 | 0.00 |
| Reg 4 | 0.00 | 0.00 | 0.00 | 0.00 | 0.00 | 0.00 | 0.00 | 0.00 | 0.00 | 0.00 | 0.00 | 0.00 | 0.00 | 0.00 | 0.00 | 0.00 | 0.00 |
| Reg 5 | 0.01 | 0.00 | 0.00 | 0.00 | 0.00 | 0.05 | 0.01 | 0.00 | 0.00 | 0.00 | 0.00 | 0.00 | 0.00 | 0.00 | 0.00 | 0.00 | 0.00 |
| Reg 6 | 0.19 | 0.00 | 0.00 | 0.00 | 0.00 | 0.07 | 0.08 | 0.01 | 0.01 | 0.01 | 0.01 | 0.01 | 0.00 | 0.00 | 0.00 | 0.00 | 0.00 |
| Reg 7 | 0.15 | 0.01 | 0.00 | 0.00 | 0.00 | 0.75 | 0.22 | 0.09 | 0.05 | 0.06 | 0.06 | 0.09 | 0.00 | 0.15 | 0.02 | 0.00 | 0.00 |
| Reg 8 | 0.00 | 0.00 | 0.00 | 0.00 | 0.00 | 0.00 | 0.00 | 0.00 | 0.00 | 0.00 | 0.00 | 0.00 | 0.00 | 0.00 | 0.00 | 0.00 | 0.00 |
| Reg 9 | 0.12 | 0.00 | 0.00 | 0.00 | 0.00 | 0.01 | 0.05 | 0.01 | 0.00 | 0.03 | 0.00 | 0.01 | 0.00 | 0.00 | 0.00 | 0.00 | 0.00 |
| Reg 10 | 0.95 | 0.00 | 0.00 | 0.00 | 0.00 | 0.00 | 0.20 | 0.01 | 0.06 | 0.69 | 0.21 | 0.36 | 0.00 | 0.00 | 0.18 | 0.07 | 0.00 |

| Sen's Slope | Jan | Feb | Mar | Apr | May | Jun | Jul | Aug | Sep | Oct | Nov | Dec | Spring | Summer | Autumn | Winter | Annual |
|---|---|---|---|---|---|---|---|---|---|---|---|---|---|---|---|---|---|
| Reg 1 | 0.03 | 0.07 | 0.10 | 0.11 | 0.12 | 0.05 | 0.01 | 0.04 | 0.03 | 0.03 | 0.05 | 0.05 | 0.11 | 0.04 | 0.03 | 0.05 | 0.06 |
| Reg 2 | 0.05 | 0.08 | 0.10 | 0.11 | 0.10 | 0.05 | 0.04 | 0.06 | 0.05 | 0.05 | 0.06 | 0.07 | 0.10 | 0.05 | 0.05 | 0.07 | 0.06 |
| Reg 3 | 0.08 | 0.10 | 0.12 | 0.13 | 0.11 | 0.05 | 0.03 | 0.05 | 0.06 | 0.07 | 0.08 | 0.08 | 0.12 | 0.04 | 0.07 | 0.09 | 0.08 |
| Reg 4 | 0.10 | 0.11 | 0.14 | 0.13 | 0.11 | 0.06 | 0.07 | 0.08 | 0.09 | 0.09 | 0.09 | 0.11 | 0.13 | 0.06 | 0.09 | 0.11 | 0.10 |
| Reg 5 | 0.05 | 0.08 | 0.10 | 0.11 | 0.10 | 0.04 | 0.04 | 0.04 | 0.05 | 0.08 | 0.08 | 0.07 | 0.10 | 0.04 | 0.08 | 0.07 | 0.07 |
| Reg 6 | 0.03 | 0.07 | 0.08 | 0.09 | 0.09 | 0.03 | 0.03 | 0.04 | 0.04 | 0.05 | 0.05 | 0.05 | 0.09 | 0.03 | 0.05 | 0.05 | 0.05 |
| Reg 7 | 0.03 | 0.06 | 0.10 | 0.07 | 0.09 | 0.01 | 0.03 | 0.03 | 0.03 | 0.03 | 0.03 | 0.03 | 0.08 | 0.02 | 0.03 | 0.04 | 0.04 |
| Reg 8 | 0.07 | 0.11 | 0.11 | 0.10 | 0.12 | 0.05 | 0.05 | 0.06 | 0.06 | 0.04 | 0.06 | 0.06 | 0.11 | 0.05 | 0.05 | 0.08 | 0.07 |
| Reg 9 | 0.03 | 0.08 | 0.10 | 0.08 | 0.10 | 0.05 | 0.03 | 0.04 | 0.04 | 0.03 | 0.05 | 0.04 | 0.09 | 0.04 | 0.04 | 0.05 | 0.05 |
| Reg 10 | 0.00 | 0.06 | 0.11 | 0.12 | 0.14 | 0.06 | 0.02 | 0.03 | 0.02 | 0.01 | 0.02 | 0.01 | 0.11 | 0.04 | 0.02 | 0.03 | 0.05 |

Annexure 5: Characteristics of long-term monthly average precipitation at Bahir Dar

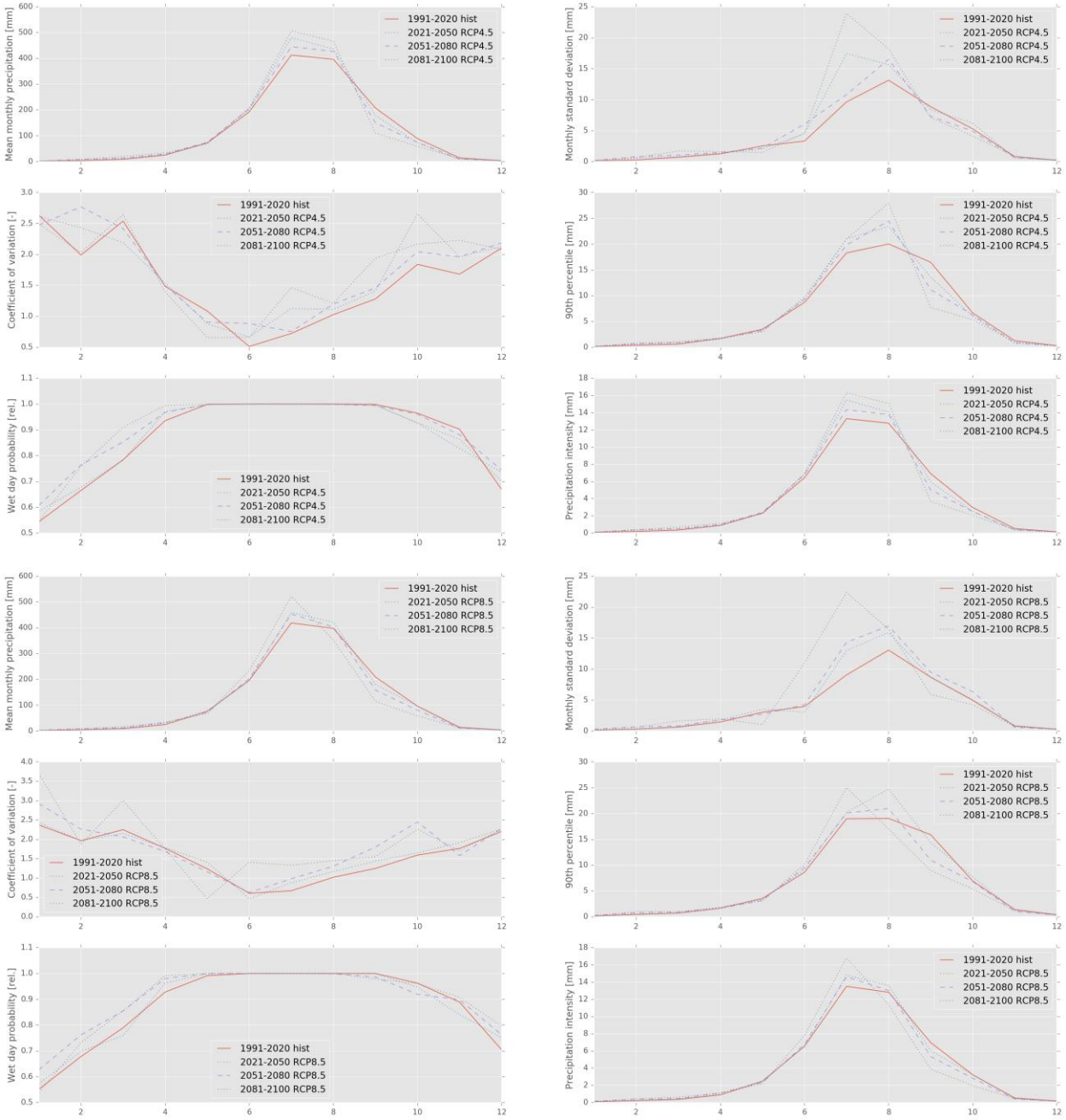

Annexure 6: Precipitation projection at Bahir Dar using RCP4.5 & RCP8.5

Annexure 7: Characteristics of long-term monthly temperature at Bahir Dar (RCP4.5)

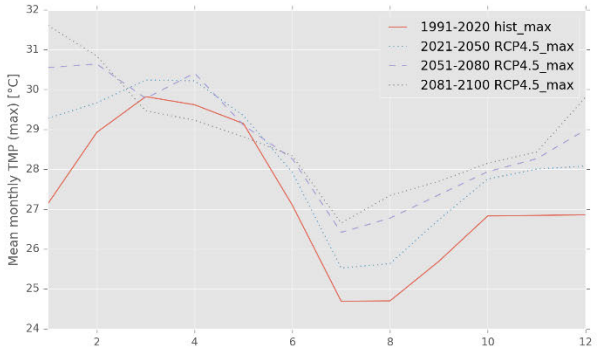


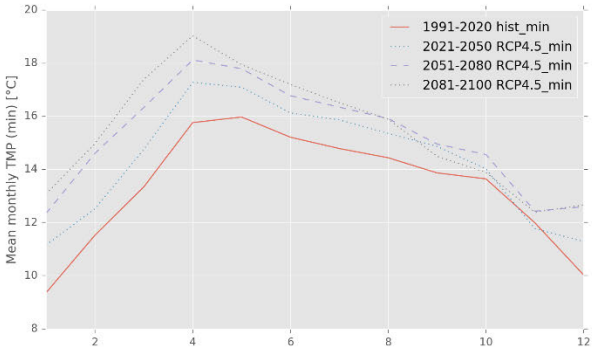


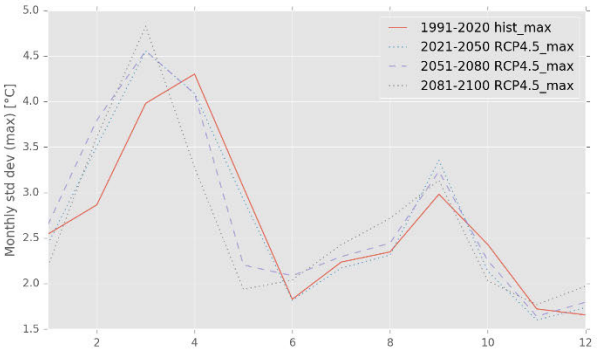


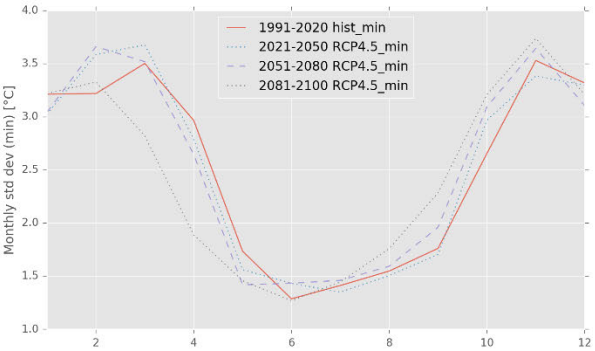


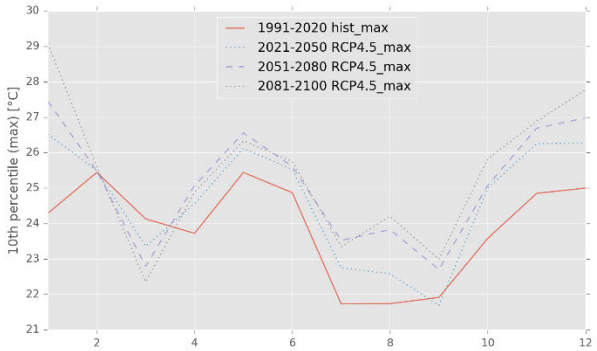


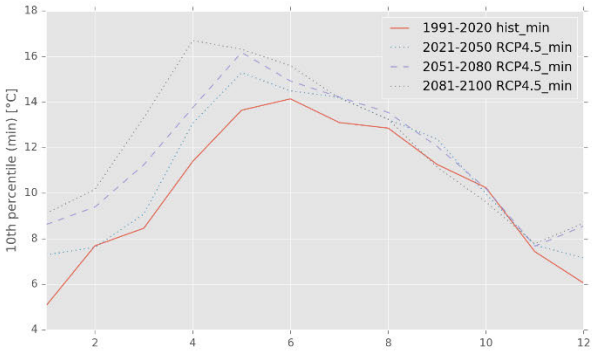


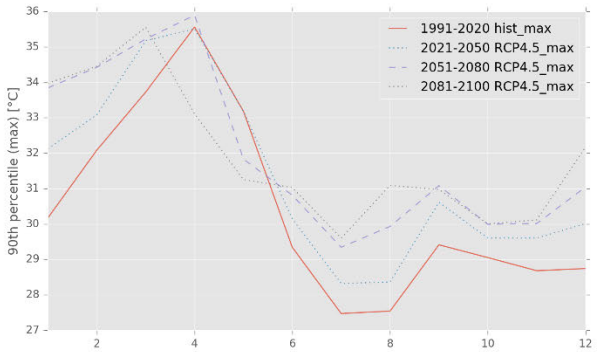


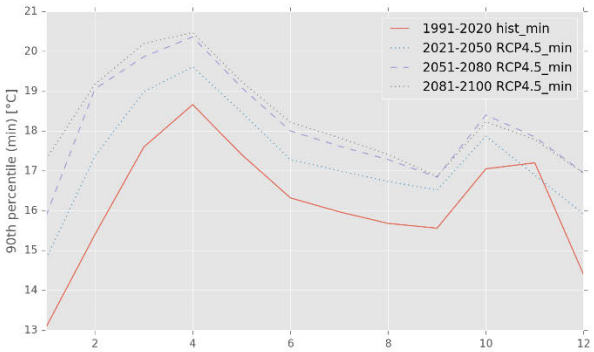

Annexure 8: Characteristics of long-term monthly temperature at Bahir Dar (RCP8.5)

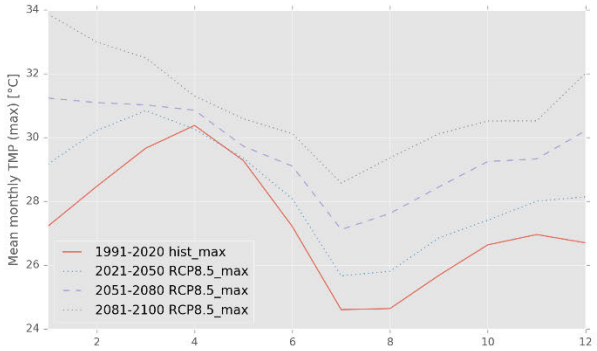


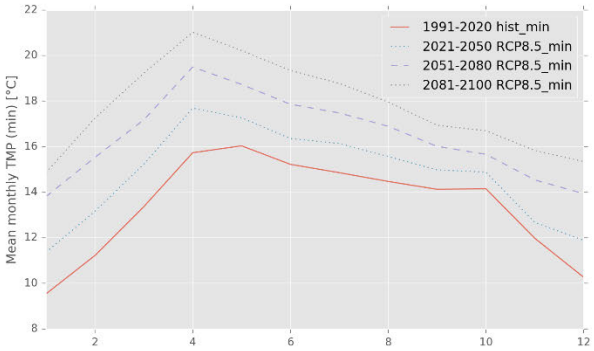


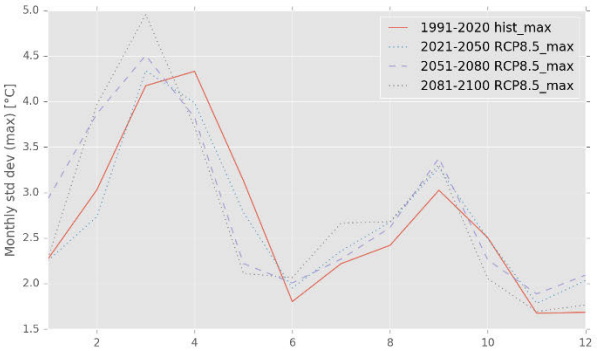


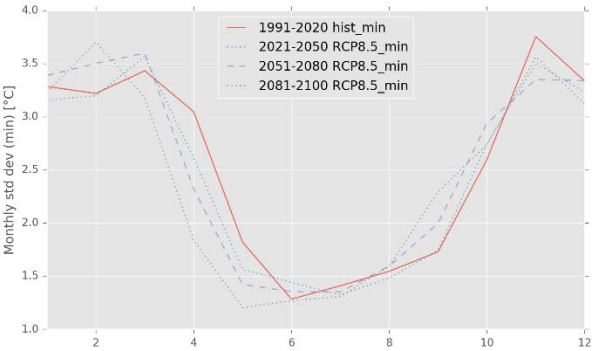


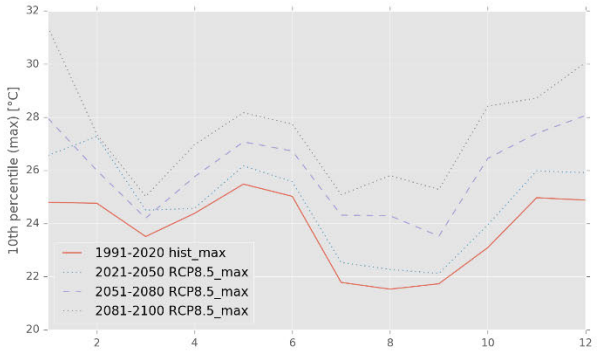


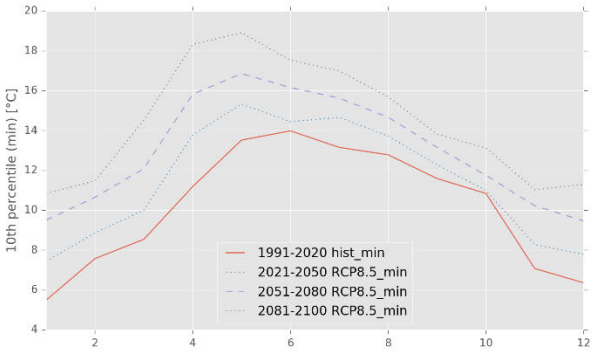


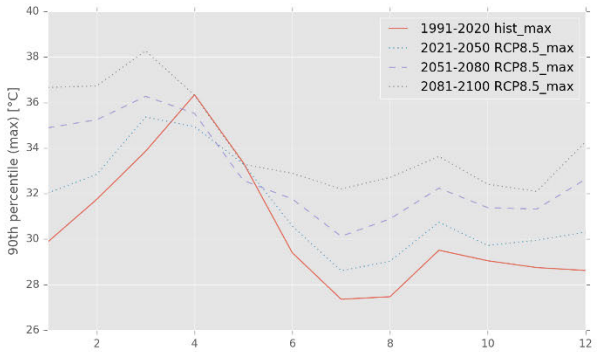


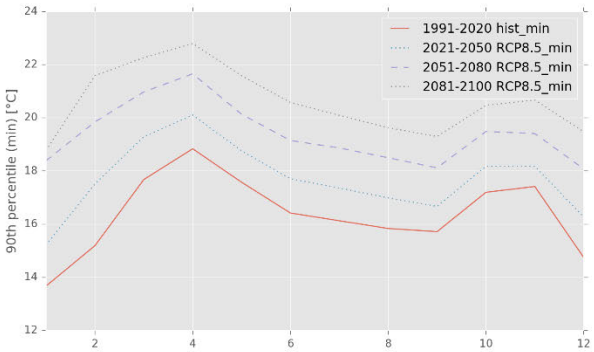

Annexure 9: Characteristics of long-term monthly average precipitation at Dangila

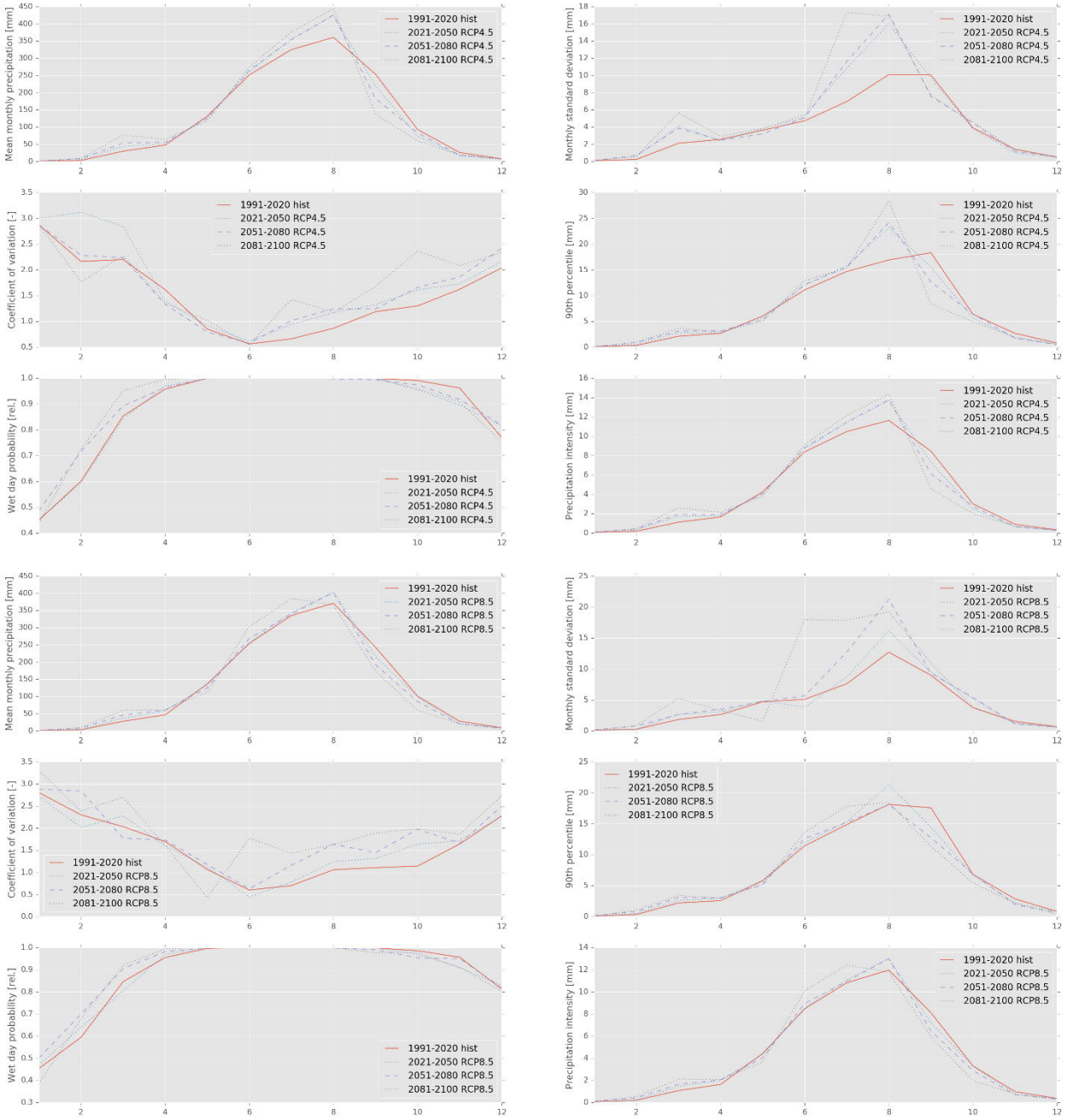

Annexure 10: Precipitation projection at Dangila using RCP4.5 & RCP8.5

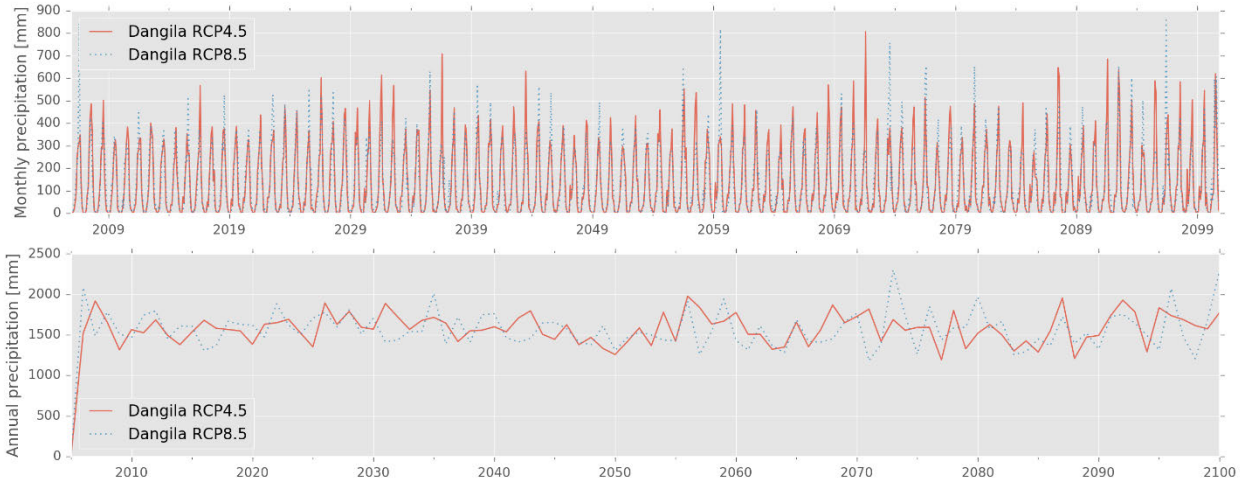

Annexure 11: Characteristics of long-term monthly temperature at Dangila (RCP4.5)

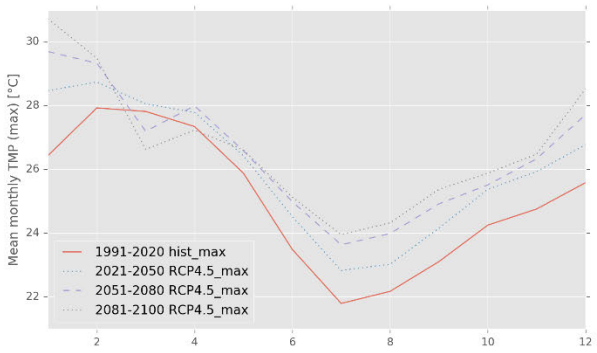


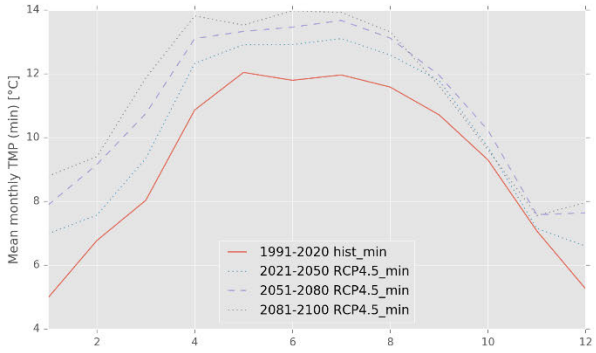


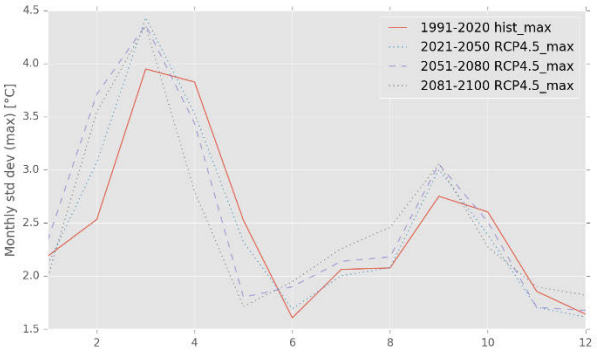


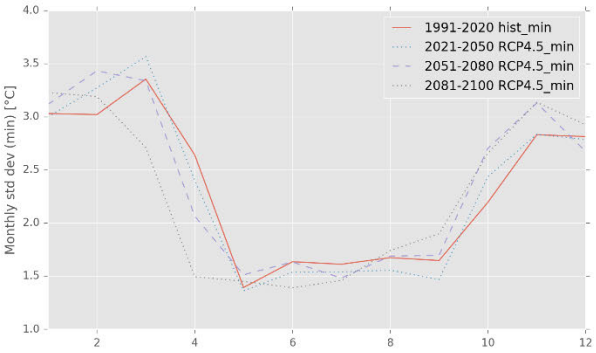


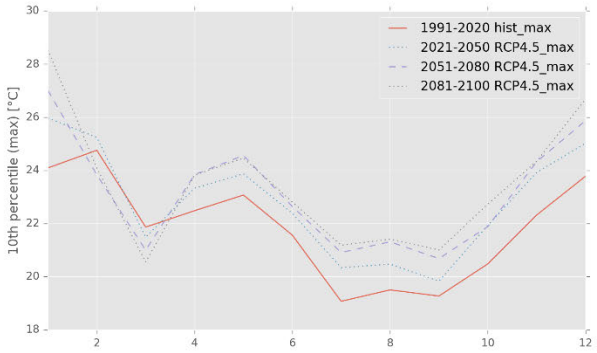


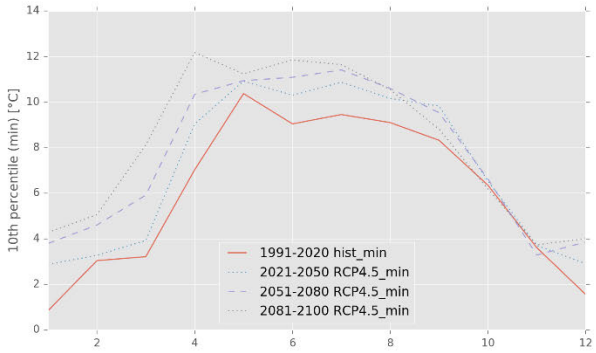


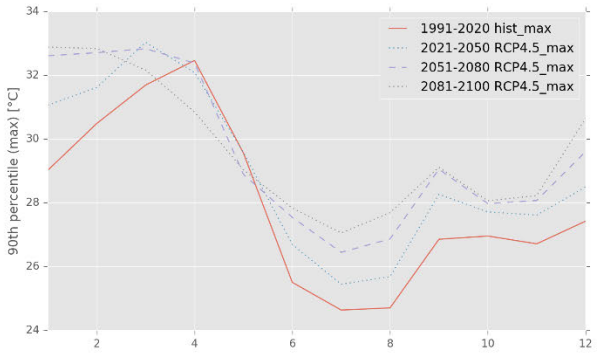


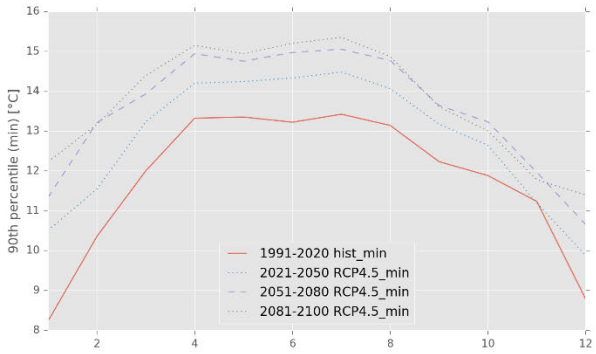

Annexure 12: Characteristics of long-term monthly temperature at Dangila (RCP8.5)

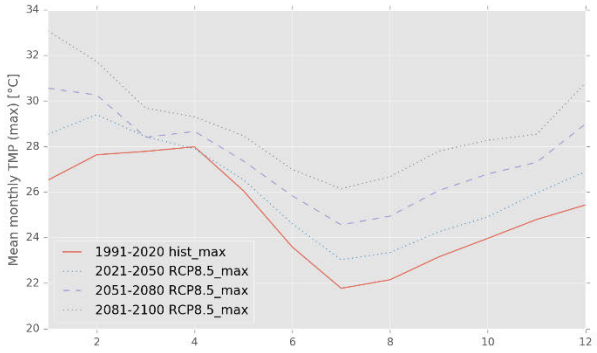


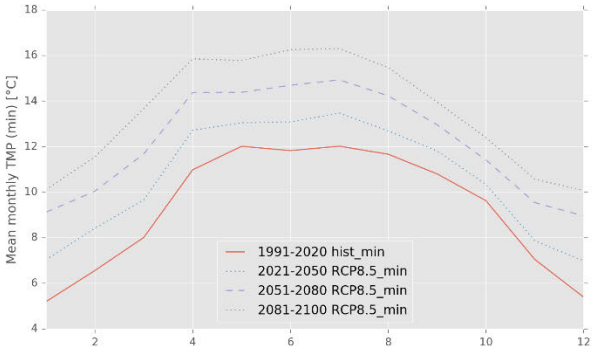


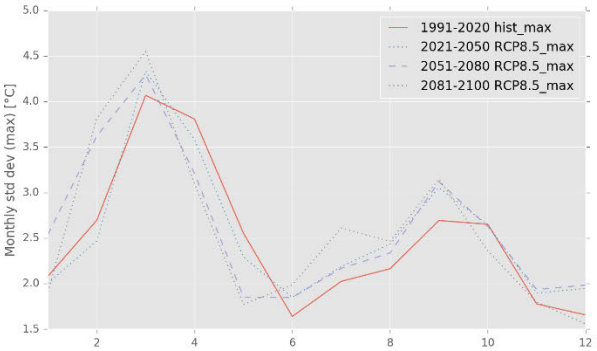


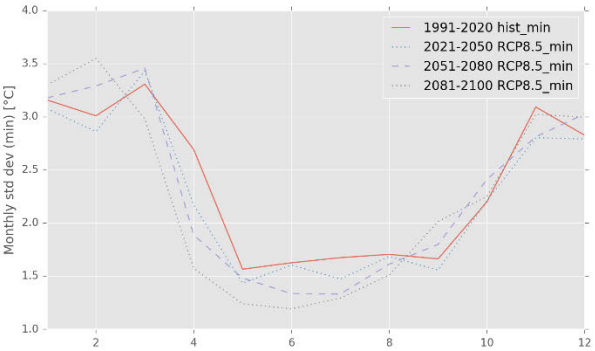


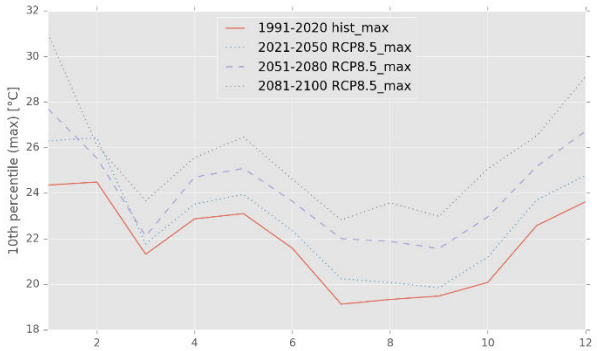


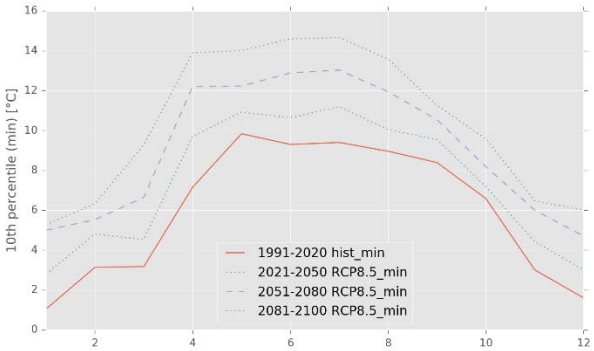


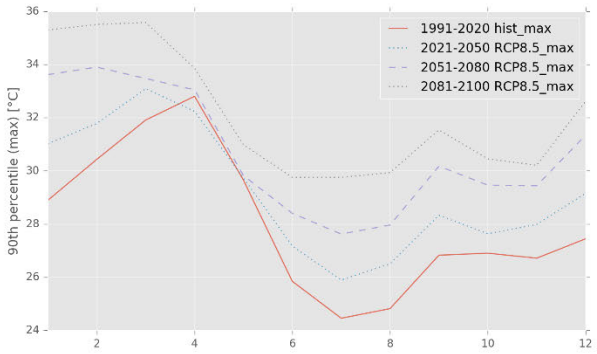


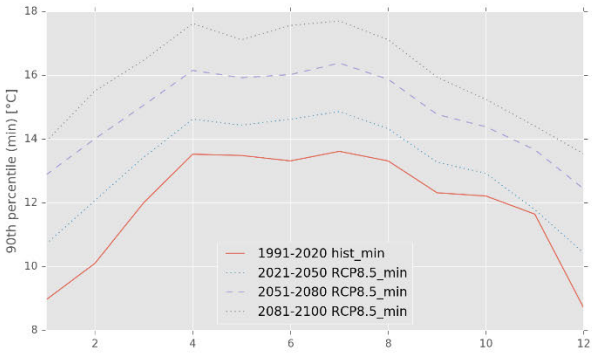

Annexure 13: Characteristics of long-term monthly average precipitation at Debre Tabor

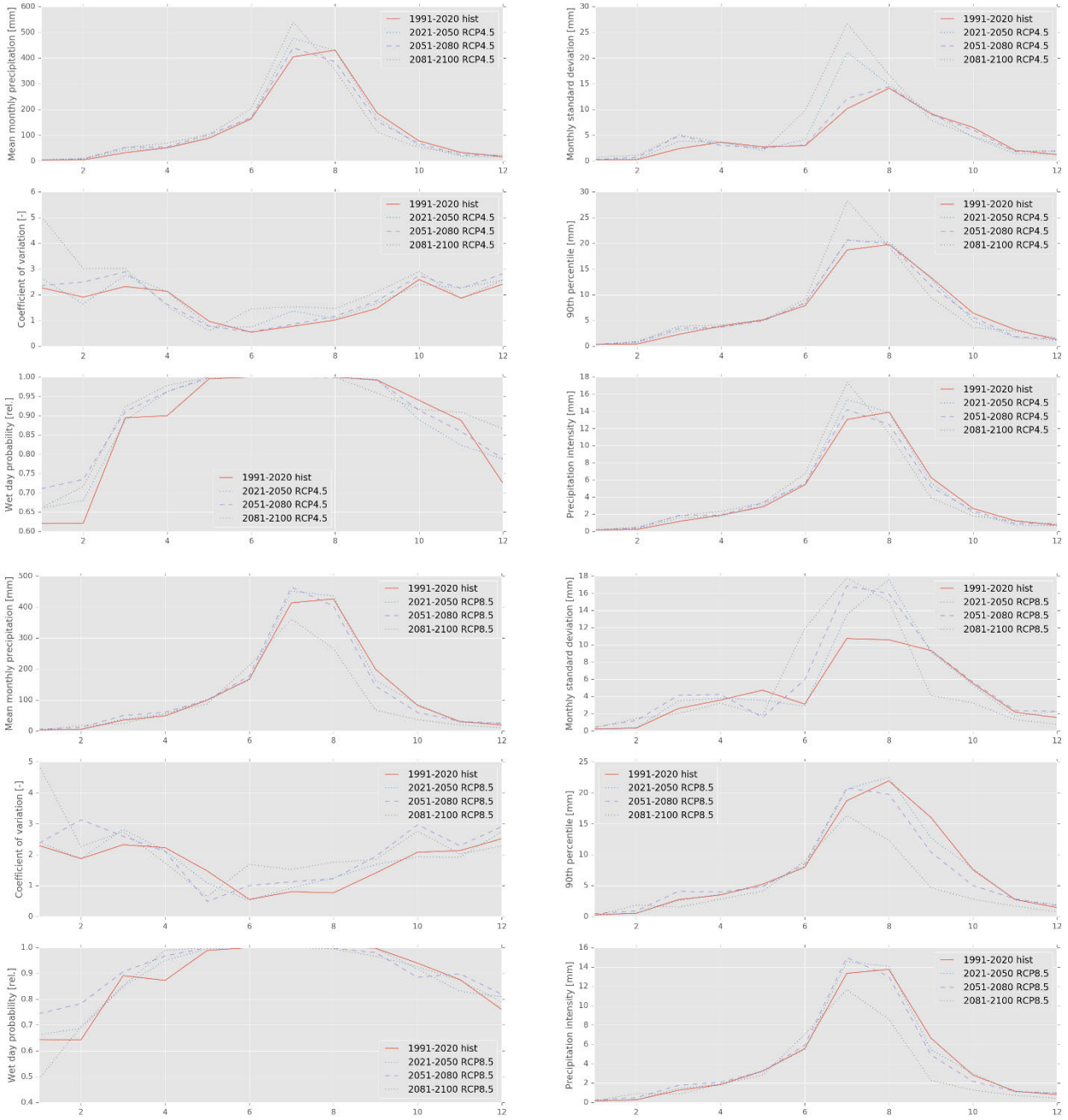

Annexure 14: Precipitation projection at Debre Tabor using RCP4.5 & RCP8.5

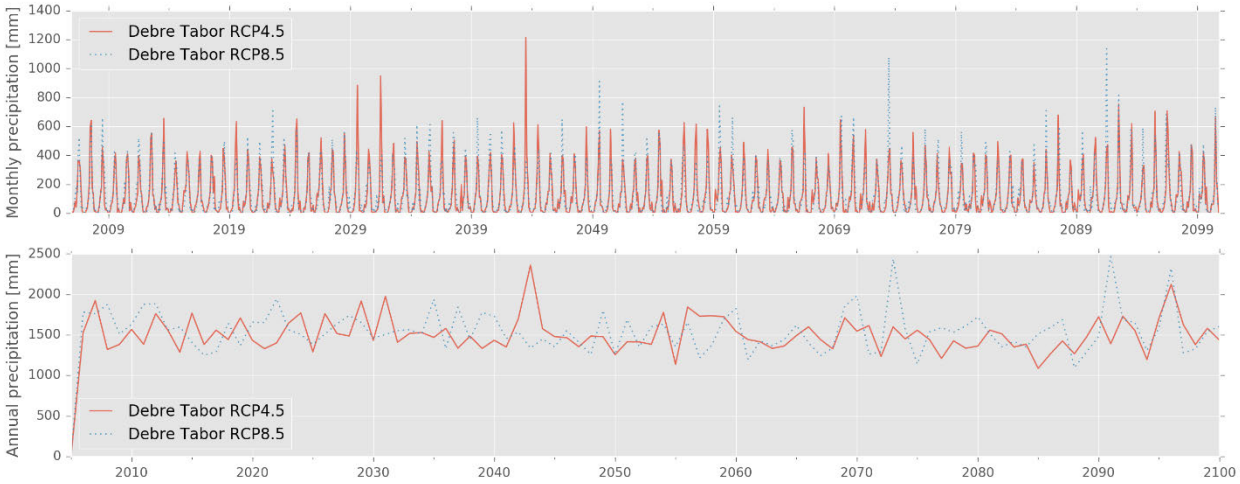

Annexure 15: Characteristics of long-term monthly temperature at Debre Tabor (RCP4.5)

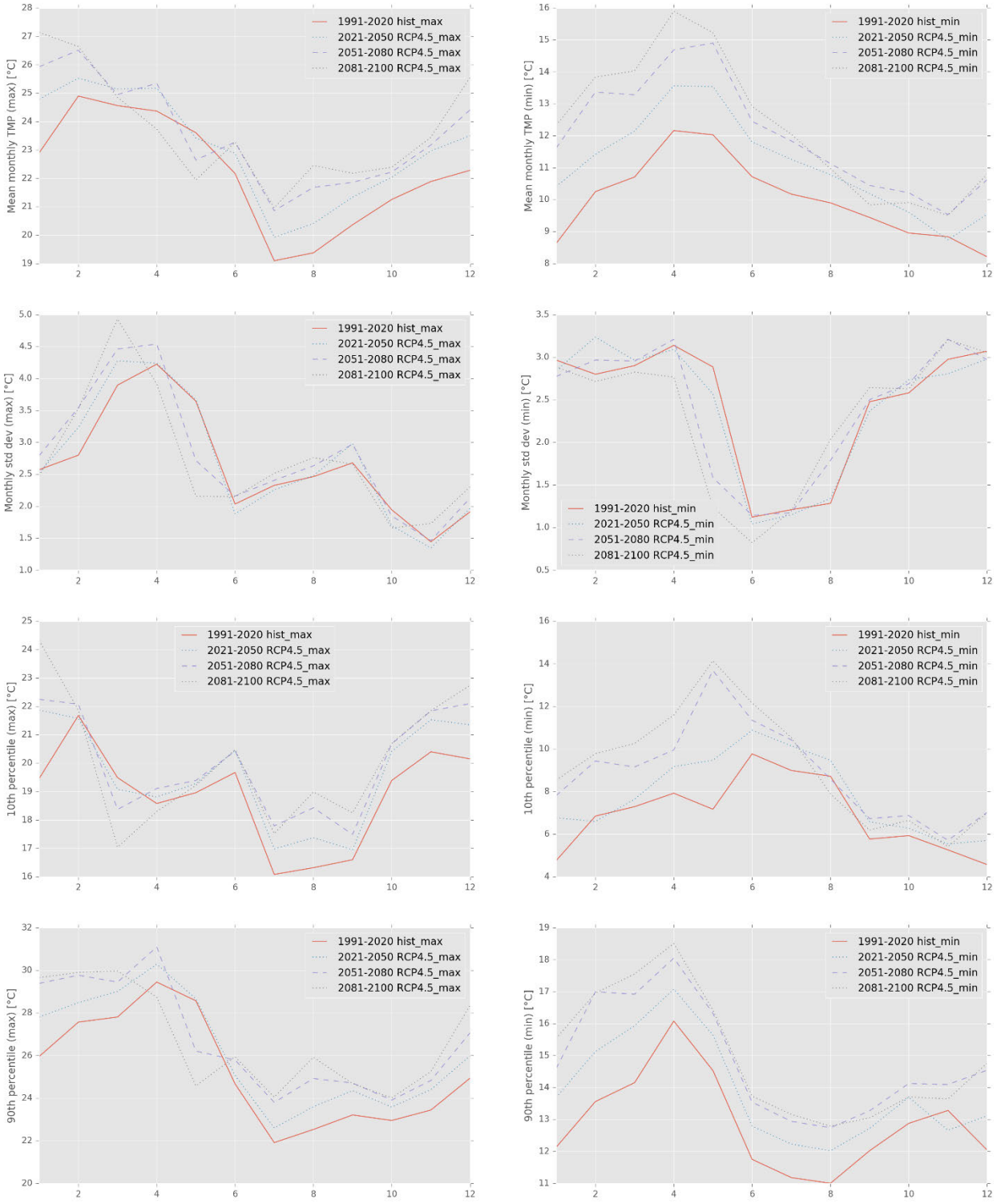

Annexure 16: Characteristics of long-term monthly temperature at Debre Tabor (RCP8.5)

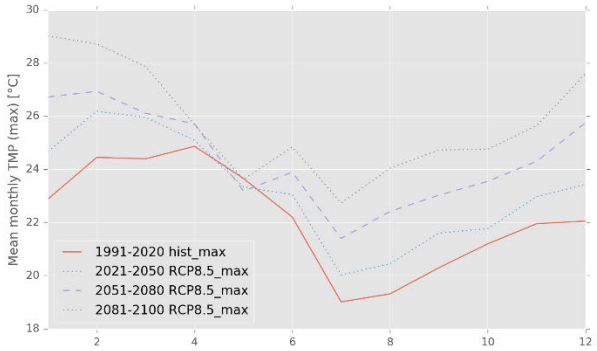


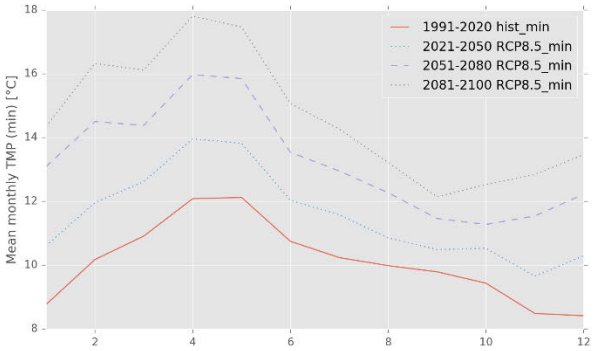


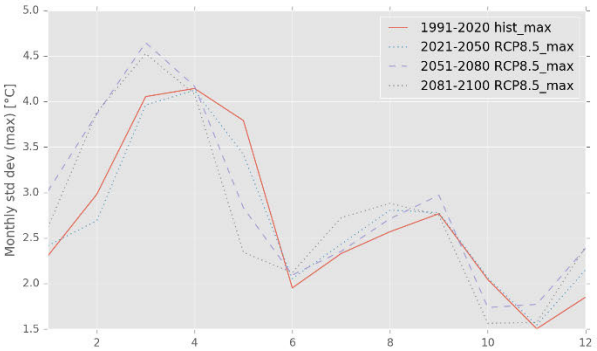


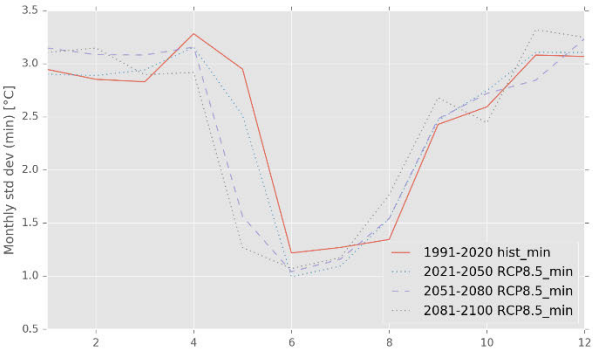


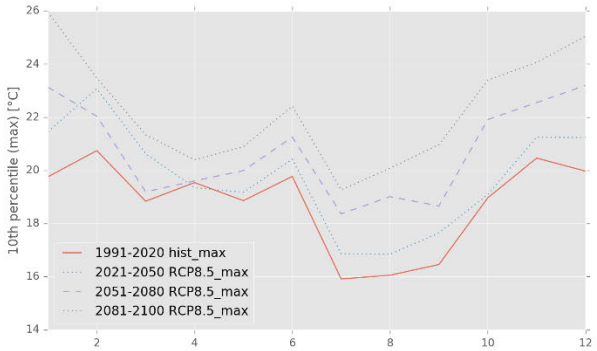


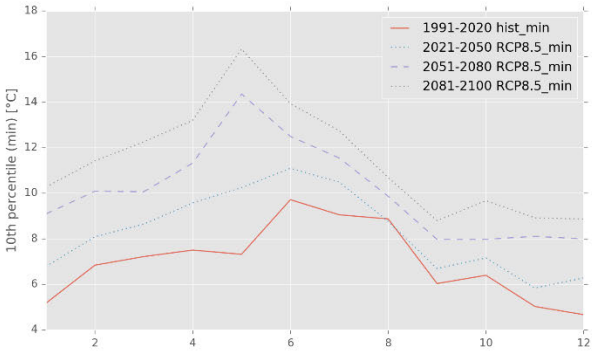


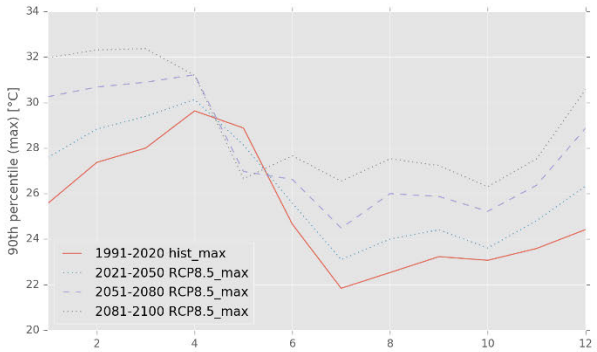


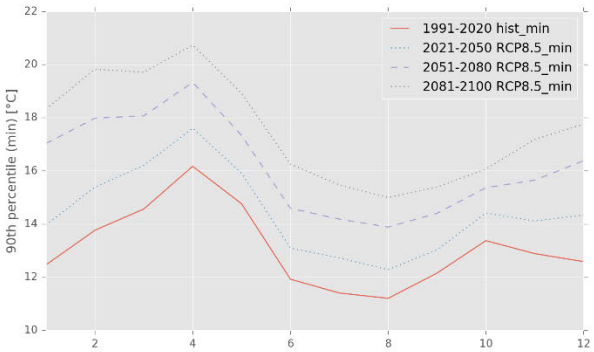

Annexure 17: Characteristics of long-term monthly average precipitation at Gonder

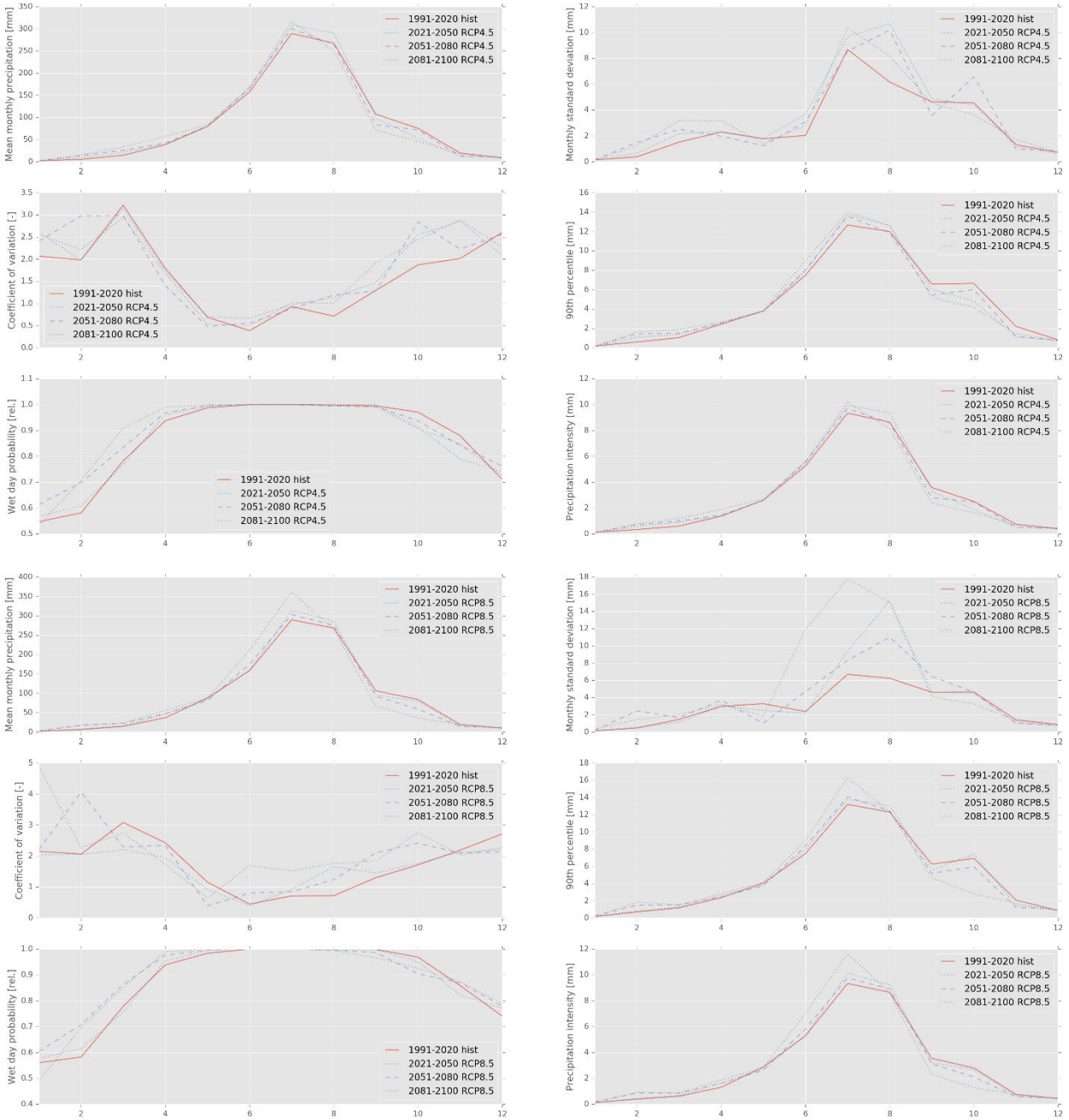

Annexure 18: Precipitation projection at Gonder using RCP4.5 & RCP8.5

Annexure 19: Characteristics of long-term monthly temperature at Gonder (RCP4.5)

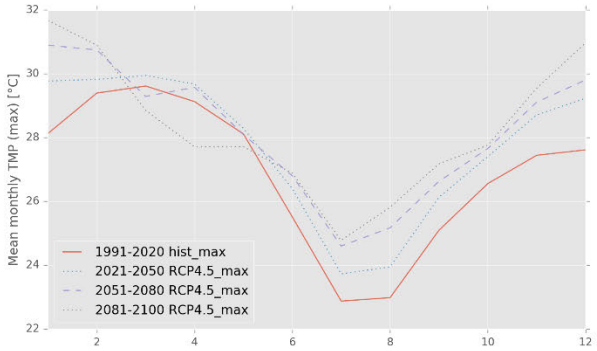


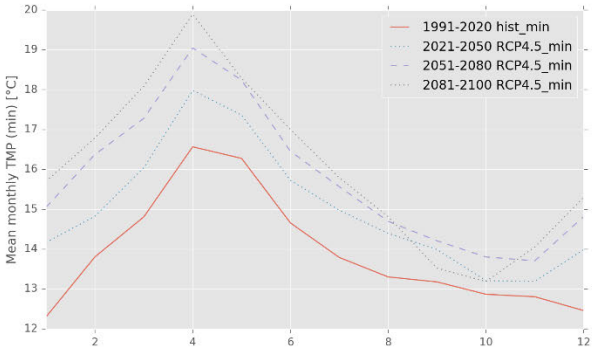


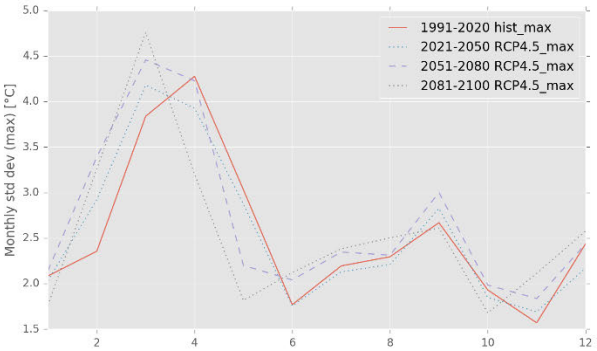


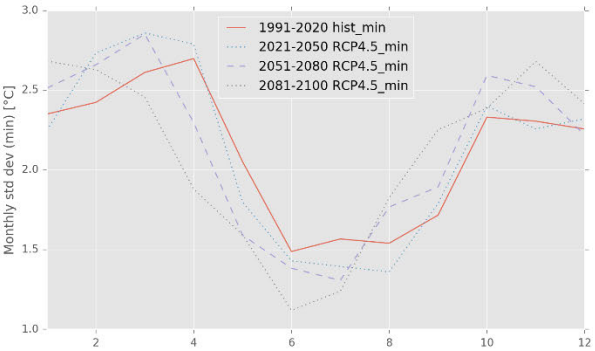


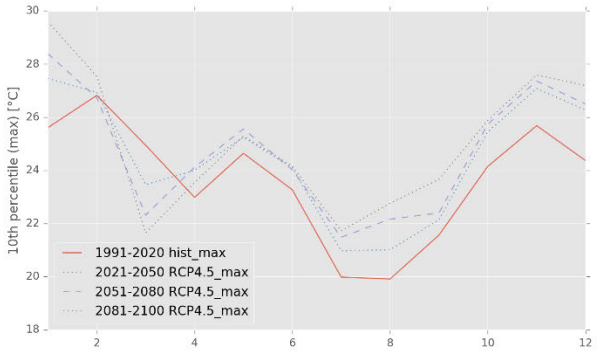


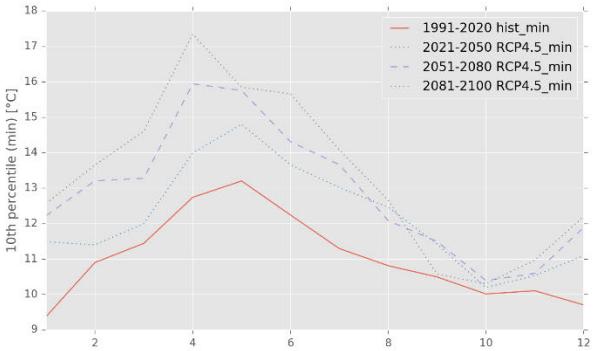


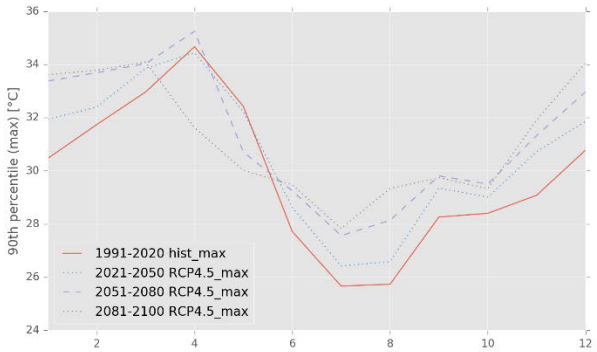


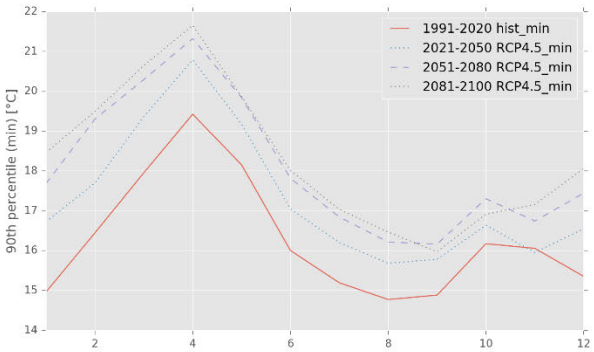

Annexure 20: Characteristics of long-term monthly temperature at Gonder (RCP8.5)

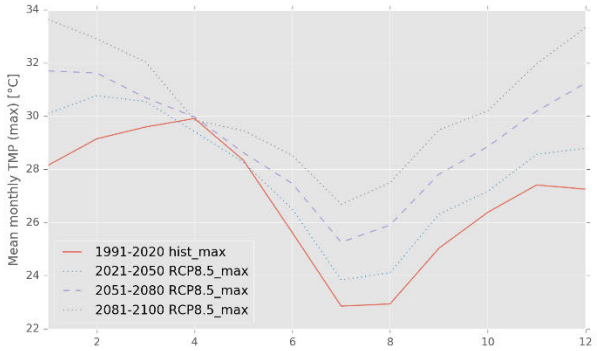


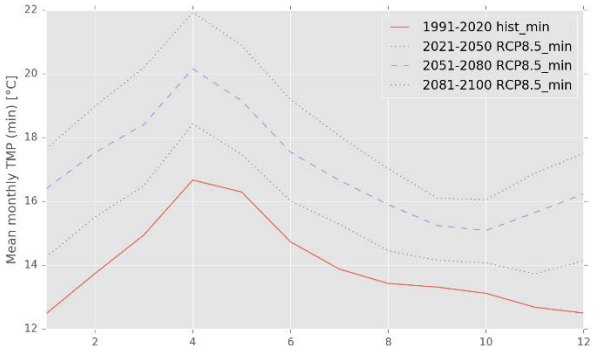


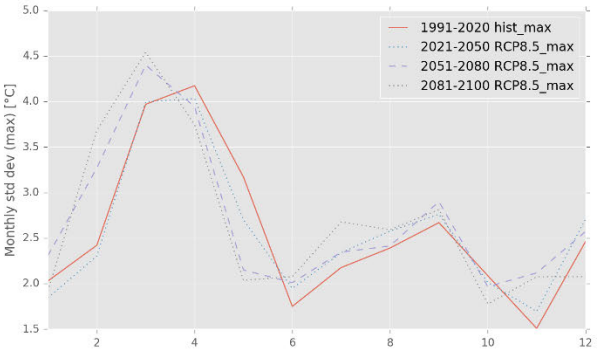


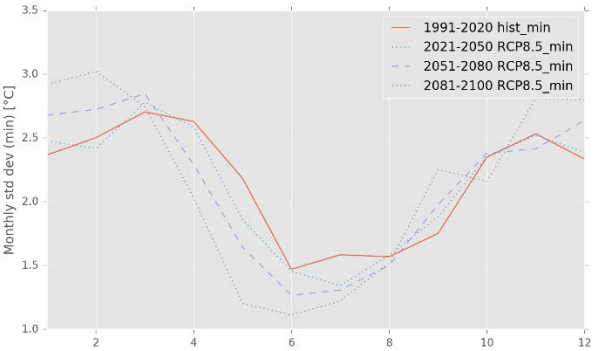


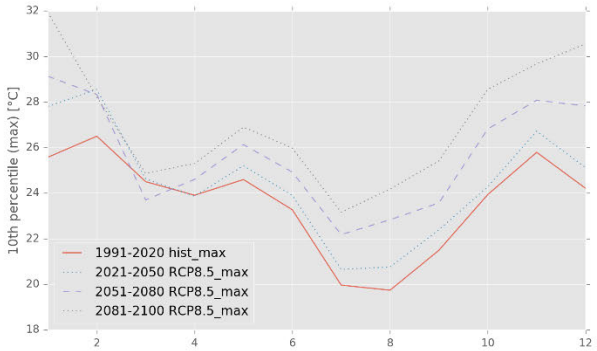


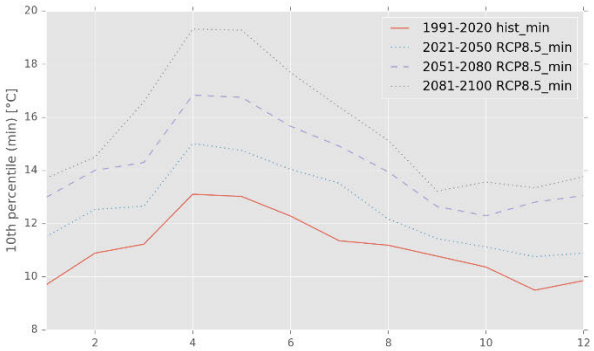


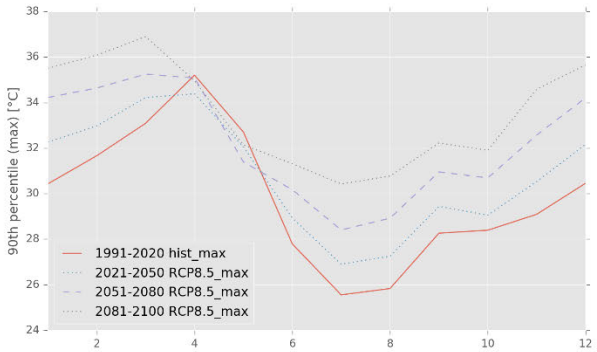


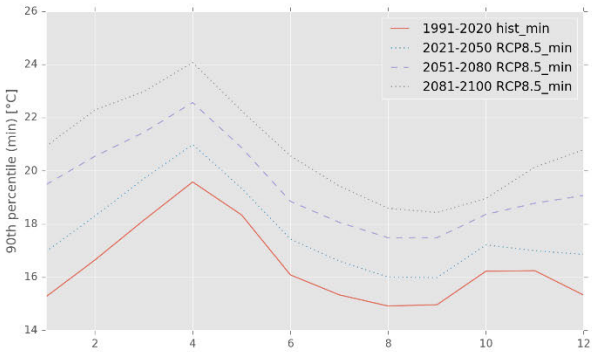

Annexure 21: Drought frequency (%) in different drought categories: SPI3

| Catchment | Normal (>=0) | Mild drought (<0 and >-1) | Moderate drought (-1.0 to -1.49) | Severe drought (-1.5 to -1.99) | Extreme drought (<-2.0) |
|---|---|---|---|---|---|
| Reg 1 | 48.12 | 36.82 | 9.83 | 2.72 | 2.51 |
| Reg 2 | 48.74 | 36.82 | 8.37 | 3.97 | 2.09 |
| Reg 3 | 49.16 | 36.40 | 7.95 | 4.39 | 2.09 |
| Reg 4 | 48.54 | 35.56 | 9.41 | 5.44 | 1.05 |
| Reg 5 | 48.33 | 35.56 | 10.04 | 4.39 | 1.67 |
| Reg 6 | 48.95 | 35.15 | 10.04 | 3.77 | 2.09 |
| Reg 7 | 48.33 | 35.15 | 9.83 | 4.39 | 2.30 |
| Reg 8 | 49.16 | 35.77 | 8.37 | 4.60 | 2.09 |
| Reg 9 | 49.16 | 36.82 | 7.95 | 3.35 | 2.72 |
| Reg 10 | 47.07 | 39.12 | 8.37 | 3.14 | 2.30 |

Annexure 22: Drought frequency (%) in different drought categories: SPI6

| Catchment | Normal (>=0) | Mild drought (<0 and >-1) | Moderate drought (-1.0 to -1.49) | Severe drought (-1.5 to -1.99) | Extreme drought (<-2.0) |
|---|---|---|---|---|---|
| Reg 1 | 49.05 | 32.84 | 12.21 | 3.79 | 2.11 |
| Reg 2 | 49.68 | 32.84 | 11.79 | 4.42 | 1.26 |
| Reg 3 | 51.58 | 29.89 | 12.21 | 4.63 | 1.68 |
| Reg 4 | 53.26 | 29.26 | 9.26 | 6.32 | 1.89 |
| Reg 5 | 52.00 | 29.68 | 11.16 | 5.26 | 1.89 |
| Reg 6 | 49.68 | 32.21 | 11.79 | 4.63 | 1.68 |
| Reg 7 | 52.84 | 29.05 | 9.47 | 5.68 | 2.95 |
| Reg 8 | 51.37 | 31.58 | 9.05 | 5.05 | 2.95 |
| Reg 9 | 52.21 | 32.42 | 8.21 | 4.21 | 2.95 |
| Reg 10 | 50.95 | 34.53 | 8.21 | 3.79 | 2.53 |

Annexure 23: Drought frequency (%) in different drought categories: SPI12

| Catchment | Normal (>=0) | Mild drought (<0 and >-1) | Moderate drought (-1.0 to -1.49) | Severe drought (-1.5 to -1.99) | Extreme drought (<-2.0) |
|---|---|---|---|---|---|
| Reg 1 | 50.96 | 28.14 | 13.01 | 7.68 | 0.21 |
| Reg 2 | 53.30 | 27.29 | 14.50 | 4.26 | 0.64 |
| Reg 3 | 53.30 | 25.59 | 13.86 | 6.82 | 0.43 |
| Reg 4 | 57.57 | 22.39 | 9.81 | 8.32 | 1.92 |
| Reg 5 | 57.78 | 22.81 | 10.87 | 6.18 | 2.35 |
| Reg 6 | 49.47 | 35.18 | 8.96 | 4.05 | 2.35 |
| Reg 7 | 52.45 | 28.57 | 13.22 | 3.41 | 2.35 |
| Reg 8 | 54.37 | 27.08 | 10.87 | 5.54 | 2.13 |
| Reg 9 | 51.60 | 30.28 | 8.96 | 7.04 | 2.13 |
| Reg 10 | 49.68 | 33.90 | 9.38 | 4.48 | 2.56 |

Annexure 24: Spatial precipitation index for 3, 6, 12, & 24 months from regions 1 to 5

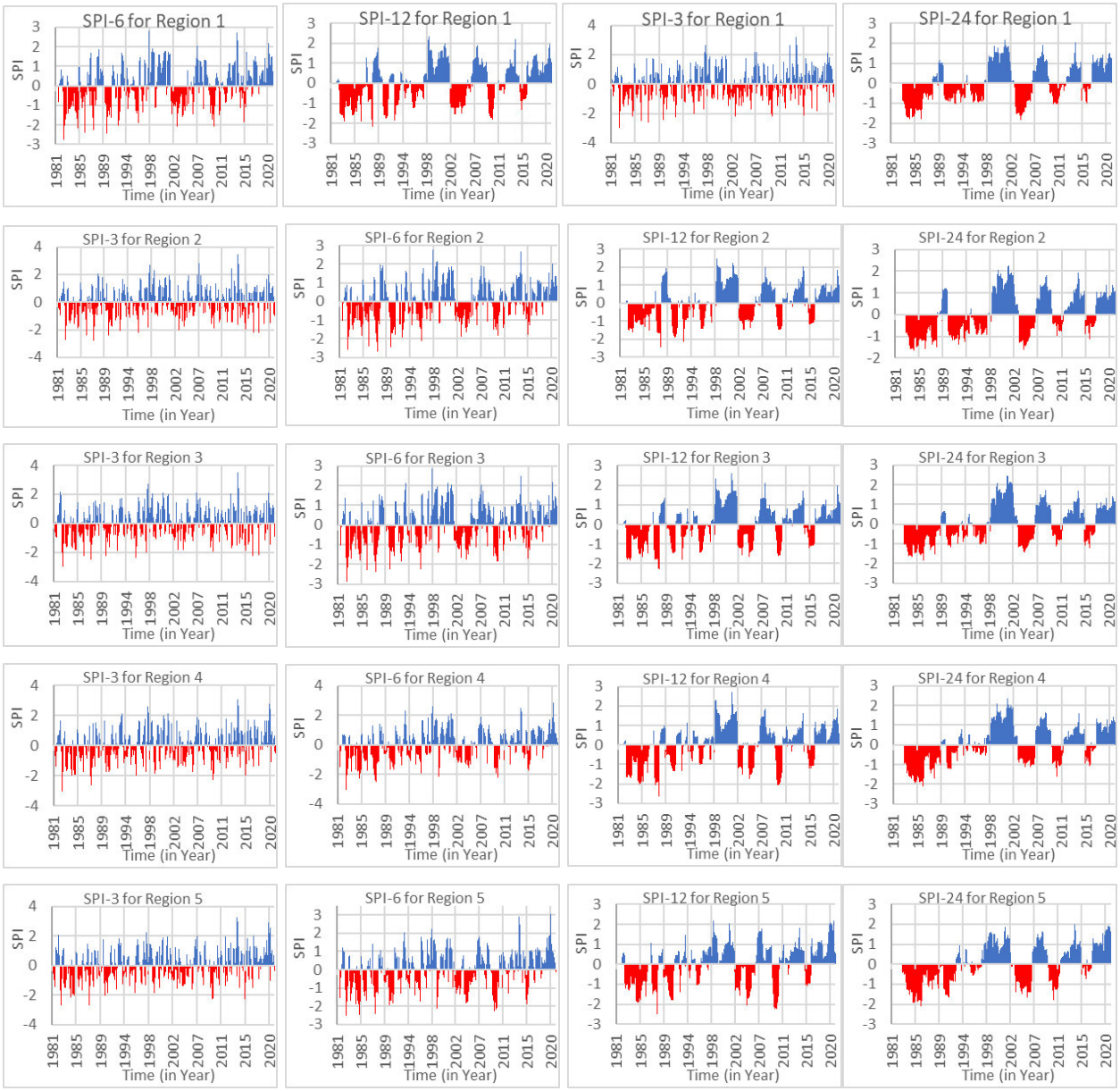

Annexure 25: Spatial precipitation index for 3, 6, 12, & 24 months from regions 6 to 10

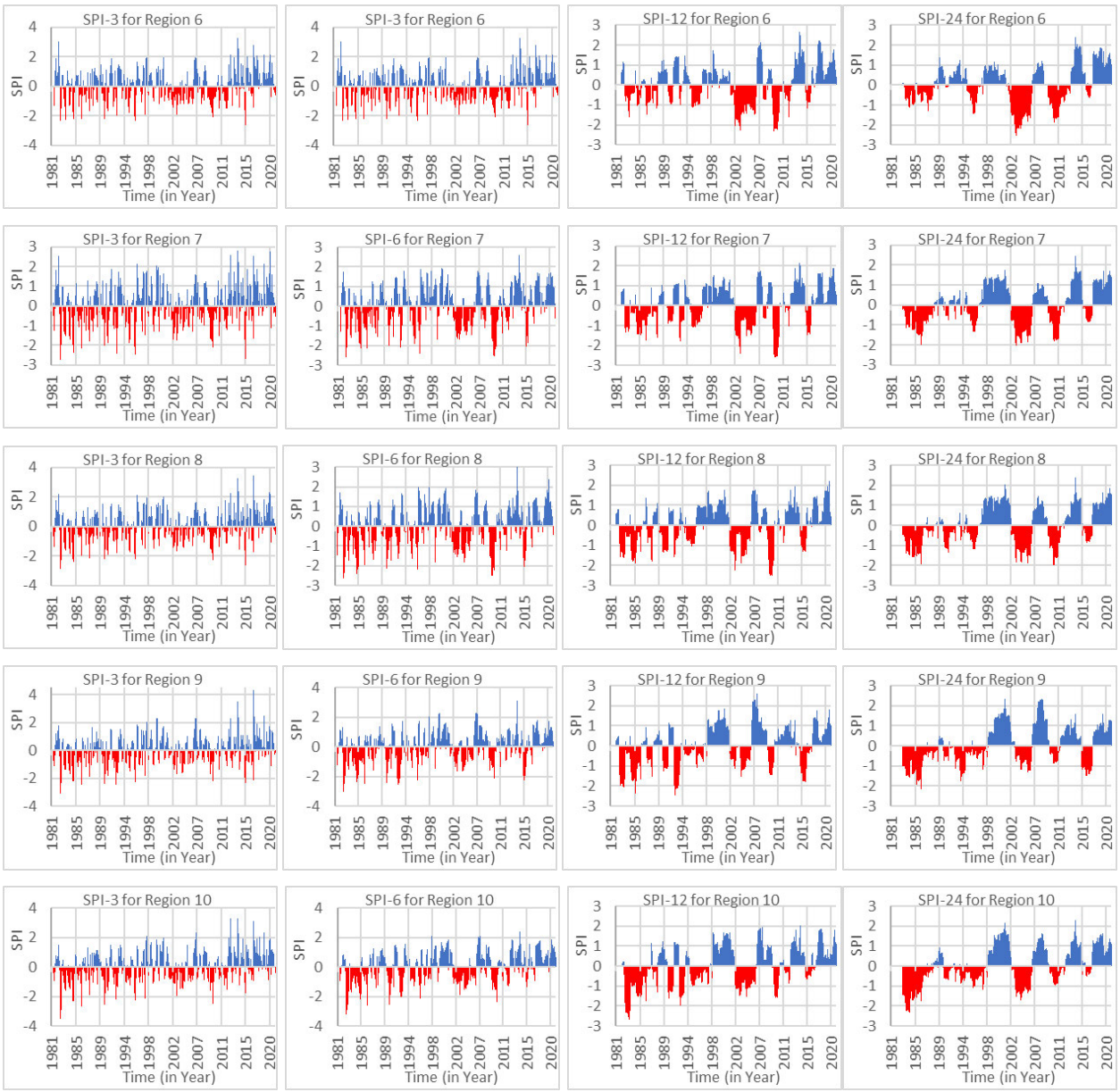

Annexure 26: Spatial distribution of precipitation drought index value

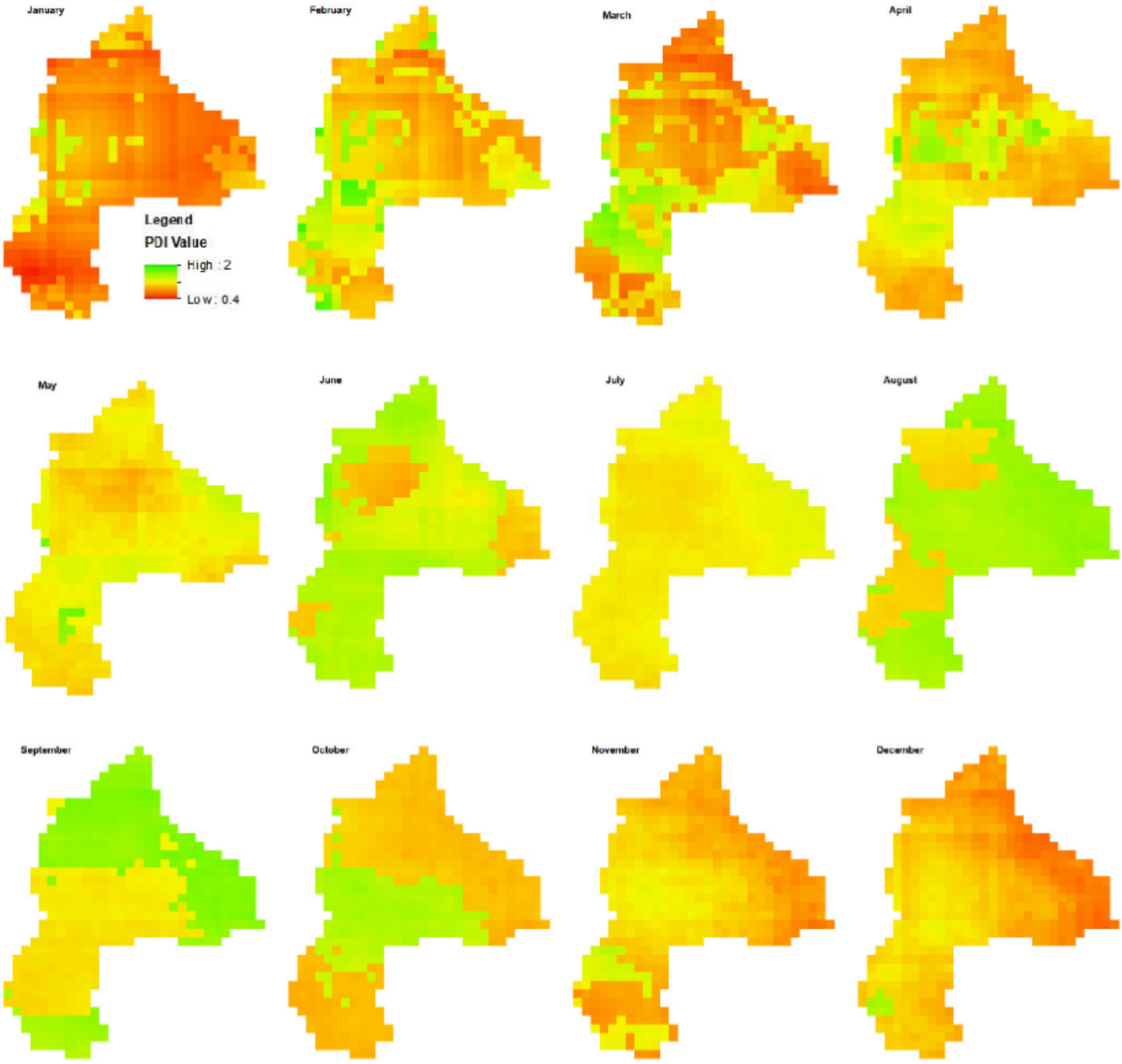

Annexure 27: Spatial distribution of temperature drought index value

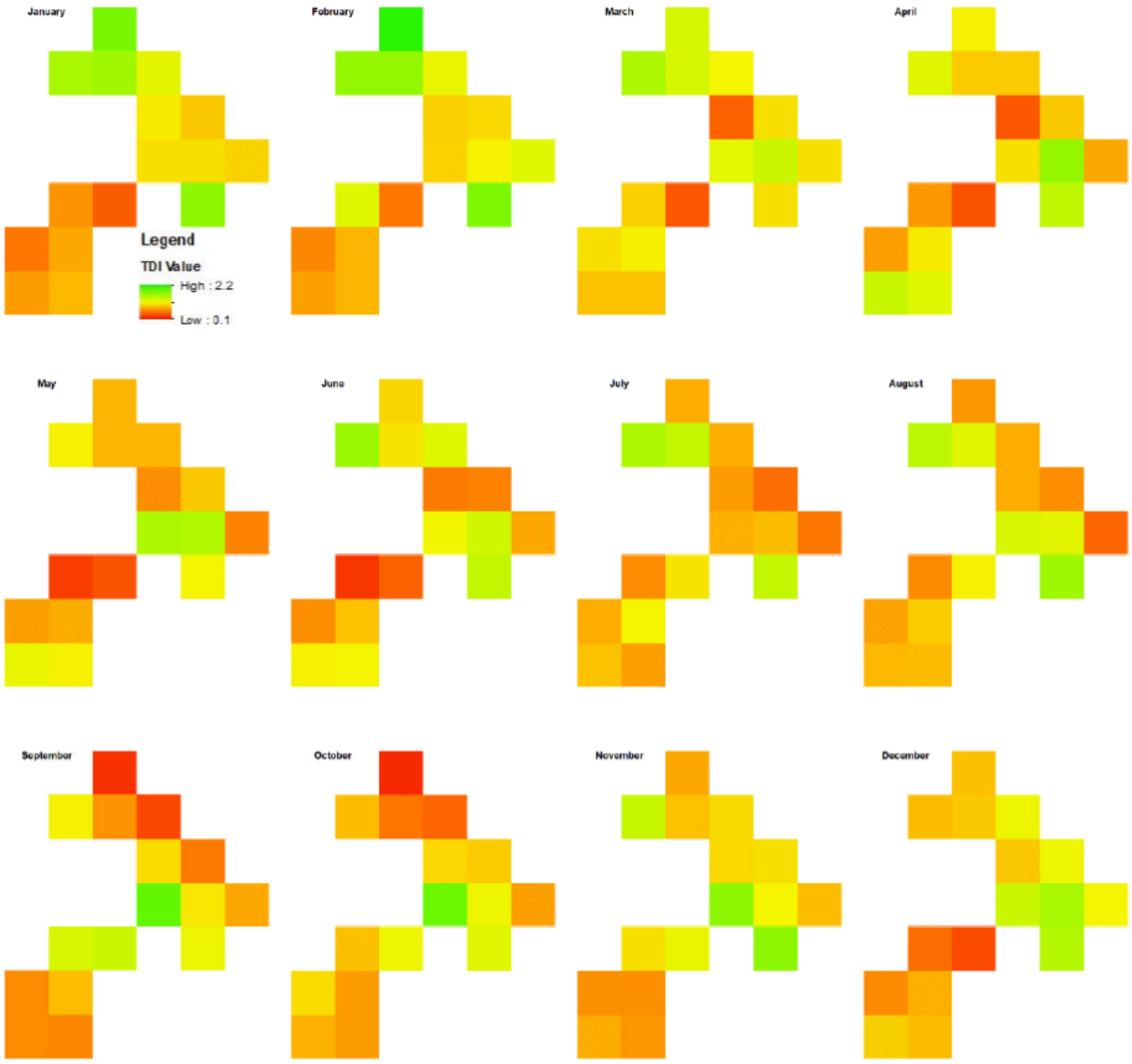

Annexure 28: Spatial distribution of vegetation drought index value

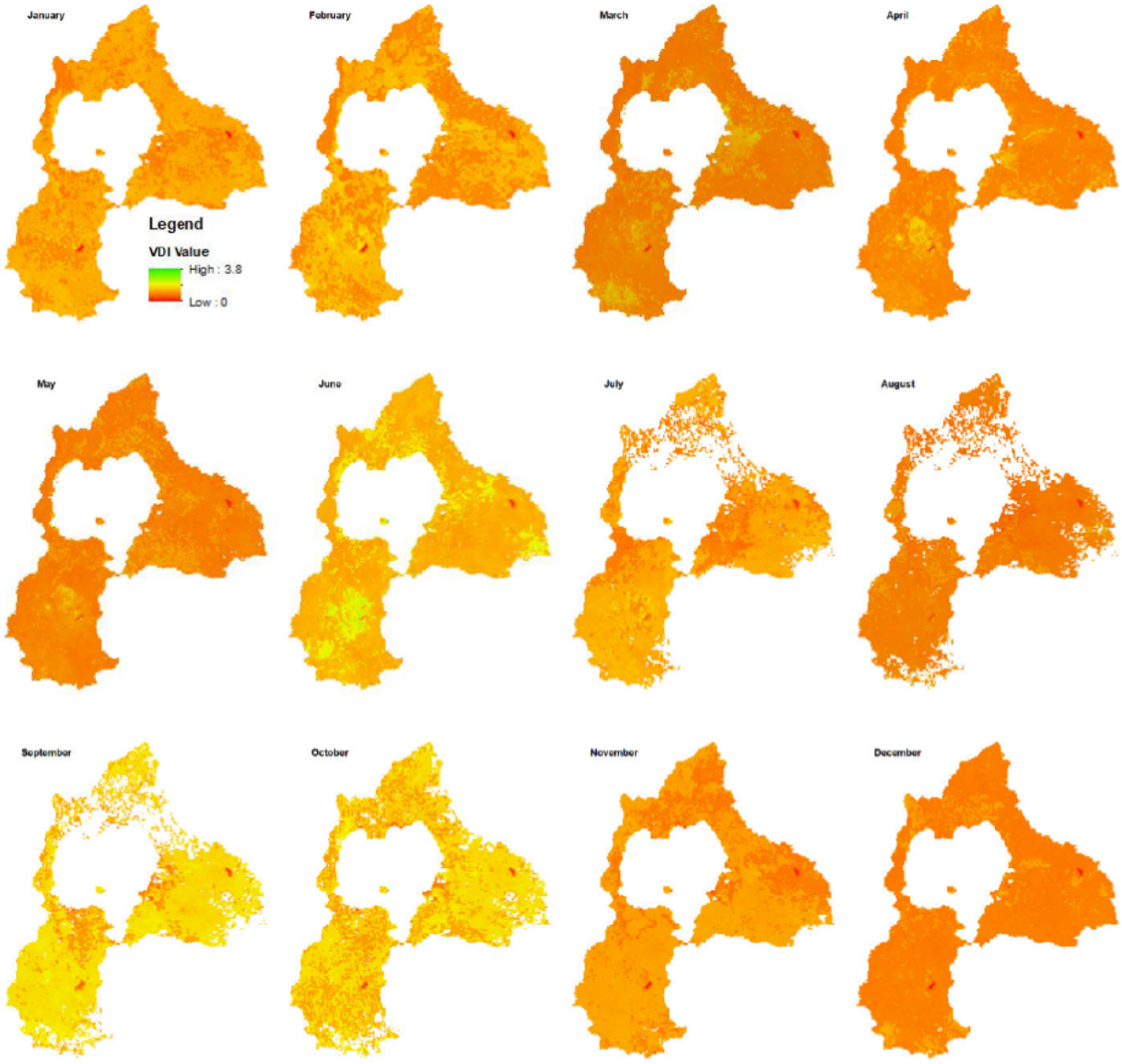

Annexure 29: LULC in 1986, 2000 and 2014 for four major watersheds

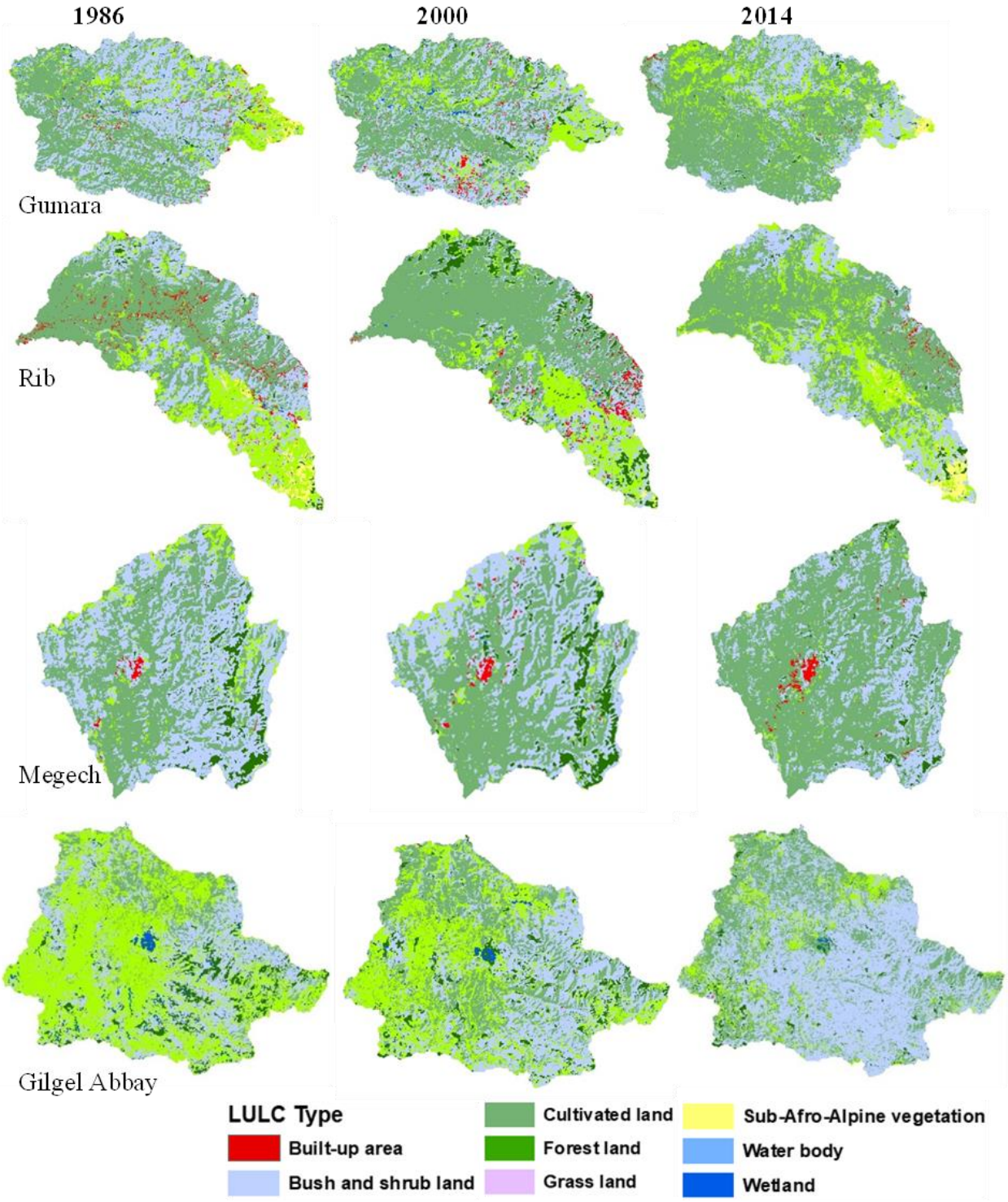

Annexure 30: Transformed versus unchanged LULC matrix for Gilgel Abbay (2000-1986)

| 1986 | 2000 | | | | | | | |
|---|---|---|---|---|---|---|---|---|
| | Afroalpine and sub-afroalpine vegetation | Built-up area | Bush and shrub land | Cultivated land | Forest land | Grass land | Water body | Wetland |
| Afroalpine and sub-afroalpine vegetation | 0.076 | 0.025 | 9.843 | 2.846 | 0.375 | 4.069 | ..... | 0.066 |
| Built-up area | ..... | 0.055 | 0.978 | 0.089 | 0.017 | 0.023 | ..... | ..... |
| Bush and shrub land | 0.018 | 0.086 | 402.607 | 159.269 | 4.517 | 74.037 | 0.014 | 1.474 |
| Cultivated land | ..... | 0.001 | 45.095 | 118.399 | 0.466 | 12.675 | ..... | 0.083 |
| Forest land | 0.098 | 0.002 | 183.392 | 14.950 | 42.268 | 17.437 | 0.163 | 3.068 |
| Grass land | 0.017 | 0.001 | 131.785 | 157.658 | 2.173 | 248.979 | 4.333 | 0.325 |
| Water body | ..... | ..... | 0.000 | ..... | ..... | ..... | 0.096 | ..... |
| Wetland | 0.006 | ..... | 3.769 | 0.807 | 0.921 | 2.735 | 0.017 | 2.841 |

Annexure 31: Transformed versus unchanged LULC matrix for Gilgel Abbay (2014-2000)

| 2000 | 2014 | | | | | | | |
|---|---|---|---|---|---|---|---|---|
| | Afroalpine and sub-afroalpine vegetation | Built-up area | Bush and shrub land | Cultivated land | Forest land | Grass land | Water body | Wetland |
| Afroalpine and sub-afroalpine vegetation | ..... | ..... | 0.072 | 0.095 | 0.014 | 0.034 | ..... | ..... |
| Built-up area | ..... | 0.087 | 0.014 | 0.069 | ..... | ..... | ..... | ..... |
| Bush and shrub land | 0.005 | 0.713 | 545.282 | 173.660 | 17.845 | 39.689 | 0.002 | 0.273 |
| Cultivated land | 0.032 | 0.051 | 199.217 | 206.831 | 2.837 | 45.044 | ..... | 0.007 |
| Forest land | ..... | 0.007 | 12.670 | 6.234 | 30.544 | 0.976 | 0.047 | 0.258 |
| Grass land | 0.001 | 0.145 | 89.332 | 115.749 | 4.808 | 149.790 | ..... | 0.130 |
| Water body | ..... | ..... | 0.041 | 0.141 | ..... | ..... | 0.110 | ..... |
| Wetland | ..... | 0.008 | 0.998 | 4.216 | 1.750 | 0.017 | ..... | 0.868 |

Annexure 32: Transformed versus unchanged LULC matrix for Gilgel Abbay (2014-1986)

| 1986 | 2014 | | | | | | | |
|---|---|---|---|---|---|---|---|---|
| | Afroalpine and sub-afroalpine vegetation | Built-up area | Bush and shrub land | Cultivated land | Forest land | Grass land | Water body | Wetland |
| Afroalpine and sub-afroalpine vegetation | ..... | 0.062 | 7.289 | 6.464 | 1.198 | 2.390 | ..... | ..... |
| Built-up area | ..... | 0.078 | 0.676 | 0.380 | 0.016 | 0.011 | ..... | ..... |
| Bush and shrub land | 0.035 | 0.479 | 406.442 | 186.184 | 9.195 | 39.536 | 0.009 | 0.142 |
| Cultivated land | ..... | 0.011 | 75.221 | 85.753 | 1.011 | 14.699 | ..... | 0.023 |
| Forest land | ..... | 0.128 | 166.627 | 44.378 | 37.062 | 12.398 | 0.107 | 0.581 |
| Grass land | 0.003 | 0.253 | 188.525 | 179.230 | 8.346 | 164.409 | ..... | 0.172 |
| Water body | ..... | ..... | ..... | 0.053 | ..... | ..... | 0.042 | ..... |
| Wetland | ..... | ..... | 2.846 | 4.544 | 0.969 | 2.107 | ..... | 0.619 |

Annexure 33: Transformed versus unchanged LULC matrix for Megech (2000-1986)

| 1986 | 2000 | | | | | | | |
|---|---|---|---|---|---|---|---|---|
| | Afroalpine and sub-afroalpine vegetation | Built-up area | Bush and shrub land | Cultivated land | Forest land | Grass land | Water body | Wetland |
| Afroalpine and sub-afroalpine vegetation | ..... | 0.002 | 0.682 | 0.213 | 0.042 | 0.091 | ..... | ..... |
| Built-up area | ..... | 1.861 | 1.447 | 0.786 | 0.000 | 0.022 | ..... | ..... |
| Bush and shrub land | ..... | 0.819 | 158.401 | 66.982 | 3.497 | 4.550 | ..... | 0.125 |
| Cultivated land | ..... | 0.645 | 33.625 | 174.850 | 0.116 | 4.284 | ..... | 0.049 |
| Forest land | ..... | 0.002 | 18.758 | 0.459 | 22.247 | 0.062 | ..... | ..... |
| Grass land | ..... | 0.002 | 7.032 | 5.547 | 0.193 | 6.882 | ..... | 0.024 |
| Water body | ..... | ..... | ..... | ..... | ..... | ..... | ..... | ..... |
| Wetland | ..... | ..... | ..... | ..... | ..... | ..... | ..... | ..... |

Annexure 34: Transformed versus unchanged LULC matrix for Megech (2014-2000)

| 2000 | 2014 | | | | | | | |
|---|---|---|---|---|---|---|---|---|
| | Afroalpine and sub-afroalpine vegetation | Built-up area | Bush and shrub land | Cultivated land | Forest land | Grass land | Water body | Wetland |
| Afroalpine and sub-afroalpine vegetation | ..... | ..... | ..... | ..... | ..... | ..... | ..... | ..... |
| Built-up area | ..... | 1.845 | 0.166 | 1.318 | 0.000 | ..... | ..... | ..... |
| Bush and shrub land | ..... | 3.129 | 98.220 | 114.674 | 3.313 | 0.546 | 0.063 | ..... |
| Cultivated land | ..... | 1.449 | 15.424 | 227.397 | 0.562 | 3.691 | 0.314 | ..... |
| Forest land | ..... | 0.012 | 12.394 | 1.839 | 11.738 | 0.111 | ..... | ..... |
| Grass land | ..... | 0.237 | 2.075 | 10.237 | 0.302 | 3.039 | ..... | ..... |
| Water body | ..... | ..... | ..... | ..... | ..... | ..... | ..... | ..... |
| Wetland | ..... | ..... | 0.000 | 0.114 | 0.084 | ..... | ..... | ..... |

Annexure 35: Transformed versus unchanged LULC matrix for Megech (2014-1986)

| 1986 | 2014 | | | | | | | |
|---|---|---|---|---|---|---|---|---|
| | Afroalpine and sub-afroalpine vegetation | Built-up area | Bush and shrub land | Cultivated land | Forest land | Grass land | Water body | Wetland |
| Afroalpine and sub-afroalpine vegetation | ..... | 0.002 | 0.489 | 0.462 | 0.069 | 0.009 | ..... | ..... |
| Built-up area | ..... | 2.228 | 0.306 | 1.547 | 0.028 | 0.006 | ..... | ..... |
| Bush and shrub land | ..... | 2.810 | 82.746 | 143.843 | 3.491 | 1.384 | 0.099 | ..... |
| Cultivated land | ..... | 1.307 | 14.427 | 193.488 | 0.931 | 3.157 | 0.258 | ..... |
| Forest land | ..... | 0.055 | 27.062 | 3.558 | 10.665 | 0.188 | ..... | ..... |
| Grass land | ..... | 0.272 | 3.250 | 12.678 | 0.816 | 2.642 | 0.021 | ..... |
| Water body | ..... | ..... | ..... | ..... | ..... | ..... | ..... | ..... |
| Wetland | ..... | ..... | ..... | ..... | ..... | ..... | ..... | ..... |

Annexure 36: Transformed versus unchanged LULC matrix for Rib (2000-1986)

| 1986 | 2000 | | | | | | | |
|---|---|---|---|---|---|---|---|---|
| | Afroalpine and sub-afroalpine vegetation | Built-up area | Bush and shrub land | Cultivated land | Forest land | Grass land | Water body | Wetland |
| Afroalpine and sub-afroalpine vegetation | 3.783 | 0.097 | 36.617 | 1.661 | 3.816 | 24.377 | ..... | ..... |
| Built-up area | ..... | 5.250 | 22.712 | 37.159 | 0.034 | 1.259 | ..... | 0.101 |
| Bush and shrub land | 0.427 | 5.139 | 230.713 | 66.275 | 14.956 | 23.141 | ..... | 0.966 |
| Cultivated land | ..... | ..... | ..... | ..... | ..... | ..... | ..... | ..... |
| Forest land | 2.306 | 0.031 | 12.821 | 0.782 | 34.689 | 0.638 | ..... | 0.466 |
| Grass land | 1.634 | 0.109 | 37.739 | 26.256 | 1.746 | 93.524 | ..... | 0.005 |
| Water body | ..... | 2.042 | 32.851 | 578.443 | 0.272 | 11.337 | ..... | 0.355 |
| Wetland | ..... | ..... | 0.211 | 0.020 | 0.019 | 0.074 | ..... | 0.326 |

Annexure 37: Transformed versus unchanged LULC matrix for Rib (2014-2000)

| 2000 | 2014 | | | | | | | |
|---|---|---|---|---|---|---|---|---|
| | Afroalpine and sub-afroalpine vegetation | Built-up area | Bush and shrub land | Cultivated land | Forest land | Grass land | Water body | Wetland |
| Afroalpine and sub-afroalpine vegetation | 5.916 | ..... | 1.382 | 0.057 | 0.050 | 0.744 | ..... | ..... |
| Built-up area | ..... | 0.111 | 0.579 | 11.133 | 0.037 | 0.786 | ..... | 0.023 |
| Bush and shrub land | 14.775 | 9.489 | 127.654 | 147.412 | 2.545 | 71.751 | 0.008 | 0.031 |
| Cultivated land | 0.911 | 0.316 | 33.286 | 525.081 | 0.093 | 150.835 | 0.002 | 0.071 |
| Forest land | 0.836 | 0.879 | 30.434 | 2.639 | 18.130 | 2.601 | ..... | 0.013 |
| Grass land | 4.478 | 0.023 | 17.703 | 5.232 | 0.439 | 126.473 | 0.000 | 0.003 |
| Water body | ..... | ..... | ..... | ..... | ..... | ..... | ..... | ..... |
| Wetland | ..... | 0.002 | 0.879 | 0.923 | 0.212 | 0.201 | ..... | ..... |

Annexure 38: Transformed versus unchanged LULC matrix for Rib (2014-1986)

| 1986 | 2014 | | | | | | | |
|---|---|---|---|---|---|---|---|---|
| | Afroalpine and sub-afroalpine vegetation | Built-up area | Bush and shrub land | Cultivated land | Forest land | Grass land | Water body | Wetland |
| Afroalpine and sub-afroalpine vegetation | 16.164 | 0.047 | 13.251 | 2.041 | 2.779 | 36.069 | ..... | 0.000 |
| Built-up area | 0.019 | 0.540 | 6.195 | 44.413 | 0.075 | 15.265 | ..... | 0.008 |
| Bush and shrub land | 2.386 | 7.643 | 118.405 | 143.456 | 4.347 | 65.369 | 0.010 | .... |
| Cultivated land | 0.013 | 0.449 | 24.594 | 486.043 | 0.253 | 113.847 | ..... | 0.099 |
| Forest land | 2.489 | 2.098 | 28.522 | 4.272 | 11.897 | 2.441 | ..... | 0.013 |
| Grass land | 5.845 | 0.037 | 20.938 | 11.788 | 2.154 | 120.229 | ..... | 0.021 |
| Water body | ..... | ..... | ..... | ..... | ..... | ..... | ..... | ..... |
| Wetland | ..... | 0.002 | 0.014 | 0.463 | 0.001 | 0.169 | ..... | ..... |

Annexure 39: Transformed versus unchanged LULC matrix for Gumara (2000-1986)

| 1986 | 2000 | | | | | | | |
|---|---|---|---|---|---|---|---|---|
| | Afroalpine and sub-afroalpine vegetation | Built-up area | Bush and shrub land | Cultivated land | Forest land | Grass land | Water body | Wetland |
| Afroalpine and sub-afroalpine vegetation | 1.109 | 0.029 | 17.431 | 0.429 | 0.969 | 4.545 | ..... | 0.002 |
| Built-up area | ..... | 1.917 | 19.449 | 11.006 | 0.069 | 1.094 | ..... | 0.194 |
| Bush and shrub land | 0.139 | 6.519 | 369.739 | 126.718 | 5.378 | 35.121 | ..... | 2.319 |
| Cultivated land | ..... | 5.522 | 134.202 | 417.289 | 0.461 | 30.818 | ..... | 1.280 |
| Forest land | 0.211 | 0.008 | 15.123 | 1.014 | 16.458 | 1.509 | ..... | 2.147 |
| Grass land | 0.403 | 0.029 | 27.660 | 24.849 | 0.751 | 63.488 | ..... | 0.169 |
| Water body | ..... | ..... | ..... | ..... | ..... | ..... | ..... | ..... |
| Wetland | 0.005 | **0.009** | 1.524 | 0.147 | 0.110 | 0.203 | ..... | 0.900 |

Annexure 40: Transformed versus unchanged LULC matrix for Gumara (2014-2000)

| 2000 | 2014 | | | | | | | |
|---|---|---|---|---|---|---|---|---|
| | Afroalpine and sub-afroalpine vegetation | Built-up area | Bush and shrub land | Cultivated land | Forest land | Grass land | Water body | Wetland |
| Afroalpine and sub-afroalpine vegetation | 1.739 | ..... | 0.077 | 0.006 | 0.009 | 0.034 | ..... | ..... |
| Built-up area | ..... | 0.041 | 0.596 | 13.165 | 0.014 | 0.216 | ..... | ..... |
| Bush and shrub land | 6.592 | 2.806 | 173.169 | 346.135 | 3.607 | 52.781 | ..... | 0.037 |
| Cultivated land | 0.460 | 0.711 | 42.832 | 434.504 | 0.348 | 102.597 | ..... | ..... |
| Forest land | 0.324 | 0.037 | 8.923 | 1.626 | 12.184 | 1.102 | ..... | ..... |
| Grass land | 1.502 | 0.016 | 23.888 | 22.291 | 0.587 | 88.482 | ..... | 0.012 |
| Water body | ..... | ..... | ..... | ..... | ..... | ..... | ..... | ..... |
| Wetland | 0.087 | 0.043 | 1.536 | 3.306 | 1.515 | 0.525 | ..... | 0.087 |

Annexure 41: Transformed versus unchanged LULC matrix for Gumara (2014-1986)

| 1986 | 2014 | | | | | | | |
|---|---|---|---|---|---|---|---|---|
| | Afroalpine and sub-afroalpine vegetation | Built-up area | Bush and shrub land | Cultivated land | Forest land | Grass land | Water body | Wetland |
| Afroalpine and sub-afroalpine vegetation | 6.062 | 0.044 | 7.451 | 1.061 | 0.856 | 9.040 | ..... | ..... |
| Built-up area | 0.042 | 0.111 | 5.280 | 24.731 | 0.206 | 3.359 | ..... | ..... |
| Bush and shrub land | 1.382 | 1.798 | 160.340 | 304.527 | 4.397 | 73.407 | ..... | 0.080 |
| Cultivated land | 0.026 | 1.297 | 39.263 | 464.737 | 0.615 | 83.631 | ..... | 0.002 |
| Forest land | 0.779 | 0.275 | 15.726 | 5.618 | 10.523 | 3.511 | ..... | 0.038 |
| Grass land | 2.305 | 0.094 | 22.149 | 18.837 | 1.315 | 72.636 | ..... | 0.013 |
| Water body | ..... | ..... | ..... | ..... | ..... | ..... | ..... | ..... |
| Wetland | 0.020 | 0.036 | 0.811 | 1.520 | 0.355 | 0.152 | ..... | 0.004 |

Annexure 42: Generated watersheds using SWAT for LULC, 1986, 2000, and 2014

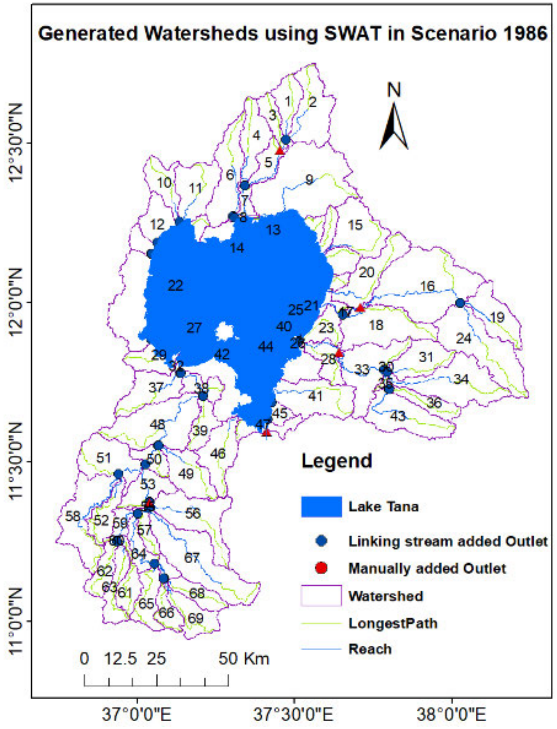


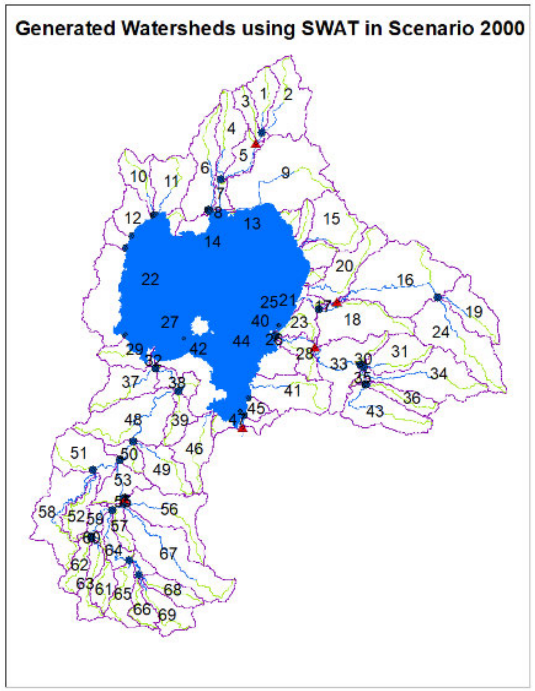


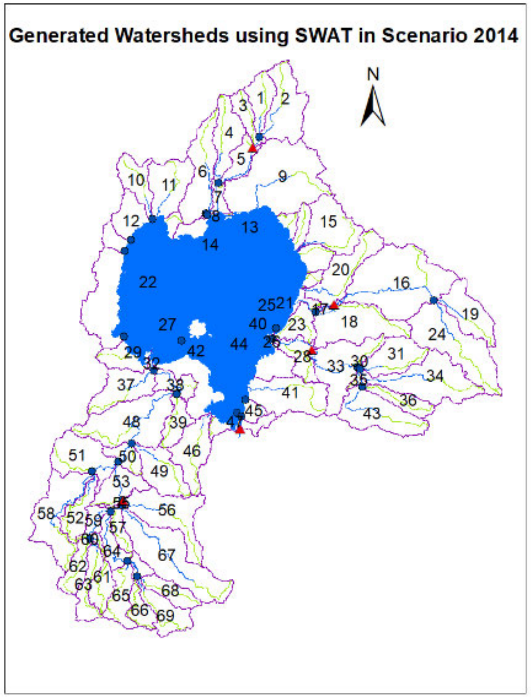

Annexure 43: Hydrological parameters used for sensitivity analysis

| No. | Parameters | Minimum value | Maximum value |
|---|---|---|---|
| 1 | r__CN2.mgt | -0.2 | 0.2 |
| 2 | v__ALPHA_BF.gw | 0.0 | 1.0 |
| 3 | a__GW_DELAY.gw | -40 | 80 |
| 4 | v__RCHRG_DP.gw | 0.0 | 1.0 |
| 5 | v__ALPHA_BNK.rte | 0.0 | 1.0 |
| 6 | r__SOL_K().sol | -0.2 | 0.2 |
| 7 | v__ALPHA_BF_D.gw | 0.0 | 1.0 |
| 8 | v__CH_ERODMO().rte | 0.0 | 1.0 |
| 9 | v__CH_COV2.rte | 0.0 | 1.0 |
| 10 | v__CH_COV1.rte | 0.0 | 1.0 |
| 11 | v__TLAPS.sub | 0.0 | 60 |
| 12 | v__SURLAG.bsn | 0.0 | 10 |
| 13 | r__SOL_Z().sol | -0.2 | 0.2 |
| 14 | r__SOL_AWC().sol | -0.2 | 0.2 |
| 15 | r__SOL_ALB().sol | -0.25 | 0.25 |
| 16 | a__REVAPMN.gw | -800 | 800 |
| 17 | v__GW_REVAP.gw | -0.03 | 0.2 |
| 18 | v__ESCO.hru | 0.0 | 1.0 |
| 19 | a__EPCO.hru | 0.0 | 1.0 |
| 20 | v__CH_N2.rte | 0.0 | 1.0 |
| 21 | v__CH_K2.rte | 0.0 | 20 |
| 22 | a__CANMX.hru | 0.0 | 20 |
| 23 | v__BIOMIX.mgt | 0.0 | 1.0 |
| 24 | a__GWQMN.gw | -1000 | 1000 |

Annexure 44: Dotty plots of parameter values versus objectives function in Rib

Calibration Validation

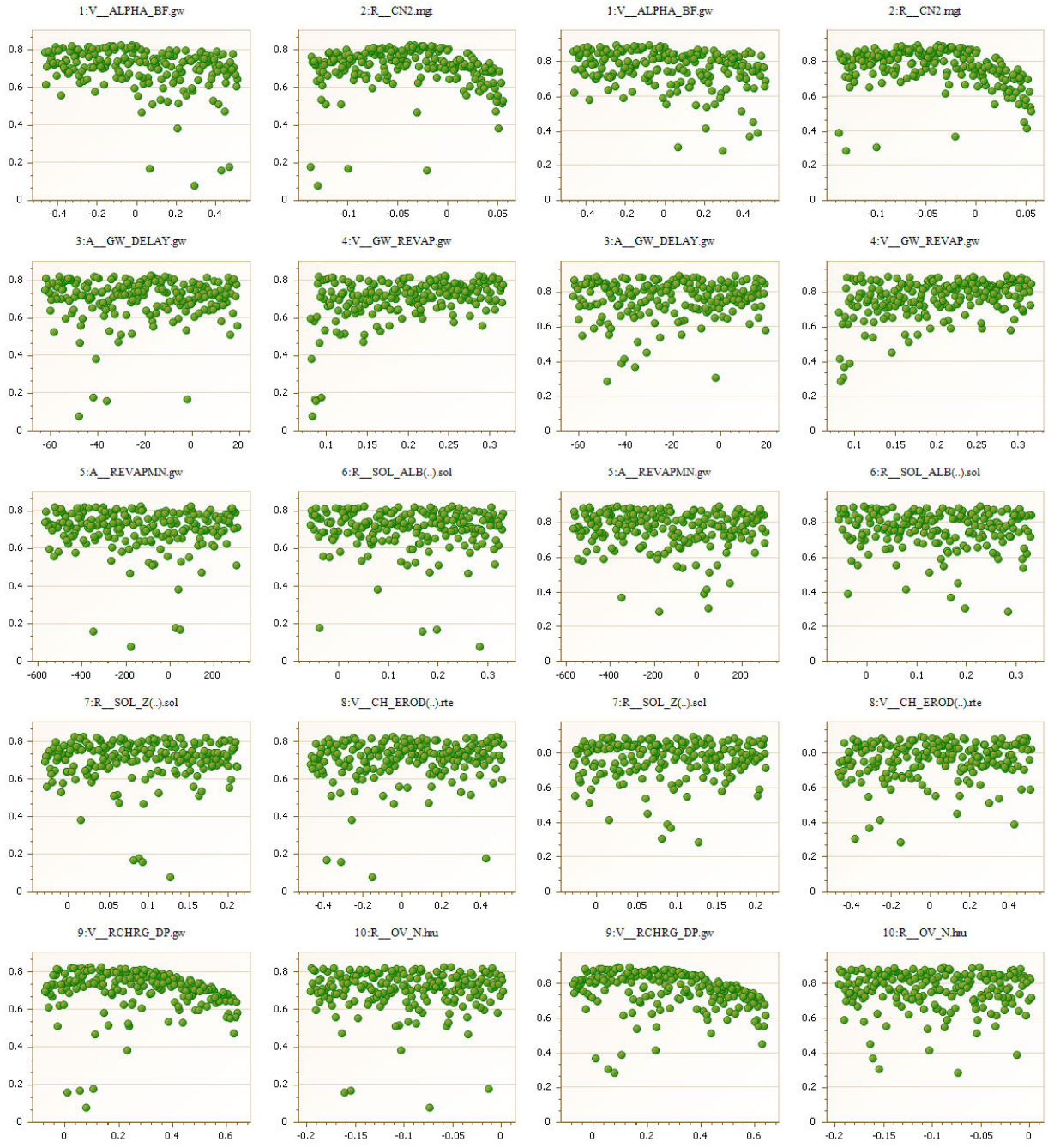

Annexure 45: Dotty plots of parameter values versus objectives function in Gumara

Calibration

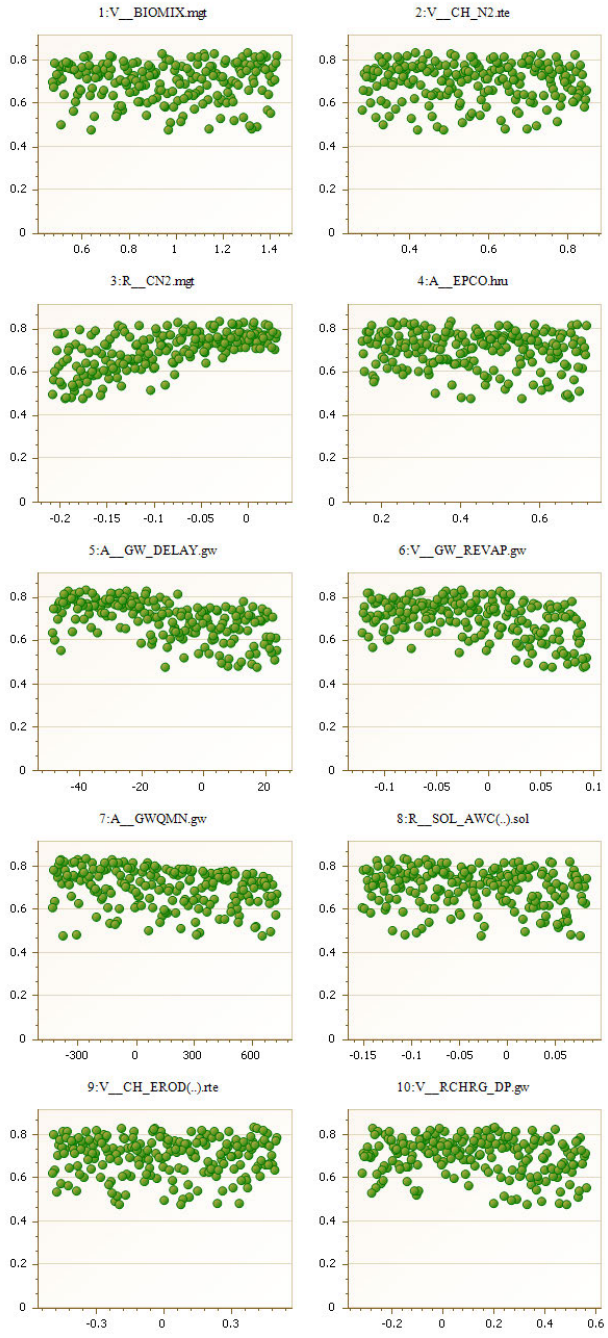


Validation

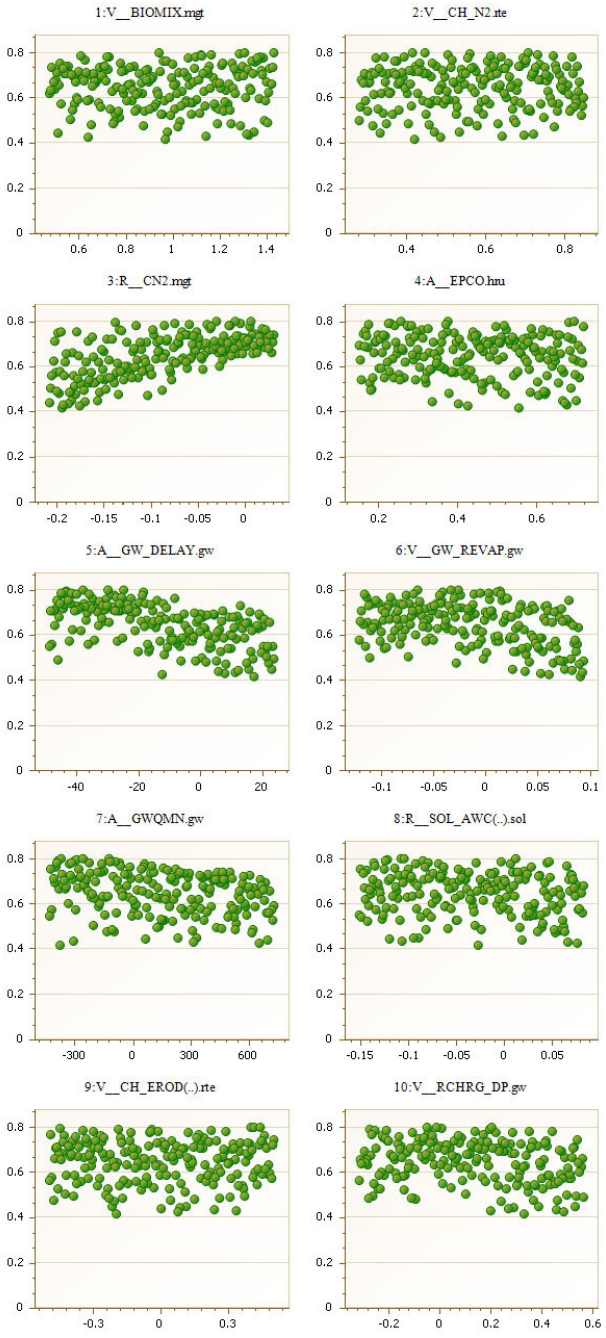

Annexure 46: Dotty plots of parameter values versus objectives function in Megech

Calibration

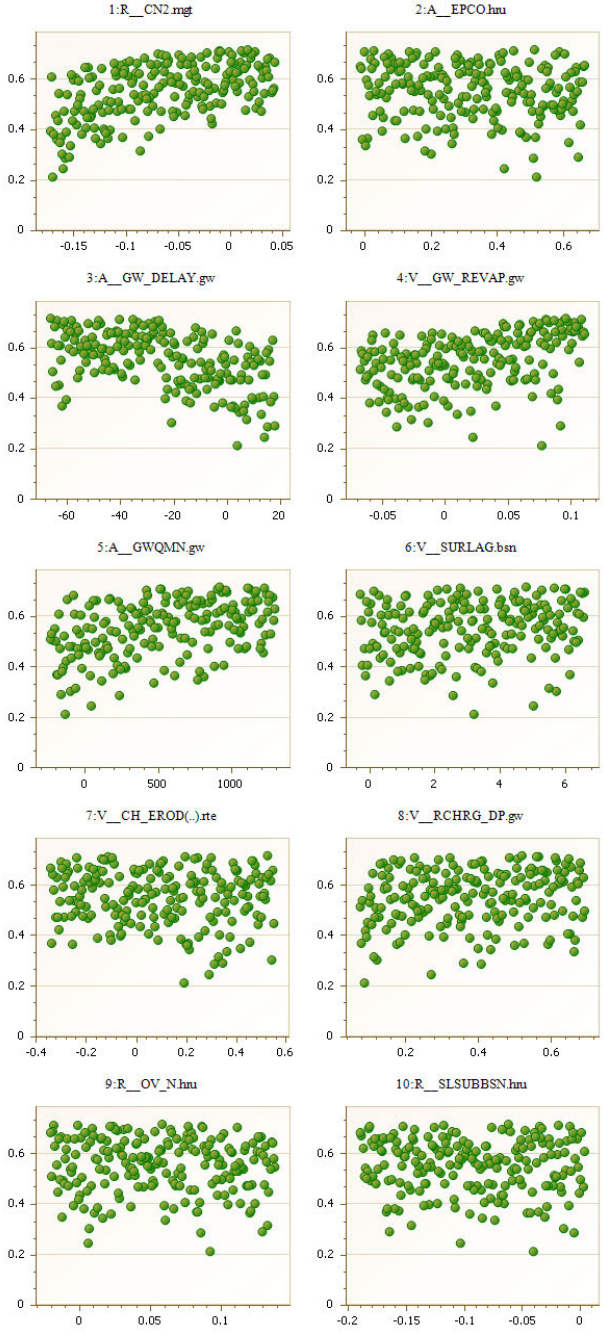


Validation

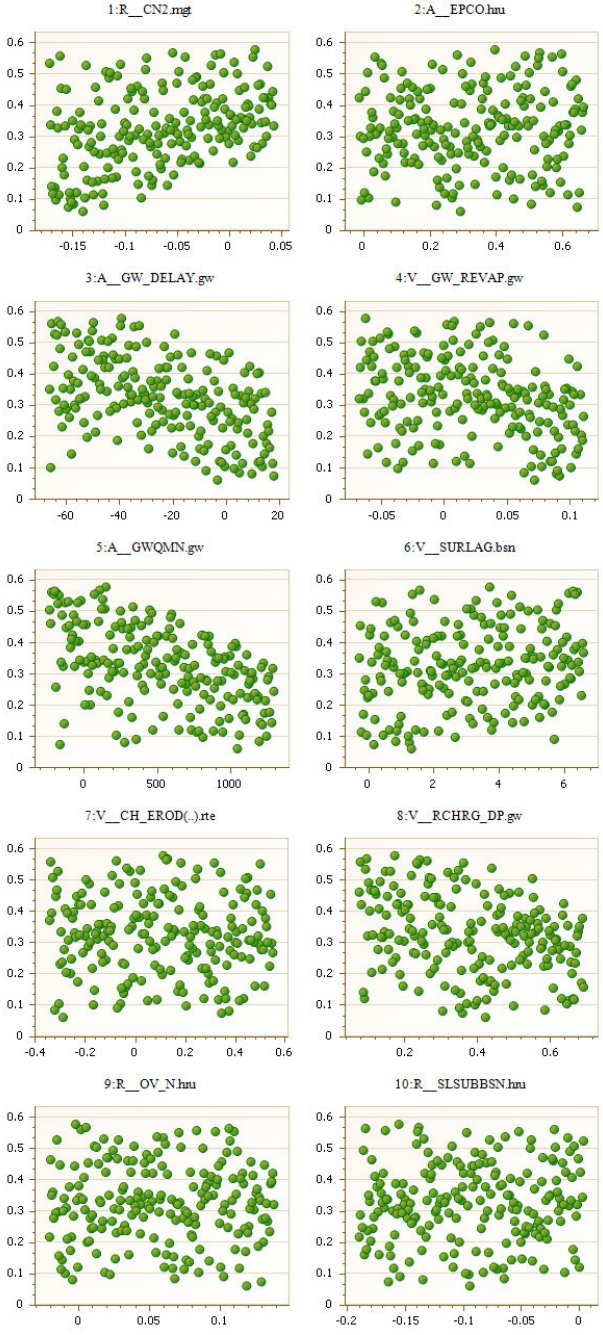

Annexure 47: Dotty plots of parameter values versus objectives function in Gilgel Abbay

Calibration

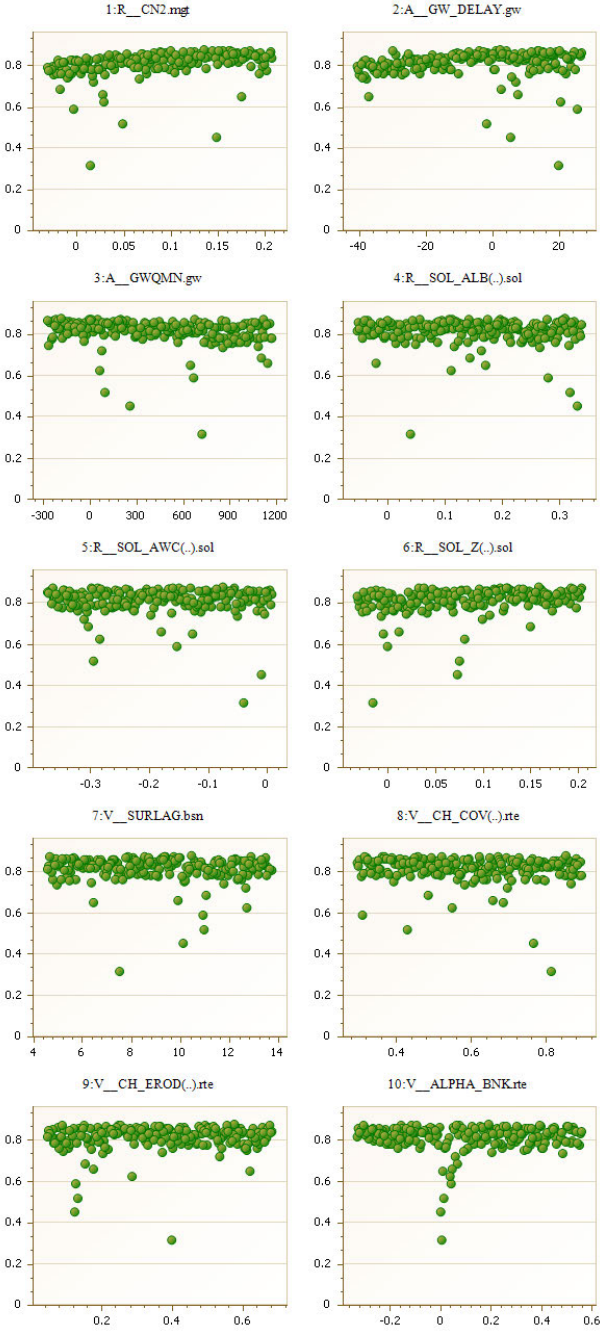


Validation

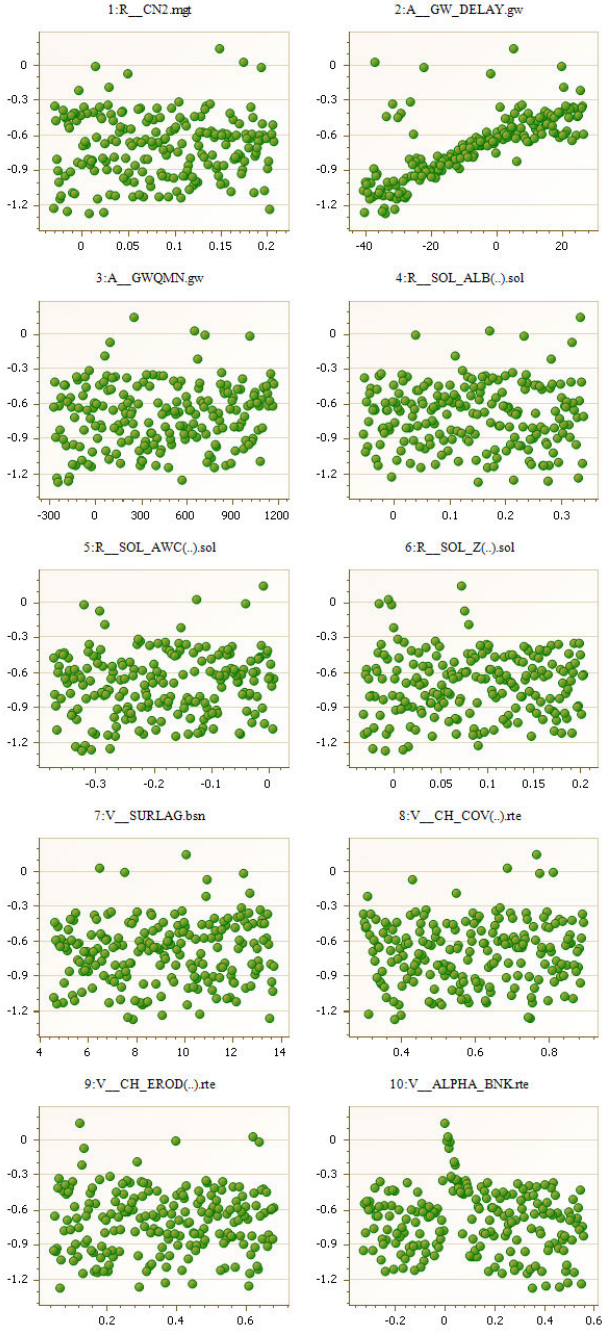

Annexure 48: Hydrology component of SWAT output using LULC, 1986

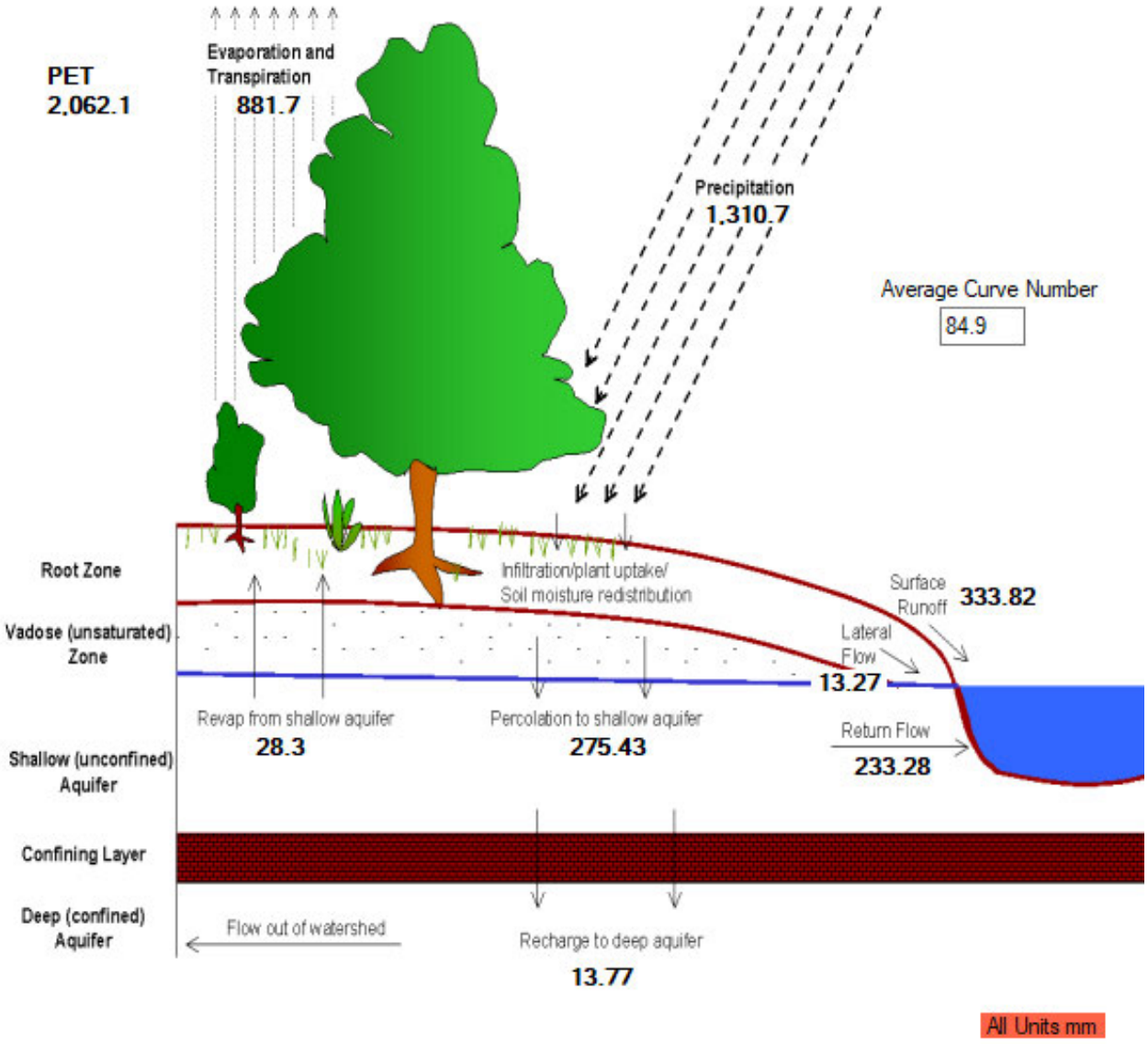

Annexure 49: Hydrology component of SWAT output using LULC, 2000

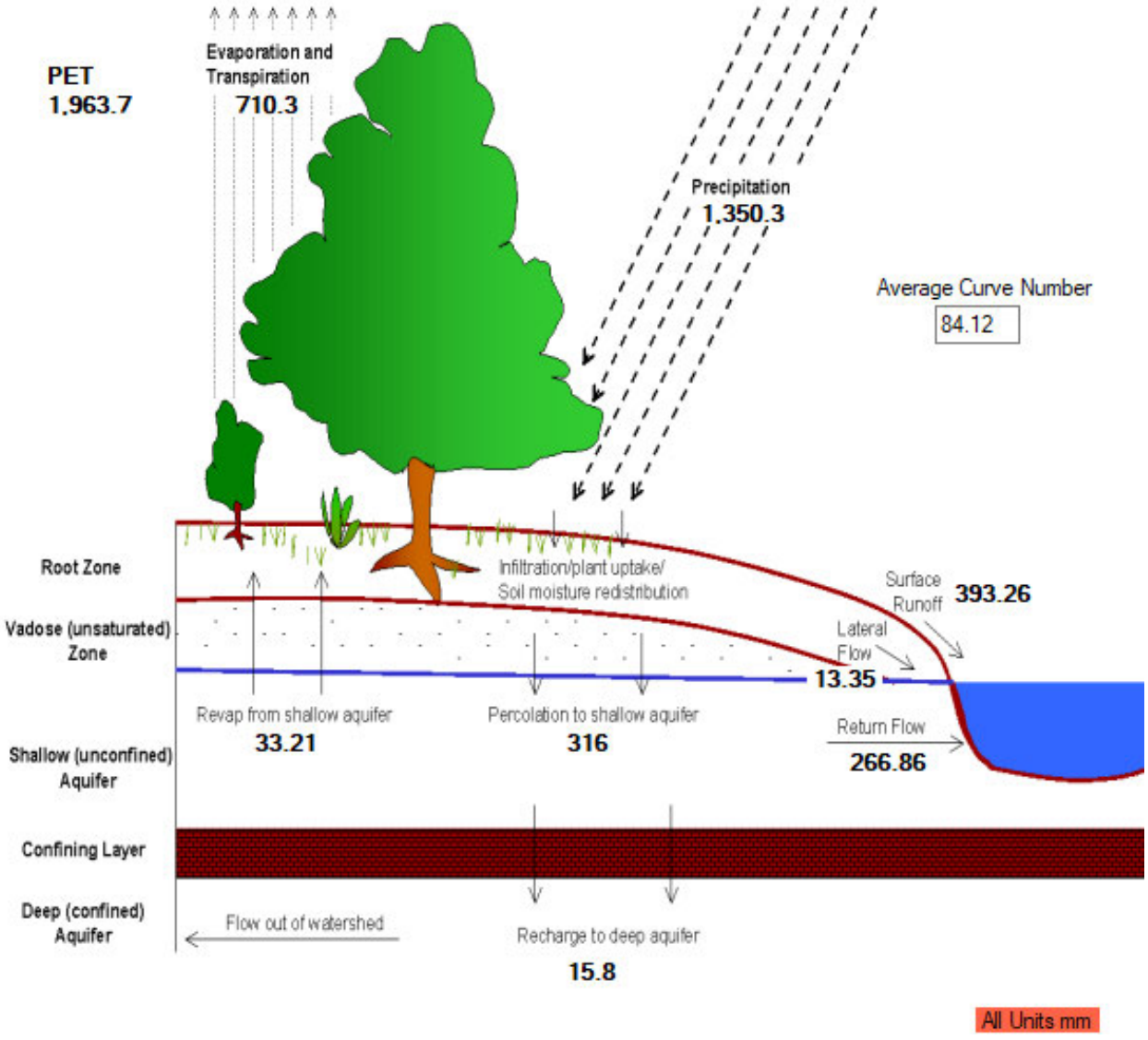

Annexure 50: Hydrology component of SWAT output using LULC, 2014

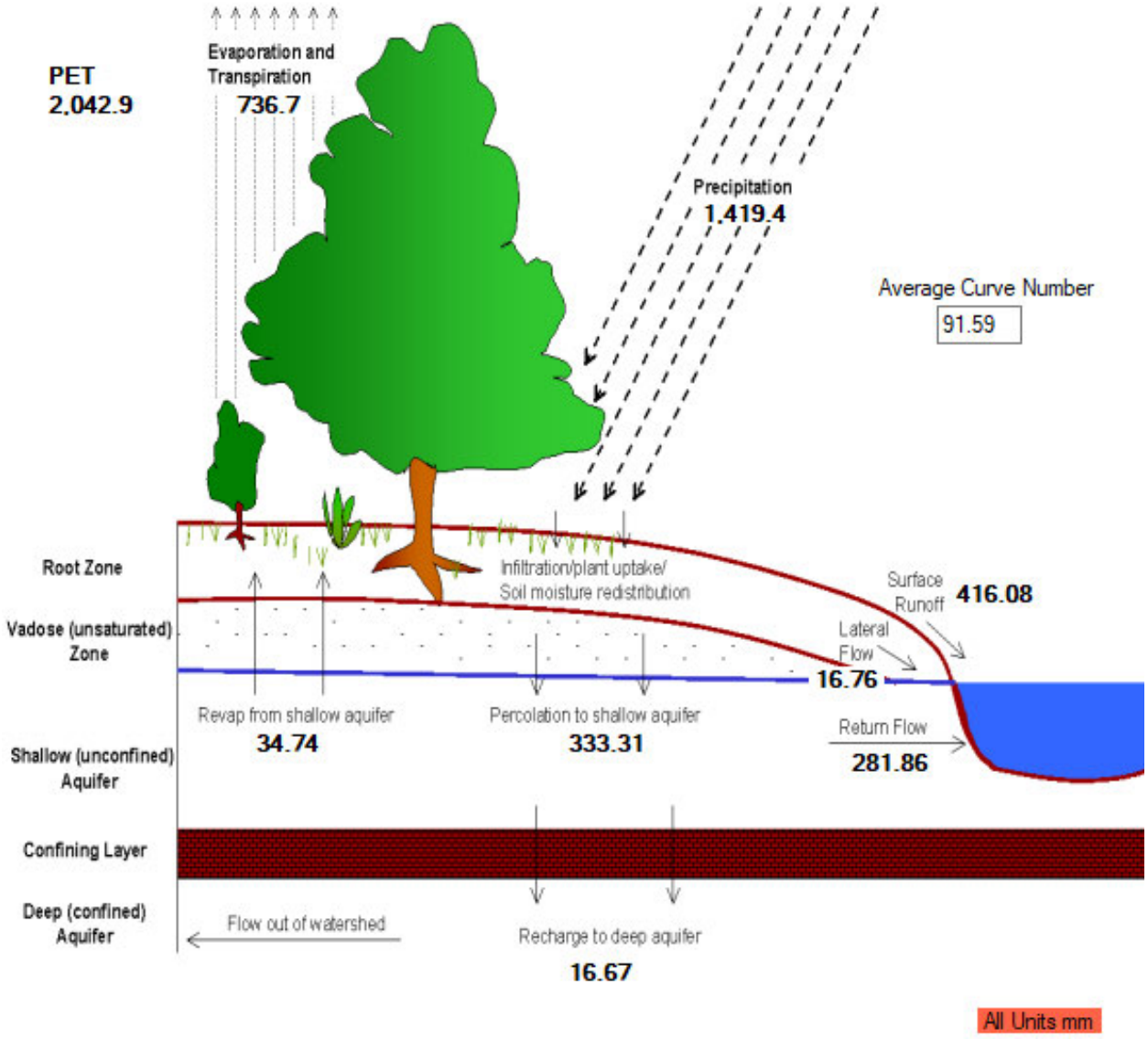

Annexure 51: Water balance components using 1986, 2000, and 2014 LULC

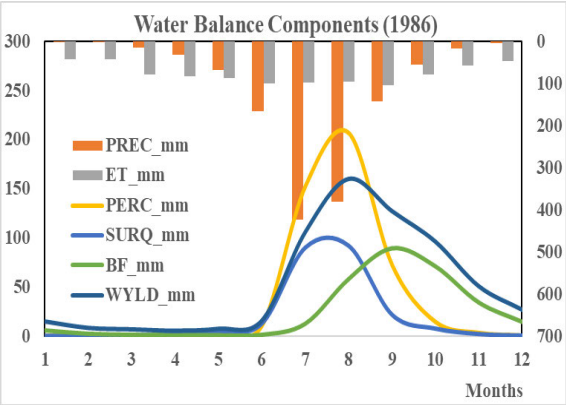


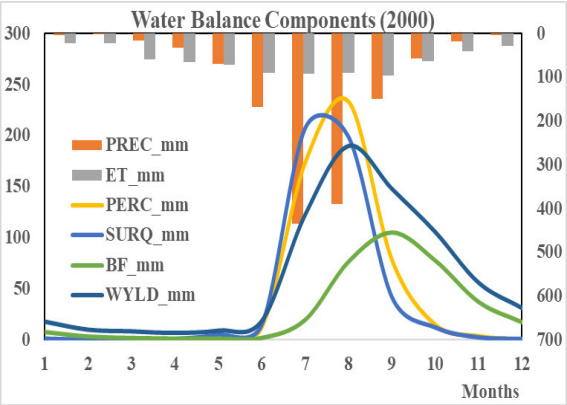


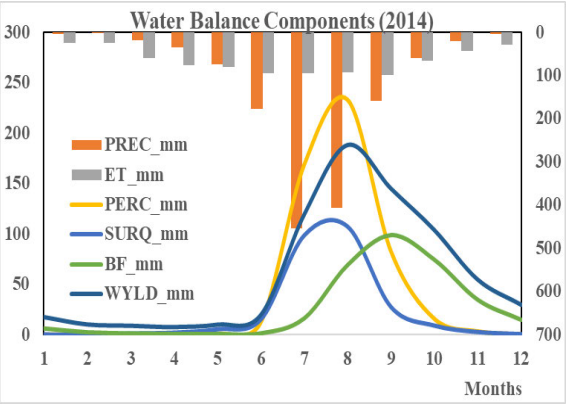

Annexure 52: Design and current domestic water yield in 2020

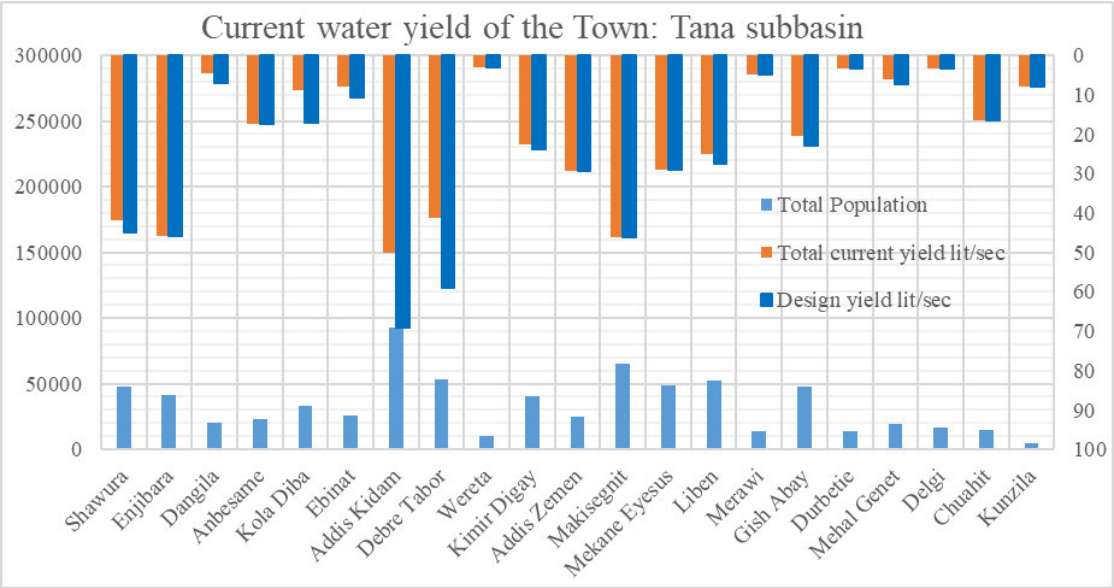


Annexure 53: Design and current water yield in 2020

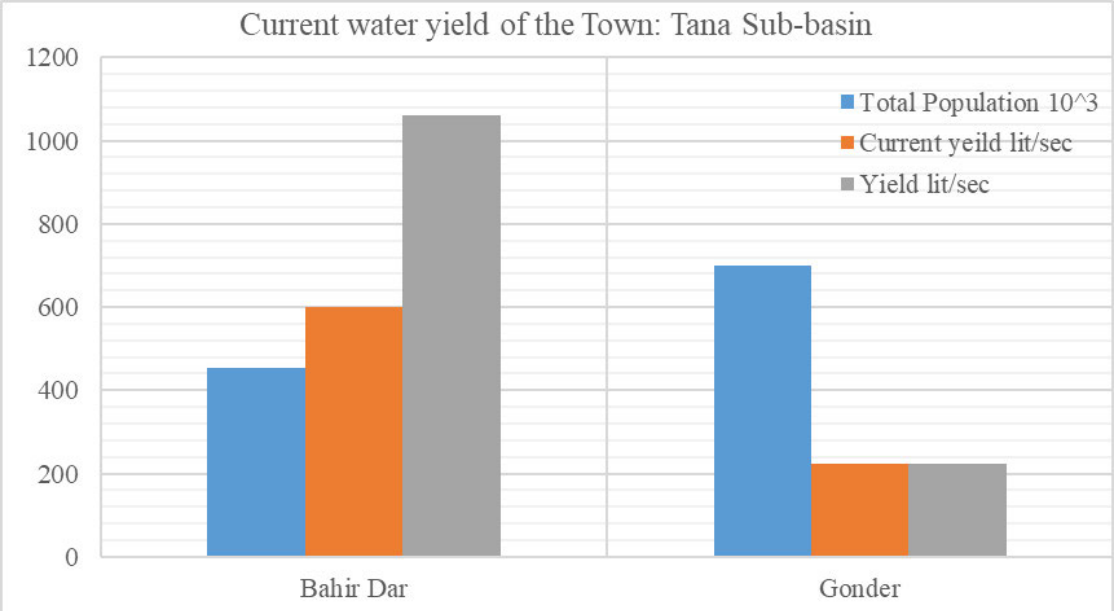

Annexure 54: Annual water production, distribution, and loss in 2020

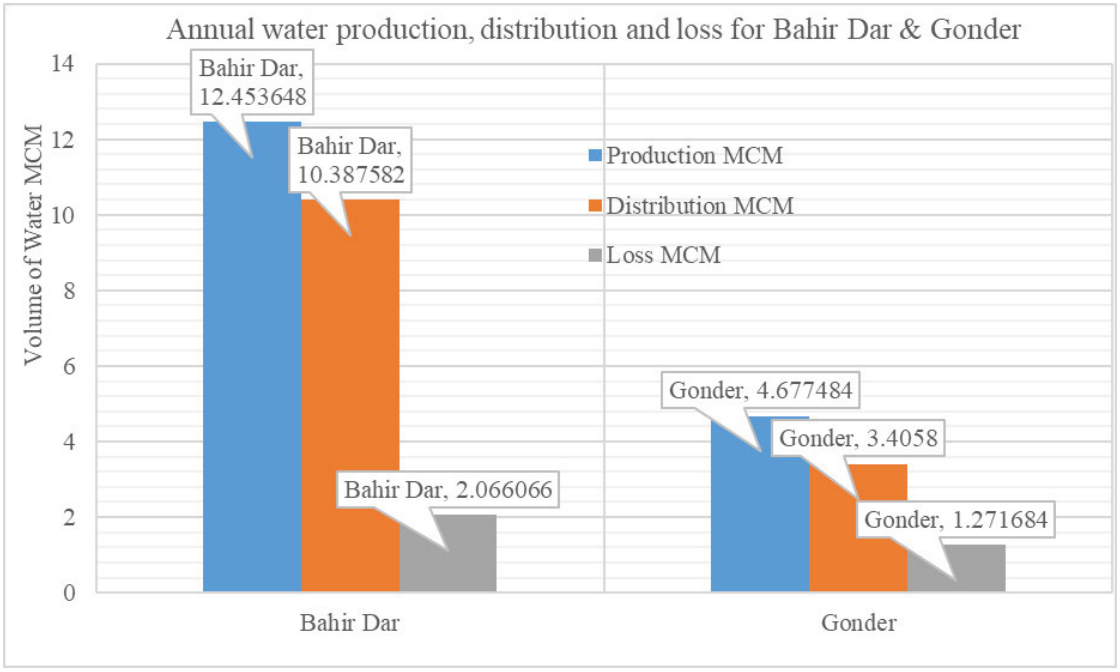


Annexure 55: Current water abstraction in Tana Sub-basin for domestic use in 2020

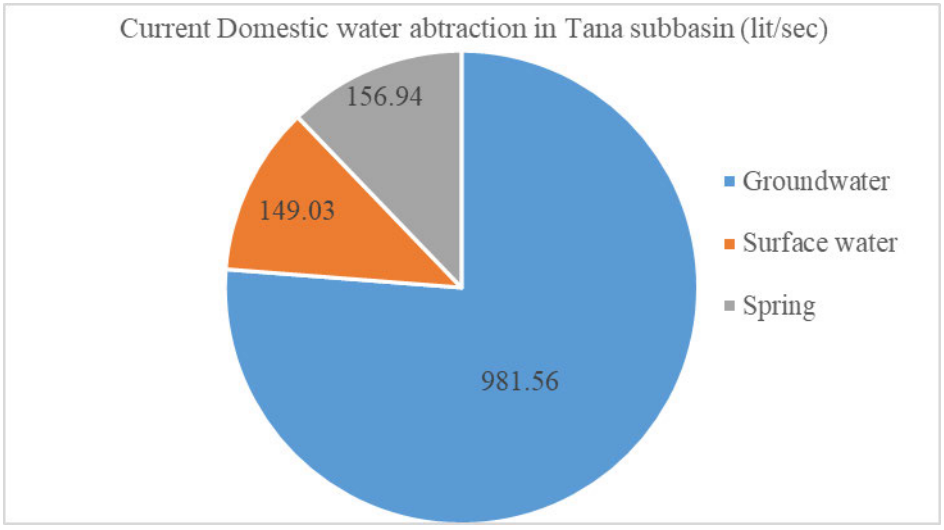

Annexure 56: Current domestic water loss in the Tana Sub-basin Towns in 2020

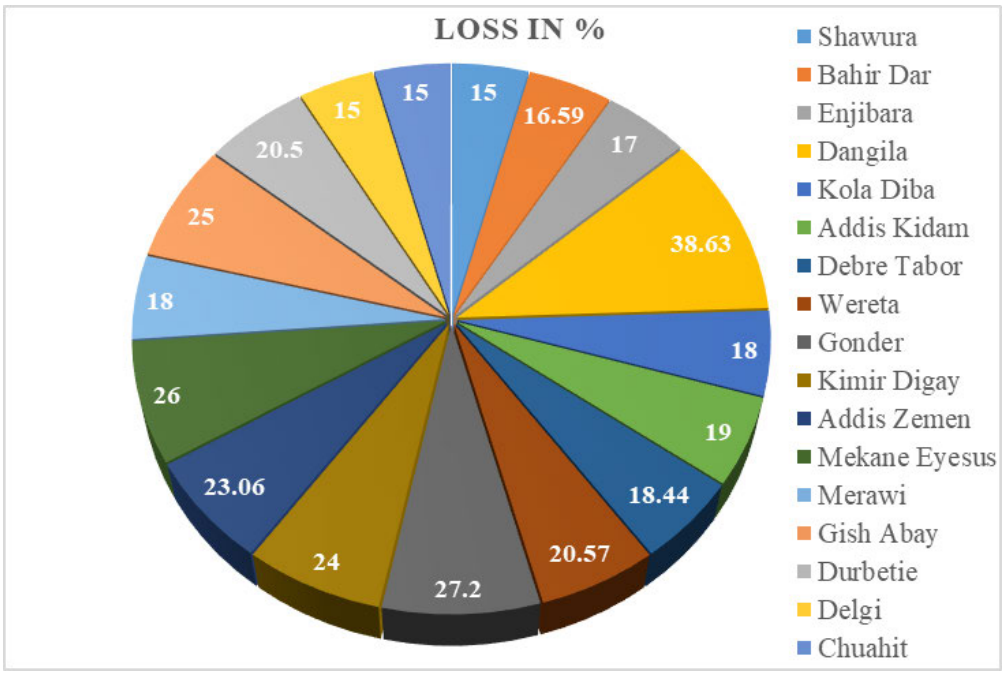


Annexure 57: Livestock population and water consumption in Tana Sub-basin in 2020